

Republic of Iraq  
Ministry of Higher Education  
And Scientific Research  
University of Babylon  
College of Materials Engineering  
Department of Metallurgical Engineering



*Investigation the Influence of Alloying  
Elements/Ceramic Additions on The Ni-  
Cr-Mo-Co Alloy Behavior as Bio-  
Material*

A Thesis

Submitted to the Council of the College of Materials  
Engineering /University of Babylon in Partial Fulfillment of  
the Requirements for the Degree of Doctor of Philosophy in  
Materials Engineering/ Metallurgical

By

*Ban Ahmed Shanan Jassim*

(B.Sc. In Metallurgical Engineering, 2011)

(M.Sc. In Metallurgical Engineering, 2017)

Supervised by

*(Prof.) Dr. Ali Hubi Haleem*

*(Prof.) Dr. Haydar H. Jamal Al Deen*

2022 A.D

1444 H.D

بِسْمِ اللَّهِ الرَّحْمَنِ الرَّحِيمِ

{ يَرْفَعُ اللَّهُ الَّذِينَ آمَنُوا مِنْكُمْ وَالَّذِينَ أُوتُوا

الْعِلْمَ دَرَجَاتٍ وَاللَّهُ بِمَا تَعْمَلُونَ خَبِيرٌ }

صدق الله العلي العظيم

{ سورة المجادلة/اية 11 }

## **Supervisor Certificate**

We certify that this thesis entitled (*Investigation the Influence of Alloying Elements/Ceramic Additions on The Ni-Cr-Mo-Co Alloy Behavior as Bio-Material*) is Prepared by (*Ban Ahmed Shanan*) under my supervision at the Department of Metallurgical Engineering / College of materials Engineering/ University of Babylon in partial fulfillment of the requirements for the degree of Doctor of Philosophy in Materials Engineering/ Metallurgical.

**Signature:**

**Dr. Ali Hubi Haleem**

**Date: / / 2022**

**Signature:**

**Dr. Haydar H. Jamal Al Deen**

**Date: / / 2022**

## ***Examination Committee Certification***

*We certify that we had read this thesis entitled (Investigation the Influence of Alloying Elements/Ceramic Additions on The Ni-Cr-Mo-Co Alloy Behavior as Bio-Material) and as an Examination Committee examined the student (Ban Ahmed Shanan) in its contents and that in our opinion it meets the standard of a thesis and is adequate for the award of the Degree of Doctor of Philosophy in Material's Engineering/ Metallurgical Engineering.*

***Signature:***

***Prof.Dr. Jassim M. Salman Al-Murshdy***

***(Chairman )***

***Date: / / 2022***

***Signature:***

***Prof. Dr. Zuheir Talib Khulief***

***(Member)***

***Date: / / 2022***

***Signature:***

***Asst. Prof. Dr. Ali Munder Mustafa***

***(Member)***

***Date: / / 2022***

***Signature:***

***Asst.Prof.Dr.Fatimah Jaffar Al-Hasani***

***(Member)***

***Date: / / 2022***

***Signature:***

***Asst.Prof.Dr.Nabaa Sttar Radhi***

***(Mamber)***

***Date: / / 2022***

***Signature:***

***Prof. Dr. Ali Hubi Haleem***

***(Supervisor)***

***Date: / / 2022***

***Signature***

***Prof.Dr. Haydar Hassan Jaber***

***(Supervisor)***

***Date: / / 2022***

***Signature:***

***Prof. Dr. Saad Hameed Najem***

***Head of the Metallurgical Engineering Dep.***

***University of Babylon***

***Date: / / 2022***

***Signature:***

***Prof. Dr. Imad Ali Disher Al-Hydary***

***Dean of Materials Engineering College/***

***University of Babylon***

***Date: / / 2022***

# *Dedication*

*To The One whose throne is in the sky... To the One whom we praise and thank... Allah*

*To The Messenger of Allah... Mohammed (peace and blessings of Allah be upon him and his progeny)*

*To The one who embraced me like my mother..... The one who is my light in life..... My dear father*

*To The secret of my existence, strength and joy..... My beloved mother*

*To The whispers of flowers and fragrance of morning..... The shoulder of tenderness and miracle of all time..... My brothers and sisters*

*To All teachers and colleagues who were supported and pushed me forward. I present this research with my regards.*

*Ban 2022*

# *Acknowledgements*

As I approached the completion of my (PhD) at the Babylon University, many people helped me with their advice, patience and support. To all those, I want to express my deepest thanks.

First of all, I would like sincerely to thank my supervisors, Prof. Dr. *Ali Hubi Haleem* and Prof. Dr. **Haydar H.Jamal Al Deen** for their tremendous time and effort spent in leading, supporting and encouraging me during study years. Their passion for challenges has given me inspiration; his knowledge of science and their guidance helped me in all the time of research and writing of this thesis. Without their help and effort, it would be impossible for me even to get close to this point.

Additional thanks go to my colleagues in the laboratories for their passion, supporting and helping me in my work. It was a real pleasure to work with you, all.

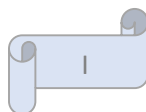
# Abstract

Metal-based dental alloy is one of the most widely used materials in dentistry. Alloys of Cobalt-chromium and nickel-chromium have many applications in the field of dentistry besides alloys Gold and precious metals used in this field. This study focused on the manufacture and characterization of nickel-chromium alloy compounds reinforced by adding some elements (Boron, Zirconium, Indium and Zirconia ceramic material), and their effect on the physical, mechanical, biological and electrochemical properties of this alloy.

Powder metallurgy method used to prepare alloys, each of the Boron, Zirconium and Indium was added in a different proportion (0.4,0.8,1.2) wt% while Zirconia was added in different proportions (3,6 and 9) wt%. The mixing process took place for 6hr, then compacted at a constant pressure of 600 Mpa. The dimensions of the samples after the pressing process were  $d=13\text{mm}$  and  $t = 4 \text{ mm}$ . The sintering process accomplished at temperature  $1000^{\circ}\text{C}$  for 8 hr for all samples are sufficient completely to transform all element into alloy structure.

Various tests were carried out on the samples, including mechanical tests (hardness, young's modules, compressive strength, and wear) , physical tests (density and porosity ), microstructure test( X-ray diffraction analysis, optical and field emission scanning electron microscope ) , electrochemical tests( open circuit potential, potentiodynamic polarization and ion release), and biological tests (Antibacterial) .

The results indicate that the addition of Boron, Zirconium and Indium to alloy lead to a clear decrease in the porosity, while the addition of Zirconia led to a noticeable increase in the porosity values of the alloy. Density results after sintering show an increase in the density of both Boron, Zirconium and Indium containing



specimens and a significant decrease in the density of Zirconia -containing specimens.

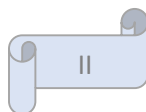
The results of XRD showed that all specimens (with and without additives) at room temperature, just three phases structure appear in all alloys,  $\gamma$  (Ni),  $\text{Cr}_3\text{Ni}_2$ ,  $\text{MoNi}_4$ . But in the case of adding Zirconia to the alloy, it showed previous phases with clear peak of Zirconia in the diagram.

The brinall hardness of the prepared alloy was significantly increased with the addition of a little boron and Zirconium in all proportions, the addition of Indium had slight effect on hardness value. Specimens with 1.2wt% Zirconium has the higher hardness of all adding elements.

The wear resistance increased with addition of B,Zr,In and  $\text{ZrO}_2$  to NiCrMoCo alloys , The specimen of (1.2wt%) Zr has lower weigh loss during wear test under different loads.

From the electrochemical properties results , the corrosion resistance of NiCrMo Co alloy showed significant improvement after the addition of each B, Zr,In and  $\text{ZrO}_2$  in artificial saliva and normal saline solutions . It was shown that higher improvement with the addition of the (0.8wt%)B where the percentage of improvement was 84.6% , 87.2% in Saliva and normal saline solutions , respectively.

The ion release test for all alloys for 21 days in artificial saliva and normal saline solutions illustrate that very low concentrations of metals ions release are observed. In the antibacterial test It was notice that the presence of samples led to a reduction in the effect of bacteria. where it was notice a noticeable decrease in the percentage of bacteria after incubation for 12 hours. Sample with addition (1.2wt%)indium and the sample with addition (6 wt%)  $\text{ZrO}_2$  had the highest antibacterial effect on both indices compared to other samples.



## Contents

<i>Subject</i>		<i>Page No.</i>
Abstract		I
Contents		III
List of Figures		VI
List of Tables		X
List of Abbreviation and Symbols		XI
<b>Chapter One : Introduction</b>		
1.1	General view	1
1.1.2	The Materials Used in Dental Application	2
1.1.3	Effect Oral Enviroment on Dental Alloys	5
1.2	Applications of Dental Alloys	7
<b>Chapter Two: Theoretical Part and Literature Review</b>		
2.1	Introduction	14
2.2	What are Dental Materials ?	15
2.3	The Clinically Important Characteristics and Requirements of The Dental Alloys	16
2.3.1	Biocompatibility	17
2.3.2	Color and appearance of dental materials	17
2.3.3	Resistance to tarnish and corrosion	17
2.3.4	Modulus of elasticity	17
2.3.5	Thermal properties	17
2.3.6	Hardness	18
2.3.7	Ease of fabrication	19
2.3.8	Bonding to ceramic	19
2.3.9	Laboratory costs	19
2.4	Classification of Dental Alloys	20
2.5	Amalgam	20
2.6	High Noble Metals Alloys	21
2.7	Noble Metals Alloys	22
2.8	Base Metals Alloys	23
2.8.1	Titanium alloy	23
2.8.2	Co Cr alloy	24
2.8.3	Ni Cr alloy	24
2.9	The Ni - Cr – Mo System	27
2.9.1	Role of Nickel	28
2.9.2	Role of Cr	29
2.9.3	Role of Mo	29
2.10	Properties of Ni Cr alloy	29
2.11	Corrosion of alloys used in dentistry	30
2.11.1	Corrosion of Ni Cr alloy	35

2.12	Wear in Dental Alloys	37
2.12.1	Wear Types	38
2.13	Powder Metallurgy	40
2.14	Boron	42
2.15	Indium	43
2.16	Zirconium	43
2.17	Zirconia	44
2.18	Literature Review	45
<b>Chapter Three: Experimental part</b>		
3.1	Introduction	58
3.2	Powders and Their Tests	60
3.3	Particle size analysis	60
3.4	Samples Preparation	63
3.4.1	Mixing	63
3.4.2	Compacting	65
3.4.3	Sintering Process	66
3.5	Preparation the specimens for testing	68
3.6	Characterization Tests	68
3.6.1	X-RAY Diffraction Test (XRD)	68
3.6.2	Optical Microstructure	68
3.6.3	Field Emission Scanning Electron Microscope ( FESEM) Test	69
3.6.4	Energy Dispersive X-ray Spectroscopy (EDX)	69
3.7	Physical properties	69
3.7.1	Green Porosity and Density	69
3.7.2	Porosity and Density of Sintered Samples	70
3.8	Mechanical properties	71
3.8.1	Hardness Measurement	71
3.8.2	The Modules of Elasticity Measurement	71
3.8.3	Compression Test	71
3.8.4	Wear Test	73
3.9	Electrochemical properties	73
3.9.1	Open Circuit Potential	73
3.9.2	Potentiodynamic Polarization Test	75
3.9.3	Ion release test	76
3.10	Biological Test	76
3.10.1	Antibacterial Test	76
<b>Chapter Four: Results and Discussion</b>		
4.1	Introduction	78
4.2	Xray Diffraction Analysis	78
4.3	Microstructure Test	82
4.3.1	Light Optical Microscope	82
4.3.2	Field Emission Scanning Electron Microscopy (FESEM)	85
4.3.3	Energy Dispersive X-ray Spectroscopy (EDX)	95

4.4	Physical Properties Tests	109
4.4.1	Compacting Pressure	109
4.4.2	Effect of B addition on density and porosity	110
4.4.3	Effect of Zr addition on density and porosity	118
4.4.4	Effect of In addition on density and porosity	120
4.4.5	Effect of ZrO <sub>2</sub> addition on density and porosity	121
4.5	Mechanical properties	124
4.5.1	Brinal Hardness Test	124
4.5.2	Compression Test	127
4.5.3	Ultrasonic wave test	130
4.5.4	Wear Test	132
4.6	Electrochemical Tests	142
4.6.1	Open circuit potential (OCP)-time measurement	142
4.6.2	Potentiodynamic Polarization	146
4.6.3	Ni and Cr ions release measurement:	158
4.6	Biological Test	161
4.6.1	Antibacterial Test	161
<b>Chapter Five :</b>		
5.1	Conclusions	164
5.2	Suggestions for future works	166
<b>References</b>		

## List of Figures

Fig. No.	Subject	Page No.
<b>Chapter One: Introduction</b>		
1.1	Clinical applications of metals in dentistry	11
1.2	Representation regarding the implant-crown constructions in gingiva and bones	11
<b>Chapter Two: Theoretical Part and Literature Review</b>		
2.1	Metallic gold crown	22
2.2	Ni-Cr phase diagram	27
2.3	Ni - Cr - Mo ternary isothermal diagram calculated at 1250 ° C	28
2.4	Tarnish. (A) Tarnish on the surface of a silver amalgam restoration seen at 5 years. (B) The same restoration when polished regains its luster, without loss of material	33
2.5	(a) Potential galvanic current pathway when dissimilar metals contact.(b) A current pathway may exist even in a single metallic restoration	34
2.6	Schematic drawing of inter-oral movements of teeth.	38
2.7	fundamental process of powder metallurgy	42
2.8	Illustration of the sintering stages with a focus on the changes in pore structure during sintering	45
<b>Chapter Three: Experimental part</b>		
3.1	The Flow Chart of Work	62
3.2	The Better Size2000 Laser Particles Size Analyzer	63
3.3	Particle Size Analysis for Ni Powder	63
3.4	Particle Size Analysis for Cr Powder.	64
3.5	Particle Size Analysis for Mo Powder.	64
3.6	Particle Size Analysis for B Powder.	64
3.7	Particle Size Analysis for Zro2 Powder	65
3.8	Particle Size Analysis for Zr Powder	65
3.9	Particle Size Analysis for Co Powder	65
3.10	Particle Size Analysis for In Powder	66
3.11	Electric hydraulic press and die	68
3.12	The furnace used for sintering process	69
3.13	Program of sintering process for NiCrMo-x (B,Zr,Zro2).	70
3.14	Program of sintering process for NiCrMo- In	70
3.15	The specimen after grinding and polishing	71
<b>3.16</b>	FESEM device	72
<b>3.17</b>	Vacuum drying furnace type (DZF-6020)	75
<b>3.18</b>	The specimens before and after compression test	77
<b>3.19</b>	The open circuit potential measurement	78
<b>3.20</b>	The schematic diagram of potential dynamic polarization	80

<b>3.21</b>	The Atomic Absorption spectrophotometer	81
<b>Chapter Four: Experimental Part</b>		
4.1	XRD pattern of the A alloy before the sintering	84
4.2	XRD pattern of A alloy after sintering	84
4.3	XRD pattern of B3 alloy after sintering	85
4.4	XRD pattern of C3 alloy after sintering	85
4.5	XRD pattern of D3 alloy after sintering	86
4.6	XRD pattern of E2 alloy after sintering	86
4.7	Microstructure for Sintered Alloys (400X): A) A Alloy, B) B <sub>1</sub> Alloy, C) B <sub>2</sub> Alloy, D) B <sub>3</sub> Alloy, E) C <sub>1</sub> Alloy, F) C <sub>2</sub> Alloy, G) C <sub>3</sub> Alloy, H) D <sub>1</sub> Alloy, I) D <sub>2</sub> Alloy and J) D <sub>3</sub> Alloy, K) E <sub>1</sub> Alloy, L) E <sub>3</sub> Alloy .	89
4.8	FESEM images for A alloy with different magnification	92
4.9	FESEM images for B <sub>1</sub> alloy with different magnification	93
4.10	FESEM images for B <sub>3</sub> alloy with different magnification	94
4.11	FESEM images for C <sub>1</sub> alloy with different magnification	95
4.12	FESEM images for C <sub>3</sub> alloy with different magnification	96
4.13	FESEM images for D <sub>1</sub> alloy with different magnification	97
4.14	FESEM images for D <sub>3</sub> alloy with different magnification	98
4.15	FESEM images for E <sub>1</sub> alloy with different magnification	99
4.16	FESEM images for E <sub>3</sub> alloy with different magnification	100
4.17	EDX for A alloy	102
4.18	EDX for B <sub>1</sub> alloy	103
4.19	EDX for B <sub>2</sub> alloy	104
4.20	EDX for B <sub>3</sub> alloy	105
4.21	EDX for C <sub>1</sub> alloy	106
4.22	EDX for C <sub>2</sub> alloy	107
4.23	EDX for C <sub>3</sub> alloy	108
4.24	EDX for D <sub>1</sub> alloy	109
4.25	EDX for D <sub>2</sub> alloy	110
4.26	EDX for D <sub>3</sub> alloy	111
4.27	EDX for E <sub>1</sub> alloy	112
4.28	EDX for E <sub>2</sub> alloy	113
4.29	EDX for E <sub>3</sub> alloy	114
4.30	The compacting pressure for base (A) alloy versus green density	115
4.31	Effect B content on green density of A,B <sub>1</sub> ,B <sub>2</sub> ,B <sub>3</sub> alloys	116
4.32	The final density of A,B <sub>1</sub> ,B <sub>2</sub> ,B <sub>3</sub> alloys	117
4.33	The green and final porosity of A,B <sub>1</sub> ,B <sub>2</sub> ,B <sub>3</sub> alloys	117
4.34	Effect Zr content on green density of A,C <sub>1</sub> ,C <sub>2</sub> ,C <sub>3</sub> alloys	118
4.35	The final density of A,C <sub>1</sub> ,C <sub>2</sub> ,C <sub>3</sub> alloys	119
4.36	The green and final porosity of A,C <sub>1</sub> ,C <sub>2</sub> ,C <sub>3</sub> alloys	119
4.37	Effect In content on green density of A,D <sub>1</sub> ,D <sub>2</sub> ,D <sub>3</sub> alloys	120
4.38	Effect In content on final density of A,D <sub>1</sub> ,D <sub>2</sub> ,D <sub>3</sub> alloys	121

4.39	The green and final porosity of A,D <sub>1</sub> ,D <sub>2</sub> ,D <sub>3</sub> alloys	121
4.40	Effect ZrO <sub>2</sub> content on green density of A,E <sub>1</sub> ,E <sub>2</sub> ,E <sub>3</sub> alloys.	122
4.41	Effect ZrO <sub>2</sub> content on final density of A,E <sub>1</sub> ,E <sub>2</sub> ,E <sub>3</sub> alloys	123
4.42	Effect ZrO <sub>2</sub> content on final density of A,E <sub>1</sub> ,E <sub>2</sub> ,E <sub>3</sub> alloys.	123
4.43	Brinall hardness of A,B <sub>1</sub> ,B <sub>2</sub> ,B <sub>3</sub> alloys	124
4.44	Brinall hardness of A,C <sub>1</sub> ,C <sub>2</sub> ,C <sub>3</sub> alloys	125
4.45	Brinall hardness of A,D <sub>1</sub> ,D <sub>2</sub> ,D <sub>3</sub> alloys	126
4.46	Brinall hardness of A,E <sub>1</sub> ,E <sub>2</sub> ,E <sub>3</sub> alloys	127
4.47	The compressive strength of A,B <sub>1</sub> ,B <sub>2</sub> ,B <sub>3</sub> alloys	128
4.48	The compressive strength of A,C <sub>1</sub> ,C <sub>2</sub> ,C <sub>3</sub> alloys	128
4.49	The compressive strength of A,D <sub>1</sub> ,D <sub>2</sub> ,D <sub>3</sub> alloys	129
4.50	The compressive strength of A,E <sub>1</sub> ,E <sub>2</sub> ,E <sub>3</sub> alloys	129
4.51	young modulus of samples	131
4.52	Wear rate for A, B <sub>1</sub> , B <sub>2</sub> and B <sub>3</sub> alloy under 5N load	132
4.53	Wear rate for A, B <sub>1</sub> , B <sub>2</sub> and B <sub>3</sub> alloy under 10N load	133
4.54	Wear rate for A, B <sub>1</sub> , B <sub>2</sub> and B <sub>3</sub> alloy under 15N load.	133
4.55	Wear rate for A, C <sub>1</sub> , C <sub>2</sub> and C <sub>3</sub> alloy under 5N load .	134
4.56	Wear rate for A, C <sub>1</sub> , C <sub>2</sub> and C <sub>3</sub> alloy under 10N load	134
4.57	Wear rate for A, C <sub>1</sub> , C <sub>2</sub> and C <sub>3</sub> alloy under 15N load	135
4.58	Wear rate for A, D <sub>1</sub> , D <sub>2</sub> and D <sub>3</sub> alloy under 5N load	136
4.59	Wear rate for A, D <sub>1</sub> , D <sub>2</sub> and D <sub>3</sub> alloy under 10N load	136
4.60	Wear rate for A, D <sub>1</sub> , D <sub>2</sub> and D <sub>3</sub> alloy under 15N load	137
4.61	Wear rate for A, E <sub>1</sub> , E <sub>2</sub> and E <sub>3</sub> alloy under 5N load	137
4.62	Wear rate for A, E <sub>1</sub> , E <sub>2</sub> and E <sub>3</sub> alloy under 10N load	138
4.63	Wear rate for A, E <sub>1</sub> , E <sub>2</sub> and E <sub>3</sub> alloy under 15N load	138
4.64	Comparison of wear rate of all alloys under 5N load.	139
4.65	Topographic for (A)alloy by use light optical microscope with magnification 200X under(10N) load and (30min)time	139
4.66	Topographic for (B <sub>3</sub> )alloy by use light optical microscope with magnification 200X under(10N) load and (30min)time	140
4.67	Topographic for (C <sub>3</sub> )alloy by use light optical microscope with magnification 200X under(10N) load and (30min)time	140
4.68	Topographic for (D <sub>3</sub> )alloy by use light optical microscope with magnification 200X under(10N) load and (30min)time	141
4.69	Topographic for (E <sub>2</sub> )alloy by use light optical microscope with magnification 200X under(10N) load and (30min)time	142
4.70	The OCP-time in saliva solution at 37±1 C° for all (A,B <sub>1</sub> ,B <sub>2</sub> ,B <sub>3</sub> ) alloys measurement in ringer solution pH =7.4 and temp. 37 °c.	142
4.71	The OCP-time in saliva solution at 37±1 C° for all (A,C <sub>1</sub> ,C <sub>2</sub> ,C <sub>3</sub> ) alloys.	143
4.72	The OCP-time in saliva solution at 37±1 C° for all (A,D <sub>1</sub> ,D <sub>2</sub> ,D <sub>3</sub> ) alloys	143

4.73	The OCP-time in saliva solution at $37\pm 1\text{ C}^\circ$ for all (A,E <sub>1</sub> ,E <sub>2</sub> ,E <sub>3</sub> ) alloys	144
4.74	The OCP-time in 0.9%NaCl solution at $37\pm 1\text{ C}^\circ$ for all (A,B <sub>1</sub> ,B <sub>2</sub> ,B <sub>3</sub> ) alloys	144
4.75	The OCP-time in 0.9%NaCl solution at $37\pm 1\text{ C}^\circ$ for all (A,C <sub>1</sub> ,C <sub>2</sub> ,C <sub>3</sub> ) alloys	145
4.76	The OCP-time in 0.9%NaCl solution at $37\pm 1\text{ C}^\circ$ for all (A,D <sub>1</sub> ,D <sub>2</sub> ,D <sub>3</sub> ) alloys	145
4.77	The OCP-time in 0.9%NaCl solution at $37\pm 1\text{ C}^\circ$ for all (A,E <sub>1</sub> ,E <sub>2</sub> ,E <sub>3</sub> ) alloys	146
4.78	Potentiodynamic Polarization for (A,B <sub>1</sub> ,B <sub>2</sub> ,B <sub>3</sub> ) specimens in artificial saliva solution.	146
4.79	Potentiodynamic Polarization for (A,C <sub>1</sub> ,C <sub>2</sub> ,C <sub>3</sub> ) specimens in artificial saliva solution	148
4.80	Potentiodynamic Polarization for (A,D <sub>1</sub> ,D <sub>2</sub> ,D <sub>3</sub> ) specimens in artificial saliva solution	149
4.81	Potentiodynamic Polarization for (A,E <sub>1</sub> ,E <sub>2</sub> ,E <sub>3</sub> ) specimens in artificial saliva solution	150
4.82	Potentiodynamic Polarization curve for (A,B <sub>1</sub> ,B <sub>2</sub> ,B <sub>3</sub> ) specimens in 0.9%NaCl solution	151
4.83	Potentiodynamic Polarization curve for (A,C <sub>1</sub> ,C <sub>2</sub> ,C <sub>3</sub> ) specimens in 0.9%NaCl solution	153
4.84	Potentiodynamic Polarization curve for (A,D <sub>1</sub> ,D <sub>2</sub> ,D <sub>3</sub> ) specimens in 0.9%NaCl solution	153
4.85	Potentiodynamic Polarization curve for (A,E <sub>1</sub> ,E <sub>2</sub> ,E <sub>3</sub> ) specimens in 0.9%NaCl solution	154
4.86	SEM for Alloys (A) A alloy before corrosion test (B) A alloy after corrosion in Artificial Saliva solution & (C) B2 alloy after corrosion in Artificial Saliva solution .	157
4.87	Nickel ion release values for all samples in artificial saliva solution.	158
4.88	Nickel ion release values for all samples in 0.9%NaCl solution	159
4.89	Chromium ion release values for all samples in artificial saliva solution.	160
4.90	Chromium ion release values for all samples in 0.9%NaCl solution.	160
4.91	The effect of adding samples on the percentage of reduction after 1h and 12h for all samples in Bacteria( <i>Streptococcus mutans</i> ) and Fungi ( <i>Candida albicans</i> )	163

## List of Tables

<i>Table No.</i>		<i>Page No.</i>
<b>Chapter One: Introduction</b>		
1.1	Chronological list of events in the development of dental alloys	2
1.2	Metal tolerances in human body	7
<b>Chapter Two: Theoretical Part and Literature Review</b>		
2.1	Classification of casting alloys for metal ceramic prosthesis and partial dentures	20
2.2	Different types of corrosion commonly occurring in the oral cavity	31
2.3	Alloying elements and their major effects on the aqueous corrosion of Ni-Cr-Mo alloys	36
<b>Chapter Three : Experimental part</b>		
3.1	Powders Specifications	61
3.2	Chemical composition of alloys under study	67
3.3	The chemical composition of saliva solution	79
<b>Chapter Four: Result and Discussion</b>		
4.1	The Compressive strength for all alloys in MPa	130
4.2	The mechanical properties[Longitudinal velocity (VL), Transverse velocity VT, young's modulus (E), poissons ratio ( $\nu$ )] of each samples	131
4.3	The Corrosion Current (I <sub>corr.</sub> ), Corrosion Potential (E <sub>corr.</sub> ) and Corrosion Rate (C.R.) for All Alloys in saliva solution at 37±1°C.	151
4.4	The Corrosion Current density (I <sub>corr.</sub> ), Corrosion Potential (E <sub>corr.</sub> ) and Corrosion Rate(C.R.) for All Alloys in 0.9%NaCl at 37±1°C	154
4.5	Concentration of Ni and Cr ions released from the all samples in synthetic saliva and 0.9%NaCl solutions after 3 weeks of immersion at 37 °C	159
4.6	The antibacterial test results include (viable count, reduction percentage and Log.reduction) for all samples at Bacteria ( Streptococcus mutans (Gr+, Facultative Anaerobe)) and Fungi( Candida albicans ) after 1h and 12h.	162

## List of Abbreviation and Symbols

<b>Symbol</b>	<b>Discreption</b>	<b>Units</b>
<b>ADA</b>	American Dental Association	
<b>FDP</b>	fixed dental prostheses	
<b>RDP</b>	removable dental prostheses	
<b>HN</b>	high noble	
<b>N</b>	noble	
<b>PB</b>	predominantly base metal	
<b>HV</b>	Hardness Vickers	Kg/mm <sup>2</sup>
<b>PM</b>	Powder Metallurgy	
<b>HB</b>	Brinell hardness	Kg/mm <sup>2</sup>
<b>E</b>	Young's modulus	GPa
<b>SLM</b>	selective laser melting	
<b>SM</b>	soft milling	
<b>XRD</b>	X- Ray Diffraction	-
<b>FESEM</b>	Field Emission Scanning Electron Microscopy	
<b>EDX</b>	Energy Dispersive X-ray	-
<b>ASTM</b>	American Society of Testing and Materials	
<b>V<sub>L</sub></b>	longitudinal ultra-sonic wave velocity	
<b>V<sub>S</sub></b>	shear ultra-sonic wave velocity.	
<b>S</b>	Sliding Velocity	
<b>E.W</b>	The equivalent weight	
<b>EIS</b>	electro-chemical impedance spectroscopy	
<b>SIM</b>	selective laser melting	
<b>SM</b>	soft milling	

## Chapter one

### Introduction

#### **1.1 General View:**

Dental restorations and implants have a long history, dating back to ancient Etruscans' use of gold wires and bones to restore missing teeth and Egyptians' placement of sea shells on corpses for burial. Using a variety of precious metals, along with a few efforts to employ steel, zinc, brass, and copper, started in the contemporary era of dental restorations following the turn of the twentieth century. The efficiency regarding a few of such materials, along with variations in the availability and price of gold, which exploded to about \$900 an ounce in the year 1980, are credited with propelling dentistry towards the usage and development of alternative metal alloys. Many studies' attempts over the twentieth century resulted in the invention of new alloys which are not just less expensive compared to gold, yet also have qualities that are better suited to certain applications [1].

In the twentieth century, dental materials science progressed to include nickel and chromium, gold, cobalt and chromium, polymers, titanium, and composites. Dentistry has embraced new processing techniques and ceramic materials in the twenty-first century [2]. Since the introduction of cobalt-chromium alloys as cast dental appliances in 1928 and subsequent development of nickel-chromium and cobalt-nickel-chromium alloys, base metal alloys have gained widespread acceptance as the predominant choice for the fabrication of removable partial denture frameworks. Because of the high cost of noble metals, these base metals have been adapted also for dual applications such as the production of all-metal and metalceramic prostheses [3]. These base metals soon replaced the gold alloys for

partial denture use because of their light weight, lower cost and tarnish resistance[4]. List of events in the development of dental alloys are shown in Table (1.1).

**Table (1.1): Chronological list of events in the development of dental alloys [5].**

Year	Event
For 2500 years	For 2500 years, gold is the oldest known metal used in dentistry
1789	Jean Darcet introduced low-fusing metal alloy
1847	Platinum-gold alloy consisting of three-fourths gold and one-fourth platinum was introduced
1880	Richmond patented a porcelain tooth soldered to gold backing
1907	Lost wax technique was introduced by W.H. Taggart
1933	Co-Cr was introduced in removable partial dentures, replacing gold
1950	Resin veneers for gold alloys were developed
1959	“Porcelain fused to metal” concept was introduced
1968	Palladium-based alloys were introduced
1971	Base metal alloys (Ni-based) were introduced
1980	All-ceramic concept and technology was introduced

### 1.1.2 The Materials Used in Dental Application

When a dentist considers the type of restoration to place in a patient's mouth, the choice may be between different varieties of the same material, for example, different types of amalgam, or between two kinds of the same basic material, such as two kinds of metal amalgam and cast gold. With the rapid developments in dental materials over the past several years, it is more common that the dentist's choice is between two basic materials, such as between a metal amalgam and a polymer-and-ceramic composite, or between a metal crown and an all-ceramic crown. For example, although metals exhibit a wide range of strengths, melting ranges, and so on, they resemble one another in their ductility, thermal and electrical conductivity, and metallic luster. Similarly, ceramics can be characterized as strong yet brittle, and polymers tend to be flexible (low elastic modulus) and weak. In fact, simply understanding one key concept for each of the three basic materials gives us

significant insight into how each class of materials behaves as a restorative dental material, as well as an idea of the potential of these materials if some of their limitations can be overcome. Certain inherent properties of materials will influence their selection for use in dentistry[6].

Alloys and metals are commonly employed as bio-medical materials and are essential in the area of medicine. Metals have a significant edge over polymers and ceramics based on the strength and fracture resistance. Elasticity, toughness, electrical conductivity, and rigidity are all important characteristics of metals utilized in medical equipment [7].

There are various classification systems for dental alloys, yet the American Dental Association (ADA) compositional classification system is the most often utilized by dentists. Only platinum, gold, and palladium are considered noble metals in ADA system, which is separated into 3 groups via the noble metal content. The first category, high-noble dental alloys, has 60wt.% or more noble metals, with 40 wt.% or more gold content. The second group includes noble dental alloys that contain (25-60) wt.% or more noble metals, yet do not specify the gold concentration. The last group consists primarily of base-metal dental alloys that contain no more than 25wt.% noble metals and have no other composition requirements. Nonetheless, they may or may not include platinum, gold, or palladium [8].

Chromium and Nickel are the most common base metal dental alloys, yet Co-Cr and iron-based alloys are also available. Due to the fact that they are not noble metals, their corrosion resistance is determined by chemical qualities other than noble metals. A thin, invisible chromium oxide layer offers an impervious and complete film which passivates the alloy's surface. Because the passive layer is

extremely thin, it has little effect on the finish of the surface. In ordinary stainless steel, a comparable passive oxide layer prevents surface corrosion [6].

The most often used dental cast base-metal alloys for those application are Co–Cr and Ni–Cr [9]. The majority of Ni-Cr alloys are composed of (60-80)% Ni, (10-27)% Cr, and (2-14)% molybdenum [10]. Despite its benefits, such as high strength and toughness at high temperatures, good acid/alkali resistance, Ni–Cr alloys provide a larger biologic risk compared to other alloys due to the prevalent hypersensitivity to Ni. As a result, Co–Cr alloys are considered to be the most popular base-metal substitute for the Ni-allergic individuals. Yet, apart from Ti-based alloys, Co–Cr alloys have largest melting ranges of casting alloys, making lab manipulations (finishing, casting, and polishing) problematic. Furthermore, the Co–Cr alloy surface oxide is hard to mask, while coefficients of thermal expansion regarding the Co–Cr alloys are not always as compatible with the porcelains as those of the Ni–Cr alloys. The 2<sup>nd</sup> most common of the metal allergens is Co [9]. The galvanic corrosion behaviors of Ni-Cr alloys have been found to be unstable. With regard to physiological solutions like artificial saliva, balanced salt, artificial sweat solutions, and human saliva, they do corrode. A few Ni-based alloys, in particular, were proven to be vulnerable to crevice corrosion and/or pitting [11].

Due to the possibility of the allergic reactions to the Nickel ions, the Nickel-based alloys biocompatibility in the oral environment has raised a few concerns. The characteristics and microstructure regarding the Nickel-based alloys could be changed with the addition of other elements. The microstructure, composition, and formation of a passive layer of the film all have an impact on Ni-Cr alloys corrosion characteristics [12]. The complex composition related to Ni-Cr alloys is responsible for their exceptional characteristics. These alloys are primarily made up of Cr (11.9-26.3)% and Ni (68-80)%, yet they must be alloyed with other elements to provide

corrosion resistance and mechanical, porcelain bonding, and castability. In Ni-Cr alloys, (0.1-14)% of iron, molybdenum, aluminum, beryllium, silicon, cobalt, manganese, niobium, carbon, titanium, copper, magnesium, gallium, and tin is added [13]. Because it is in contact with the human body, bio-materials engineering coatings must demonstrate a high resistance to corrosion reactions, as well as a high resistance to wear, hardness, biocompatibility, and ductility. A ceramic veneer fired onto an alloy may be the outcome of utilizing dental alloys in fixed prosthesis for aesthetic reasons [14].

### **1.1.3 Effect Oral Environment on Dental Alloys**

Dental alloys are typically placed in patients' mouths to last for several years, in which they must withstand corrosive environments and mechanical load. As a result, it's critical to understand not just such materials' mechanical and physical qualities, yet also their corrosion resistance and biocompatibility [15]. The biologic nature related to the oral environment, as well as the size of the mouth cavity, limit the materials that can be used. Biting forces which could fracture replacement material and teeth are among the limits. Corrosion of metals and dental cavities are examples of material degradation. Changes in temperature result in restorations to compress and expand differently compare to the teeth, resulting in leakage and tooth sensitivity surrounding the restoration. Bio-compatibility (lack of harmful effects to the patient) and Esthetic demands of the patient [2].

Safety to the human body is essential in biomaterials; therefore, no toxic material is used for biomaterials. Metals implanted in tissues do not show any toxicity unless there is metal ion dissolution from corrosion and/or the generation of debris from wear. Therefore, corrosion resistance is absolutely essential for metals

in biomedical use, necessitating the use of noble or corrosion-resistant metals and alloys for medicine and dentistry [7]. Almost all dental materials release substances into the oral cavity, from where they may enter the human body through different routes, including swallowing of saliva and inhalation, with subsequent passage of the epithelial barriers in the gastrointestinal tract or the lungs. These substances may, via the blood circulation, be transported to different organs [16].

Corrosion is the unintended wearing of metal surfaces. The inner and outer layers of metallic surface are damaged when being exposed to electrochemical or chemical reactions in the surrounding area. For electrochemical reactions, an electrolyte is required. In the mouth, saliva serves as an electrolyte. Saliva is an extremely corrosive media. There is an increase in corrosion potential of saliva with the decrease in the pH factor and the chloride content rises[17]. Corrosive materials include acidic drinks and foods that contain sodium chloride. Aggressive media, like chloride ions, and acidic environments, speed up corrosion process. It is further boosted by fluoride ions found in mouthwash and toothpaste products, which operate as a major element in speeding corrosion [18].

The abrasive action of some antagonistic teeth contacts and foods commonly result in wear of the structure of the human tooth, which is natural occurrence. Pathological methods like acids and bruxism can frequently speed up abrasion. Artificial denture materials can occasionally alter the teeth's natural wear pattern. Abrasion can be caused by differences in wear properties of restorative materials and natural teeth. Discrepancies between the restoration and tooth surface could cause rapid wear, and reduced wear resistance regarding restorative materials which cause an occlusal contact loss, leading to supraeruption of antagonist and appearance of the occlusal interferences [19]. Table (1.2) shows metal tolerances in the human body.

Table(1.2) Metal tolerances in human body [20].

Metal	Normal Amount	Comments
Fe	4-5 g in whole body	Element of red blood cells. One of the least toxic trace elements
Co	Releted to B <sub>12</sub> amount	Element of vitamin B <sub>12</sub> ,No biological function of free Co.May Pure Co is toxic to bone tissue .Co-Cr alloys are not toxic .High dose may be carcinogenic.
Cr	2.8 µg/100g in blood	Toxic and Affecting cell viability and diminishing DNA synthesis .Hexavalent Cr is carcinogenic
Mn	12-20 mg in whole body	Essential elements in cells .One of the least toxic trace elements .
Mo	1-3 ppm in liver	Necessary for certain enzymes to function ,toxic in high dose .Also possible interfere with metabolism of Ca and P.
Ni	5mg/L in blood	Essential element for limited biological activities .High dose is toxic and may be carcinogenic.
Ag		Not inert in body.Strong in inhibitory and bactericidal effects.
Ti		No normal function ,but no carcinogenic.
Al		Having adverse effects.Causing deficiencies in bone calcification and neural disorders.
V		Toxic

## 1.2 Applications of Dental Alloys

Dental alloys have applications in the restoration and correction of lost, deteriorated or misaligned dental pieces. They are used for crowns, bridges, incrustations, implants, or in the form of wires in orthodontic appliances . To fulfill these functions, a variety of materials must be chosen that meet biocompatibility requirements, have adequate physical properties, resistance to wear and corrosion deterioration, and acceptable and stable appearance [21]. An enormous variety of dental applications are available to restore or replace decayed dental elements. Dental applications can be categorized as dental restorations or dental fillings, fixed

dental prostheses (FDP), removable dental prostheses (RDP), dental implants and orthodontic appliances[22].

- 1- **Dental Fillings or Dental Restorations** are used for repairing damage to the tooth's internal parts. This type of damage is almost commonly induced by caries, however it can also result from trauma[23]. Intraorally (direct method), it's used in a soft form. The fundamental benefit of direct restorative materials such as resin composite and dental amalgam is that they require less time in the chair. Furthermore, dental amalgam represents a common material for the restoration in the posterior teeth [24].
  
- 2- **Fixed dental prostheses (FDP)**, also known as (partial) dental crowns and bridges, are used for restoring severely decayed or missing teeth. Those restorations have been made outside of the mouth (i.e. through an indirect approach) and subsequently cemented into place. Also, endosseous dental implants might be screwed or cemented to such structures. These structures are majorly built of alloys and are frequently veneered with porcelain. Since veneers might be complicated to differentiate from natural teeth, diagnosing adverse reactions might be more challenging. Because of their inexpensive cost, Ni-Cr and Cr-Co alloys are still broadly utilized for FDPs. Titanium and Titanium alloys are regarded as 'bio-compatible,' and are mostly employed in the endosseous dental implants and suprastructures [22].Figure(1.1)shows fixed dental prostheses (FDP).

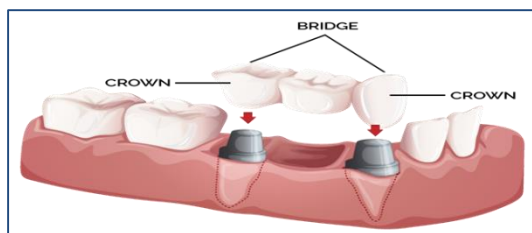


**Figure (1.1) :Fixed dental prostheses (FDP)(26).**

- 3- **Removable Dental Prostheses (RDP):** Partial dentures are also prevalent in circumstances when a fixed bridge cannot be anchored due to a lack of a distal abutment tooth. Partial dentures have a stiff alloy framework which rests on certain abutment teeth and evenly distributes occlusal biting forces to the remaining teeth. Clasps that engage the abutment teeth secure the acrylic teeth to the framework, which is after that bonded to the framework. RPDs have the advantage of allowing the patient to inspect and clean their remaining teeth, yet they are often less comfortable and attractive to wear compared to permanently fixed prostheses like implants or bridges [23].Figure(1.2)shows Removable Dental Prostheses (RDP).



**RPD**

**Figure(1.2): Removable Dental Prostheses (RDP)(26).**

- 4- **Dental implants** are becoming more popular as a way for replacing missing teeth. Special titanium-based alloys or, more recently, ceramics are used to make dental implants. Endosseous implants are implanted into the bone using specialized approaches to achieve bone integration, and after that indirect restorations are placed on the implants. Furthermore, implants do not require the restoration of adjacent teeth and are simpler to clean compared to bridges or removable partial dentures [23]. Figure (1.3) shows dental implant.

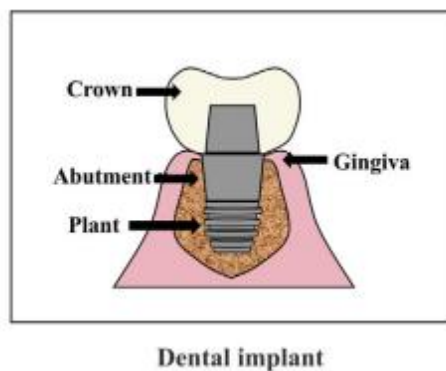


**Figure (1.3) : Dental implant(26).**

- 5- **Orthodontic Appliances:** Orthodontic appliances are utilized for moving teeth within the jaw into a more aesthetic or functional position. Stainless steel (316 L) is frequently combined with flexible alloys such as Ni-Ti. In addition, the active orthodontics appliances are typically in situ for about tow–three years. Yet, a wire of retention is frequently put behind front teeth to maintain the treatment result, and it remains in place for decades. Stainless steel is typically used for such retainers [22]. Figure (1.4) shows orthodontic appliances

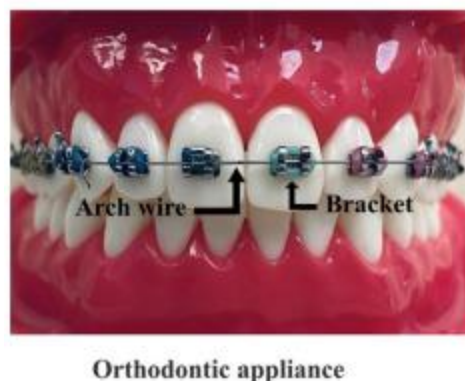


**Figure (1.4): Orthodontic Appliances (26).**

Dental alloys containing Ni are still being utilized efficiently in a variety of dental procedures. A lot of such alloys are used in the construction of long-lasting restorations such as fixed bridgework, crowns, and removable partial dentures. Ni-containing alloys are also widely used in orthodontics, where they are used in arch wires, metallic brackets, springs, bands, and ligature wires. Ni is found in various tools and devices, including endodontic instruments [25]. Clinical applications of metals in dentistry are shown in Figure (1.1). Schematic representation of implant-crown construction in bone and gingiva appeared in Figure (1.2) . Figure (1.5) shows clinical applications of metals in dentistry

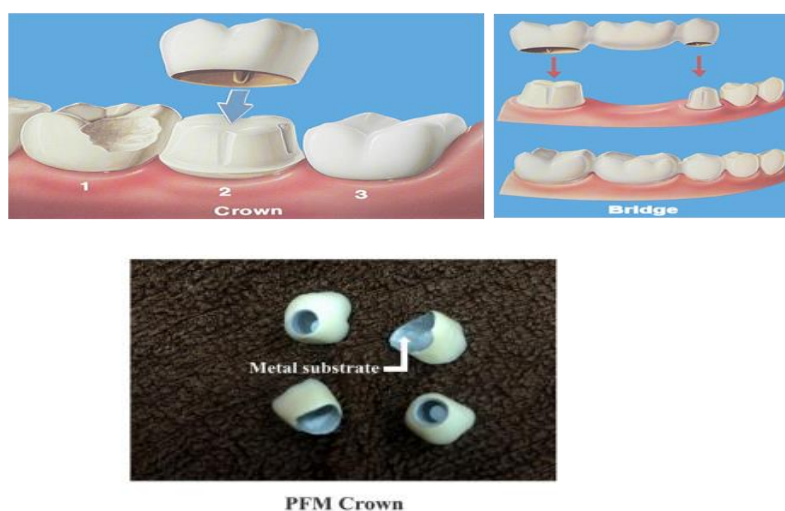


**Figure (1.5): Clinical applications of metals in dentistry[26].**

Figure (1.6) shows representation regarding the implant-crown constructions in gingiva and bones.

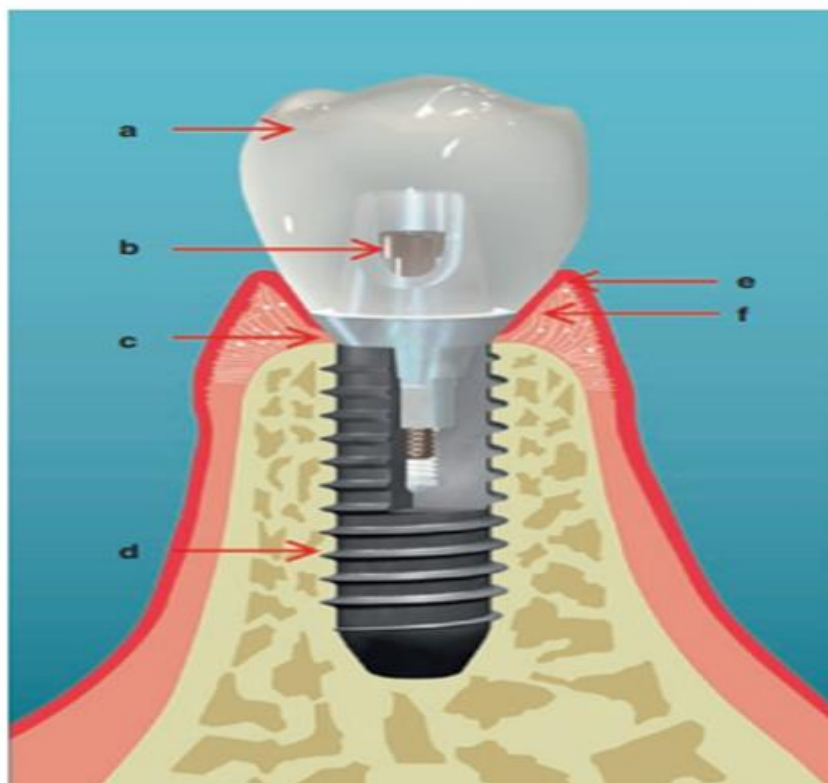


Figure (1.6) representation regarding the implant-crown constructions in gingiva and bones. (a) Metals, among other materials, could be used to make the dental crown. (b) The abutment screw secures the implant to abutment (majorly made of the Ti alloy). (c) Abutment for supporting and connecting the crown to the implant (majorly made of the Ti alloy). (d) A dental implant in the bone for replacing a lost natural root. (e) The dental sulcus is indicated (maximum of 1mm). (f) Junctional epithelium (1–2 mm) toward the bone [22].

### 1.3 Aims of the research

The problem of the NiCrMo alloy was the release of Nickel. Since this alloy is used in the human body, this will affect the biocompatibility of the alloy, due to the possibility of allergic reactions to nickel ions. So the objective of this study is improving the chemical, physical, biological and mechanical properties of Ni-Cr-Mo dental alloy by changing chemical composition of the alloy. This improvement will be achieved based upon several considerations as follows:

- 1- Preparation of Ni Cr Mo dental alloy by powder metallurgy and the determination of the physical and mechanical properties.
- 2- Inspect the influence of alloying elements addition (Boron, Indium, Zirconium) and Zirconia ceramic particle in different amounts on the mechanical properties, physical properties .
- 3- To support the use of these materials in the human physical structure, biocompatibility and corrosion behavior of fabricated materials will be investigated in saliva and normal saline solution as a bio media.
- 4- Improve the wear resistance of the alloy and reduce the release of nickel from Ni Cr Mo dental alloy after adding alloying elements .

## **Chapter Two**

### **Theoretical Part and Literature Review**

#### **2.1 Introduction:**

In the past few years, there was an increase in the emphasis on the applications of the materials in the bio-medical fields. None-the-less, the term "biomaterials" might've encountered a variety of the interpretations, in the clinical medicine as well as the materials sciences. Here the bio-material can be defined as synthetic material that is utilized for the replacement of part of a living system or to function in intimate[20]. The human body is a highly corrosive environment; therefore, a biomaterial for human use must fulfill mechanical, chemical, and biological performance criteria. Depending on the intended clinical target, typical clinical performance properties of the biomaterial must be considered: biocompatibility, bioactivity, and biomechanical functionality[27].

Biocompatibility is the ability of a material to perform with an appropriate host response in a specific application. Examples of "appropriate host responses" include resistance to blood clotting, resistance to bacterial colonization, and normal, uncomplicated healing. Many materials used as biomaterials such as metals, ceramics, polymers, glasses, carbons, and natural and composite materials [28]. Metals, one of the most commonly used biomaterials, have been used in clinical settings for centuries, primarily because of their mechanical properties this affords the metal alloy the unique ability of being interwoven physically and mechanically, which is an important influence on alloy strength and ductility. Essential characteristics of metals with respect to metal alloy biomaterials include the yield stress, elastic modulus, ultimate tensile stress, and fatigue stress of a given metal[27]. The high toughness and mechanical strength of metal alloys

represent the most important advantages in comparison with the bio-active ceramics that are intrinsically brittle or weak [29].

Mechanical and performance requirements each biomaterial and device has imposed upon it mechanical and performance requirements that originate from the physical (bulk) properties of the material. These requirements can be divided into three categories: mechanical performance, mechanical durability, and physical properties. First, consider mechanical performance. A hip prosthesis must be strong and rigid. A tendon material must be strong and flexible. A heart valve leaflet must be flexible and tough. A dialysis membrane this design criterion is met when a new biomaterial is under must be strong and flexible, but not elastomeric [30] .

There are a variety of materials which can be used to help with each of the above-mentioned conditions. Dental materials science is concerned with the chemical composition, manipulation, characteristics, mechanism of action, chemical reaction, indications, contraindications, and clinical uses of dental materials. Because every material that comes into contact with the human body is referred to as a biomaterial, most dental materials could be classified as biomaterials [5].

## **2.2 What are Dental Materials?**

Historically, a wide variety of materials have been used as tooth crown and root replacements, including animal teeth, bone, human teeth, ivory, seashells, ceramics, and metals. Restorative materials for the replacement of missing portions of tooth structure have evolved more slowly over the past several centuries. Dental materials may fall into any of the following classes: metals, ceramics, polymers, or composites. In general, polymers, cements, and composites are used for preventive

as well as restorative applications. Pure metals are rarely used for dental applications, although commercially pure titanium can be used to make dental implants, inlays, onlays, crowns, and bridges. Pure gold in a foil form can be used to make dental restorations (“fillings”) directly on teeth, but this technique is used only rarely today. Metals and alloys can also be used to construct orthodontic appliances, partial denture frameworks and clasp arms, and these materials may require auxiliary products such as matrix bands, burs, cutting blades, endodontic files, brooches, and reamers to ensure proper adaptation and placement [3].

Dental alloys, rather than pure metals, play a prominent role in the treatment of dental disease because pure metals do not have the appropriate physical properties to function in different types of restorations. Other materials may lack a combination of strength, modulus of elasticity, wear resistance and biologic compatibility that a material must have to survive long term in the mouth as fixed prosthesis[31].

### **2.3 The Clinically Important Characteristics and Requirements of The Dental Alloys:**

The diversity in available alloys exists so that alloys with specific properties can be used when needed. For instance, alloys used for bridge and crown applications have distinctive mechanical property requirements than alloys utilized for porcelain fused to alloy restorations. Although crown and bridge alloys must have appropriate rigidity and hardness when utilized in stress-bearing restorations, excessive strength is a drawback when it comes to polishing, grinding, and burnishing. Excessive wear of the occluding teeth is also a possibility. Alloys utilized in porcelain fused to metal restorations are employed as

overlaying porcelain substrates. The alloys' high rigidity and strength better match the qualities of the porcelain in this case. Because the alloy has a stronger sag resistance at the temperatures required to fire the porcelain, there is less residual stress and distortion. Comparably, alloys utilized in partial denture and implant applications should have improved mechanical qualities to provide failure resistance [5,32].

### **2.3.1 Biocompatibility:**

The bio-compatibility can be defined as the material's capability for eliciting a suitable biological response in a certain application. In the case of the close examination, it includes interaction amongst a material, a host, and an expected function of that material. All of the three factors have to be in harmony prior to when a material could be considered as bio-compatible [33]. Different alloy type for the fixed prostheses and dental restorations are currently available on the market. The capacity to remain in the oral cavity for an extended duration without being removed by the patient is a major characteristic for all of such fixed prosthodontic materials. As a result, understanding the biocompatibility regarding dental alloys is critical [31].

### **2.3.2 Color and appearance of dental materials :**

The color of alloys ranges from white to yellow for noble metals, while base metal alloys are darker in color. Although color has no bearing on the clinical performance of the alloy, the color of the underlying metal substructure in a metal–ceramic crown does play a role in the final restoration esthetics [5].

### **2.3.3 Resistance to Tarnish and Corrosion:**

Tarnish is a discoloration of the surface that results from formation of hard and soft deposits, for example, sulphides and chlorides. Tarnish causes no

deterioration of the actual material, however, it may could be unsightly, and is easily removed from the surface by polishing the metal. On the other hand, corrosion represents a chemical reaction between the material and its environment, and is therefore a potentially much more serious issue [34]. The corrosion happens in the case where two dissimilar materials are in contact with or are surrounded by some conductive liquid, such as saliva that leads to degrading the metal from a chemical reaction[35].

#### **2.3.4 Modulus of elasticity:**

The stress-shielding impact of metallic prostheses put in the body (i.e. dental implants) is a serious concern because of the major differences in the Young's or elastic modulus of metallic prosthesis and bone tissue. In the case when a load is applied, the material with maximum elastic modulus—in most cases, metallic prosthesis—adsorbs the load, inhibiting bone growth and promoting bone resorption. The elastic modulus of cortical bone is 20 GPa [36].

#### **2.3.5 Thermal properties:**

The dental materials have different levels of their capability for conducting heat. The metals have higher value of the thermal conductivity compared to the porcelain or resins. Which is why, a patient that has amalgam restoration could have temporary sensitivity to the heat changes within the oral cavity[35]. There are numerous significant thermal conductivity applications in the dental materials. For instance, a large amalgam filling or gold crown in proximity to pulp could result in causing patient considerable discomfort in the case where cold or hot foods produce changes of the temperature; this effect has been

mitigated in the case where adequate remains of the tooth tissue or cavity liners are placed between tooth and filling for the insulations [37].

### **2.3.6 Hardness:**

The surface hardness of a dental material can be measured readily by a number of techniques, resulting in a hardness value that can then be used to compare different composites. At one time, it was thought that the hardness would provide a good indicator of the wear resistance of a composite, and this is true up to a point[34]. The alloy's hardness should be sufficient for resisting occlusal forces while not wearing opposing teeth. In general, the alloys with Vickers hardness of no more than 125kg/mm<sup>2</sup> are prone to wear, while alloys with a Vickers hardness of more than 340kg/mm<sup>2</sup> (hardness of enamel<sup>24</sup>) are more likely to wear opposing teeth [38].

### **2.3.7 Ease of fabrication:**

It refers to a material's capability to be molded to fit a specific purpose. As a result, the material should be able to be molded cost-effectively with the use of engineering fabrication procedures [39].

### **2.3.8 Bonding to Ceramic:**

The alloy used in metal–ceramic restorations should be able to form a thin, adherent layer of oxide on its surface to enable proper bonding with ceramic [5].

### **2.3.9 Laboratory Costs:**

Cost is an additional factor that impacts the alloy selection. In contrast to the many bio-medical markets, the dental market is rather small and is highly sensitive

to economic forces. Precious alloy costs, in combination with other competing systems, like the all-ceramic restorations and milled alloys, suggest a gradual decline in utilization of the precious dental alloys [40].

## 2.4 Classification of Dental Alloys

Dental alloys can be classified according to the following five categories:

(1) **use** (all-metal inlays, bridges and crowns, cores and posts, metal-ceramic prostheses, implants, and removable partial dentures);

(2) **major elements** (palladium-based, gold-based, nickel-based, silver-based, titanium-based, and cobalt-based).

(3) **nobility** (noble, high noble, and predominantly base metal (PB)).

(4) **three principal elements** (Pd-Ag-Sn, Au-Pd-Ag, Co-Cr-Mo, Ni-Cr-Be, Fe-Ni-Cr, and Ti-Al-V).

(5) **dominant phase system** (eutectic, single phase, peritectic, and intermetallic types).

To specify the type of a particular alloy for dental applications, we can use a simple classification system such as the revised classification that was proposed by the American Dental Association in 2003 (high noble HN, noble N and predominantly base metal PB), or we can be much more specific by listing the concentration of the most abundant and/or the most important elements contained in the alloy [3, 4]. The classification of dental alloys is listed in Table (2.1).

Table(2.1) Classifications of casting alloys for metal ceramic prosthesis and partial dentures[41].

Metal Type	All-metal prostheses	Metal ceramic prostheses	Partial denture frameworks
High Noble (HN)	Au-Ag-Pd	Pure Au (99.7%)	Au-Ag-Cu-Pd
	Au-Pd-Cu-Ag	Au-Pt-Pd	
	HN metal ceramic alloys	Au-Pd-Ag (5-12 wt. % Ag) Au-Pd-Ag (>12 wt. % Ag) Au-Pd	
Noble (N)	Ag-Pd-Au-Cu	Pd-Au	
	Ag-Pd	Pd-Au-Ag	
	Noble metal ceramic alloys	Pd-Ag Pd-Cu-Ga Pd-Ga-Ag	
Predominantly Base metal (PB)	CP Ti	CP Ti	CP Ti
	Ti-Al-V	Ti-Al-V	Ti-Al-V
	Ni-Cr-Mo-Be	Ni-Cr-Mo-Be	Ni-Cr-Mo-Be
	Ni-Cr-Mo	Ni-Cr-Mo	Ni-Cr-Mo
	Co-Cr-Mo	Co-Cr-Mo	Co-Cr-Mo
	Co-Cr-W	Co-Cr-W	Co-Cr-W
	Cu-Al		

## 2.5 Amalgam

An amalgam can be defined as a mixture of any metallic element and the liquid element mercury in general. Dental amalgam can be defined as one of the silver alloys with mercury that is mixed together. A chemical reaction occurs in the case when the silver alloy—a powder made largely of copper, silver, and tin—is combined with mercury [42]. Dental amalgams are made by mixing (45–55)% Hg with a powder mixture of Sn, Ag, and Cu (in certain cases, small amounts of Pd, Zn, In, or Se are added) and mechanically vibrating the mixture, resulting in a putty-like material which is easy to manipulate and fill [43]. Dental amalgam restorations are generally simple to place, aren't too

method sensitive, have appropriate fracture resistance, preserve anatomical shape, can be employed in stress-bearing areas, avoid marginal leakage after a period in the oral cavity, and have long service life. The main drawbacks of dental amalgam is that its silver color is not matching to the teeth structure. Furthermore, amalgam restorations have susceptibility to the galvanic action and corrosion, brittle, might show a degree of break-down at the tooth-amalgam margins, and don't aid in the retention of weakened tooth structure. Lastly, there are issues regarding amalgam being disposed of in waste-water because to regulatory problems. In spite of such flaws, dental amalgam has long history as one of the cost-effective and reliable restorative materials [37].

## **2.6 High Noble Metals Alloys: -**

High noble metal alloys should be containing equal to or more than 40% gold by weight and equal to or more than 60% noble metal elements. Gold has a long history of biocompatibility in the oral cavity, and it has the lowest reactivity of any metal. Pure gold, on the other hand, is too ductile and soft to be used as a crown restorative. To increase its qualities, it is alloyed with other metals [44]. Copper is added to gold to make it stronger, and silver to make it more workable. Corrosion resistance is excellent in this alloy, which contains 75wt.% 18-carat gold. The mechanical qualities are improved by the addition of platinum and palladium. Zinc is used to enhance the alloy's casting. For promoting the growth of nucleation centers, small quantities of ruthenium or iridium (0.0005 - 1%) are introduced. They also produce a fine-grained structure in the alloy [41]. Au-Pd-Cu-Ag alloys and Au-Ag-Pd alloys are two examples of the high noble metal alloys

utilized for all-metal prosthetic restoration processes [44]. Figure (2.1) shows Metallic gold crown.



**Figure (2.1): Metallic gold crown[41].**

## **2.7 Noble Metals Alloys: -**

Noble metal alloys should contain equal to or more than 25% by weight noble metals. The emergence of less expensive palladium-based alloys in seventh decade of the 19<sup>th</sup> century stemmed from a rise in gold prices [44]. Platinum group metals like palladium, platinum, ruthenium, iridium, or rhodium shall make up the remaining noble metal components. The solution hardening effects regarding alloying metals that all form solid solutions with the gold, is mainly responsible for increasing the hardness that is identified when nobility decreases [45]. Those alloys are white and they mostly include silver; nevertheless, they should be containing at least 25% Pd to offer corrosion resistance and nobility. Copper and a small amount of gold might also be present. Ag-Pd-Au-Cu and Ag-Pd are two alloys that are commonly utilized for all metal crown restoration. Yet, such alloys were linked to a number of disadvantages. In the molten state, both silver and palladium have a tendency to dissolve oxygen, leading to porous castings. Second, low gold concentration reduces density

regarding these alloys, lowering the kinetic energy of liquid metal throughout casting and, thus, reducing their castability [44].

## **2.8 Base Metals Alloys: -**

Silver, gold, palladium, and platinum are not included in the composition of base metals. They are classified as Co–Cr alloys, Ti and its alloys, and Ni–Cr alloys in general [43]. Other base metals utilized in dental alloys include cobalt, nickel, iron, titanium, and indium. These elements might be present in trace levels for eliciting certain qualities, or they might be the alloy's main element. For instance, trace amounts of iron can be added to improve the bonding regarding ceramic to gold-based alloys, or indium can be added to induce small grain size. Due to the low cost of cobalt and nickel, alloys with such metals as the most frequent component are becoming more popular. Ti alloys are frequently utilized as endosseous implants [42].

### **2.8.1 Titanium Alloy**

Since the 1970s, Ti and its alloys were employed in dental applications. Ti-based crown restoration is increasingly seen as a viable substitute to more conventional noble and base metal alloys; nonetheless, success requires precise processing techniques and laboratory expertise. Ti can be defined as one of the highly-reactive metals that easily reacts with oxygen to generate a thin passivating oxide film (about 10 nm thick) on the surface, which is responsible for its high corrosion resistance [44]. Ti and Ti alloys were utilized increasingly in the medical implants due to their exceptional bio-compatibility, corrosion resistance and rather low density. Like the stainless steel, Ti alloys form passive films on their surfaces - in which case a  $\text{TiO}_2$  film which is their corrosion

resistance source [20]. The focus on the Ti-based castings for the fixed and removable prosthodontics have come about at about the same time as Ti dental implant development. Clinically, two Ti forms gained the most interest. One of them represents the commercially pure Ti form (cpTi) and the other one is an alloy of titanium–6% aluminum–4% vanadium[34].

### **2.8.2 Cobalt Chromium Alloy**

Due to its corrosion resistance and tarnish, Cr is an important component regarding such alloys; nevertheless, adding 30% or more of Cr makes the alloy harder to cast and might lead to a brittle sigma phase, therefore dental casting alloys must be containing 29% or less of Cr. The strength and elastic modulus of Co are higher compared to those of Ni. Molybdenum is used to improve corrosion resistance and reduce the value of the thermal expansion coefficient. Tungsten improves corrosion resistance and decreases the amount of Cr-depleted intermetallic areas. Ni improves ductility, whereas decreasing the alloy's hardness. Additional alloying elements in Co-based alloys include manganese, silicon, iron, and carbon. A lot of such alloying elements create carbides when they react with carbon, altering the characteristics of Co-Cr alloys. In addition, the Co-Cr alloys, like the Ni-Cr base alloys, have a nonhomogeneous microstructure due to the large number of alloying elements. A solid-solution austenitic matrix containing intermetallic compounds makes up the microstructure. The strength, hardness, and modulus characteristics of such alloy system are comparable to the ones of the Ni-Cr alloys. Nonetheless, Co-Cr castings are less ductile when compared to Ni-Cr based alloys [46].

### **2.8.3 Nickel Chromium Alloy**

The use of Ni-containing alloys for the bio-medical applications was perennially controversial. In the field of the dentistry, the increase in the utilization was driven by superior physical characteristics of the Nickel alloys and their economy relative to palladium-based or gold alternative options [47]. The bulk composition of Ni-Cr alloys is split into groups depending on the amounts of molybdenum, Cr, and beryllium (Be). Several researchers divided alloys into 2 or 3 compositional groups, with a few differences in exact criteria. Be is used to improve the castability through decreasing the alloy's melting range and as a grain refiner. Additions of Ti, molybdenum, and manganese all improve corrosion resistance. Also, Molybdenum has been utilized in order to reduce the thermal expansion coefficient. The inclusion of aluminum causes an increase in hardness and strength. Carbon is used in partial denture frameworks to improve hardness and yield strength, although it affects ductility. The various alloying elements present a wide spectrum of the micro-structures with solid solution matrices and inter-metallic compounds in Ni-Cr alloys. Due to the preferential ion release from some areas on surface that can result in internal galvanic coupling, heterogeneous surfaces and oxide layers play a role in a wide variety of the corrosion resistance[46]. Ni–Cr casting alloys generally comprise 70–80% Ni and 10–25% Cr, with minor amounts of additional metals like tungsten, molybdenum, and Be. Those alloys have a high melting temperature and a high modulus, which are both advantages. The following are their drawbacks: (1) A high degree of casting shrinkage, which, if not adequately balanced by the investment, might impact fit accuracy. (2) A proclivity for voids in the castings due to poor castability. (3) A bond strength with porcelain that is incomparable to that of the other alloys [45].

The Nickel-based alloys are ductile FCC materials with excellent corrosion resistance, stress resistance, and high temperature resistance. They also have a high creep resistance. They are corrosion resistant in fresh water, deaerated non-oxidizing acids, atmospheric conditions, and dilute caustics. Ni has a higher solubility for Mo and Cr due to properties like electronic configuration and atomic radius, which allow an Ni solvent to accommodate large amounts of solutes without forming a 2<sup>nd</sup> phase. As a result, alloys can be developed for specific service environments through modifying minor and major additions, and a few were improved for use in both oxidizing and reducing acids. At room temperature, Ni-Cr-Mo alloys are frequently developed up to solubility limits, and following quick quenching, there is a meta-stable solid solution below solutionizing temperature (1150°–1050°C) [48]. In addition, a melting temperature of Ni-Cr-Mo dental alloy is between 1360 and 1410 degrees Celsius. Minor additions regarding the other elements are used in Ni-Cr based dental alloys to enhance characteristics. The higher the Ni-Cr dental alloy's melting temperature, the less dental laboratory technicians like it. A higher melting point necessitates a more powerful furnace, as well as more time and energy for casting and melting. When casting and melting at higher temperature degrees, the number of absorbed gases in a molten alloy rises, increasing the impurities and inclusion index in the alloy and creating brittleness. It's also nearly impossible to recycle the alloy. When the alloy is molten, it has a strong capability for absorbing gases from the atmosphere such as oxygen, hydrogen, carbon, and nitrogen, making it brittle [49]. The Ni-Cr phase diagram is depicted in Figure (2.2).

The binary phase diagram for the system Ni-Cr demonstrates that Cr has a high solid solubility in Ni. Thus, precipitation hardenability is not possible for binary alloys. At room temperature, around 37 wt% Cr might remain dissolved in

the matrix known as gamma. To make Ni-Cr alloys stronger, alloying elements are required. Other additions are employed to produce greater solid solution hardening or precipitate formation, whereas Cr offers some solid solution hardening and corrosion resistance. Differences in mechanical behavior, castability, and oxide development are caused by the presence of alloying additives [50].

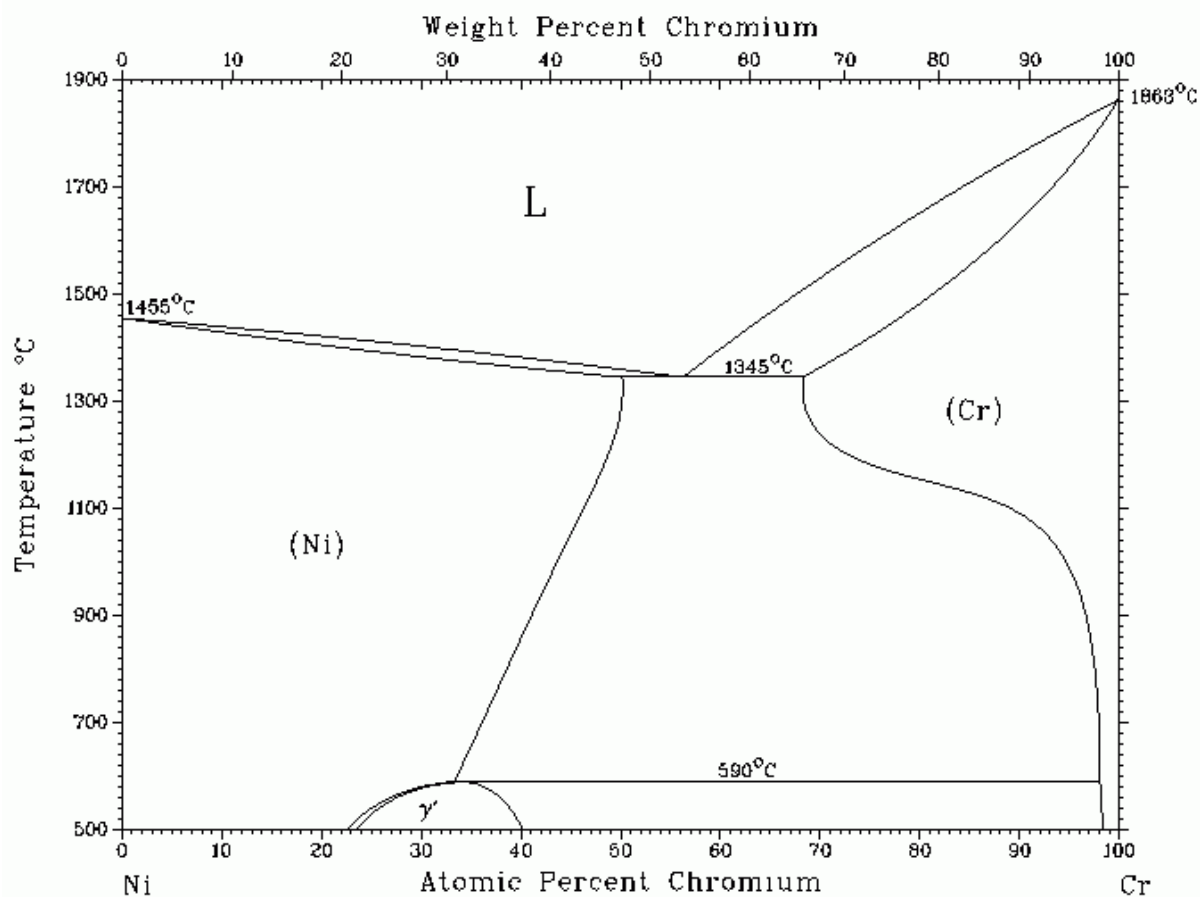
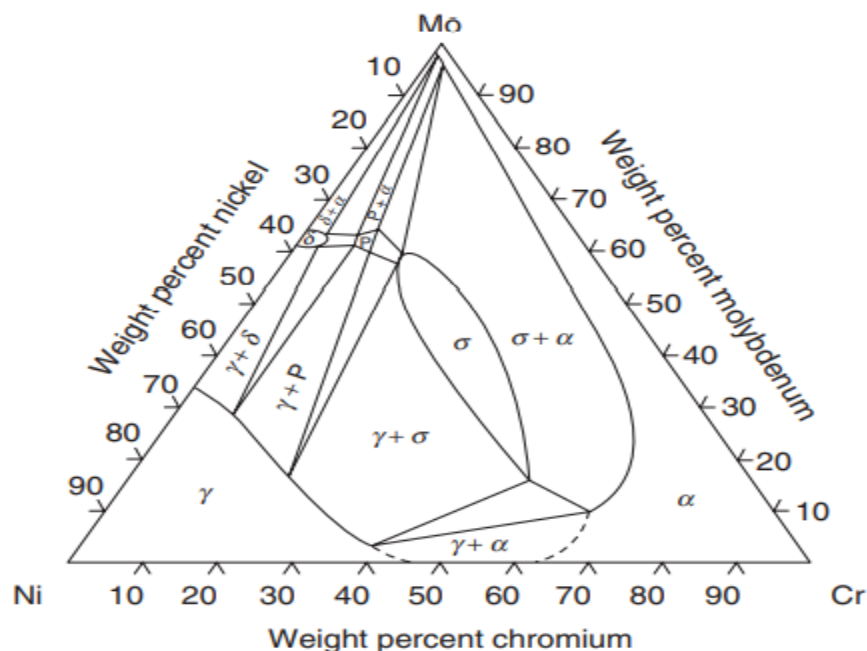


Figure (2.2): Phase diagram of Ni-Cr [51].

## 2.9 The Ni - Cr – Mo System

The Ni-Cr-Mo system provides the base for the solid-solution strengthened alloys, as well as a matrix for several precipitation-hardened alloys. Figure

(2.2) shows the liquidus projection for Ni - Cr - Mo system. In the figure, the boxed composition space indicates Cr (10–30 wt%) and Mo (0–15 wt%) levels observed in commercial alloys. Those diagrams show the system's phase stability in different ways. The existence of Mo, first, stabilizes a wide spectrum of intermetallic compounds. A lot of such phases, like P and  $\sigma$ , can be found in commercial alloy welds. Second, austenite is frequently the first phase of solidification in such alloys. Throughout solidification, Mo aggressively segregates to the liquid, resulting in a high Mo enrichment in the liquid. According to the liquidus projection, which will result in promoting the production of the intermetallic compounds in the inter-dendritic regions as solidification progresses. The susceptibility of fusion zone solidification cracking is influenced by the creation of such terminal solidification phases. Finally, as a result of the diminishing solubility of Cr and Mo in Ni as the degree of the temperature decreases, such intermetallic phases could develop in the solid state via precipitation processes [52].



**Figure(2.3 ) Ni - Cr - Mo ternary iso-thermal diagram that has been calculated at 1250°C [51] .**

### 2.9.1 Role of Nickel

For the alloying elements in the solid solution without creating the inter-metallic particles, Nickel has an FCC structure with high solubility. For a variety of alloys, the Ni matrix has high malleability, ductility, and formability. Nickel has been considered more noble compared to Fe and less noble compared to Cu in terms of corrosion [53].

### 2.9.2 Role of Cr

The role of chromium in the alloys of Ni-Cr-Mo is similar to it in the stainless steels, in other words, it promotes the formation of passive film under the oxidizing conditions like the aerated acids[54]. A Cr content of 20% or more is required to form a compact layer of  $\text{Cr}_2\text{O}_3$  oxide on the alloy's surface. If the Cr level is less than that essential threshold, the oxide forms in loose stacks that aren't corrosion resistant [49]. While more Cr concentration results in wider passive range and reduced corrosion rates, too much Cr results in brittleness and a loss of mechanical characteristics [55].

### 2.9.3 Role of Mo

reduce the rate of corrosion of the alloys under active corrosion conditions. Molybdenum and tungsten also result in increasing those alloys' mechanical strength [54]. Yet, Mo is reasonably expensive, and a larger Mo percentage in an alloy improves its hardness, making machining more complex [55].

## 2.10 Properties of Ni Cr alloy

They are the cheapest of the casting alloys. They are white in color. A typical melting range is 1155–1304 °C. The melting range of these alloys like the gold ceramic alloys are high. Density ranges from 7.8 to 8.4 g/cm<sup>3</sup>. They have just

half the density of the gold alloys making them much lighter. One can get more castings per gram compared to the gold alloys. Hardness and workability ranges from 175 to 360 HV. They tend to be much harder than the high noble metal ceramic alloys. Unlike the gold alloys these alloys are extremely difficult to work with in the laboratory. Their high hardness makes them very difficult to cut (sprue cutting), grind and polish. In the mouth, more chair time may be needed to adjust the occlusion. Cutting and removing a defective crown or FDP can be quite demanding. The high hardness results in rapid wear of carbide and diamond burs. Yield strength ranges from 310 to 828 MPa. These alloys are stronger than the gold and palladium based alloys. This property denotes the stiffness of the alloy. Base metal alloys are twice as stiff as the gold ceramic alloys. Practically, this means that we can make thinner, lighter castings or use it in long span FDPs where other metals are likely to fail because of flexing. Porcelain bonding these alloys form an adequate oxide layer which is essential for successful porcelain bonding. However, occasionally the porcelain may delaminate from the underlying metal. This has been blamed on a poorly adherent oxide layer which occurs under certain circumstances which have not been fully understood. Biological considerations Nickel may produce allergic reactions in some individuals. It is also a potential carcinogen[4].

## **2.11 Corrosion of Alloys Utilized in Dentistry**

Corrosion represents the undesirable chemical reaction of a metal with its surroundings, leading to the ongoing degradation of the metal into hydroxides, oxides, and other compounds. In addition to that, the corrosion shows oral environment as an electrochemical or chemical process through which the metal is attacked by the natural agents, like the water and air, which leads to complete or partial dissolution, weakening or deterioration of any of the solid substances [56,

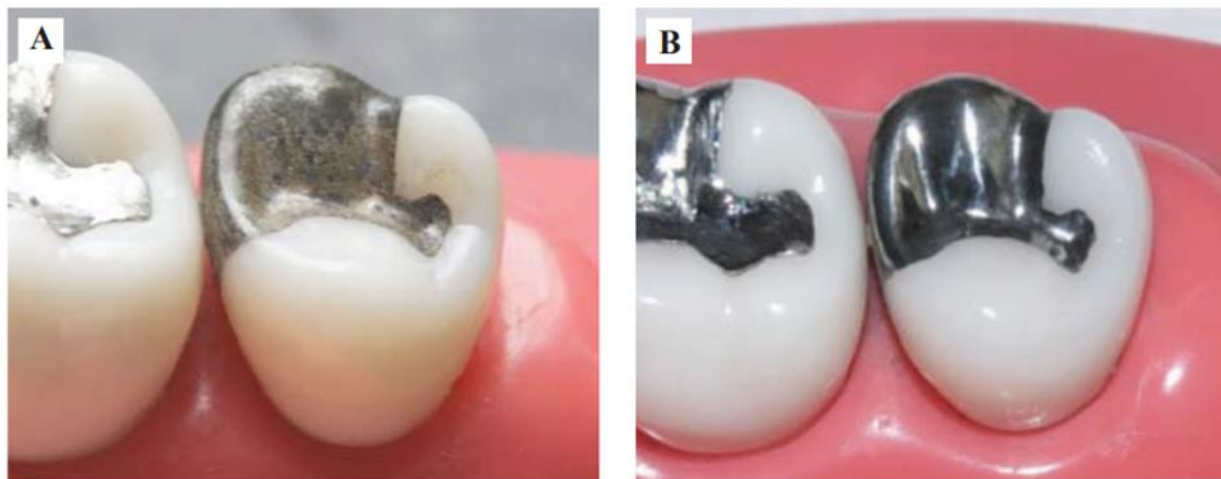
57]. Dissolved oxygen, water, proteins, and different ions like hydroxide and chloride make up tissue fluid in the human body. Therefore, metals utilized for implantation face an aggressive environment in the human body [57]. Other elements, yet, might also induce corrosion, especially in the oral environment. Oxygen, water, sulfides, and chloride ions such as ammonium sulfide or hydrogen sulfide all contribute to oral cavity corrosion. Acetic, phosphoric, and lactic acids are among the acids found. The ions oxygen and chloride were involved in amalgam corrosion both within the amalgam body and at the tooth interface. The corrosion of silver-containing casting alloys was linked to sulfide [4]. The oral cavity provides an extremely favorable environment for the formation of corrosion products, one of the main requisites of any of the metals is that in the case where utilized in the mouth it mustn't result in the production of harmful products of the corrosion. The mouth is a warm, moist, acidic, and salty environment, and it is continually subjected to the temperature fluctuations. The liquid and food that one consumes have a wide variety of the values of the pH. All of those environmental factors play a role in degrading the metals that are utilized in the oral cavity. The corrosion within this environment has been defined as a continuous procedure, due to the fact that the ions, in interfacial layer metal-oral fluids, are continuously removed with the abrasion of liquids, food, and tooth-brushes.[5, 58]. Table (2.2) shows different types of corrosion commonly occurring in the oral cavity.

Table (2.2): Different types of corrosion commonly occurring in the oral cavity[59].

Types of corrosion	Description
Uniform corrosion	A uniform, regular removal of metal from the surface is the usually expected mode of corrosion.
Pitting corrosion	A form of localized, symmetric corrosion in which pits form on the metal surface. It usually occurs on base metals, which are protected by a naturally forming, thin film of an oxide.
Crevice corrosion	Crevice corrosion occurs between two close surfaces or in constricted places where oxygen exchange is not available.
Galvanic corrosion	Galvanic corrosion occurs when dissimilar alloys are placed in direct contact within the oral cavity or within the tissues.
Stress corrosion	Stress corrosion occurs because of fatigue of metal when it is associated with a corrosive environment.
Fretting and erosion-corrosion	The combination of a corrosive fluid and high flow velocity results in erosion-corrosion. Fretting corrosion is responsible for most of the metal release into tissues.
Intergranular corrosion	Reactive impurities may segregate, or passivate elements such as chromium may be depleted at the grain boundaries.
Microbial corrosion	Microorganisms affect the corrosion of metal and alloys immersed in an aqueous environment. The formation of organic acids during glucolysis pathways from sugars by bacteria may reduce pH levels. A low pH level creates a favorable environment for aerobic bacteria for corrosion.

Generally, all dental materials are exposed to the aggressiveness of the oral environment, and they will chemically degrade with time, whether shorter or longer. The term "degradation of biomaterials in a biological environment" refers to the interaction between metallic biomaterials, ceramic and polymeric biomaterial corrosion, and host tissue reaction [60]. Corrosion of the metal is either a chemical or an electrochemical process, in each of which the first step is the loss of an electron. **Chemical corrosion** is the direct metallic and nonmetallic element combination for the purpose of yielding a chemical compound via the reactions of the oxidation. One of the good examples is silver discoloration by the sulfur, where the silver sulfide is formed with the chemical corrosion. It may as well be a product of corrosion of the dental Au alloys containing Ag. This corrosion mode has also been known as the dry corrosion, due to the fact that it takes place in absence of the water or a different fluid electrolyte. Another example is the oxidation of silver-copper alloy particles that are mixed with the mercury to prepare certain dental amalgam products. These alloy particles contain a silver-copper eutectic phase; oxidation results in limiting their reactivity with the mercury, thereby affecting the setting reaction of the dental amalgam product. This

is why it is prudent to store the alloy in a dry, cool, location for ensuring an adequate shelf life[3]. Figure (2.4) shows the tarnish.



**Figure (2.4) Tarnish. (A) Tarnish on the surface of a silver amalgam restoration seen at 5 years. (B) The same restoration when polished regains its luster, without loss of material[5].**

*Electrochemical corrosion*, also known as galvanic corrosion happens in the case where 2 or more different practical nobility metals are connected electrically and immersed in one environment: the metal with the lower nobility experiences a corrosion rate increase that results from presence of a higher nobility one [61]. In applications of the dentistry, the galvanic corrosions occur in the case where two or more dental prosthetic devices with the dissimilar alloys come into contact whereas subjected to the oral liquids such as the saliva; the difference between the potentials of the corrosion results in an electric current flow between them. Which is why, galvanic cell is created and results in causing the increase in the rate of the corrosion of the anode and improving the amount of the released metal ions [62]. The applications of the dental alloys are deployed in restoring and correcting deteriorated, misaligned or lost, dental pieces. They're utilized for the bridges, crowns, implants, incrustations, or as wires in the orthodontic appliances. For the purpose of fulfilling those functions, various materials have to be selected, meeting

the requirements of the bio-compatibility, have sufficient physical characteristics, resistances to the wear and corrosion deterioration, and stable and acceptable appearance. The various restoration types usually necessitate using a variety of the materials whose dissimilarity in the mouth results in increasing galvanic interactions [21]. Figure (2.5) shows galvanic corrosion in dental alloy .

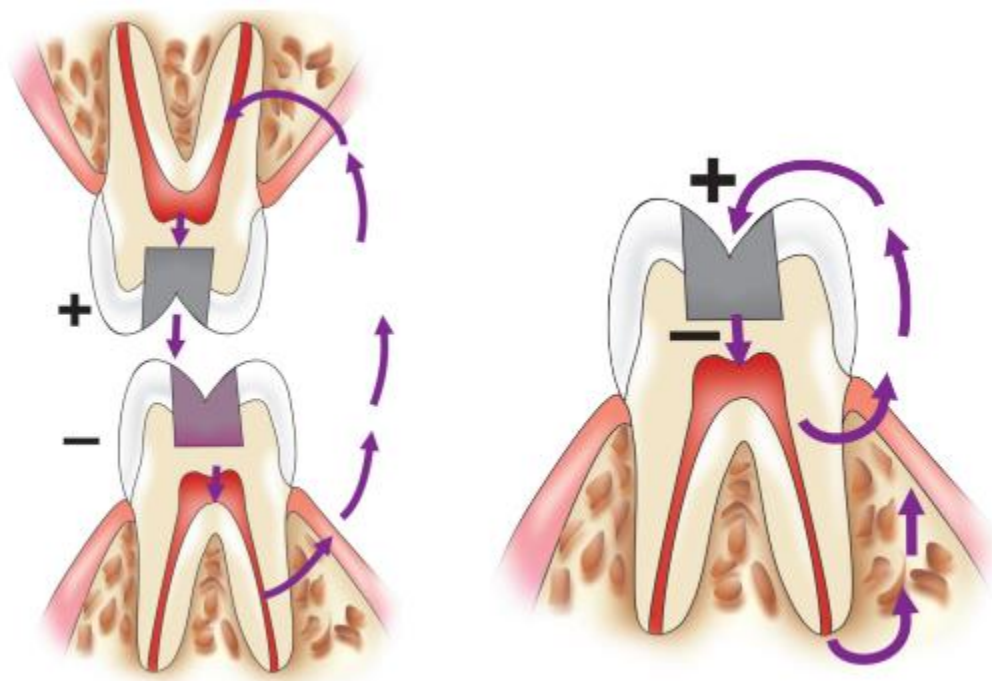


**Figure (2.5):** (a) Possible galvanic current path-way in the case of the contact between dissimilar metals. The saliva and tissue fluid behave as electrolyte. (b) current path-way could exist even in one metallic restoration. In such case, the fluid of the tissue behaves as cathode (due to a higher  $\text{Cl}^-$  ions' concentration in the tissue fluid in comparison with the saliva) while the saliva behaves like anode. This current typically has a lower intensity [21].

It is possible to prevent the galvanic corrosions in mouth with the use of the same alloy type for all of the metal prosthetic reconstruction types in the oral cavity, particularly for the ones coming in a direct contact. Simultaneously, using homogeneous alloys that can't produce possibly different phases, results in the

reduction of risks of the intrinsic galvanic corrosions of ally or perfect polishing of the metal works (amalgam or dentures obturation) reducing risks of the crevicular corrosions [60]. **2.11.1 Corrosion of Ni Cr Alloy and NiCrMo Alloy**

Chromium and nickel impart corrosion resistance and mechanical strength to nonprecious alloys. The presence of the chromium results in the improvement of alloys' corrosion resistance in corrosive environments as a result of formation of chromium-rich, passive oxide film that has high resistance to the acids. Mo in Nickel-chromium based alloy results in increasing resistance to the localized corrosions in environments that contain the chloride. Which is why, for the base-alloy dental materials, adding 12% Cr (minimal value) and 2–5% Molybdenum to alloy bulk has been recommended from the viewpoint of the corrosion resistance [63]. Molybdenum oxide ( $\text{MO}_3$ ) and Chromium oxide ( $\text{Cr}_2\text{O}_3$ ) provide initial stability for the prevention of metal ion dissolution and so result in the induction of the resistance to the corrosion and a reduced corrosion rate. The integrity and composition of surface oxide film on the Nickel-Chromium dental casting alloy are vital for their clinical performances [12]. At ordinary temperatures up to  $20^\circ\text{C}$  molybdenum dissolves in nickel in the solid state and this increases both corrosion resistance and strength[64].

The corrosion of the dental materials could lead to biologic effects. Although allergic characteristics of Ni-Cr-based alloy metal ions have to be carefully taken under consideration, those alloys are still quite popular for the applications in the dentistry field. Metal ion release from the alloys results from the process of the corrosion. It was stated that the products of the corrosion from Nickel-Chromium based alloys have no impact on the cellular viability or morphology, however, that they actually do result in decreasing the proliferation of the cells. Metal ions that are released from the Nickel-Chromium based alloys of dental casting are

interfering with the metabolism of the cellular energy. Which is why, with the biocompatibility of serious concern, a Nickel-Chromium-based dental alloy that has high resistance to corruptions would be quite desirable. Ni-Cr-Mo dental alloy in the mouth represents a great concern and may be varying with a variety of the chemical compositions [66]. Nickel chromium alloys showed unstable galvanic corrosion behaviors. They, in fact, corrode in the physiological solutions, like the artificial saliva, balanced salt, artificial sweat and human saliva solutions. In particular, some Ni-based alloys were shown to have susceptibility to pitting and/or crevice corrosion phenomenon [67].

## **2.12 Wear in Dental Alloys**

Tribology can be defined as a science of mechanisms of lubrication, friction, and wear of the interacting surfaces, which are in relative motions. In other words, the friction represents rubbing of a surface or object against another one, whereas the wear can be defined as the process occurring in the case where a surface has been under the exposure of a different surface or chemically active substances. For instance, throughout food chewing, teeth, together with any restorations, must move in contact with each other, and after that, wear and friction happen in general with lubrication of food slurry or saliva [68]. The teeth get in contact with one another throughout chewing and eating, besides other processes, like swallowing, yawning and speaking [69]. Wear of the restorative materials or teeth results from a variety of the complex processes, which are mainly dependent upon food's abrasive nature, the antagonistic material characteristics, the hardness and thickness of the enamel, chewing behavior along with the para functional habits, and neuro-muscular forces. A variety of the wear phenomena could happen in oral cavity. Wear as tribological system function includes three main elements : (i) structure—types of the materials that are in contact and the geometry of the

contact; (ii) conditions of interaction — such as stresses, loads and durations of the interaction; (iii) surface and environment conditions—which include chemistry and environment of the surface, ambient temperature and surface topography [60].

Figure (2.6) Schematic representation of the inter-oral teeth movements.

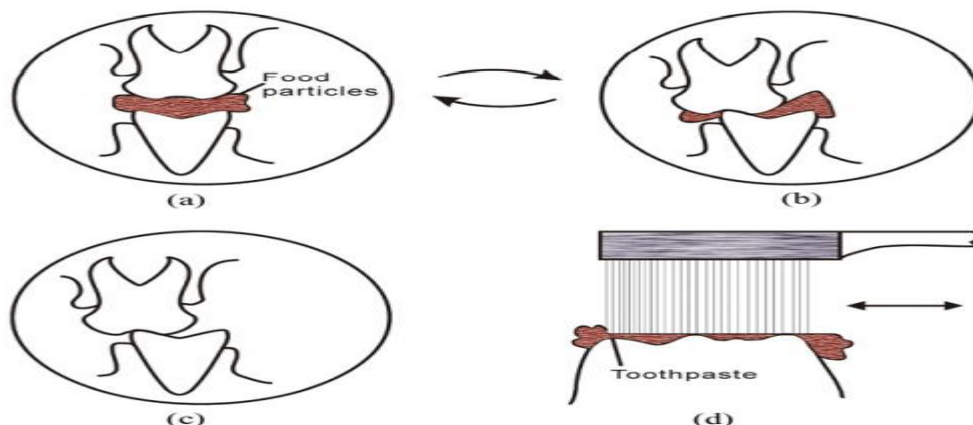


**Figure (2.6).** Schematic representation of the inter-oral teeth movements. (a) Open phase mastication, (b) closed phase mastication, (c) thegosis/bruxism (d) tooth-brushing [68].

### 2.12.1 Wear Types

The wear of material relates to surface lubrication and friction, roughness, hardness, and wear types [70]. In tribology area, five wear mechanisms instead of wear modes were often identified, which include: adhesion, abrasion, fatigue, corrosion and erosion. In the majority of the cases, two or more mechanisms of the wear are combined together and play a role in the processes of the material degradation [71].

- **Abrasion:** The wear that results from the tooth-to-restoration or tooth-to-tooth, or restoration-to-restoration frictions has been referred to as the ‘attrition’, usually considered a result of two-body interactions. The friction

between a tooth or restoration and exogenous agent (like the toothpaste, food bolus, dental floss and tooth-pick) results in causing a wear form that is referred to as the ‘abrasion’, typically considered to result from three-body interactions. In the case where the teeth have been worn by the friction from food bolus, such wear becomes referred to as the ‘masticatory abrasion’[69]. The harder materials have the tendency of having higher resistance to the abrasions compared to the than softer materials. In the dentistry area, the main concern is the abrasion (i.e. wear) resistance of the dental restorations to the opposing teeth as well as the foods. The concern is also focused upon the natural teeth opposing the dental restoration. In the case where the restorative material is too hard, then it’ll wear opposing teeth at unacceptably increased rate. Which is why, restoration has to be hard enough so that restoration doesn’t wear away, however, not so hard as to wear away opposing teeth excessively [70].

- **Adhesive wear:** adhesive wear mechanism takes place in the case where two bodies have been subjected to high contact pressure throughout relative sliding. Fundamentally, it’s related to some materials like the polymers and metals. From tribological viewpoint, superficial asperities come in contact undergoing plastic deformations and locally adhering (i.e. micro junctions) [72].
- **Fatigue wear:** this type happens in the case where the surface that is subjected to the high pressures acts over another in cyclic manner. The generated deformations allow propagation of surface molecules at sub-superficial level of the fragile materials, resulting in fractures in inter-molecular bonds. Based on the material type, the microcracks must thus, be produced around damaged surface and propagate with the increase of cycles [72].

- **Corrosive wear:** has been considered as the loss of the substance under the electro-chemical or chemical action, which is usually combined with the relative motions. The fine debris that has been detached from surface and fresh contact surface exposed to the oxidization are considered as usual wear forms [71]. The main corrosive wear reason has been associated with the fact that the molecules of the surface undergo an attack by the acids, and those molecules are removed after that, and new exposed surface is attacked once more by the acids. Thereby, this wear mechanism results from cumulative impacts of the removals of the molecular layer [73].
- **Erosion wear:** which represents the surface loss of either restorations or teeth, which results from the electrochemical or chemical actions is typically referred to as the ‘erosion’ in dental literatures. It should be noted that term ‘erosion’ has considerably different meaning between the dentistry and engineering tribology. Usually, in the dentistry, the erosion is utilized for describing the dental materials’ surface loss, which results due to solution by the acids that aren’t of the bacterial origins [68].

### 2.13 Powder Metallurgy

Powder Metallurgy, PM, is a manufacturing process in which components are directly produced by bringing a powder of the starting material into the desired final shape by compressing the powder in dies. Strength and other properties are imparted to the components by subsequent sintering operations. It is one of the cheapest mass production process for manufacturing high quality, high strength, complex parts with a high degree of accuracy. Porous parts as well as parts with high density structures may be produced. The process is commercially and economically adaptable only to mass production, due to expensive dies and

machines[74]. Powder metallurgy (PM) involves the mixing of the metallic powders as well as compacting the mix in a die. The parts that have been compacted become in the shape of the die and are sintered or heated after that in furnace of controlled atmosphere to the metallurgically bond particles [75].

P/M process highly more competitive in comparison with other approaches of fabrication, such as casting, machining or stamping. PM is the best option in the case where the requirements for the wear resistance, strength, or high operating temperature exceed the die casting alloy capabilities. PM presents a higher level of the precision, eliminating the majority or all finish machining processes that are needed for the castings. It avoids the defects of the casting, like the Shrinkage, blow holes, inclusions, porosity, micro-cracks, particles from investment, and dendritic structure. Those defects represent an important failure factor of the partial denture model [76, 77].

The PM technology was implemented in a variety of the industrial fields for several years. PM was utilized as well in the medical applications as a substitute approach for the production of the materials for the implants in dentistry as well as surgery. Presently, a considerable amount of the researches in this area had been focused upon the metallic materials that are manufactured by the PM techniques. Those materials have been considered highly promising because: a) They include almost waste-free net-shape forming; b) they present accurate choice of the chemical compositions through using hard-to machine or high-melting alloys for the improvement of the bio-compatibility of the implant; c) there's a lack of the chemical inhomogeneity that is typical for the cast as well as some plastic formed material types, thereby, enhancing the resistance to the corrosions; d) they present the porosity of suitable pore geometries. Which results in the improvement of the in-growth of the bone tissue, thereby, improving the stability of the endo-

prosthesis; and e) they present the potential for the formation of a variety of the composite material types that contain additions improving the bio-functionality [78].

During processing, the performance of metal powders and the characteristics of the products depend on the characteristics of the metal powders used, like the particle size, particle size distribution, particle shape, the flow rate of powders, the compressibility of powders, apparent density, and purity of powders. The basic steps of the powder metallurgy route are powder manufacturing, mixing of the powders, compacting, and sintering[79].

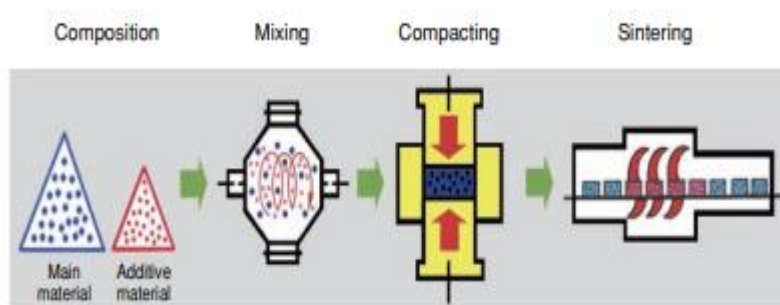


**Figure (2.7): fundamental process of powder metallurgy[80].**

## 2.14 Boron

Boron's chemical symbol is B, it has an atomic number value of 5, and relative atomic mass of 10.811, it is the 1<sup>st</sup> element of the group IIIA (13) of periodic table. B is light and hard (9.30 Mohs hardness), with a 2.08g/cm<sup>3</sup> density, and it exhibits a noticeable metalloidal character as well as physical and chemical characteristics that more resemble the characteristics of the silicon and carbon. In addition to that, like the carbon, B is a semiconductor. It is highly refractory, with increased melting point of 2330°C and a 3650°C boiling point [84]. It has three

electrons only in valence shell, which may be involved in forming covalent bonds. It can't donate, however, it can accept the electrons in some of the cases. Which is why, it is capable of easily making covalent bonds, and in the majority of the compounds, like the sulfides, oxides, halides and nitrides, B has formal oxidation state of III[85].

## 2.15 Indium

Indium, In, has an atomic number of 49 as well as an atomic weight of 114.82, it's a metallic element that is part of group 13 in periodic table and it is usually trivalent in its compounds due to the fact that they have the highest stability. The melting point of indium (156.6 C or 429.8K) and high boiling point (2353.2K)[86]. In can be described as dense, silvery-white metal that has brilliant metallic luster. The density of In is equal to  $7.31 \text{ g/cm}^3$ , crystallizes in tetragonal system ( $a = 325\text{pm}$  &  $c = 495\text{pm}$ ). Mechanically, the In is highly soft, malleable and ductile metal exhibiting Brinell hardness number (HBN) of only 0.90. which is why, it's softer compared to the tin (5.20) and lead (3.90). In, with Young's modulus of only 10.6GPa, In has resistance to the air oxidation at the temperature of the room as thin and impervious passivating oxide film protects metal like Al [84].

## 2.16 Zirconium

Zirconium represents the second metallic element in the IVB group (4) of periodic table, with the atomic number value of 40 and relative atomic mass (atomic weight) of 91.224. Its chemical symbol is Zr. Zr is a hard, grayish-white lustrous metal. It has moderate density of  $6506\text{kg/m}^3$ , and that is lower than that of the pure nickel or iron. In addition to that, it has low thermal expansion coefficient ( $5.78\mu\text{m/m} \cdot \text{K}$ ). As a result of its increased melting point temperature of  $1852^\circ\text{C}$ .

As in the case of Ti, elemental Zr exists as the hcp at room temperature[84, 85]. A slight interest in the Zr for the medical applications, especially in the dental implants, had continued throughout the years, due to its exceptional bio-compatibility[84]. Obviously, Zr has been categorized as refractory metal like the tantalum and titanium. Zr has very high corrosion resistance in the majority of the organic acids and strong mineral, saline solutions, strong alkalis, and some molten salt types [87].

## 2.17 Zirconia

Zirconia, which is referred to as the zirconium oxide,  $ZrO_2$  as well, it is a white crystalline oxide of the zirconium. It represents a common polymorph, occurring in three polymorphic forms. At the temperature of the room it exists as a monoclinic crystal structure. At temperature degrees between  $1170^{\circ}C$  and  $2370^{\circ}C$ ,  $ZrO_2$  exists in the tetragonal phase. A tetragonal– monoclinic transformation happens in the case where the  $ZrO_2$  ceramics are cooled at a temperature of lower than  $1170^{\circ}C$ . At temperatures above  $2670^{\circ}C$ , a cubic phase is formed[69]. Zirconia has high bio-compatibility, as are other ceramic types, and may be made in a form of large implants like acetabular cup and femoral head in total replacement of the hip joint [88]. The zirconia strength is directly related to phase transformation and grain size control. Young' s modulus ( 210 GPa), Hardness (Vickers, HV0.5) (1250), Density ( $6.1g/cm^3$  ) [24].

## 2.17 Literature Review

**Rao, et.al., 2011[90]** studied the corrosive behaviors of three different commercially available casting alloys of Nickel-Chromium, through the use of the potentiodynamic method of polarization, three commercially available casting alloys of Ni-Cr (Remanium CS, Wiron 99, CB Soft) have been taken for the assessment of their corrosion behaviors, utilizing the potentiodynamic polarization approach (i.e. electro-chemical approach) with the fusayama artificial saliva as electrolyte medium for the checking for their level of bio-compatibility. Obtained results have been analyzed through the classic Tafel analysis. Remanium CS has led to lower degree of the corrosive rate. Which may be explained due to its higher chromium percentage. Molybdenum as molybdenum oxide ( $\text{MoO}_3$ ) and Chromium as chromium oxide ( $\text{Cr}_2\text{O}_3$ ) provide initial stability for the prevention of metal ion dissolution and thereby provide the resistance to the corrosion and lower level of the corrosive rate. Wiron99 has been the next best amongst Nickel-Chromium casting alloys, which results due to its low percentage of molybdenum 9.5wt% and chromium 22.5wt% in comparison with the Remanium CS. Molybdenum as ( $\text{MoO}_3$ ) and Chromium as ( $\text{Cr}_2\text{O}_3$ ) are helpful in forming stable surface oxide film. The CB Soft showed maximum rate of corrosion compared with all samples that have been chosen for this study. Less chromium content amount, which was 4.9wt% and absence of the molybdenum in the CB Soft has led to absence of the formation of the surface oxide passive film onto the surface of the metal. It has been concluded that Wiron 99 and Remanium CS had shown satisfactory corrosive behaviors, except the CB Soft that had shown higher rate of corrosion and minimal corrosion resistance. Which is why, alloy selection has to be made according to the corrosion resistance and biological data from the dental manufactures.

**Gatin, et.al.,2011 [91]** investigated the electro-chemical behavior and the corrosion of two commercial dental Nickel-Chromium alloys like: Wirocer plus and Vera soft. The research has been carried out with the use of a Fusayama-Meyer artificial saliva medium. According to curves of electro-chemical impedance spectroscopy (EIS) the type and intensity of corrosion process has been established using corrosion current value. The passivation of all samples had happened in a spontaneous manner at open circuit potential. The values of the corrosion current are decreased after alloys maintenance in corrosive medium as a result of their passivation. The currents of the corrosion are decreased by increasing the time of the immersion. The Wirocer plus metal alloy is in optimal condition of corrosion resistance. The sample of the Vera Soft alloy presented a deep break-down potential (approximately 250mV). With the benefit of the dendritic structure after the process of the casting (creating a more sufficient quality of the surface), Wirocer plus alloy presented a superior bio-compatibility and electro-chemical behavior in comparison with the Vera Soft sample.

**Galo, et.al, 2012 [92]** studied effects of oral environment on dental alloy corrosion with a variety of the compositions, utilizing the electro-chemical approaches. The rates of the corrosion have been obtained from current-potential curves as well as EIS. The artificial saliva effect upon the dental alloy corrosion has been dependent upon the composition of the alloy. The dissolution of ions had happened in every tested dental alloy and results have been highly dependent upon general alloy composition. Considering alloys that contain nickel, Ni-Cr-Ti and Ni-Cr alloys release 0.62mg/L of Nickel as an average, whereas Co-Cr dental alloy had released ions between 0.01mg/L and 0.03mg/L of Cobalt and Chromium, respectively. The open-circuit potential had been stabilized at higher level with a lower level of the deviation (standard deviation: Co-Cr = 54mV/SCE and Ni-Cr-6Ti = 32mV/SCE).

The potencio-dynamic dental alloy curves had shown that Nickel-base dental alloy with >70wt% of the Nickel had similar curve and dental alloy of Co-Cr exhibited a low level of the current density and thus, high resistance to the corrosions in comparison to Nickel-based dental alloys. Some of the changes in the micro-structure have been noticed and it affected the behavior of the corrosion for alloys. In addition to that, lower resistance to corrosions has resulted as well in higher amount of nickel ion release to the medium. The Co ion amounts that have been released from Co-Cr-Mo alloy have been rather small in solutions. Moreover, the amount of the Chromium ions that have been released in artificial saliva from Co-Cr alloy has been lower in comparison with the Chromium release from Nickel-based dental alloys.

**Yavuz,et.al,2012 [93]** investigated the impacts of various surface treatments upon the stability of the elemental composition of as-received and re-cast Ni-Cr casting alloy types, six commercial Ni-Cr dental casting alloys (which are Nodelco, Kera N, Wiron99, Bellabond, Trittech D and Metaplus VK) have been utilized, 72 samples (12mm x 12mm x 1.2mm) have been prepared with the use of lost-wax process of casting. There have been 3 casting protocols established based on proportion of the as-received and re-cast alloys: Group A (100% as-received metal), Group B (50wt% once-recast metal and 50wt% new metal), and Group C (100% once-recast metal), two samples in each one of the groups had received two separate treatments of the surface, which are: oxidation firing or sand-blasting with 110 $\mu$ m Al<sub>2</sub>O<sub>3</sub>. Elemental analysis has been carried out with energy-dispersive x-ray spectroscopy. The results have been subjected to Tukey HSD and one-way analysis of variance tests. The results have shown that elemental composition has been considerably different in treatment groups and casting groups ( $p < 0.050$ ). The minimal average wt. percentage Nickel value has been recorded for the Group

C and the maximal was for the Group A. Al-oxide sand-blasting of alloy surface has resulted in the reduction of average percentage of weight for the Chromium. Re-casting the metal alloys could have adverse effects on the level of the surface quality.

**Sartori, et.al.,2013 [94]** studied the hardness and tensile mechanical characteristics, in addition to the micro-structure and composition of three different alloy types that are utilized for the implant prosthetic component casting. Alloys have been divided to three groups: Tilite (Ni – 60 to 76%, Cr – 12 to 21%Mo – 4 to 14%,Ti – 4 to 6%), Vera (Ni – balancedCr – 14%, Al – 1.70%, Mo – 8.50%, Be – 1.80%) and Malloy (Ni – 65.70%, Mo – 8%, Cr – 20%, Others – 6.30%). For tensile test, the samples (n = 10) of every one of the groups have been assessed in an “alter” form and maximal load fracture, deformation at the maximal load Vickers hardness, and Young’s modulus have been specified. The micro-structure and the composition have been determined via the analysis of two samples from every one of the groups by the metallographic analysis (MEV/EED). The maximal load tensile, the three alloys have been similar. Values have been 756.25, 722.05 and 776.03kgf for Tilite, Malloy and Vera, respectively. Young’s modulus results have shown higher values for Vera, (48.87GPa), compared with Tilite values, (40.15Gpa). Malloy values, (38.18GPa). considering the hardness, the Tilite exhibited statistically significant higher values ( $433.32 \pm 11.77$ ) in comparison with others alloys; which have been  $357.24 \pm 14.93$  for the Vera and  $377.72 \pm 32.99$  for the Malloy).

**Kim,et.al.,2014[95]** studied the bio-compatibility and corrosion behavior through the addition of various Mo amounts into the Nickel-Chromium alloys (such as Ni-13Cr-4Mo, Ni-13Cr-8Mo, Ni-13Cr-10Mo and Ni-13Cr-6Mo,).They used it in their research the incubated 6-th passage human gingival fibroblast cells for cell

viability as well as cell adhesion experimentations. The amount and the form of the human gingival fibroblast cell adhesion to the alloys have been observed with the use of the FE-SEM. For the purpose of evaluating the quantitative analyses of cell corrosion and adhesion behaviors, AC impedance approach has been utilized (at  $37^{\circ} \pm 1^{\circ}$  in 0.90% NaCl solution) and compared results that have been obtained with FE-SEM results. The Ni-13Cr-6Mo alloy micro-structure had a more uniform surface in comparison with other alloy types. Ni-13Cr-6Mo alloy showed minimal cytotoxicity level in cell viability assay, and maximum cell adhesion and corrosion resistance in the AC impedance test. They have established the fact that the Ni-Cr-xMo alloys have more sufficient cell adhesion and cell viability, as well as a higher electro-chemical impedance in comparison with the Nickel-Chromium alloys.

**Sousa, et.al., 2014 [96]** investigated corrosive Ni-Cr-Mo alloy development. The 59.60% Ni, 9.80% and 24% Cr Mo alloy had been utilized in the dental prostheses has been recast in the open fire - oxyGLP torch and cooled naturally. The electro-chemical study had exhibited that the alloy has behavior that is similar to the Cr, showing extensive passivity area as a result of chrome oxide layer formation. The development research of the corrosive process has been performed through the interruption of potentiodynamic curve of polarization in four different potentials as well as their surfaces have been analyzed with the optical microscopy and SEM. The material micrographs, prior to being subjected to electro-chemical testing, exhibited homogeneous surface, showing a few pores, which have been formed potentially throughout the process of the recasting. The process of the wear and tear starts after the potential of the trans-passivity, with the inter-granular corrosion properties with the preferential dissolution of the region that includes the minimal content of Mo, as it has been quantified by the EDS. The surface that has been

obtained appears like a sample that has been attacked electrolytically in the HCl, showing Mo-rich precipitates in grain boundaries.

**Loch,et.al.,2015[97]** studied the corrosion resistance of the Ni-Cr and Co-Cr dental alloys in the simulated artificial saliva through the electro-chemical approaches. The micro-structure of the alloys that were investigated, have been studied with the use of the optical microscopic observation, XRD measurements and SEM with the X-ray micro-analyzer. Mechanical characteristics have been identified with the micro-hardness tests. The characteristics and structure of examined Co-Cr alloys have made the latter a sufficient material to be used in the dental prosthetics. The studied Ni-Cr materials had shown Nickel-rich, Mo and Cr depleted areas in the Ni-Cr alloys undergo highly localized dissolutions, which is why, disqualifies those alloys for dental uses. Through the comparison of corrosion characteristics of the Ni-Cr and Co-Cr alloys it has been noticed that general corrosion resistance characteristic of Co-Cr alloy is superior to that of Ni-Cr alloys.

**Park,et.al.,2016 [98]** investigated corrosion properties of Ni–Cr–xMo alloys for the identification of composition that exhibits maximum resistance to the corrosions in the oral environment. All of the samples have been categorized to four different groups of the composition ratio (Group1: 83Ni–13Cr–4Mo; Group2: 81Ni–13Cr–6Mo; Group3: 79Ni–13Cr–8Mo; Group4: 77Ni–13Cr–10Mo) and embedded with the epoxy resin. The alloys' corrosion behavior has been studied by utilizing the potentiodynamic polarization method in a 0.90% NaCl solution at  $37^{\circ} \pm 1$  °C. After the potentiodynamic polarization experiment, the alloy surface has been examined by using optical and scanning electron microscopies. Notably, the 77Ni–13Cr–10Mo composition exhibited the noblest corrosion potential ( $E_{\text{corr}}$ ), highest corrosion resistance, and lowest pitting potential. Consequently, the AC impedance plots revealed that the Group four samples, i.e., the 77Ni–13Cr–10Mo

alloy, had higher corrosion resistance than the others. In conclusion, Ni–Cr–xMo alloys can be used for dental casting as they provide a valid alternative to commercial dental casting alloys.

**Augustyn-Nadzieja, et.al., 2017[99]** studied the micro-structural, XRD and corrosion resistance characteristics in an artificial saliva solution of commercial alloy of Ni-22Cr-9Mo. Within this research, examinations have been performed on commercial alloys and the alloy that has been re-melted and cast by lost wax (i.e. lost wax) approach. The micro-structure observations have been carried out by using optical and SEM. In addition to that, the structural tests of the X-ray have been carried out besides the corrosion resistance tests in a solution of the artificial saliva (pH = 6,7). It has been shown that examined Ni-22Cr-9Mo alloy characterized in dendritic structure that is typical of cast materials. The qualitative phase analyses of the X-ray showed phase  $\gamma'$  (Ni) in the two materials that have been examined, in addition to presence of the Cr<sub>23</sub>C<sub>6</sub> type carbides and Nb<sub>2</sub>C, Ta<sub>2</sub>C (commercial alloy) and NbC, Ta<sub>4</sub>C<sub>0,04</sub> (i.e. cast alloy) phases. The effects of alloy re-melting and passive layer morphology upon Ni-Cr-Mo alloy corrosion resistance has been observed. The electro-chemical test results have shown that the re-casting process had only a slight effect on micro-structure and corrosion resistance of the alloy that has been considered. The recasting process roles and homogeneity of passive film on Ni-Cr-Mo dental alloy's corrosion resistance have been examined. Results of electro-chemical study have shown that the corrosion resistance dependence upon micro-structure related to the process of re-casting is minimal.

**Liliana, et.al., 2018 [100]** investigated corrosion behaviors of four different commercial Nickel-Chromium alloys of dental casting (S1, S2, S3, S4) in the simulated oral environments, which are associated with micro-structure and

chemical composition, through the electro-chemical approaches, which include the EIS, cyclic voltammetry studies. The characterization of the samples surface has been performed with the use of the SEM prior to and post the immersion in the artificial saliva. Corroborating investigation methods of the results, the Nickel-Chromium alloys represent a proper substitute for the metal frameworks that are utilized in the prostheses dentistry. All of the dental alloys have exhibited a low tendency for the corrosion, however, S1 and S2 alloys have been the most stable against the corrosions in the artificial saliva. The optimal electro-chemical behavior must be a result of composition of alloys (which contain Mo and Cr) and to compact surface micro-structure.

**Ghasemzadeh and Nasirpouri,2019 [101]** studied the effects of the level of the artificial saliva pH on Ni-Cr-Mo alloy corrosion behavior at the temperature of 37°C. The corrosion behaviors of commercially available Ni-Cr-Mo base dental alloy has been investigated through the use of the potentiodynamic polarization and electro-chemical impedance spectroscopy approaches. Effects of the pH upon the corrosion and Nickel ion release has been researched as well by the SEM and atomic absorption spectroscopy. Results have suggested that corrosion rate order has been: pH3 > pH5 > pH9 > pH7. The rate of the corrosions in the pH3 has been considerably different with other levels of the pH. The depletion of Ni had occurred considerably in the alloy with no passivation. The ion release and corrosion resistance of the Ni-Cr-Mo alloys in various levels of the pH of the artificial saliva has been dependent upon the passive layer stability. The acidic pH levels severely corrode the Ni-Cr-Mo base metal alloys and results in increasing the release. Differences of the forward and reverse corrosion potential for pH=7 had been the maximal and for the pH=3 had been minimal. Which is an indication

of the maximum resistive passive layer in the solution in pH=7 and minimal resistive passive layer in pH=3.

**Turdean, et.al., 2019 [102]** investigated the impact of artificial saliva pH value on Ni–Cr and Co–Cr dental alloy corrosion, utilizing a variety of the electro-chemical approaches, like: open circuit potential (OCP) measurement, cyclic voltammetry, EIS and polarization curves. The results that have been obtained were complementary with the SEM coupled with the EDXS analyses, proving that the alloy of Co–Cr has a higher resistance in time, and recommending it for successfully treating the patients who have dental prosthesis with metal frameworks.

**Barros, et.al., 2020 [103]** investigated the galvanic effects of the NiCr on Ti-6Al-4V in the fluoride solutions that have been utilized on the rehabilitations of the dental implants. Alloys have been assessed in the solutions with various fluoride contents and pH in similar conditions that have been founded in the environment of the oral cavity. Electro-chemical measurements have been carried out on two steps. On initial step, the open circuit potential analysis of every one of the alloys in combination with a variety of the pH values and concentrations of fluoride have been performed. In 2<sup>nd</sup> step, the galvanic measurements have been carried out between coupled alloys with the use of precision multi-meters. The data have been assessed through one-way ANOVA test ( $\alpha=0.05$ ). Ti-6Al-4V presented decreasing resistance to the corrosions with the increase in the concentration of the fluoride and decrease in the level of pH, being in domain of thermo-dynamic corrosion for all of the evaluated combinations of the solution except the 227ppm Fat pH 5.50. In spite of that, a significant result has been obtained from galvanic measurements. In the case where it is coupled with the NiCr, Ti-6Al-4V has been capable of achieving passivity and exhibited no negative galvanic impacts with a variety of

the tested combinations of the fluoride. The potential galvanic effects in this work has been an enhancement in Ti-6Al-4V. The resistance to the corruptions in presence of the content of the fluoride when it has been coupled with the NiCr. This work provided a new significant result for safe utilization of the Ti-6Al-4V with potential presence of the fluoride in oral environment, due to the fact that they're related to the NiCr-based prostheses and implant connections.

**Yun,et.al., 2021 [104]** studied in vitro bio-compatibility of the Ni–Cr alloys that have been produced with the use of three different approaches of manufacturing (i.e. selective laser melting [SLM], casting, and soft milling [SM]) from single alloy with a similar elemental composition. The ion release, micro-structure, and cell viability of alloys have been investigated. Nickel-based  $\gamma$  phase has been characterized for those 3 alloys. A Cr and Mo segregation has been observed in cast alloy. SM and SLM alloys have shown more homogeneous elemental dispersions as well as formation of finer grains compared to the cast one. The extensive porosity and (Mo,Cr)C carbide have been produced in SM alloy. The SLM alloy had exhibited minimal nickel ion release, which has been followed by SM alloy ( $p < 0.001$ ) and after that, the cast alloy ( $p < 0.050$ ). SLM alloy had shown as well the highest density and viability of the L-929 mouse fibroblasts, which has been followed by soft milling alloy ( $p < 0.050$ ) and lastly cast alloy ( $p < 0.001$ ). It has been concluded from the results of this study that SLM alloy had better bio-compatibility, cell viability of soft milling alloy being a little less but still higher than that of the cast alloy.

Table (2.3): Summary of literature review

Reference	Process Parameters	Tests	Research Finding
[90]	Comparison of corrosion resistance between three commercial Ni-Cr dental alloys in artificial saliva.	Tafel test	The results have exhibited that the Nickel-Chromium casting alloys with higher content of Cr and Mo have considerably higher passive range and immunity to the corrosions.
[91]	Comparison of corrosion resistance between two commercial Ni-Cr dental alloys in artificial saliva.	OCP,PPC,SEM& EDX	The Mo and Cr contents have an important impact on corrosion resistance.
[92]	The effects of oral environment (i.e. saliva) on the corrosion of Ni-Cr,Ni-Cr-Ti &Co-Cr dental alloys.	PPC,SEM&EDX, Ion Concentration	The amount of the Cobalt ions that have been released from Co-Cr-Mo alloy has been rather small in solutions. Additionally, the amount of the ions of Chromium that have been released into artificial saliva from Co-Cr alloy has been less than the release of chromium from the Nickel-based dental alloys.
[93]	Effects of different surface treatments on the elemental composition stability of the as-received and re-cast Ni-Cr casting alloy types.	EDX	The very low ratio of change of elements influenced the biological and physical characteristics of the alloy. The recasting of the metal alloys could have adverse effects on the surface quality.
[94]	The mechanical properties,,the composition and micro-structure of 3 Ni- Cr alloys that have been utilized for implant prosthetic were measured	The tensile test, Vickers hardness, and Young's modulus	Higher levels of hardness and lower value of Young's modulus of Tilitite predict higher initial resistances to better strain and stress absorption to the prosthetic abutments.
[95]	Evaluate the corrosion	FE-SEM, in vitro	The Ni-Cr-xMo alloys have a superior cell

	behaviors and bio-compatibility through the addition of various Mo amounts to Ni-Cr alloys	cytotoxicity testing	viability as well as better cell adhesion and higher electro-chemical impedance in comparison with the Ni-Cr alloys.
[96]	The corrosive development of a Ni-Cr-Mo alloy, following the re-melting in open flame, in a 0.90% solution of NaCl	OCP,PPC,OP,SEM &EDX	The alloy's corrosion resistance is associated with passive layer formed on the surface and this is dependent upon the alloy's chemical composition.
[97]	The corrosion behavior of Co-Cr-Mo and Ni-Cr-Mo alloys have been fabricated with 2 different approaches of casting in the de-aerated 0.90% solution of NaCl	PPC,XRD,SEM& EDX	The dependence of the corrosion resistance upon micro-structure that is related to casting approaches is minimal. The Co-Cr alloy corrosion resistance characteristics higher than the Ni-Cr alloy.
[98]	Corrosion properties of Ni-Cr-xMo alloys in 0.9%NaCl solution.	PPC,OP,SEM	Ni-Cr-xMo alloys can be used for dental casting as they provide a valid alternative to commercial dental casting alloys.
[99]	XRD and corrosion resistance characteristics in an artificial saliva solution of commercial Ni-22Cr-9Mo alloy.	OCP,XRD,PPC,OP ,SEM&EDX	The commercial alloy shows considerably higher rate of corrosion resistance in comparison with re-cast alloy.
[100]	The corrosion behaviors of 4 various commercial Ni-Cr dental casting alloys (S1,S2, S3,S4) in the artificial saliva solution	OCP,PPC,SEM	All of the dental alloys show a low tendency for the corrosion, however, S1 & S2 alloys have been most stable to the corrosions in the artificial saliva.
[101]	Effects of the value of pH of the artificial saliva on Ni-Cr-Mo alloy's corrosion behavior at 37°C	SEM,EDS& AAS	The acidic pH level results in severely corroding Ni-Cr-Mo base metal alloys and increasing the release of the Nickel ions.
[102]	Effect the pH value of the artificial saliva on Co-Cr and Ni-Cr dental alloy corrosion	OCP,PPC,SEM& EDX	The Co-Cr alloy has more sufficient level of corrosion resistance compared to the Ni-Cr based alloys, potentially because of the

			formation of more adherent oxide layer on its surface.
[103 ]	Effect of NiCr on Ti6Al4V in solutions with various contents of the fluoride and pH that are used on dental implants rehabilitations	SEM, galvanic test, OPC	Ti-6Al-4V presented a reducing corrosion resistance with the increase in concentration of the fluoride and decreasing pH.
[104 ]	Effect manufacturing techniques on biocompatibility of Ni-Cr dental alloy.	XRD, Ion release test, SEM&EDS	The alloy of the SLM had better biocompatibility, cell viability of soft milling alloy being a little less, however, still greater than that of the cast alloys.

## Chapter Three

### Experimental part

#### 3.1 Introduction

This chapter presents work's materials, as well as the tests and methods. The alloys' preparation is the first stage, and the process of creating the alloy was done utilizing powder technology. Through this chapter we will get acquainted in detail with the stages of alloys formation using powder technology, including (mixing, compacting and sintering). The second stage includes preparing the samples for the tests as well as the tests performed on them. Figure (3.1) shows the flow chart of the experimental part.

#### 3.2 Powders and Their Tests

The properties of powders are used in this study illustrated in table (3.1). This properties included particle size, purity. The original ingredients from India/CDH fined chemical/Central Drug House (P) Ltd.

Table(3.1) Powders Specifications

Powder	Purity %	Average particles size ( $\mu\text{m}$ )
Nickel	99.9	23.53
Chromium	99.9	38.95
Molybdenum	99.95	19.76
Cobalt	99.68	18.46
Boron	99.9	4.931
Indium	99.99	27.29
Zirconium	99.99	14.23
Zirconia	99.97	0.398

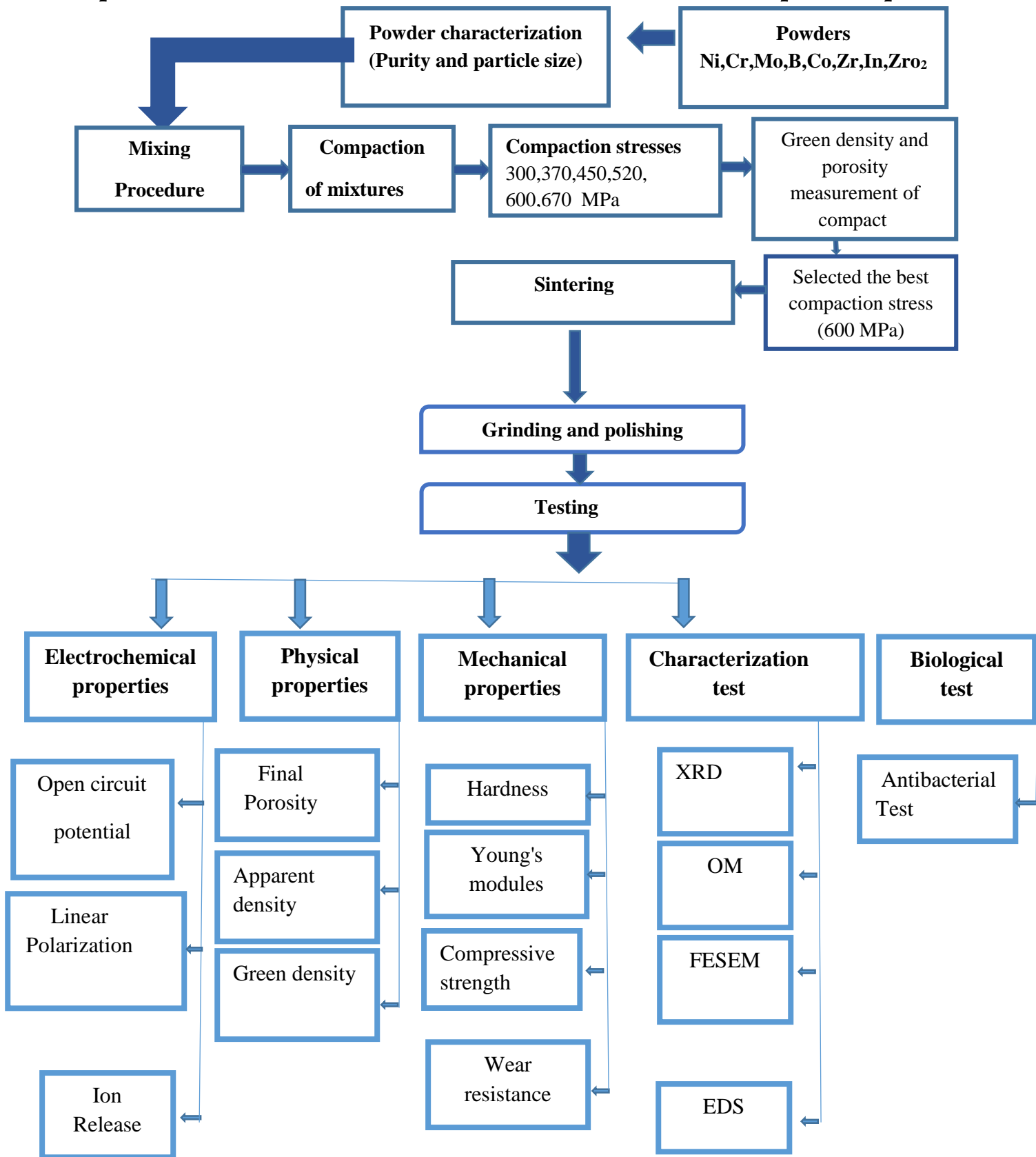


Figure (3.1): The Flow Chart of Work

### 3.3 Particle size analysis

The device used for particle size analysis is a ("best 2000" laser particle size analyzer). This device is located in the laboratories of the University of Babylon / College of Materials Engineering / Ceramics and Building Materials. Figures(3.2-3.9) shows the particle size analyses for powders .

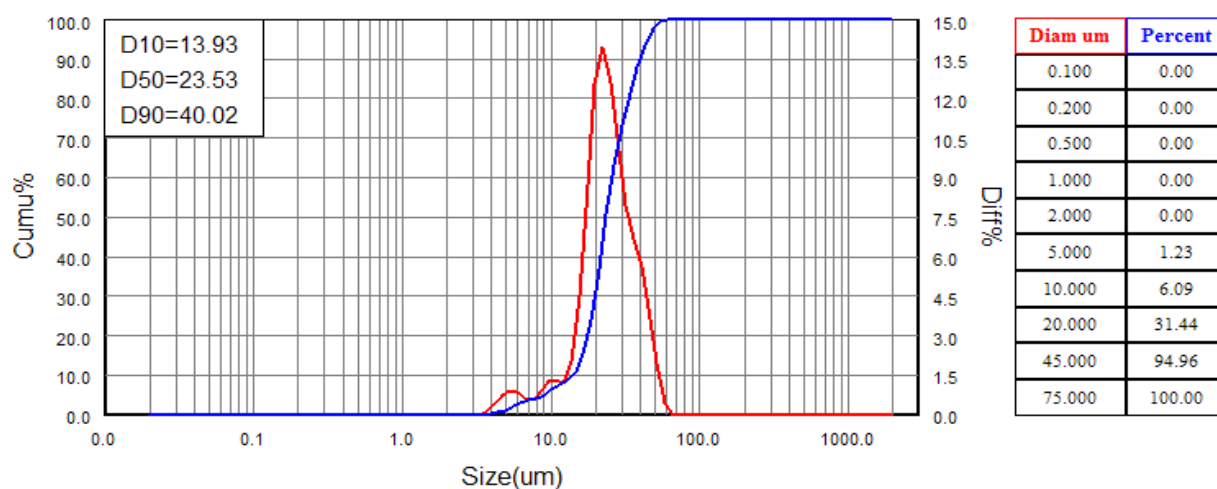
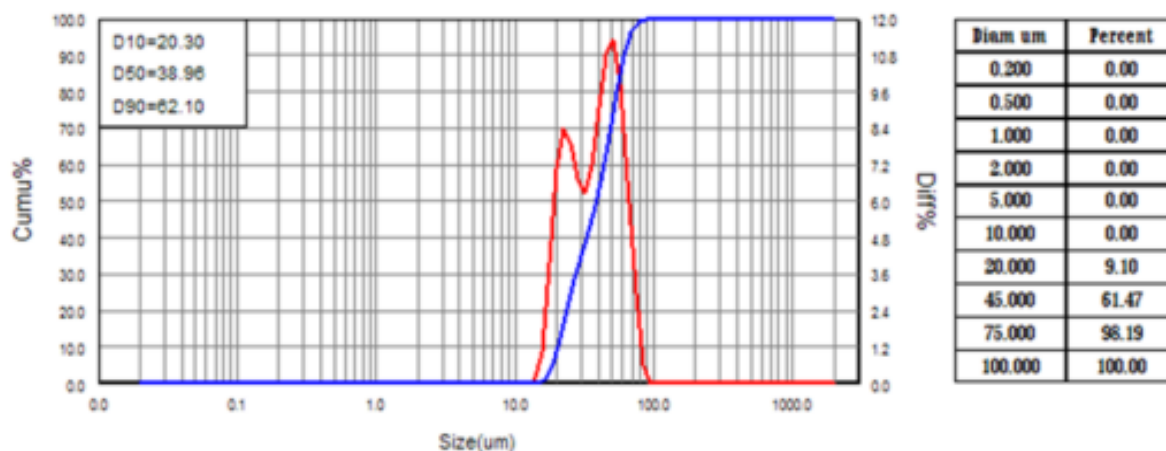
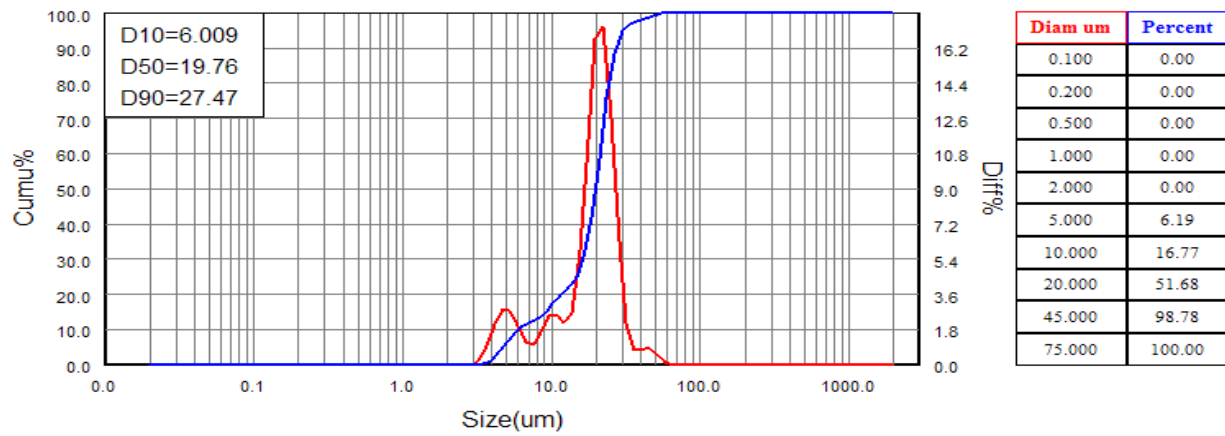


Figure (3.2): Particle Size Analysis for Ni Powder



Figure(3.3) : Particle Size Analyses for Cr Powder.



Figure(3.4): Particle Size Analyses for Mo Powder.

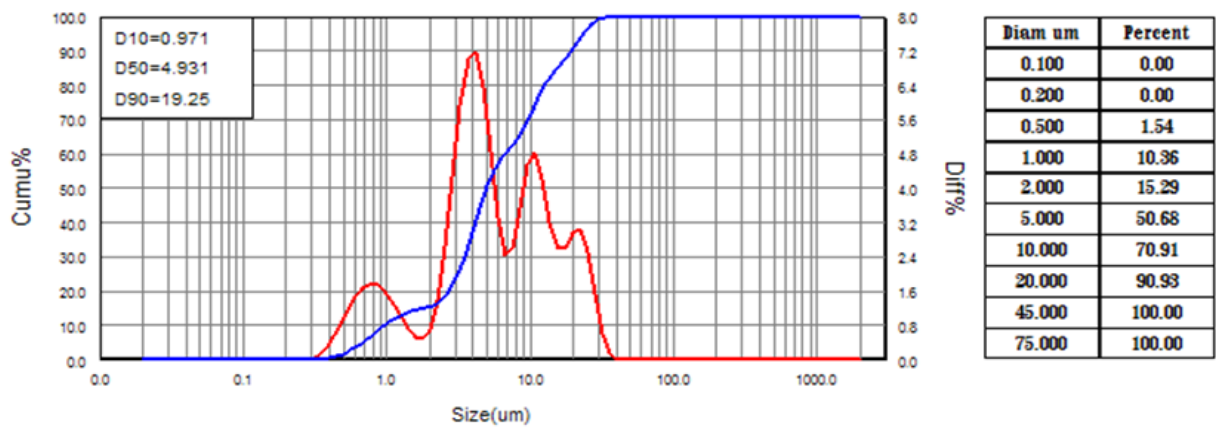


Figure (3.5): Particle Size Analyses for B Powder.

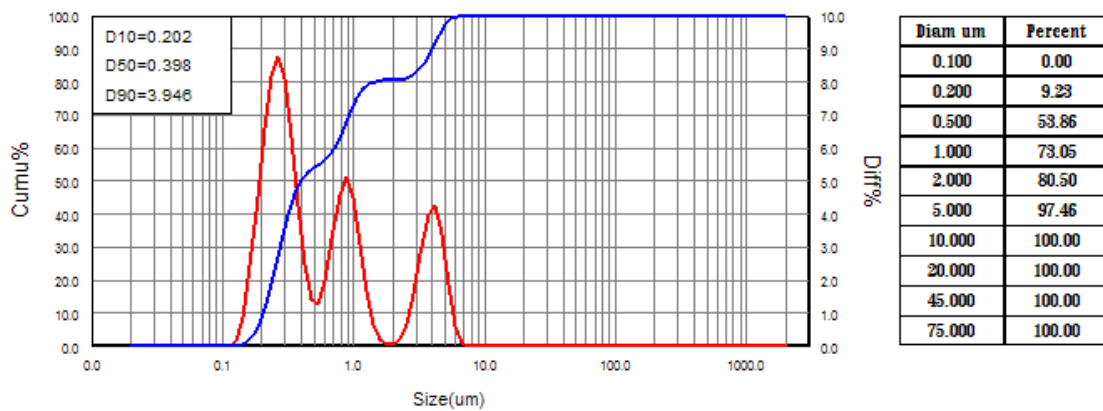


Figure (3.6): Particle Size Analyses for ZrO<sub>2</sub> Powder.

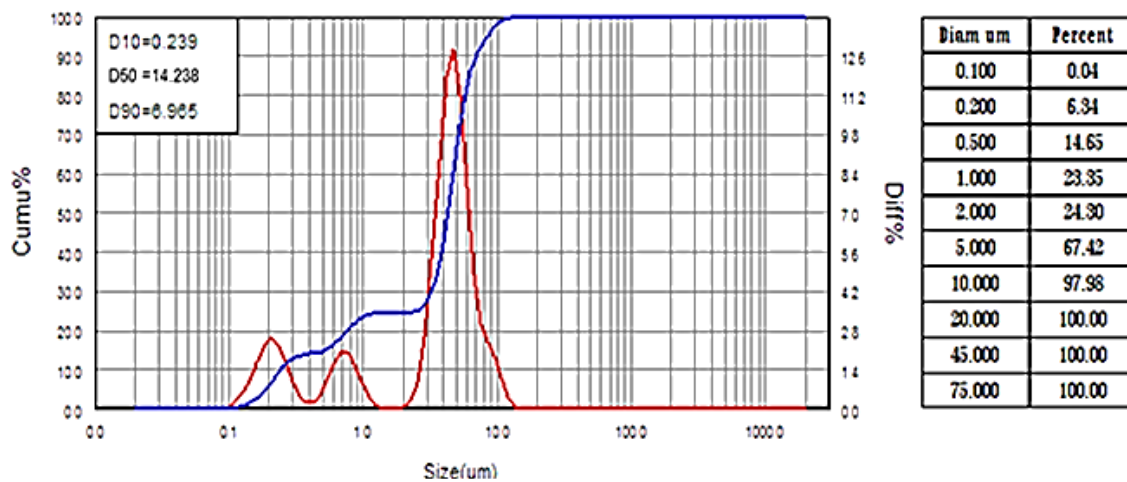
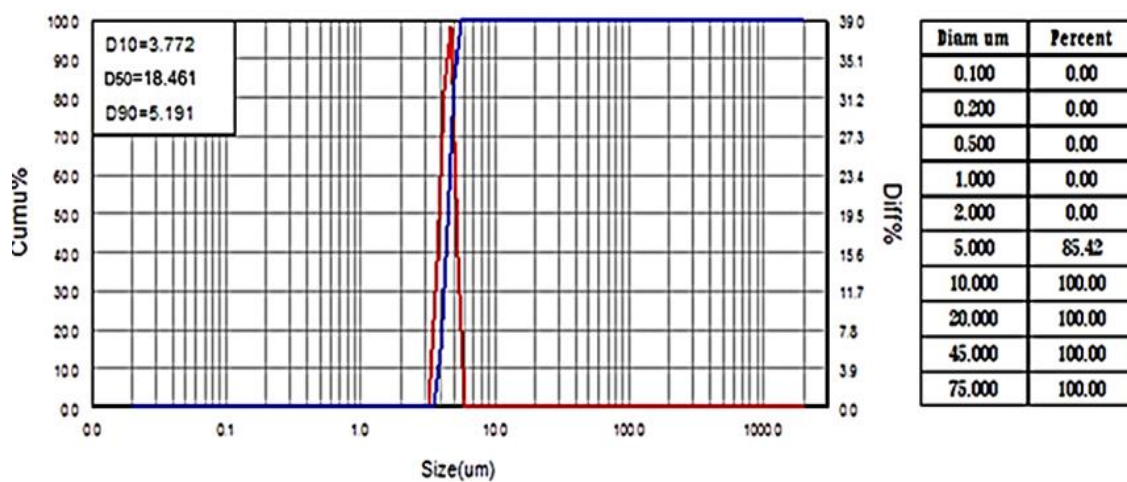


Figure (3.7): Particle Size Analyses for Zr Powder.



Figure(3.8): Particle Size Analyses for Co Powder.

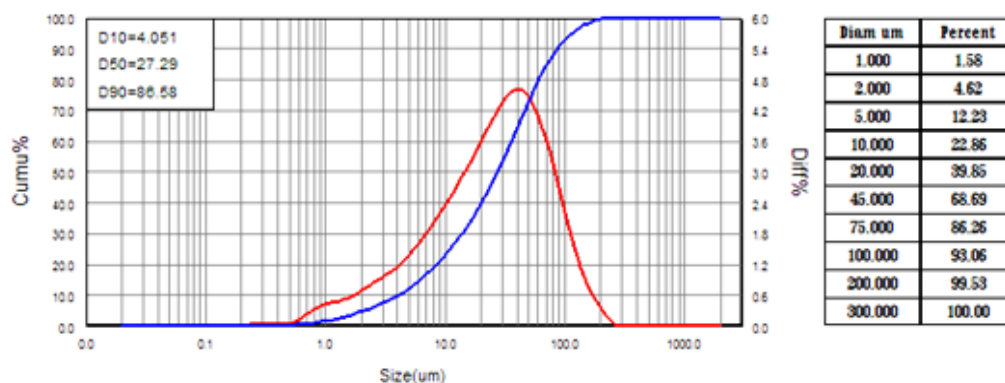


Figure (3.9): Particle Size Analysis for In Powder.

### **3.4 Samples Preparation**

The powder metallurgy method was used for samples preparation. Powder metallurgy includes several stages, mixing, compacting, sintering. All of these steps have to be done in order to have a sample ready for use and testing. Table (3.2) shows the composition and code of alloys utilized in this work. All samples were created in the metallurgical engineering department's laboratories at the University of Babylon's College of Materials Engineering.

#### **3.4.1 Mixing**

The needed amount of each powder has been weighed with the use of a Sensitive Balance type (L220S– D) with ( $\pm 0.0001$  accuracy) Germany prior to mixing. Electrical mixer type (STGQM-1/5-2) is used to combine powders. The purpose of the mixing process is to obtain a homogeneous mixture and uniform distribution of the powder. For the purpose of obtaining a good mixing, stainless steel balls of different diameters are used with small amounts of alcohol to prevent friction and oxidation of the powders during mixing. The time of mixing is 6 hours.

Table 3.2: Chemical composition of alloys under study

Synthesized Composition	Code	Ni wt. %	Cr wt. %	Mo wt. %	Co wt. %	B wt. %	Zr wt. %	In wt. %	ZrO <sub>2</sub> wt. %
Ni-21Cr-2Mo-2Co	A	75	21	2	2	-	-	-	-
Ni-21Cr-2Mo-2Co-0.4B	B1	74.6	21	2	2	0.4	-	-	-
Ni-21Cr-2Mo-2Co-0.8B	B2	74.2	21	2	2	0.8	-	-	-
Ni-21Cr-2Mo-2Co-1.2B	B3	73.8	21	2	2	1.2	-	-	-
Ni-21Cr-2Mo-2Co-0.4Zr	C1	74.6	21	2	2	-	0.4	-	-
Ni-21Cr-2Mo-2Co-0.8Zr	C2	74.2	21	2	2	-	0.8	-	-
Ni-21Cr-2Mo-2Co-1.2Zr	C3	73.8	21	2	2	-	1.2	-	-
Ni-21Cr-2Mo-2Co-0.4In	D1	74.6	21	2	2	-	-	0.4	-
Ni-21Cr-2Mo-2Co-0.8In	D2	74.2	21	2	2	-	-	0.8	-
Ni-21Cr-2Mo-2Co-1.2In	D3	73.8	21	2	2	-	-	1.2	-
Ni-21Cr-2Mo-2Co-3ZrO <sub>2</sub>	E1	72	21	2	2	-	-	-	3
Ni-21Cr-2Mo-2Co-6ZrO <sub>2</sub>	E2	69	21	2	2	-	-	-	6
Ni-21Cr-2Mo-2Co-9ZrO <sub>2</sub>	E3	66	21	2	2	-	-	-	9

### 3.4.2 Compacting

The compacting process of mixed powder is done by using an electrical uniaxial hydraulic press type (Soil Test, Inc. USA). The compaction process includes the following steps:

- 1- Preparing a die for the compacting process with specific dimensions. The die used in this study is made of stainless steel.
- 2- Lubricate the die using graphite for the purpose of preventing friction between the die wall and the sample, ease of removing the sample from the die and avoiding cracks that affect the die.
- 3- Weighing an appropriate amount(4g) of the mixed powder and put it in the die.
- 4- We use the compaction device for the purpose of obtaining a green sample with dimensions  $D:13\text{mm}$ ,  $t:4\text{mm}$ . Different compaction pressures (300,370,450,520, 600,670 MPa) with a periodic time of 4 min were used to determine the optimum pressure giving the lowest green porosity and the highest green density.



Figure (3.10): (A) Electric hydraulic press (B) Die .

### 3.4.3 Sintering Process

The compact samples are placed in the through inert tube furnace of high temperature with existence of argon gas as the last step in sample preparation. Figure (3.11) illustrates the sintering furnace. The steps of sintering process for NiCrMo and NiCrMo  $-x$  (B, Zr, ZrO<sub>2</sub>) includes:

- 1- Heating the compact samples from room temperature to 500 C° at heat rate 20 °C/min, and soaking two hours.
- 2- Heating the furnace from temperature 500 C° to 1000 C° with soaking time (8) hours.
- 3- Cooling takes place slowly inside the furnace with the continuation of the argon flow. Figure (3.12) illustrated all above steps.

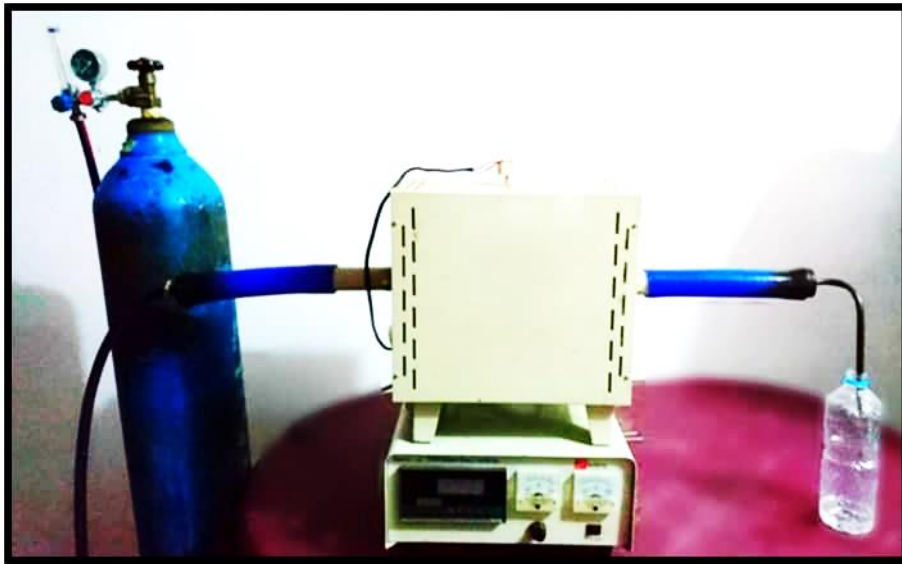


Figure (3.11): The furnace used for sintering process

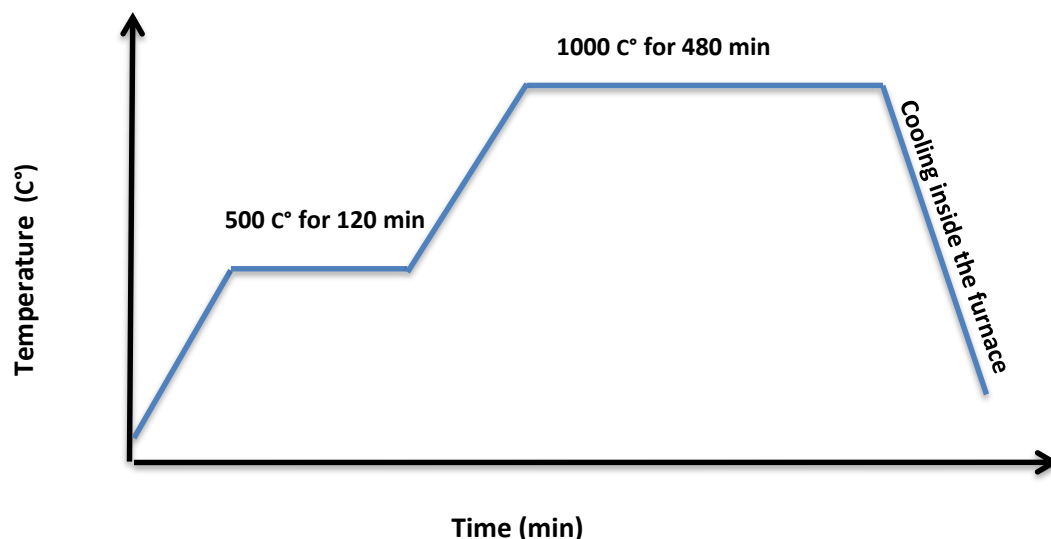


Figure (3.12): Program of sintering process for NiCrMo-x (B,Zr,ZrO<sub>2</sub>).

The steps of sintering process of NiCrMo-In includes:

- 1- Heating the compact samples from room temperature to 123 C° at heat rate 20 °C/min, and soaking one hours.
- 2- Heating the furnace from temperature 123 C° to 500 C° with soaking time (2) hours.
- 3- Heating from 500 C° to 1000 C°, and soaking (8) hours. Then cooling samples inside furnace.

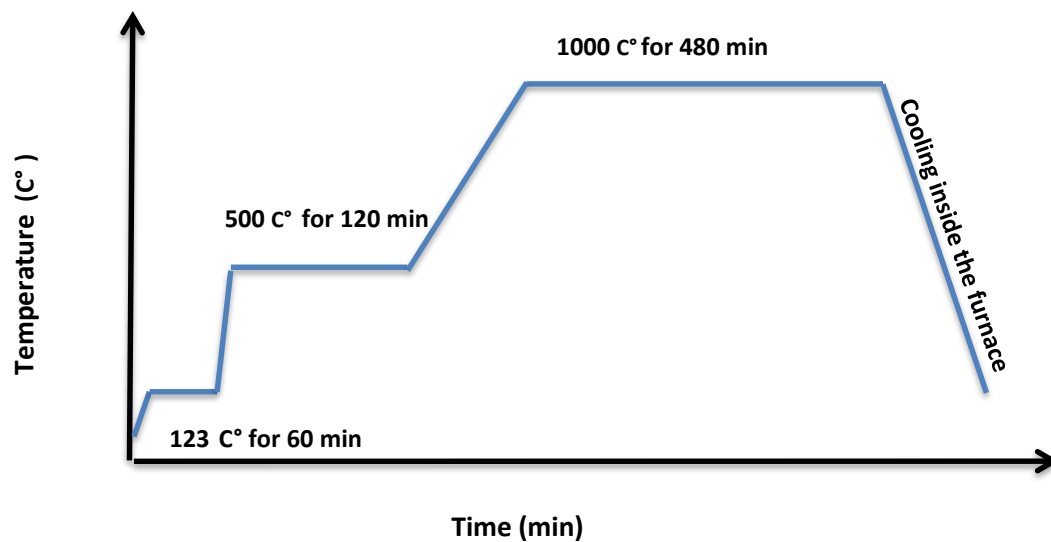


Figure (3.13): Program of sintering process for NiCrMo- In.

### 3.5 Preparation the specimens for testing

The processes of preparing specimens for testing includes grinding process and polishing process. The grinding process of the samples is carried out by using grinding papers of silicon carbide of different sizes (400, 600, 800, 1000, 1500, 2000, 2500, 3000). After the grinding process, the samples need to be polished using diamonds (particle size 1  $\mu\text{m}$ ) on a special polishing cloth, then washed with water and dried in warm air.



Figure (3.14): The specimen after grinding and polishing

### 3.6 Characterization Tests:

#### 3.6.1 XRD Test:

The XRD examination is performed on the samples for the purpose of knowing the phases that appear in the alloy. The XRD device type (Philips- PW1730) in university of Tehran-Iran. This device using radiation  $\text{CuK}\alpha$  with wavelength ( $\lambda = 1.54090 \text{ \AA}$ ) 40 KV, 30 mA at room temperature.

#### 3.6.2 Optical Microstructure:

The microstructure of the specimens can be obtained by examining the optical microscope. For the purpose of conducting this examination, specimens must be prepared by (grinding, polishing, etching). The etching process is carried out using

etching solution that consists of (100 ml HNO<sub>3</sub>, 10 ml HF). Light microscope used for testing type (1280 XEQMM300TUSB) have different magnification power (100X, 200X, 400X, 800X). The test was conducted in the laboratories of the Metallurgical Department of the College of Materials Engineering, University of Babylon.

### 3.6.3 Field Emission Scanning Electron Microscopy (FESEM) Test

To show microstructure in more magnification, clarity and showing the phases in the samples more accurately, we use the test FESEM. This device Type (TESCAN Mira3) found in university of Tehran-Iran .

### 3.6.4. Energy Dispersive X-ray (EDX) Spectroscopy

The EDX test has been conducted in order to know the chemical composition of the samples and through it can distinguish between the different phases that appear in the microstructure. The test was carried out at the University of Tehran, Iran.

## 3.7 Physical properties

### 3.7.1 Green Porosity and Density

The green density can be extracted from the compacted samples before the sintering process by taking the dimensions and weight of the samples and applying the following Eq. (3-1)[105]:

$$\rho_g = \frac{M_g}{V_g} \dots \dots \dots (3 - 1)$$

Where:

( $\rho_g$ ): The green density of a sample ( $\text{g}/\text{cm}^3$ ), ( $M_g$ ) mass of a sample (g), and ( $V_g$ ) sample's volume ( $\text{cm}^3$ ).

After calculating the green density of the samples, we can extract the green porosity by using the following Eq.(3-2)

$$p_g = 1 - \left( \frac{\rho_g}{\rho_{th}} \right) \times 100 \dots \dots \dots (3 - 2)$$

where  $P_g$  is the green porosity of the sample, and

$\rho_{th}$  is the theoretical density of the mixture ( $\text{g}/\text{cm}^3$ ).

The theoretical density of alloys is determined by their percentage ratios, according to the following relationship[105] :

$$\rho_{th} = (W_1\% * \rho_1 + W_2 \% * \rho_2 + W_3 \% * \rho_3 + \dots \dots \dots) \dots \dots \dots (3.3)$$

where  $\rho_1, \rho_2, \rho_3, \dots$  are the theoretical density

$W_1, W_2, W_3, \dots$  are the weight percentage of powder.

### 3.7.2 Porosity and Density of Sintered Samples

The final porosity of the specimens are measured according to ASTM B-328[105]:

- 1- The vacuum drying furnace used to dry the specimens at 100 degrees for 5 hours at vacuum ( $10^{-4}$ ) tor and then take the weight of the specimens, which represents mass A.
- 2- The specimens were immersed in oil with a density of  $0.8 \text{ g}/\text{cm}^3$  for half an hour where a suitable vacuum pump was used at room temperature. The weight of specimens completely immersed in air represents the mass B.
- 3- The suspended weight of the specimen immersed in water is the mass F.

Finally, the following equation was used to extract the porosity:

$$P = \frac{B - A(B - F)D^{\circ}}{D_w} \times 100 \quad (3.4)$$

$$\rho F = \frac{A(B - F)}{D_w} \quad (3.5)$$

where:  $D_w$  = density of water (0.9956 g/cm<sup>3</sup>)  $D^{\circ}$  = density of oil (0.8 g/cm<sup>3</sup>) .

### 3.8 Mechanical properties

#### 3.16.1 Hardness Measurement

The test was carried out using a Brinell hardness tester (Wilson Hard Reichrter UH250) in the laboratories of the Metallurgical Engineering Dept., Materials Engineering College, Univ. of Babylon. The test consisted of the use of ball (2.5 mm) diameter and the load used (32.25kg) for 10 seconds according to ASTM(E10-15a). Three readings were measured for each specimen and the average was taken.

#### 3.8.2 The Modules of Elasticity Measurement

Ultrasonic wave test used to measurement the modules of elasticity. In this test, ultrasound waves are used that pass from one side of the specimen and travel to the other side, and this path represents the length of the specimen(L). The time of the wave's passage through the sample is measured by electronic time instruments. The specimen used in this test have 10mm diameter, 15mm length and the test was done in laboratories Dept. of Polymer Engineering / Materials Engineering College / Univ. of Babylon.

There are several equations used to calculate the modulus of elasticity as in the following [106]:

$$E = \frac{\rho V_S^2 (3V_L^2 - 4V_S^2)}{V_L^2 - V_S^2} \dots\dots\dots (3.6)$$

Where:  $E$  represents Young's modulus of alloy,  $\rho$  represents alloy density  $V_L =$  longitudinal ultra-sonic wave velocity,  $V_S$  represents shear ultra-sonic wave velocity.

To calculate  $V_L$  and  $V_S$ , equations 3.2 and 3.3 were used [106].

$$V_L = 2l/t_L \dots\dots\dots (3.7)$$

$$V_S = 2l/t_S \dots\dots\dots (3.8)$$

$t_L$  represents longitudinal ultra-sonic wave transit time,  $t_S$  represents the shear ultra-sonic wave transit time,  $l$  represents the thickness of the samples.

### 3.8.3 Compression Test

Compression testing was performed using via computer control electronic general testing machine, Model (WDW 200, No.W1124) as per specification ASTM B925–08. The diameter of specimen 10mm and height 15mm. The rate of loading speed was 0.2mm/min.



**Figure (3.15):**The specimens before and after compression test.

### 3.8.4 Wear Test

The wear test was carried out with a pin on a disc device (MT-4003, version 10) in the College of Materials Engineering at the University of Babylon's laboratories.. For the purpose of conducting the test, three loads (5,10,15)) and a rotational speed 350 rpm in a radius of 4 mm with different sliding distance were used. The specimen is installed in the device after weighing it with a sensitive scale, and then the device is turned on. After every 5 min, the device stops and the sample weight is measured periodically. The test was performed as per specification ASTM G 99. The wear rate was calculated using the following equation[139]:

$$\text{Specific wear rate} = \Delta W / S \text{ ( g/ cm ) } \dots \dots \dots (3.9)$$

Where:  $\Delta W$  = Weight lost (g)

S = Sliding distance (263.76m)

$$S = \text{Sliding Velocity (m/sec )} \times \text{time (sec )} \dots \dots \dots (3.10)$$

$$\text{Sliding Velocity} = \pi DN / 1000$$

Where: D = wear track diameter selected (8mm).

## 3.9 Electrochemical properties

### 3.9.1 Open Circuit Potential

The open circuit was tested by immersing the samples in artificial saliva and normal saline (0.9%NaCl) solutions at  $37 \pm 1$  °C and pH 5.8 and 6.5 respectively. The specimen represents the working electrode and the calomel electrode is the reference electrode, both of which are connected to a voltmeter to measure voltages. The first reading is taken at the moment the specimen is immersed in the

solution and then other readings are recorded after every five minutes until the voltage is stabilized at a certain number that represents the specimen voltage. The figure (3.16) shows the open circuit potential measurement. Table (3.3) shows the chemical composition of saliva solution



Figure (3.16) shows the open circuit potential measurement.

Table (3.3) shows the chemical composition of saliva solution.

No.	Constituent	g/l
1	NaCl	0.4
2	KCl	0.4
3	CaCl <sub>2</sub> .2H <sub>2</sub> O	0.906
4	NaH <sub>2</sub> PO <sub>4</sub> .2H <sub>2</sub> O	0.69
5	Na <sub>2</sub> S.9H <sub>2</sub> O	0.005
6	Urea	1

### 3.9.2 Potentiodynamic Polarization Test

The specimen's polarization was examined in accordance with ASTM (GS-87), with the specimen serving as working electrode, the calomel electrode that serves as reference electrode, and platinum electrode that serves as counter electrode. At a temperature of  $37 \pm 1^\circ\text{C}$ , two solutions were utilized in the test: artificial saliva and normal saline solution. The schematic diagram regarding potentiodynamic polarization is shown in Figure 3.17. Potentiostats were used to conduct polarization investigations (Winking M Lab 200). With + 1mV/sec scan rate and initiation and end potential that equals  $\pm 0.250$  V against open circuit potential ( $E_{oc}$ ), potentiodynamic polarization was performed. Tafel plots are used for calculating corrosion potential and corrosion current density ( $i_{corr}$ ). The next equation was used to compute the corrosion rate[107]:

$$\text{corrosion rate (mpy)} = \frac{0.13 * I_{corr} * (E.W)}{\rho} \dots\dots\dots(3.11)$$

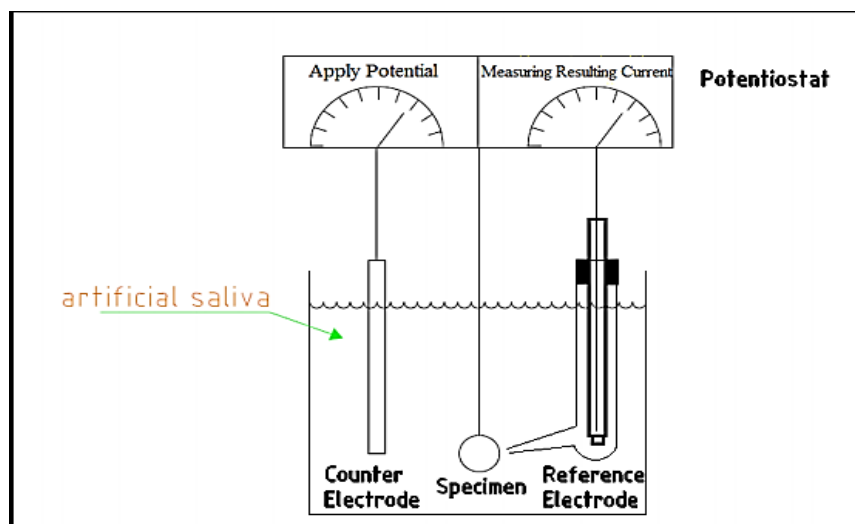
0.13 denotes the metric as well as the time conversion factor.

$i_{corr}$  denotes corrosion current density ( $\mu\text{A}/\text{cm}^2$ ).

$\rho$  denotes the alloy density ( $\text{g}/\text{cm}^3$ ).

E.W denotes the equivalent weight.

mpy denotes the rate of the Corrosion (mils per year).



(3.17) illustrates schematic diagram of potential dynamic polarization

### 3.9.3 Ion release test

The static immersion test was carried out in accordance with the current JIS T-0304 metallic biomaterial requirements. The Atomic Absorption spectrophotometer type (shimadzu AA-7000) located in the College of Science; University of Babylon was used to calculate the ions release. The specimen is immersed in plastic containers containing corrosive solutions (Saliva, normal saline) at a rate of 50 ml and at  $37 \pm 1$  °C for three weeks. The specimens are placed in a glass chamber to maintain a constant temperature at  $37 \pm 1$  °C.

## 3.10 Biological Test:

### 3.10.1 Antibacterial Test

The antibacterial test used for samples ( $B_1$ ,  $B_4$ ,  $B_7$ ,  $B_{10}$ ,  $B_{12}$ ) to measure the antibacterial effect by using test's method Viable Cell Count. The type of Bacteria was *Streptococcus mutans* (Gr+, Facultative Anaerobe) and Fungi type was *Candida albicans* ATCC 10231 (Yeast). The test was conducted in the Department of Microbiology, University of Tehran – Iran. The steps of test:

- 1) Preparation of fresh culture of target bacteria (index).
- 2) Preparation of suspension from bacteria with a concentration of 0.5 McFarland (equivalent to  $1.5 \times 10^8$  CFU/ml) with diluting solution (saline or phosphate buffer).
- 3) Dilution of the bacterial suspension to reach the desired number of cells in the diluent solution.
- 4) Contact of a certain volume of suspension ( $0.4\text{cc} < V < 1\text{cc}$ ) with the sample based on the surface and volume of the sample.
- 5) Sampling and culture of bacteria in contact with the sample, based on the desired schedule.
- 6) The amount of 0.1 cc of the sample taken by Plate Spread method is spread in solid culture medium on the plate surface and then placed in the incubator at a temperature of  $30 \pm 2$  ° C.
- 7) After 24-48 hours, the colonies formed by the Count Colony are counted.
- 8) The number of colonies per unit volume (CFU/ml) is calculated as follows:  
$$\text{CFU/ml} = (\text{no. of colonies} \times \text{dilution factor}) / \text{volume of culture plate}$$
- 9) Percentage of mortality and logarithm of reduction is calculated based on the number of colonies per unit volume

## Chapter Four

### Results and Discussion

#### 4.1. Introduction

In this chapter, the test results that were performed on the samples were discussed. These tests included tests of physical properties, mechanical properties, electrochemical properties, microstructure and biomedical test.

#### 4.2. X-ray Diffraction Analysis

Figure (4.1) and (4.2) show the X-ray diffraction results for the ( Ni-Cr-Mo) alloy before and after sintering process. From the results of tests before and after sintering, it was notice new phases were formed. This means that 1000°C for 8h was enough to complete sintering process due to the enhancement of the interdiffusion between Ni, Cr and Mo. Figure (4.2) illustrates XRD pattern for A alloy after sintering. Three phases appears in XRD pattern:  $\gamma$  (Ni),  $\text{Cr}_3\text{Ni}_2$ ,  $\text{MoNi}_4$ , this agree with the research[108]. From the Figure (4.2), it was notice that the phase  $\gamma$  (Ni) appears in the angles ( $44.6^\circ$ ,  $51.9^\circ$ ,  $76.1^\circ$ ) according to the card (04-0850), while the phase  $\text{Cr}_3\text{Ni}_2$  appears in the following angles ( $38.7^\circ$ ,  $65.1^\circ$ ,  $78.2^\circ$ ) based on the card (26-0430). Finally, phase  $\text{MoNi}_4$  appears at angles ( $44.6^\circ$ ,  $51.9^\circ$ ,  $65.1^\circ$ ) and this corresponds to card (03-1036). Figures (4.3),(4.4)and(4.5) illustrates XRD pattern for B<sub>3</sub>, C<sub>3</sub> and D<sub>3</sub> alloys after sintering process, all amount of Ni, Cr and Mo transformed to ( $\gamma$  (Ni),  $\text{Cr}_3\text{Ni}_2$ ,  $\text{MoNi}_4$ ) phases. B, Zr and In was added to a maximum percentage 1.2%, this is a small amount to be detected by the XRD technique. Figure (4.6) shows the XRD pattern of E2 alloy.  $\text{ZrO}_2$  was added to a maximum percentage 9% the amounts can be detected by the XRD method as shown in several large prominent peaks of  $\text{ZrO}_2$ . From the figure (4.6) it was notice that  $\text{ZrO}_2$  appears in three peaks having angles ( $30.35^\circ$ ,  $33.75^\circ$ ,  $50.45^\circ$ ) according to the card (37-0031).

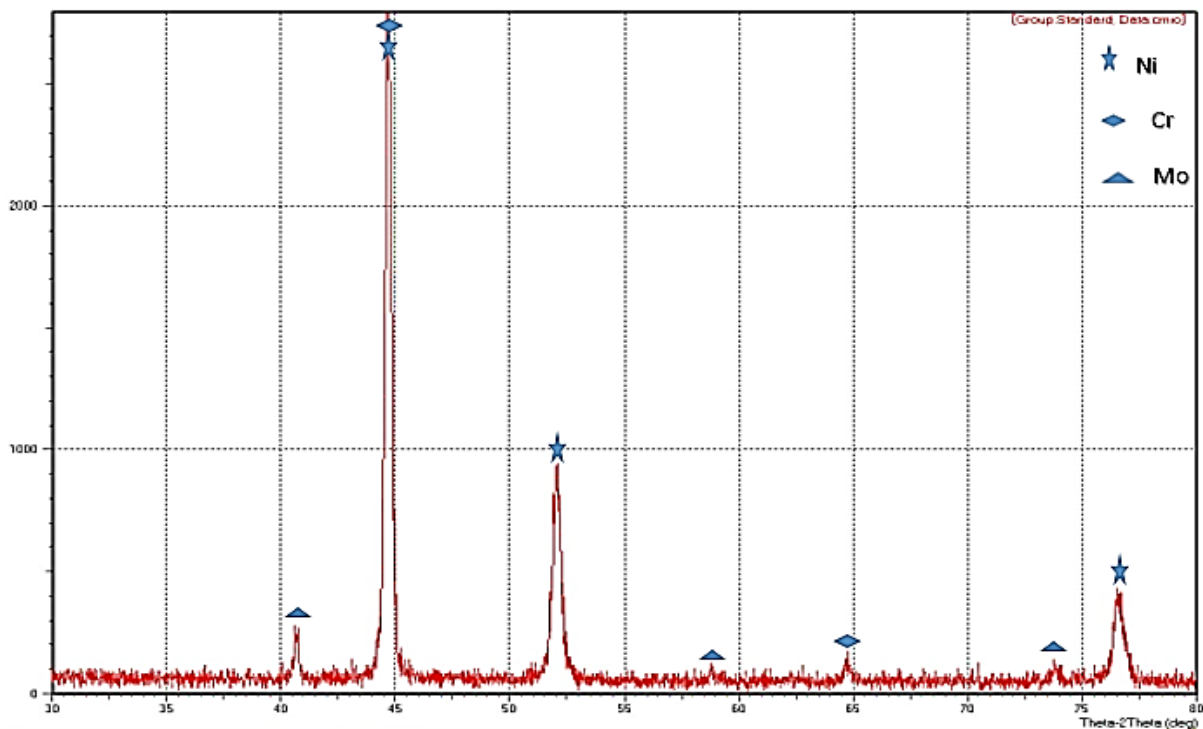


Figure (4.1): XRD pattern of the A alloy before the sintering

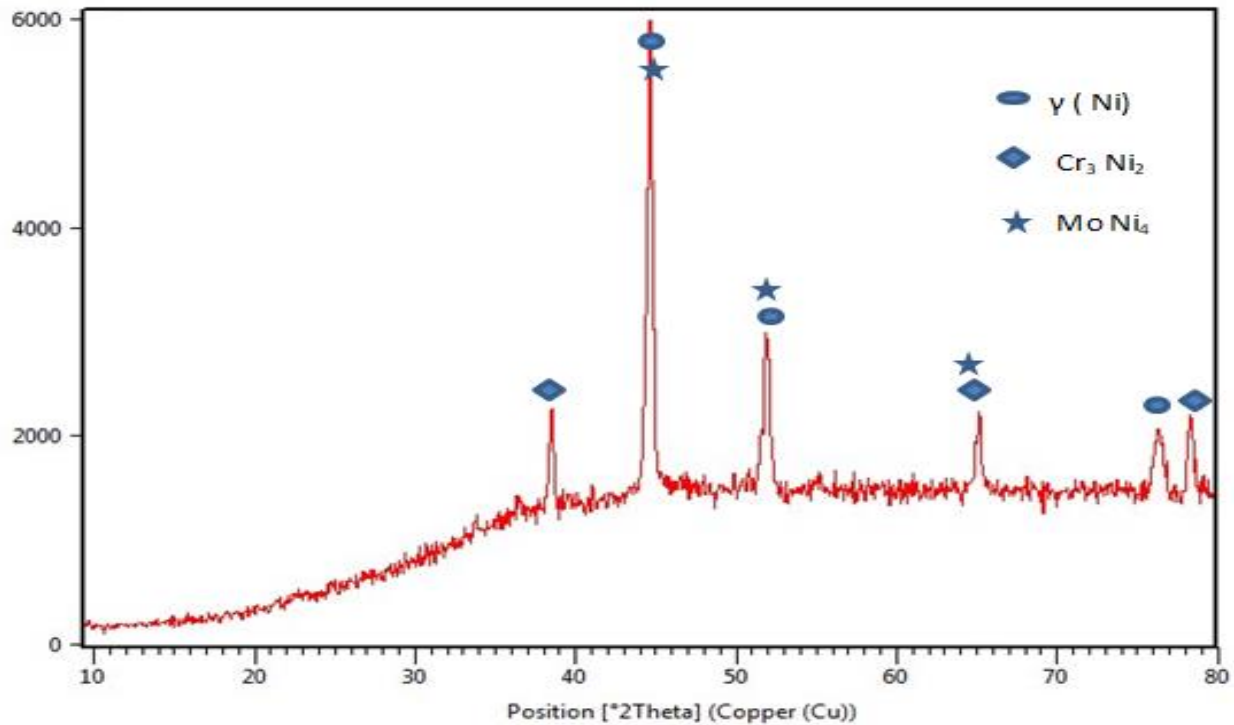


Figure (4.2): XRD pattern of the A alloy after the sintering

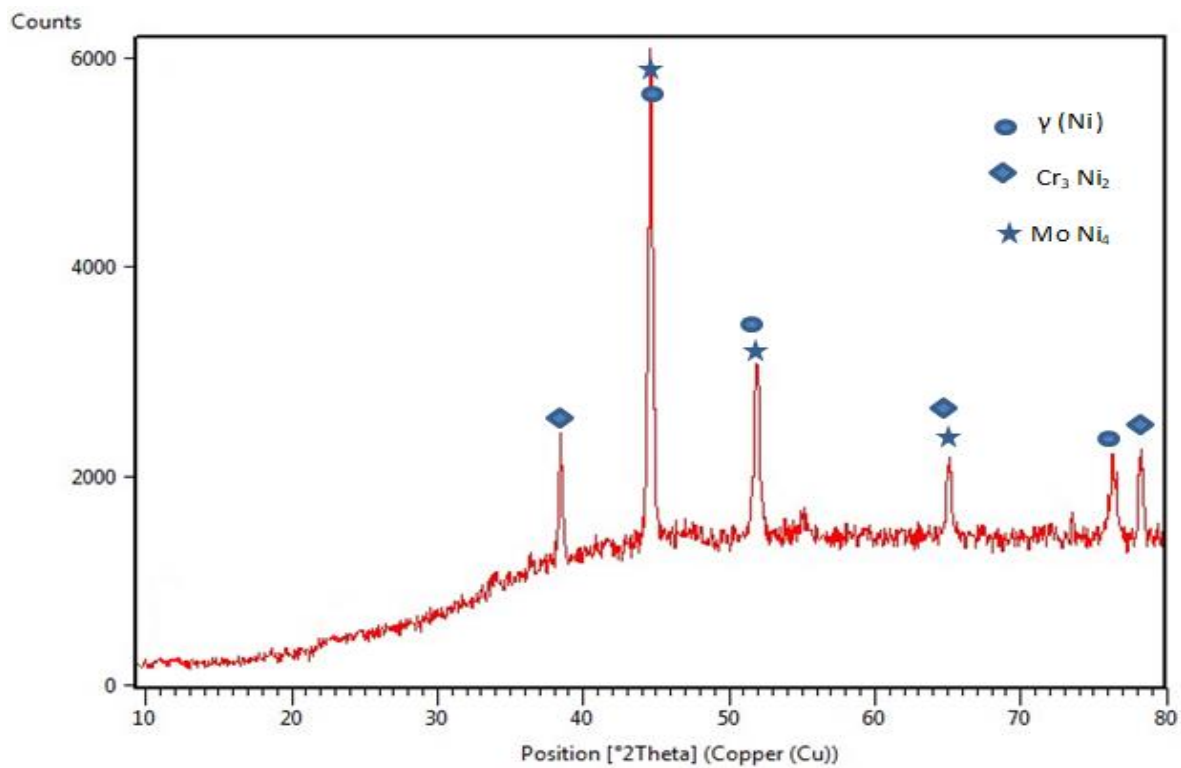


Figure (4.3): XRD patterns of the B3 alloy post the sintering

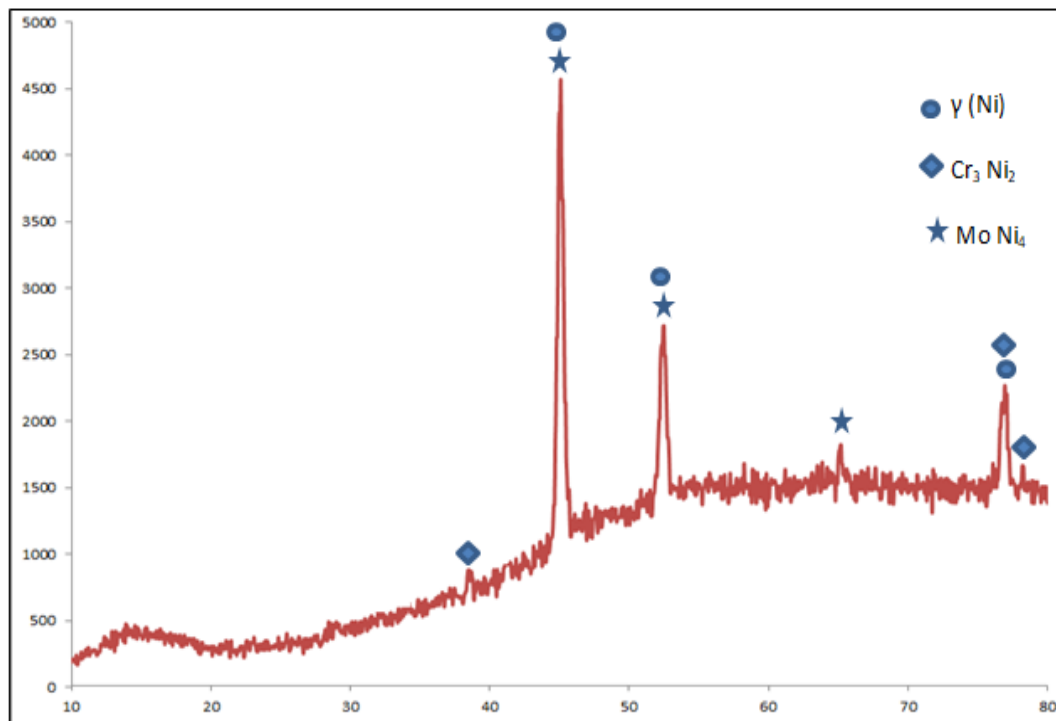
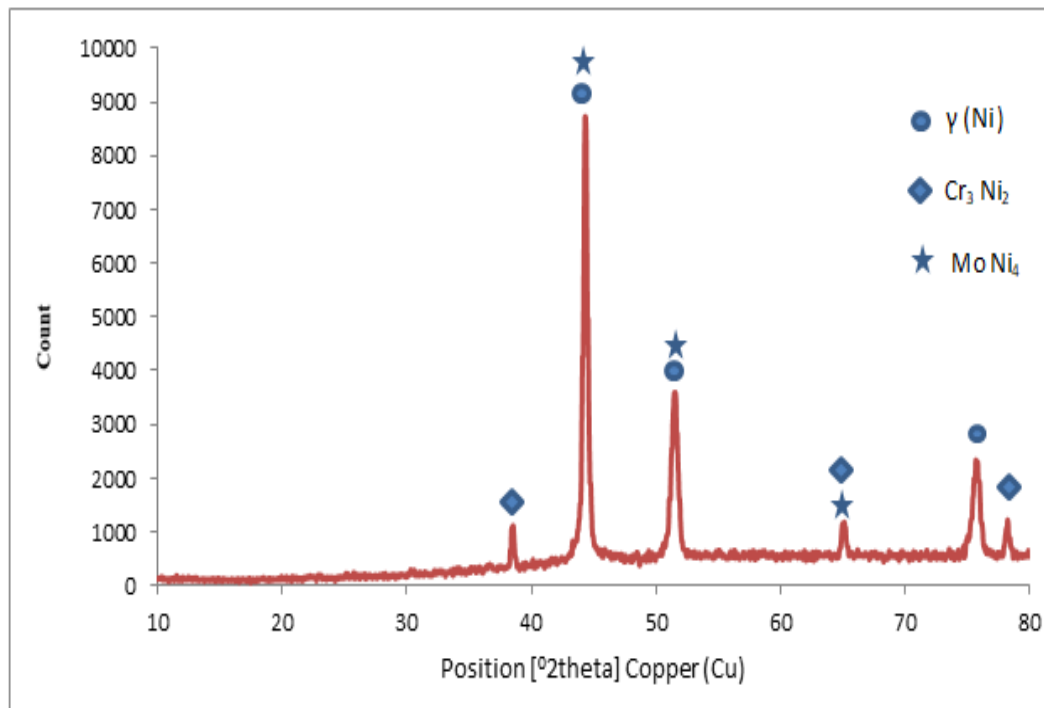


Figure (4.4): XRD patterns of the C3 alloy post the sintering



Figure(4.5): XRD patterns of the D3 alloy post the sintering

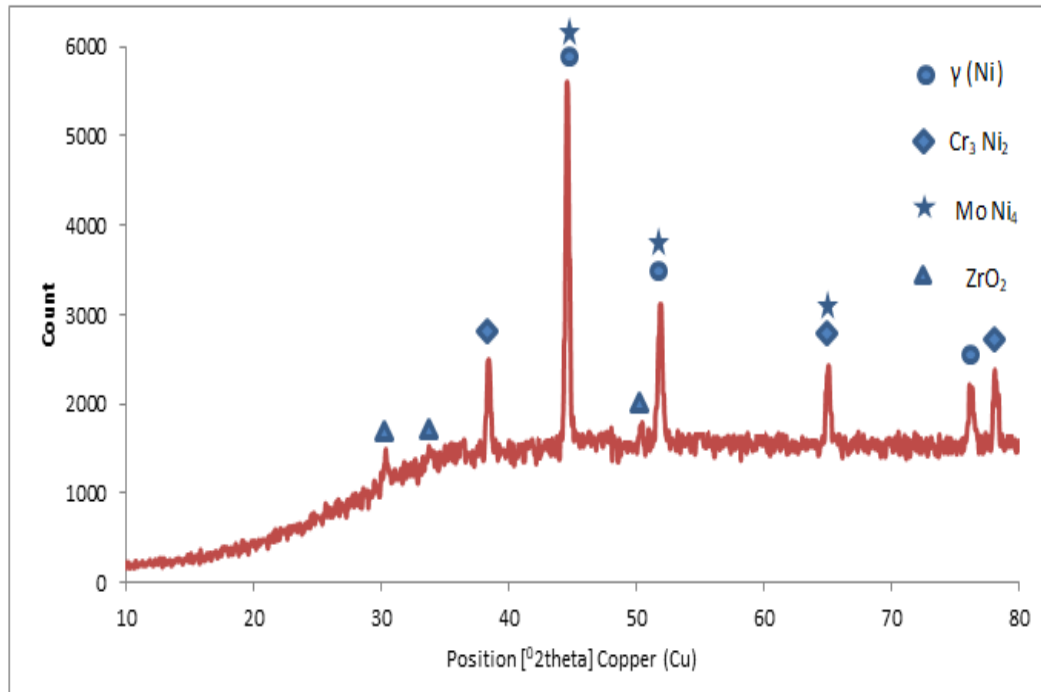
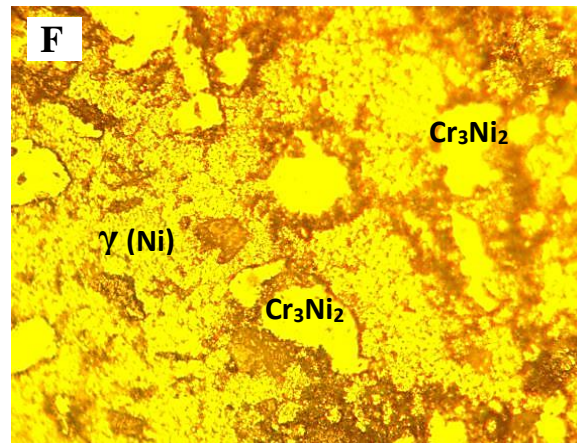
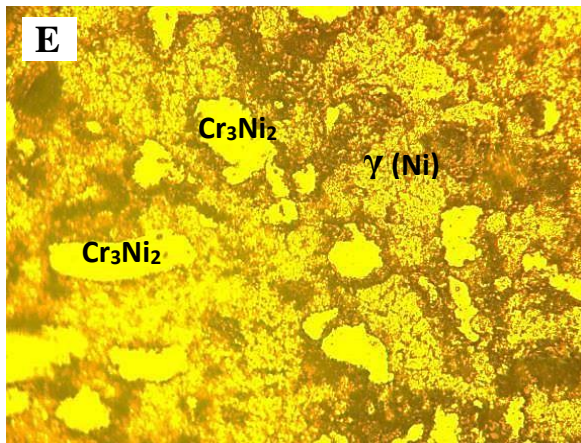
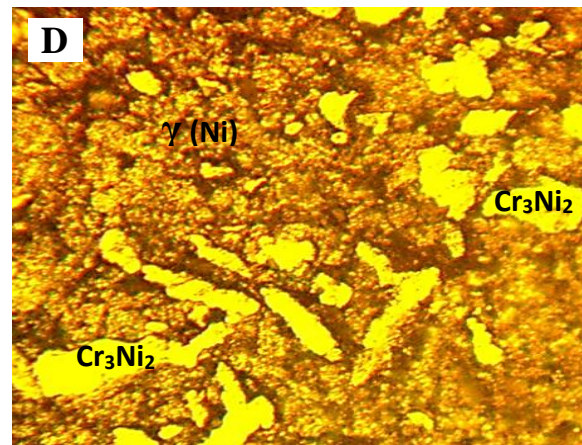
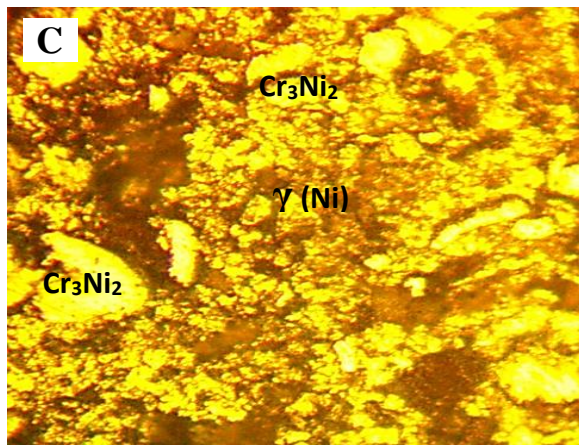
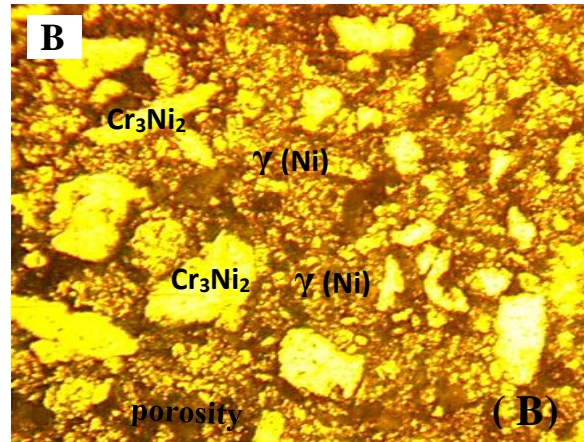
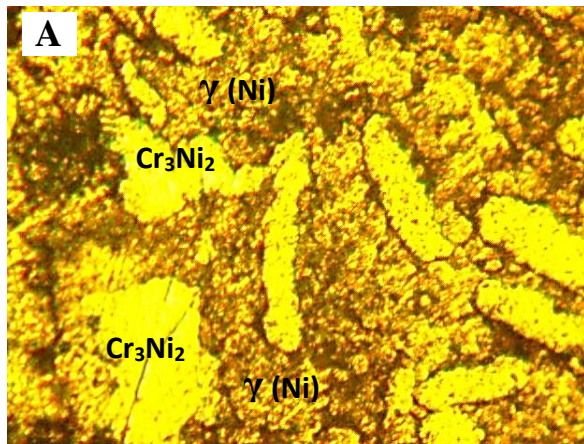


Figure (4.6): XRD patterns of the E2 alloy after sintering .

## 4.3 Microstructure Characterization

### 4.3.1 Light Optical Microscope

The metallography gives an idea about material micro-structure and its relationship to characteristics of material because the size, shape and distribution of the particles have significant effects upon behaviour of a material[110]. The compacted samples have been sintered at a temperature of 1000 °C for an 8 hr period, then the samples were grind, polished and etched. After that Optical microstructures image of the (Ni-Cr-Mo) alloy with and without addition are carried out for the samples, as shown in Figure (4.7). Figure (4.7) illustrated the microstructure of etched alloys after sintering process with 400x. The microstructure for alloys showed the grain boundaries, pores in different sizes and the present phases. There are many pores with different sizes can be seen on the surface, that is natural manner since the samples were prepared by powder metallurgy technique. The plates of  $\text{Cr}_3\text{Ni}_2$  dispersed in the matrix  $\gamma$  (Ni). the adding alloying elements (B,Zr,In, $\text{ZrO}_2$ ) effect on grain refinement and grain restricted growth rate. From the figures below, the effect of the added elements on the microstructure refining is not clearly visible because the optical magnification is low so FESEM was used for high magnification and resolution.



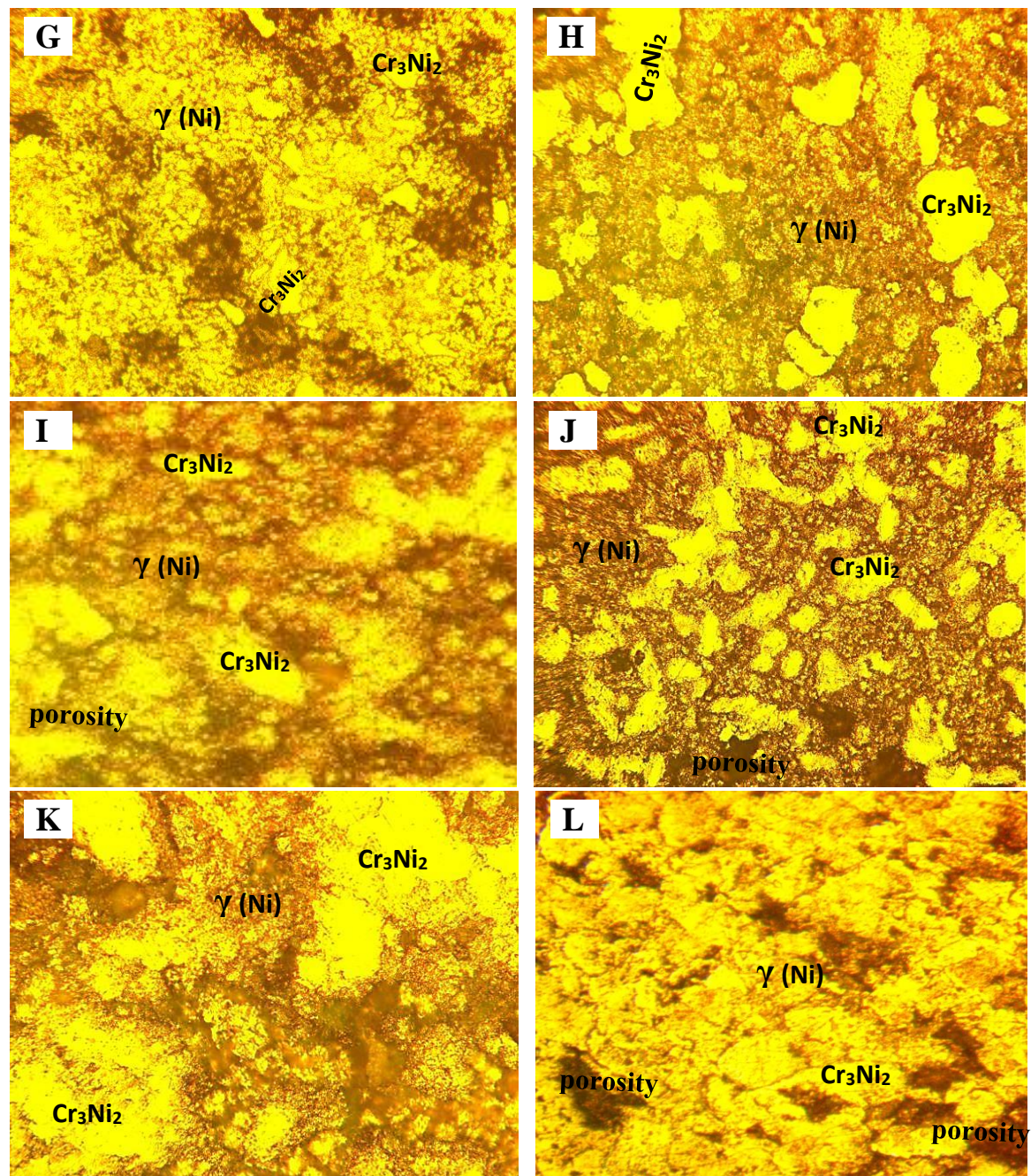


**Figure (4.7):** Microstructure for Sintered Alloys (400X): A) A Alloy, B) B<sub>1</sub> Alloy, C) B<sub>2</sub> Alloy, D) B<sub>3</sub> Alloy, E) C<sub>1</sub> Alloy, F) C<sub>2</sub> Alloy, G) C<sub>3</sub>Alloy, H) D<sub>1</sub> Alloy, I) D<sub>2</sub> Alloy and J) D<sub>3</sub>Alloy, K) E<sub>1</sub> Alloy, L) E<sub>3</sub> Alloy .

### 4.3.2 Field Emission Scanning Electron Microscopy (FESEM)

The microstructure of the specimens surfaces was studied by using FESEM test in both secondary electron (SE) and back scattered electron (BSE) mods. The figure (4.8) shows the FESEM of (A) alloy without addition in different magnification. The solid solution  $\gamma$  (Ni) and the phase ( $\text{Cr}_3\text{Ni}_2$ ) are distributed over it. The figure (4.9) showed, the effect of adding (0.4%) B in microstructure of base alloy (A) is clear, as the refining of the particles is due to the effect of the B addition in impeding the growth rate of the particles as a result of their regular distribution on the base alloy. The refining process that occurs in the base alloy when alloying elements are added is due to the formation of secondary phases or the dissolution of the elements in the alloy [111]. From the figures (4.9-4.10), it was observed that the presence of boron led to a refining of the grain size. The addition of boron is very effective in refining the particle size of the base alloy, this is due to the fact that the boron will diffuse on the grain boundaries and prevent the grain growth of the  $\gamma$  (Ni) phase this agree with [111]. Figures (4.11-4.12) illustrated the effect of adding Zr on microstructure of base alloy. FESEM images showed that the addition of zirconium affected the microstructure of the base alloy. The addition of zirconium led to a reduction in the grain size of the alloy. The refining increase with increase of Zr content in the alloy.

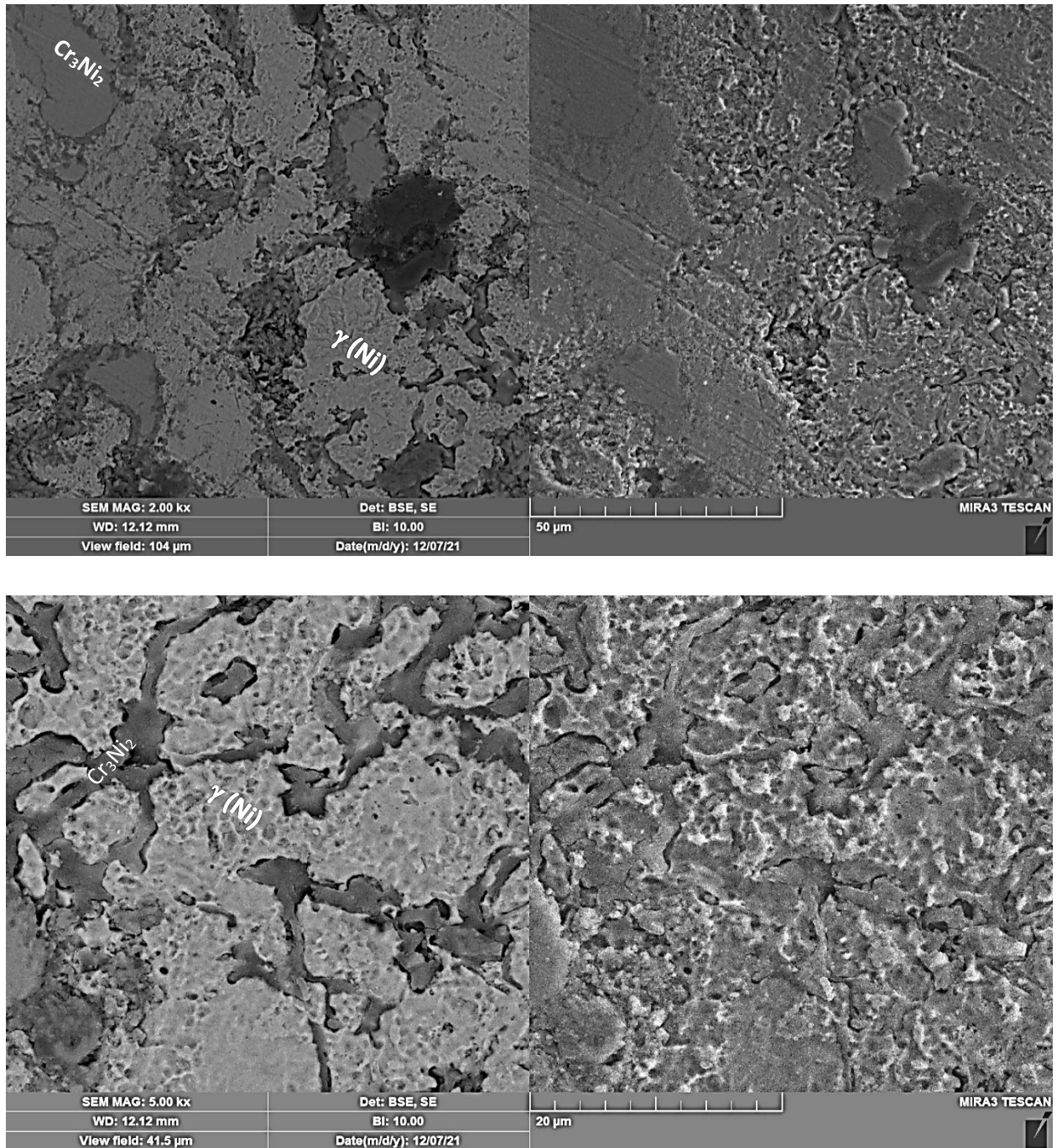


Figure (4.8) FESEM images for A alloy with different magnification

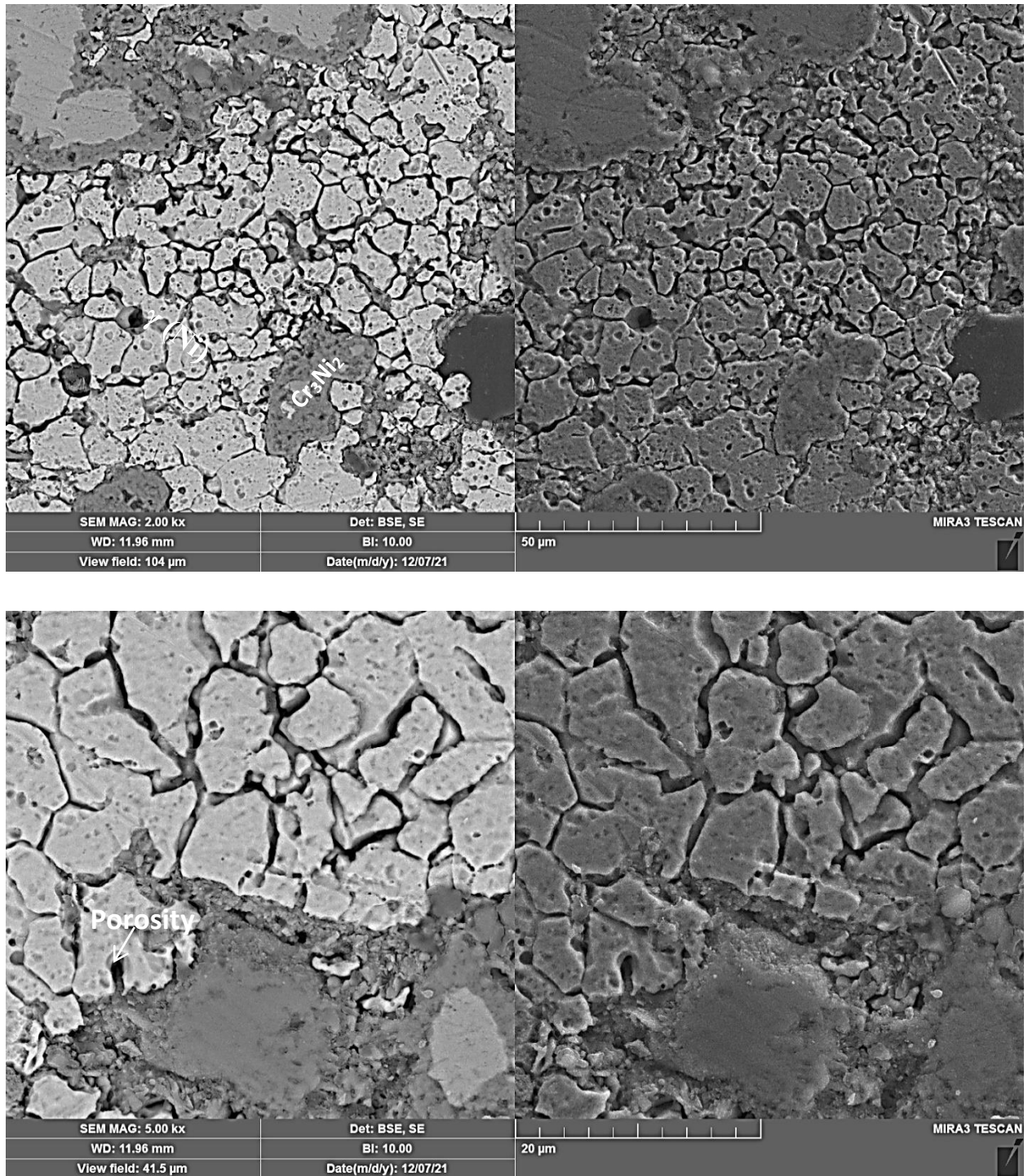


Figure (4.9) FESEM images for B<sub>1</sub> alloy with different magnification

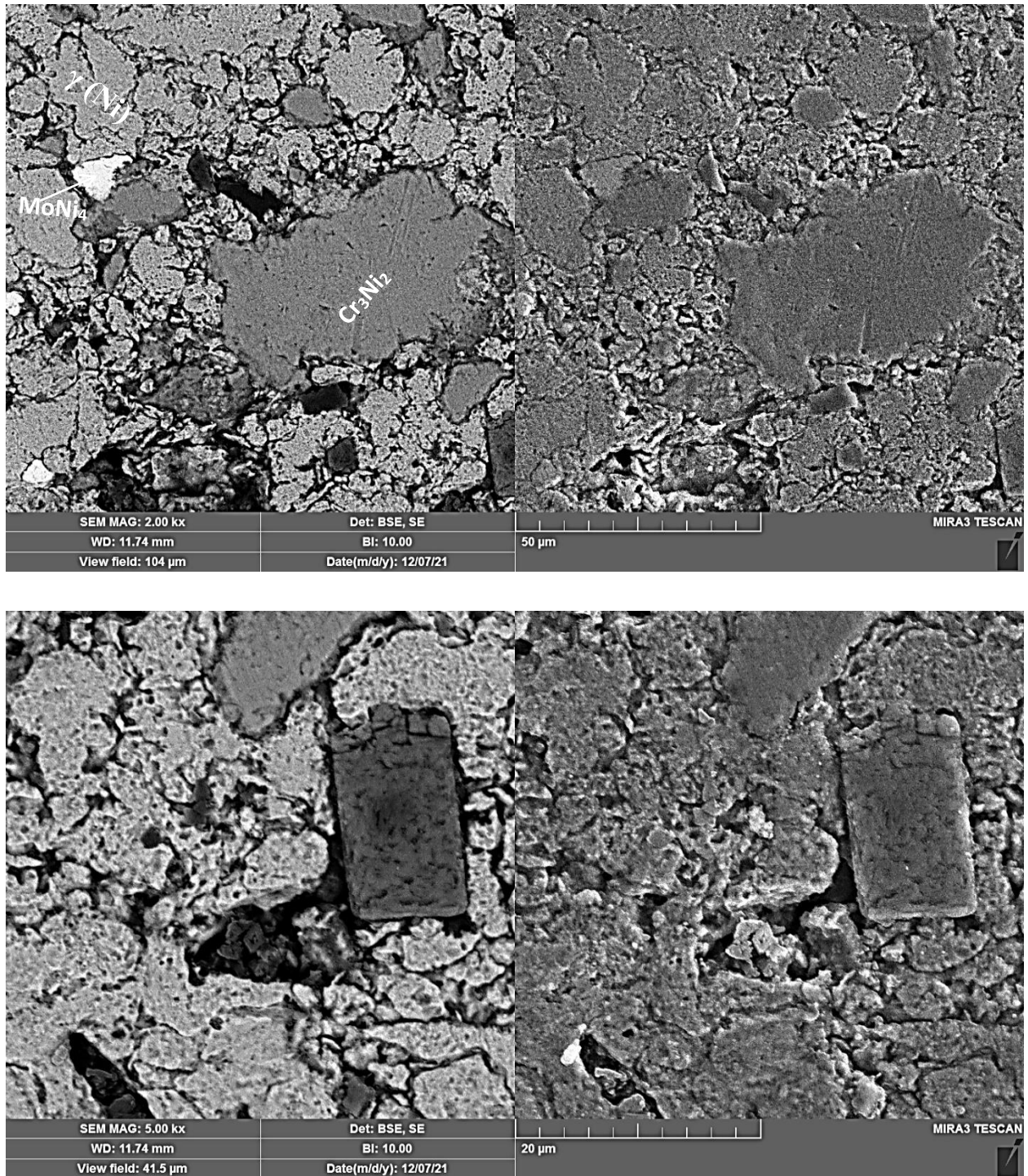


Figure (4.10) FESEM images for B<sub>3</sub> alloy with different magnification

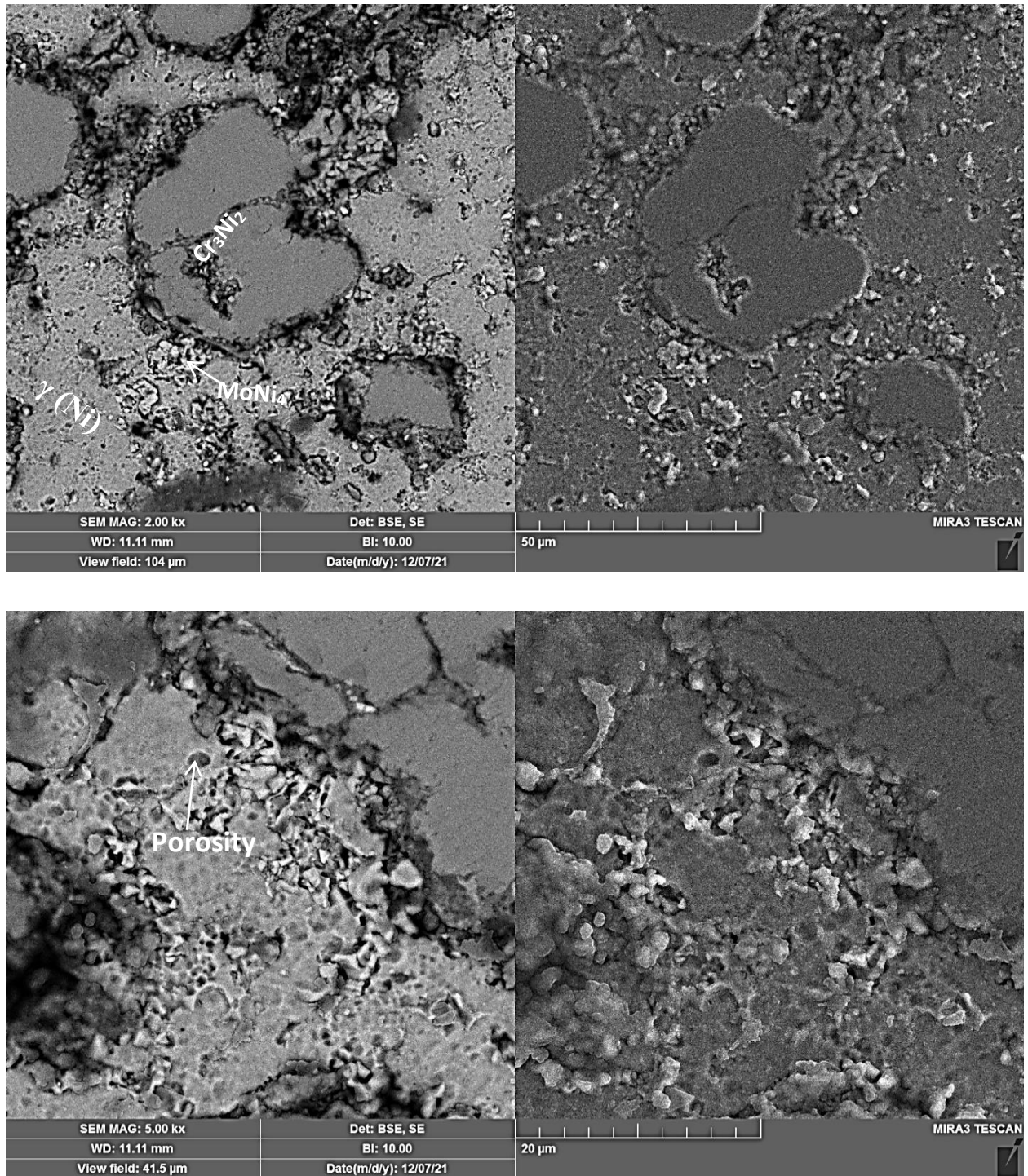


Figure (4.11) FESEM images for C<sub>1</sub> alloy with different magnification

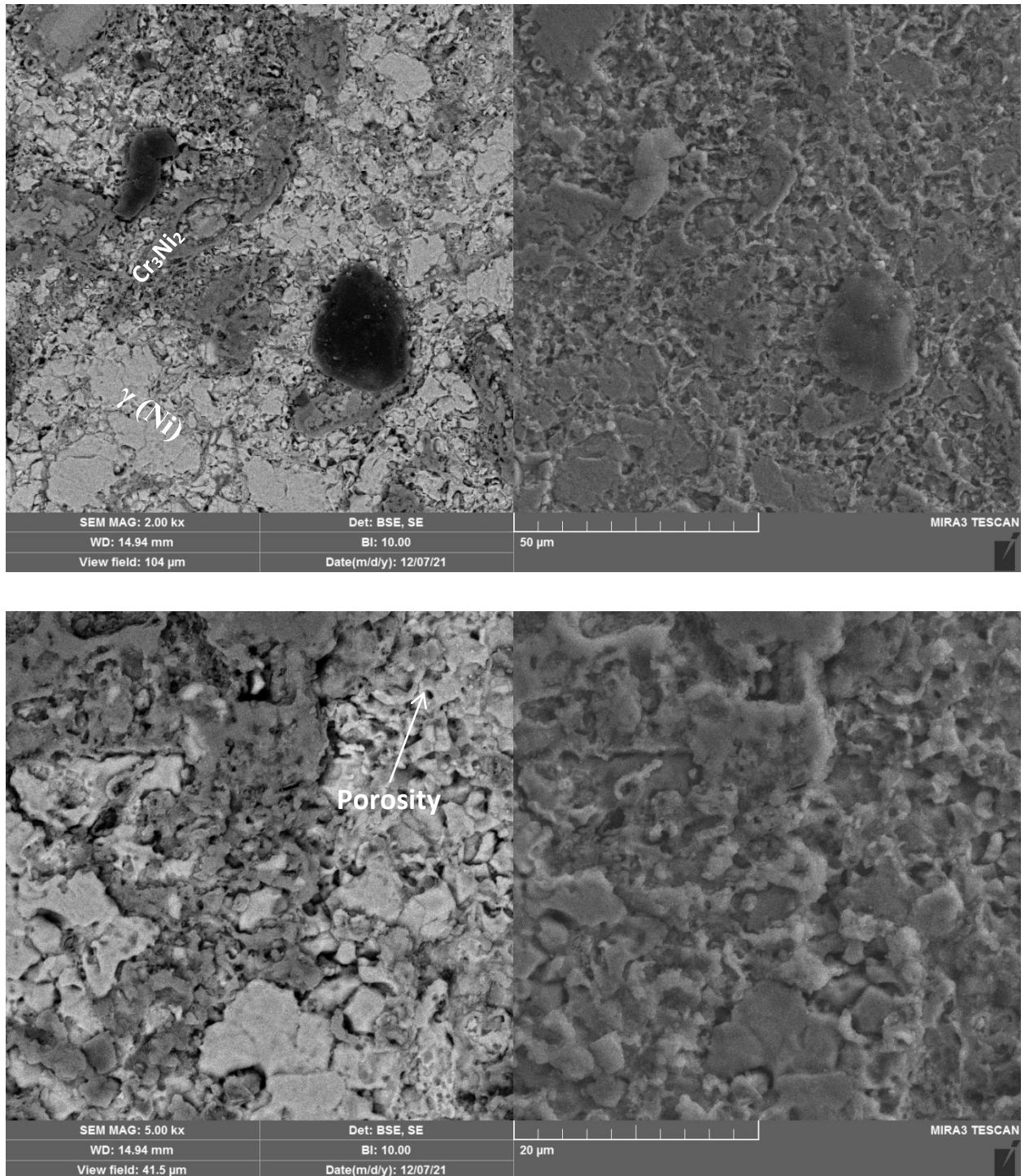
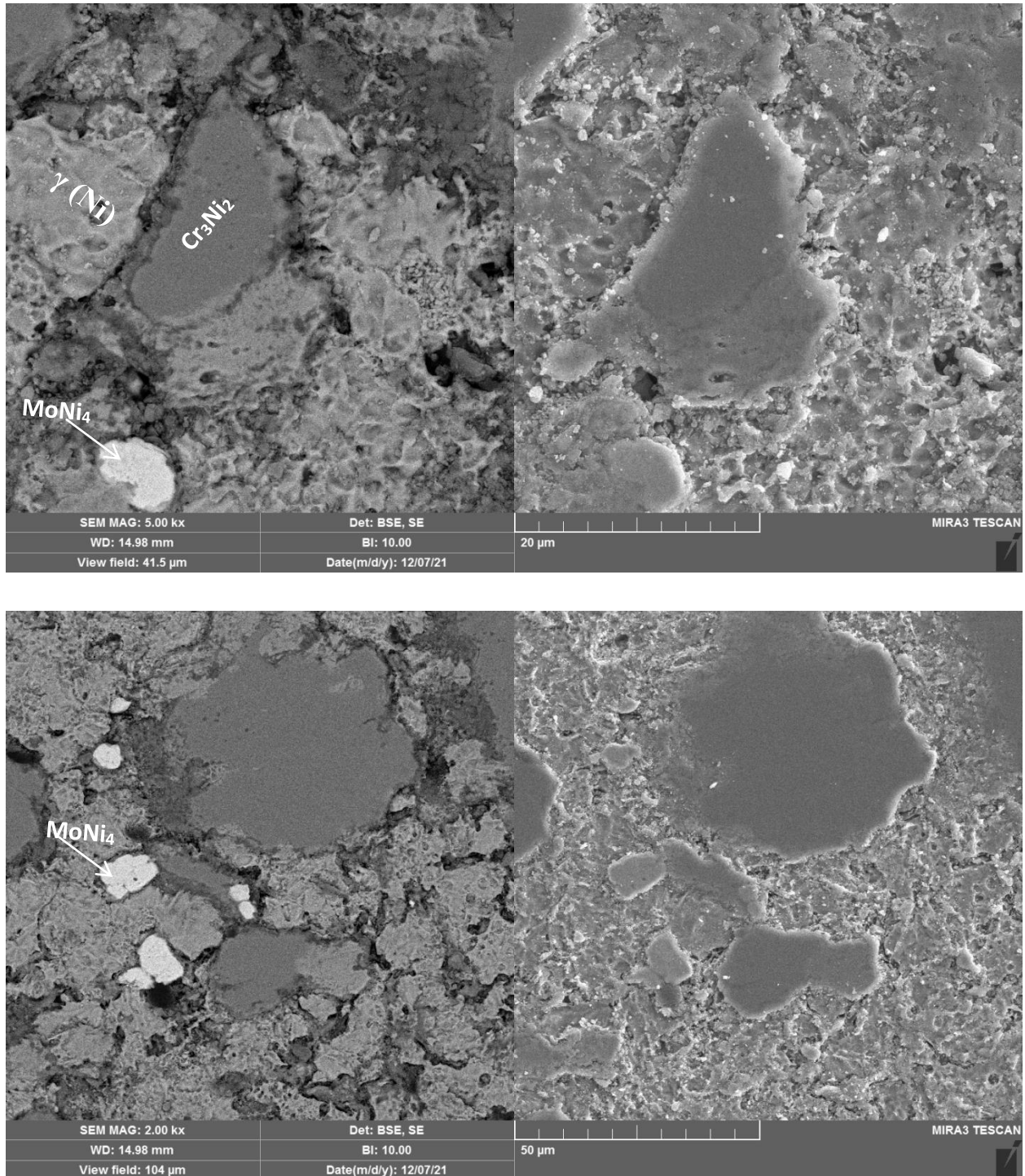


Figure (4.12) FESEM images for C3 alloy with different magnification.

Figures (4.13-4.14) showed the effect of adding Indium on microstructure of base alloy.



**Figure (4.13) FESEM images for  $D_1$  alloy with different magnification**

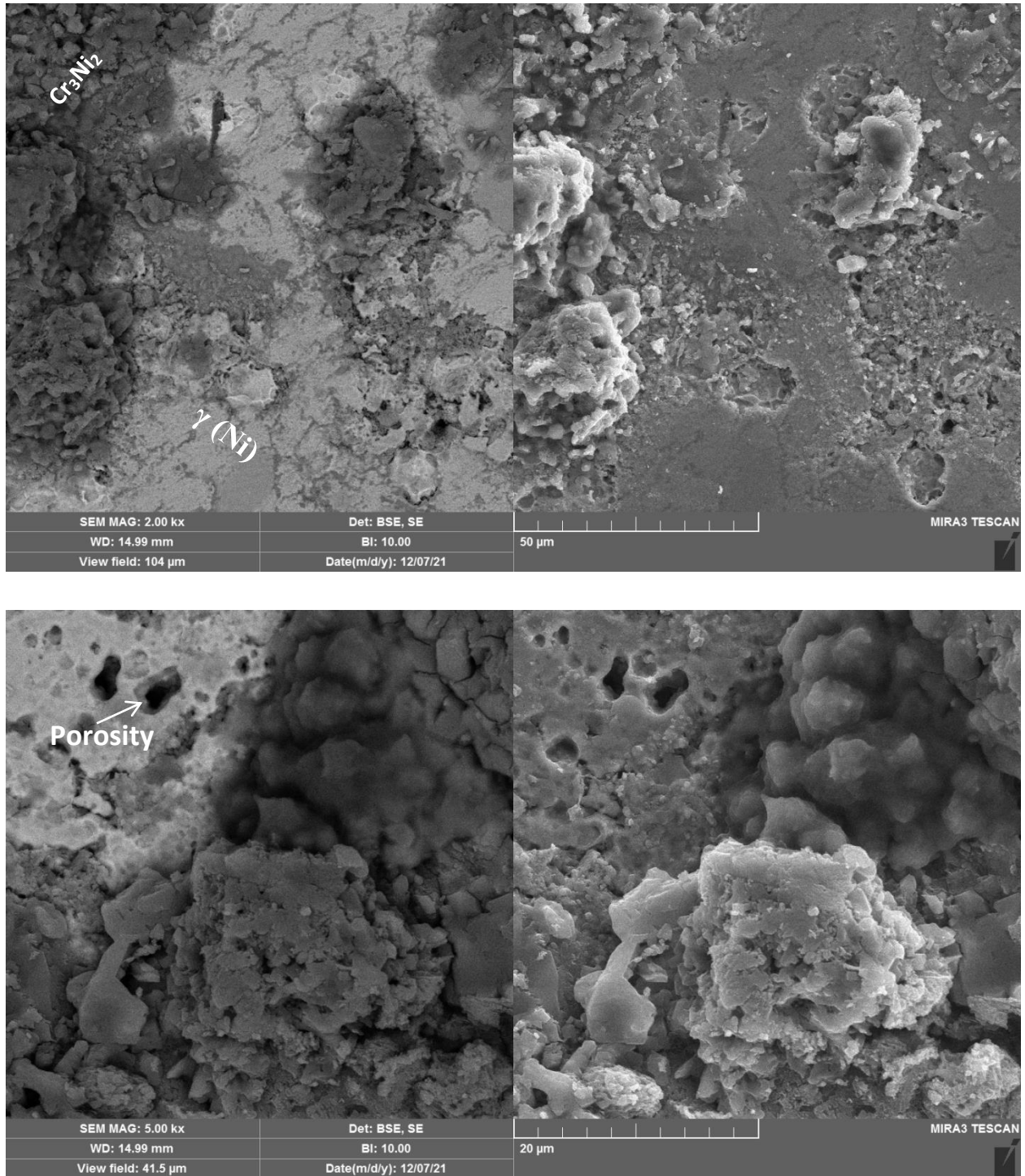


Figure (4.14) FESEM images for D<sub>3</sub> alloy with different magnification

Figures (4.15-4.16) showed the effect of adding Zirconia on microstructure of base alloy. The white particles refer to zirconia and are scattered regularly in the matrix.

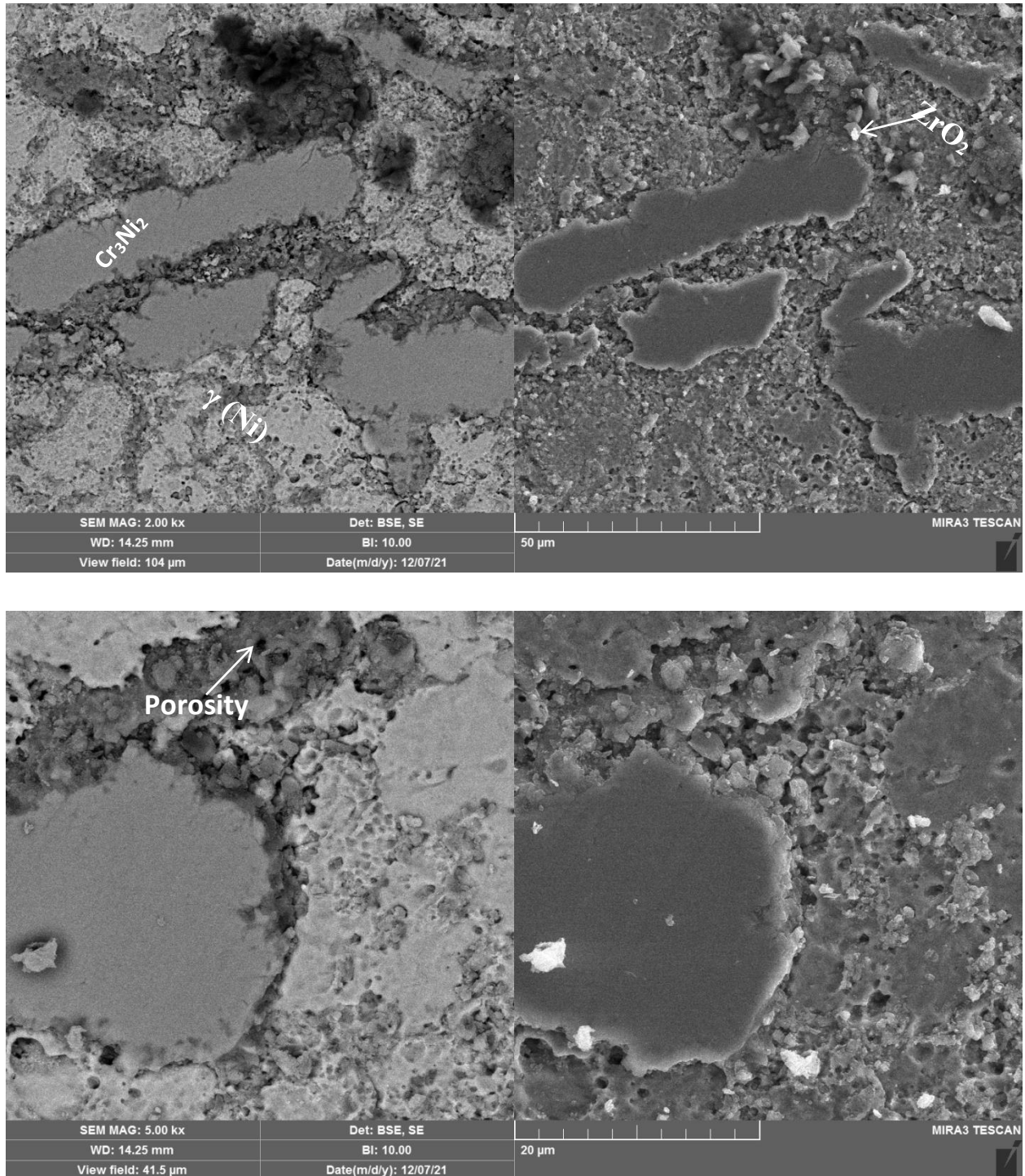


Figure (4.15) FESEM images for E<sub>1</sub> alloy with different magnification.

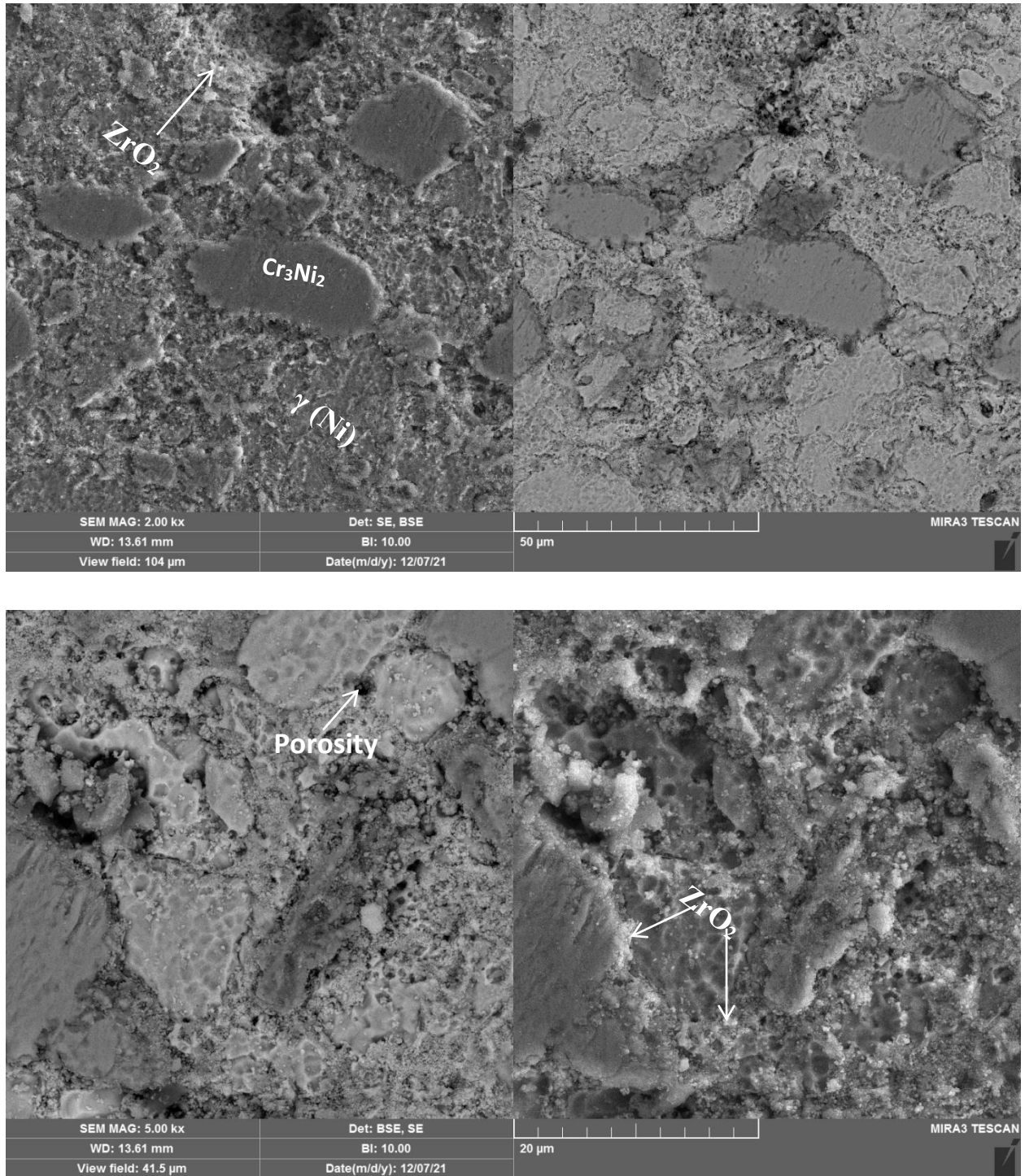


Figure (4.16) FESEM images for E3 alloy with different magnification

### 4.3.3 Energy Dispersive X-ray Spectroscopy (EDX)

Energy dispersive spectroscopy (EDX) utilized a high-energy focused electron beam to emit an X-ray spectrum of a solid specimen. EDX is able to identify the chemical composition that results from the contrast topography differences on an SEM image. Precision obtained from specimens is limited by statistical error. EDX was scanned on several different polished specimens. The chemical composition of the alloy and the distribution of the elements can be observed by the EDX test. A specific area of the alloy was taken and the elements in it were analyzed in the form of a map, where each element in the alloy is given a specific color through which the distribution of the element in the alloy can be observed. Figures (4.17) showed the EDX test of (A) alloys. By observing the images, it was noticed how the elements are distributed uniformly and homogeneously in the alloys. The test was in the form of a map where for each element there is a color that indicates it in order to be distinguished from the rest of the elements. Figures (4.18-4.20) illustrated the EDX test of alloy with boron addition. It is good distributed in the structures which indicate the successful mixing method and procedure. In figures (4.21-4.23) showed the EDX test of the Zr distribution in base alloy. Where it was noticed that there is homogeneity and regularity in the distribution of elements in the alloy. Figures (4.24-4.26) showed the EDX test of the In distribution in base alloy. Figures (4.27-4.29) showed the EDX test of the  $ZrO_2$  distribution in base alloy.

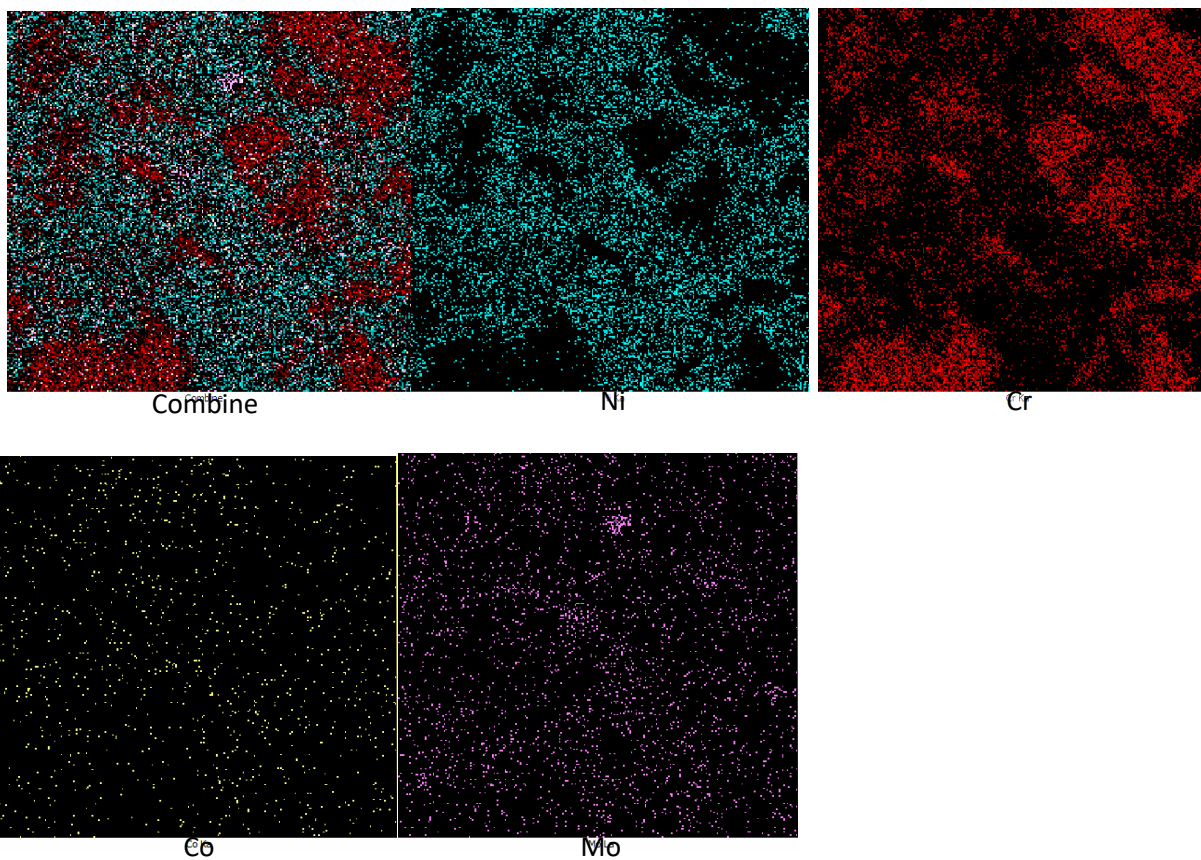
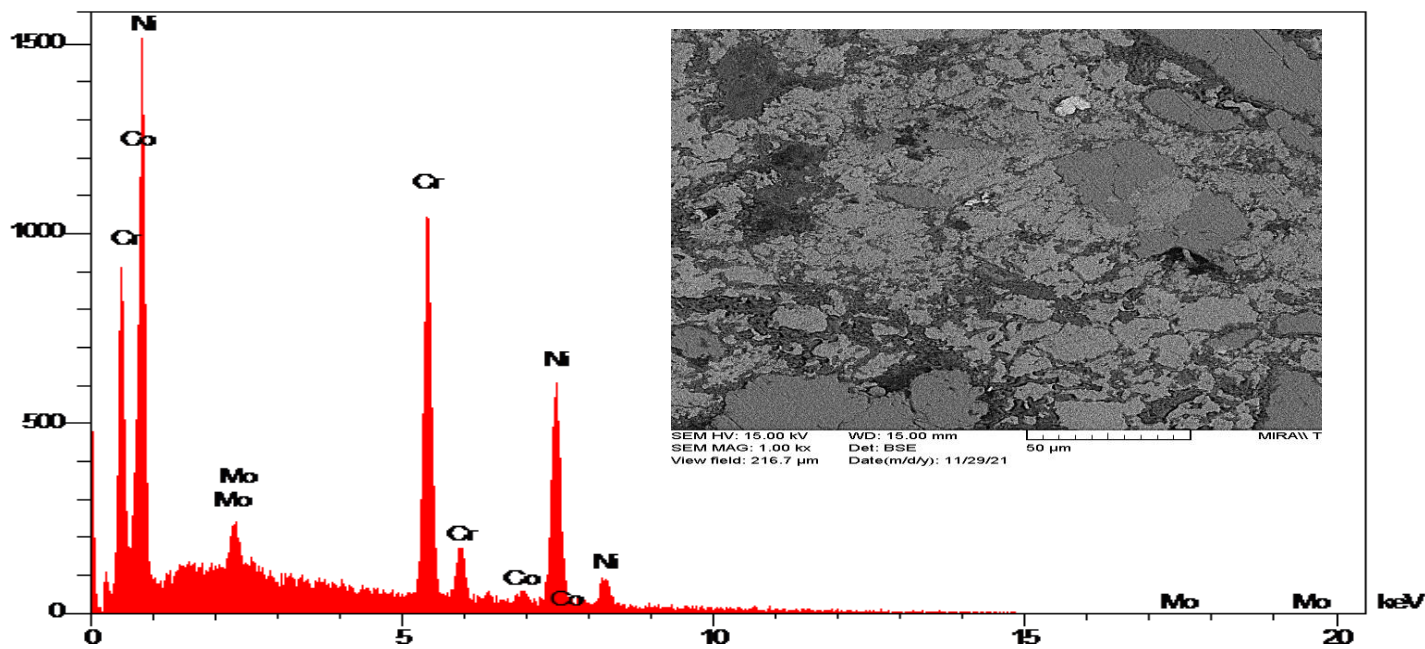


Figure (4.17):EDX for the A alloy

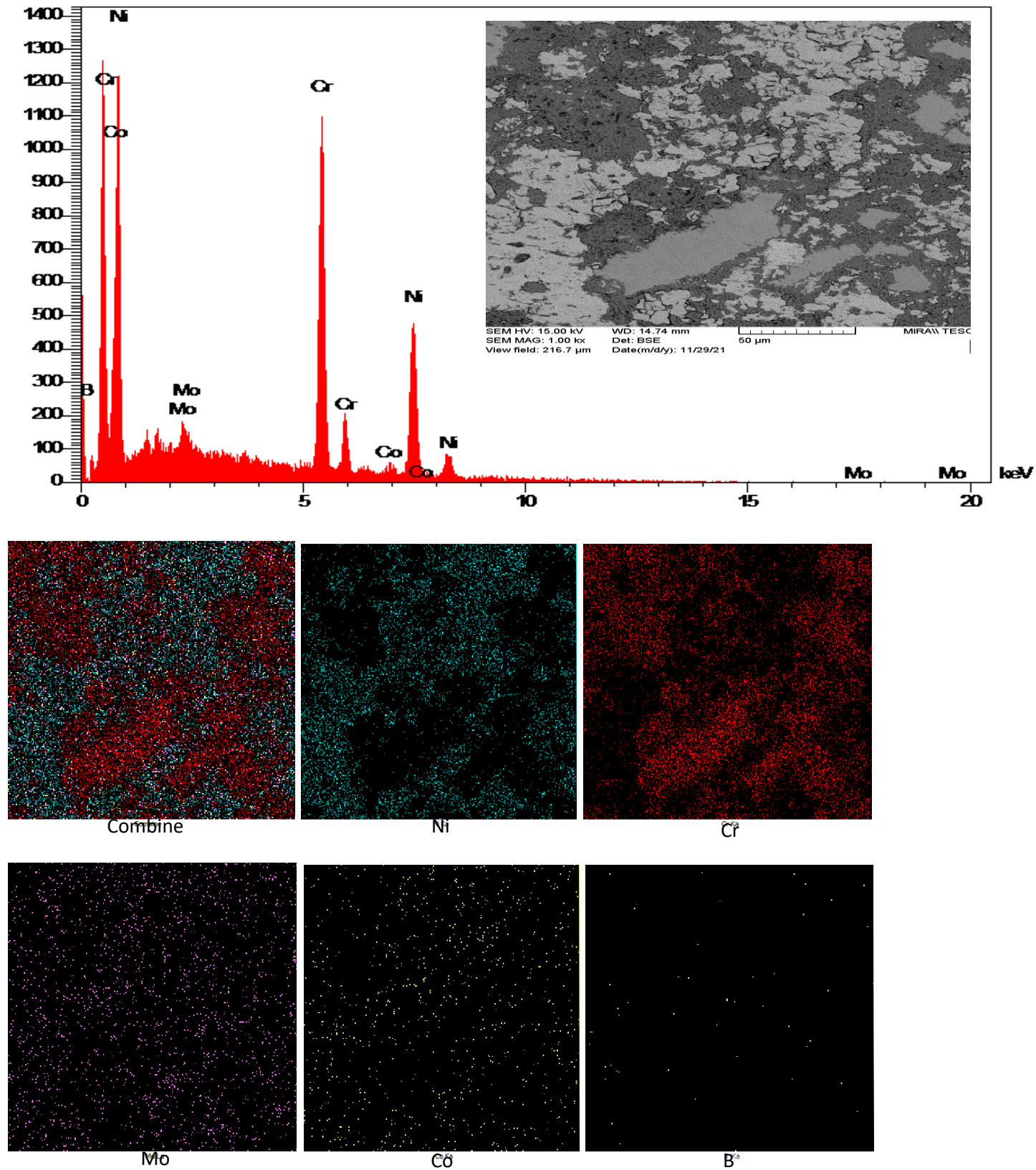


Figure (4.18): EDX for the B<sub>1</sub> alloy

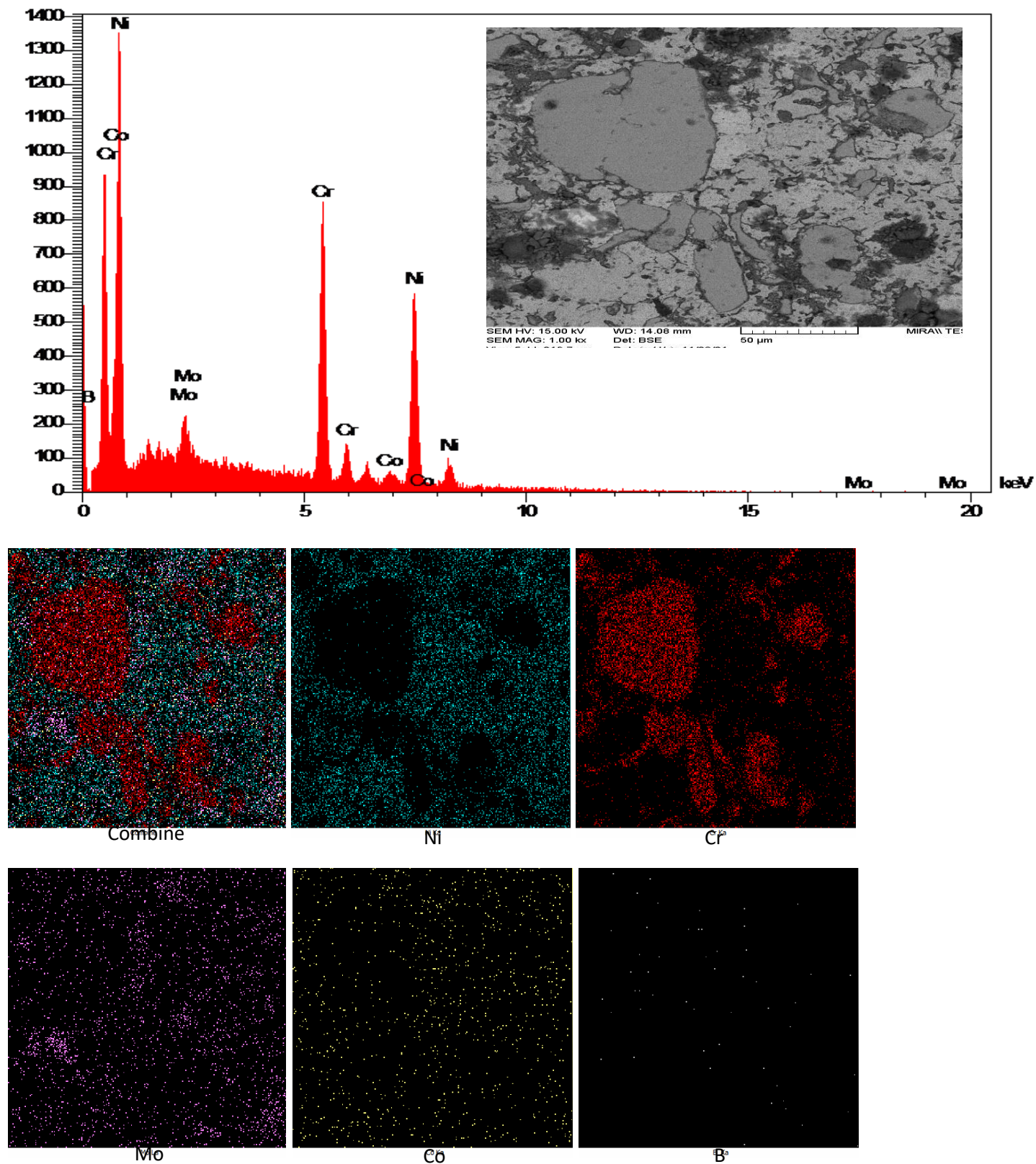


Figure (4.19):EDX for the B<sub>2</sub> alloy

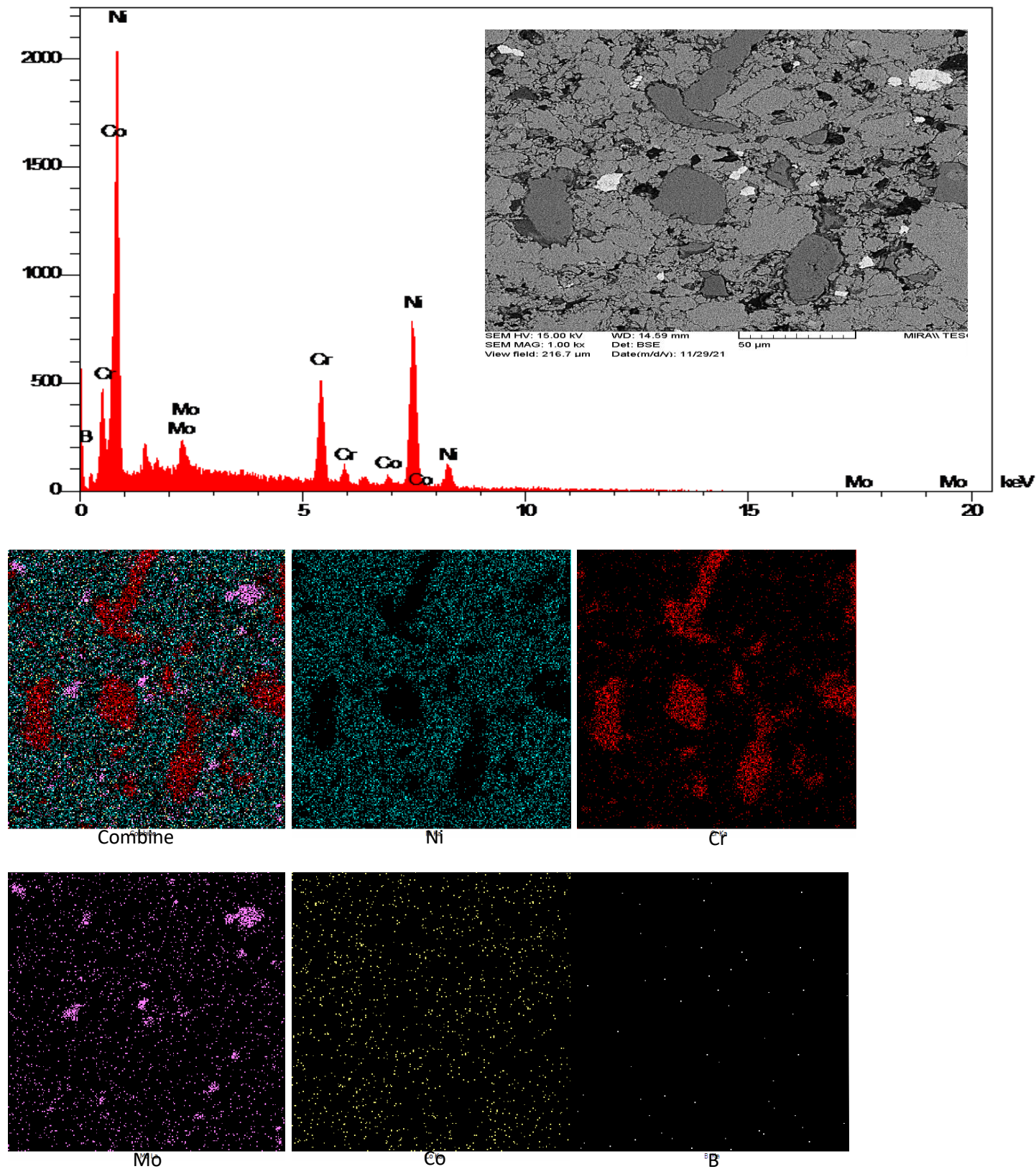
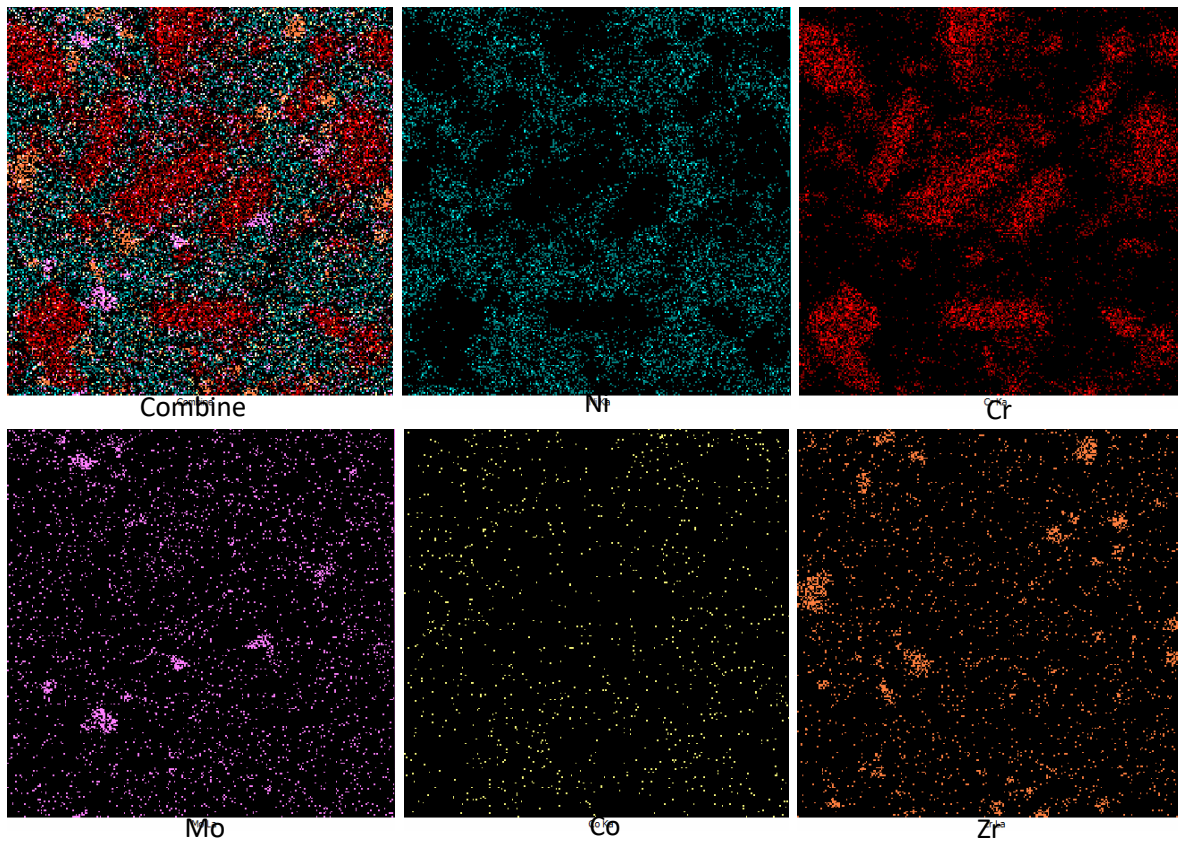
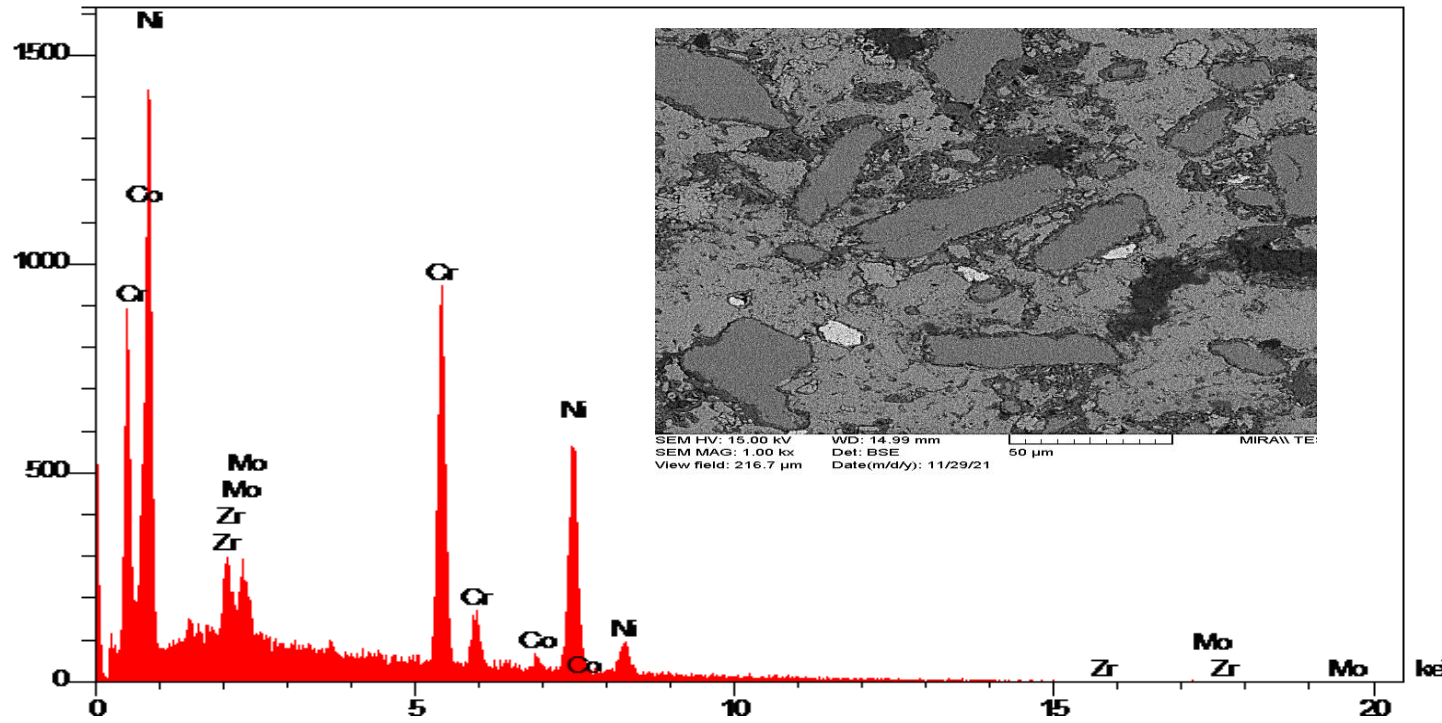
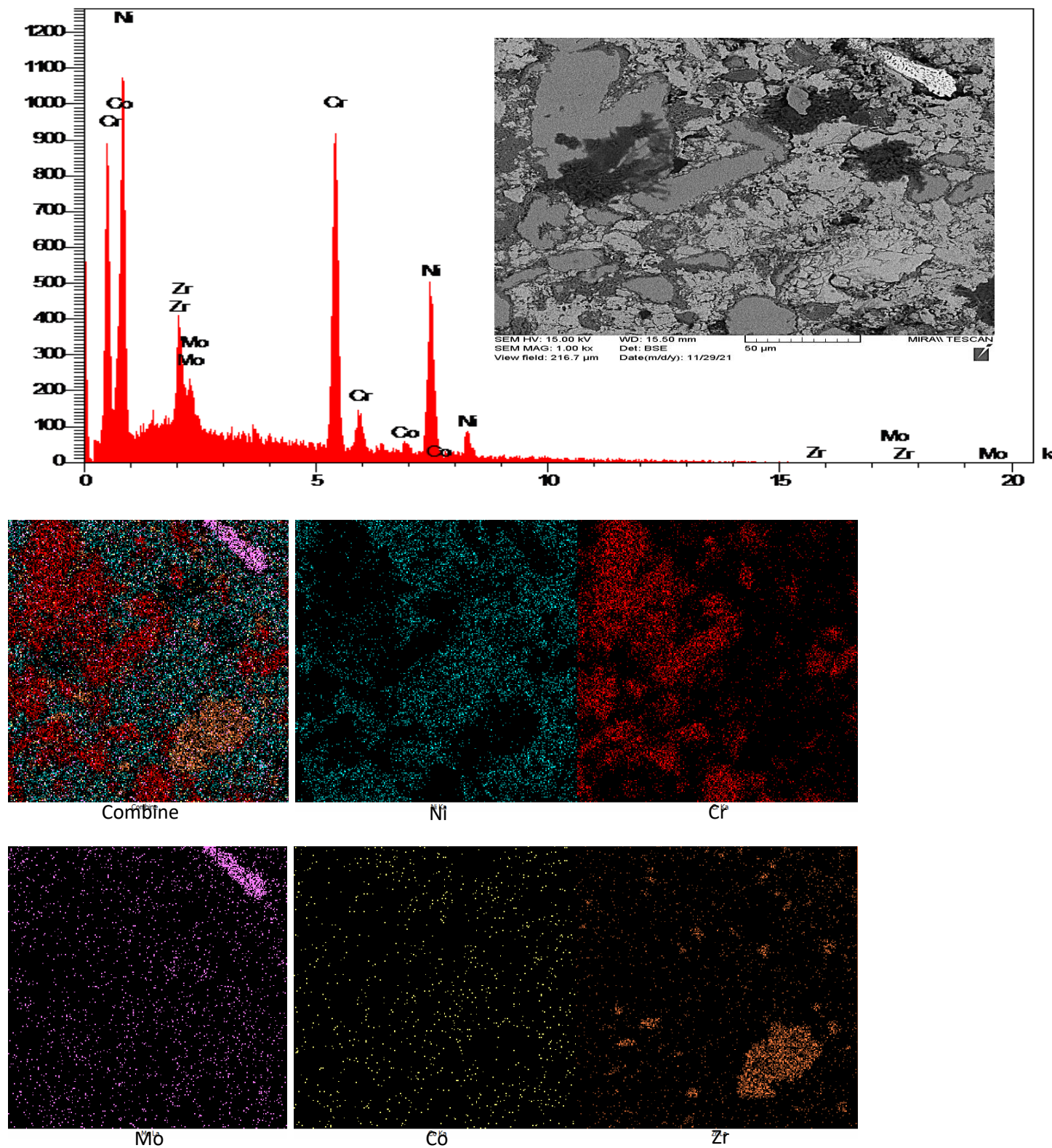


Figure (4.20):EDX for the B<sub>3</sub> alloy



Figure(4.21):EDX for C<sub>1</sub> alloy



Figure(4.22): EDX for the C<sub>2</sub> alloy

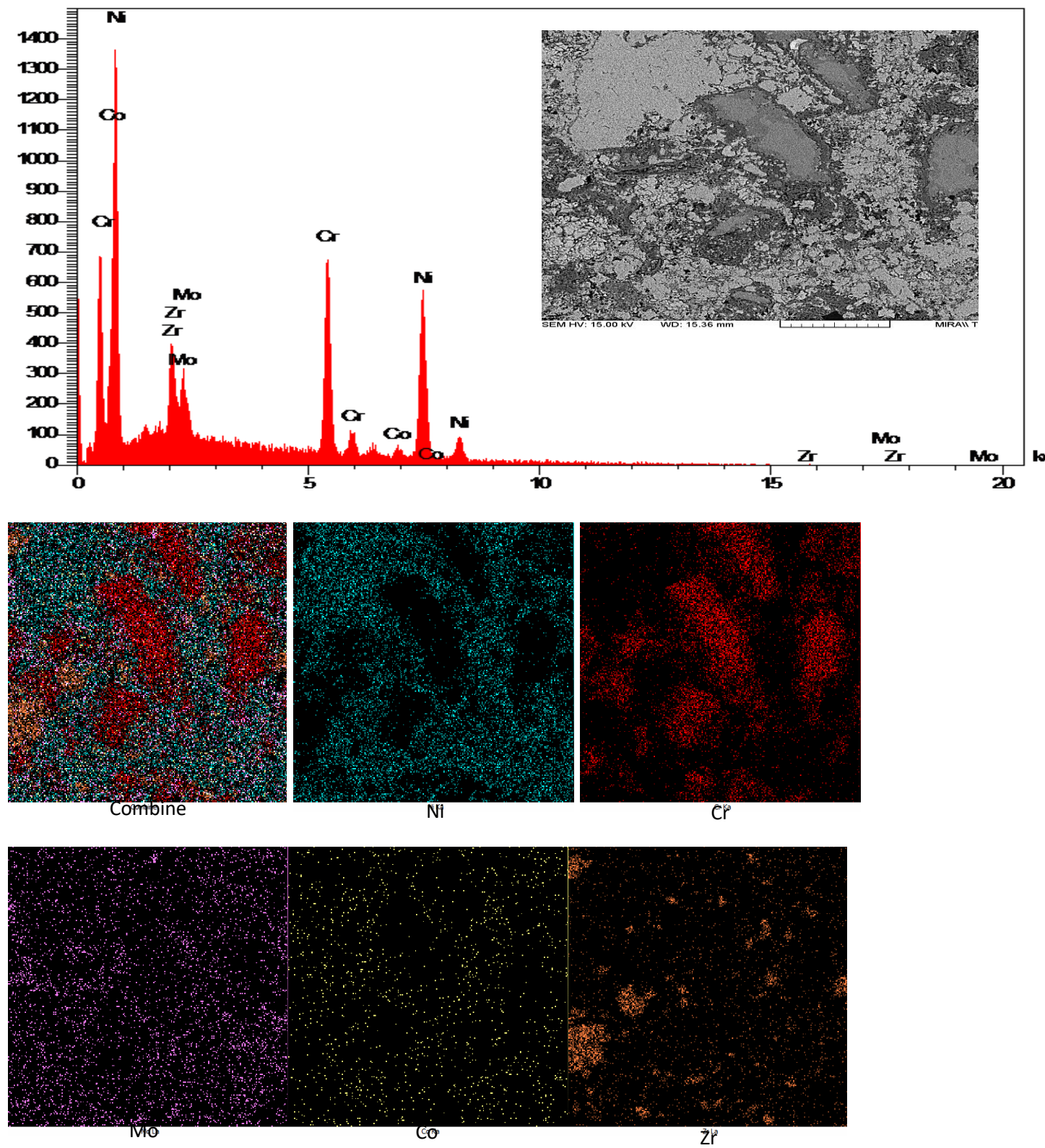
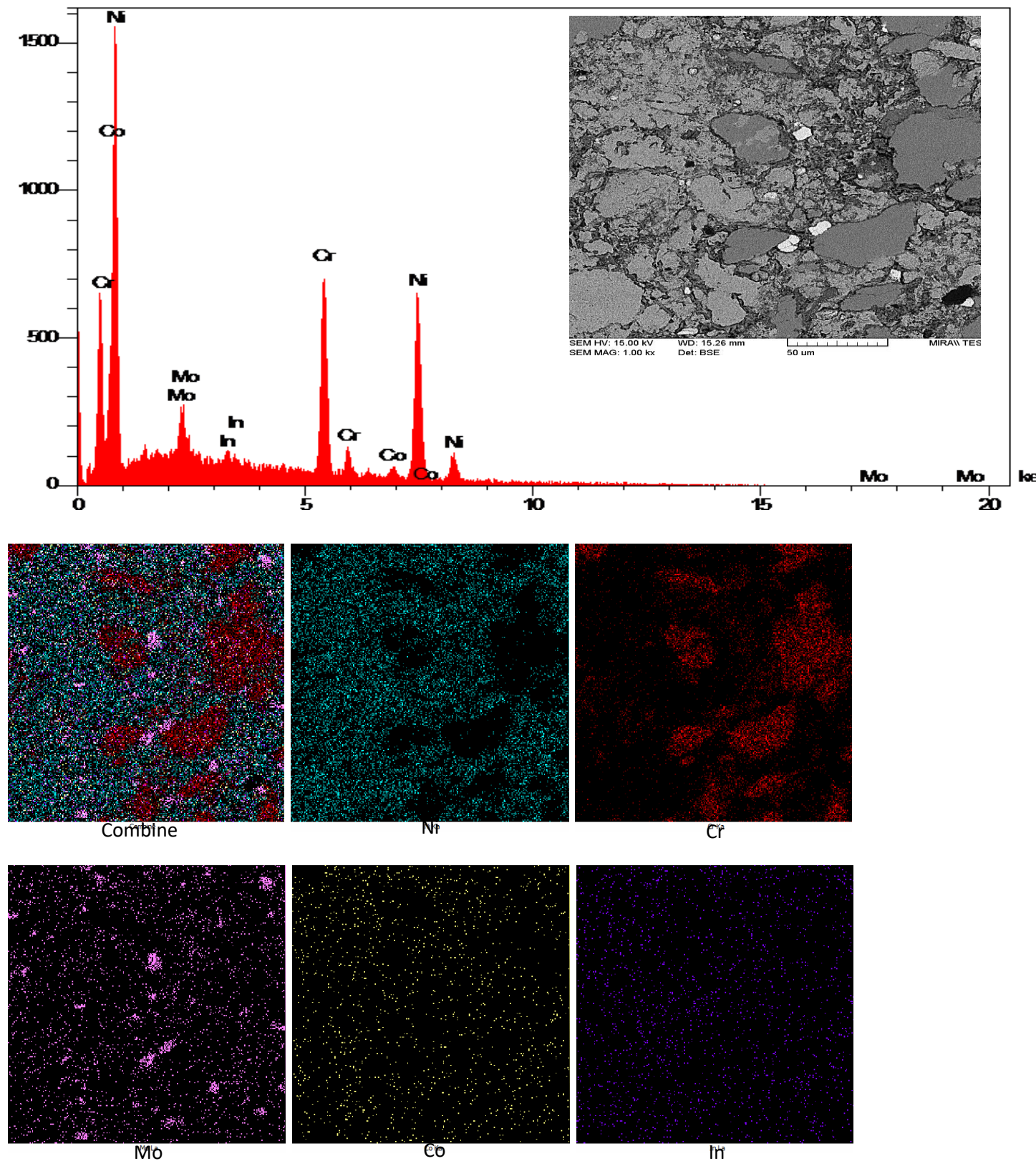
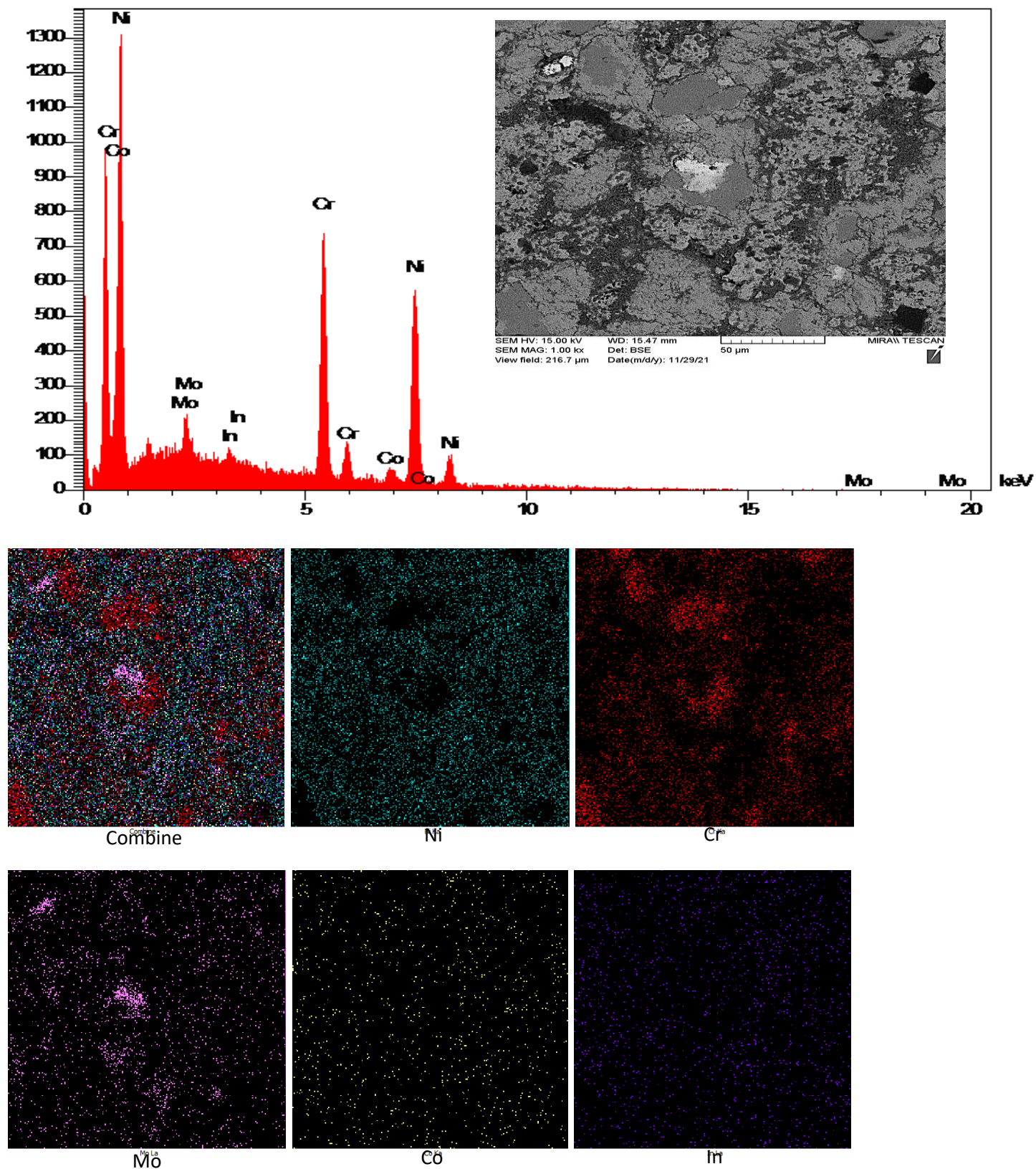


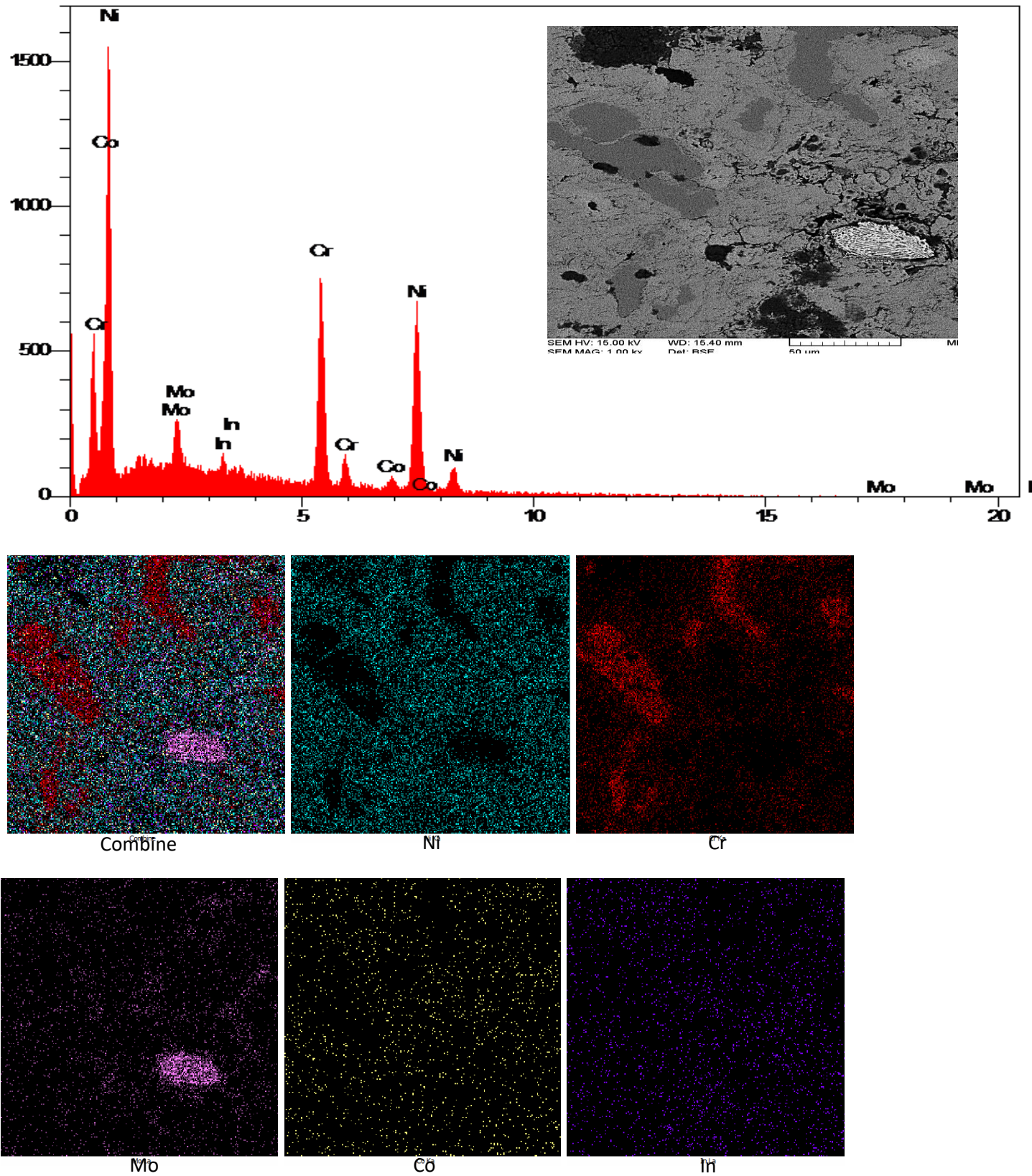
Figure (4. 23): EDX for C<sub>3</sub> alloy



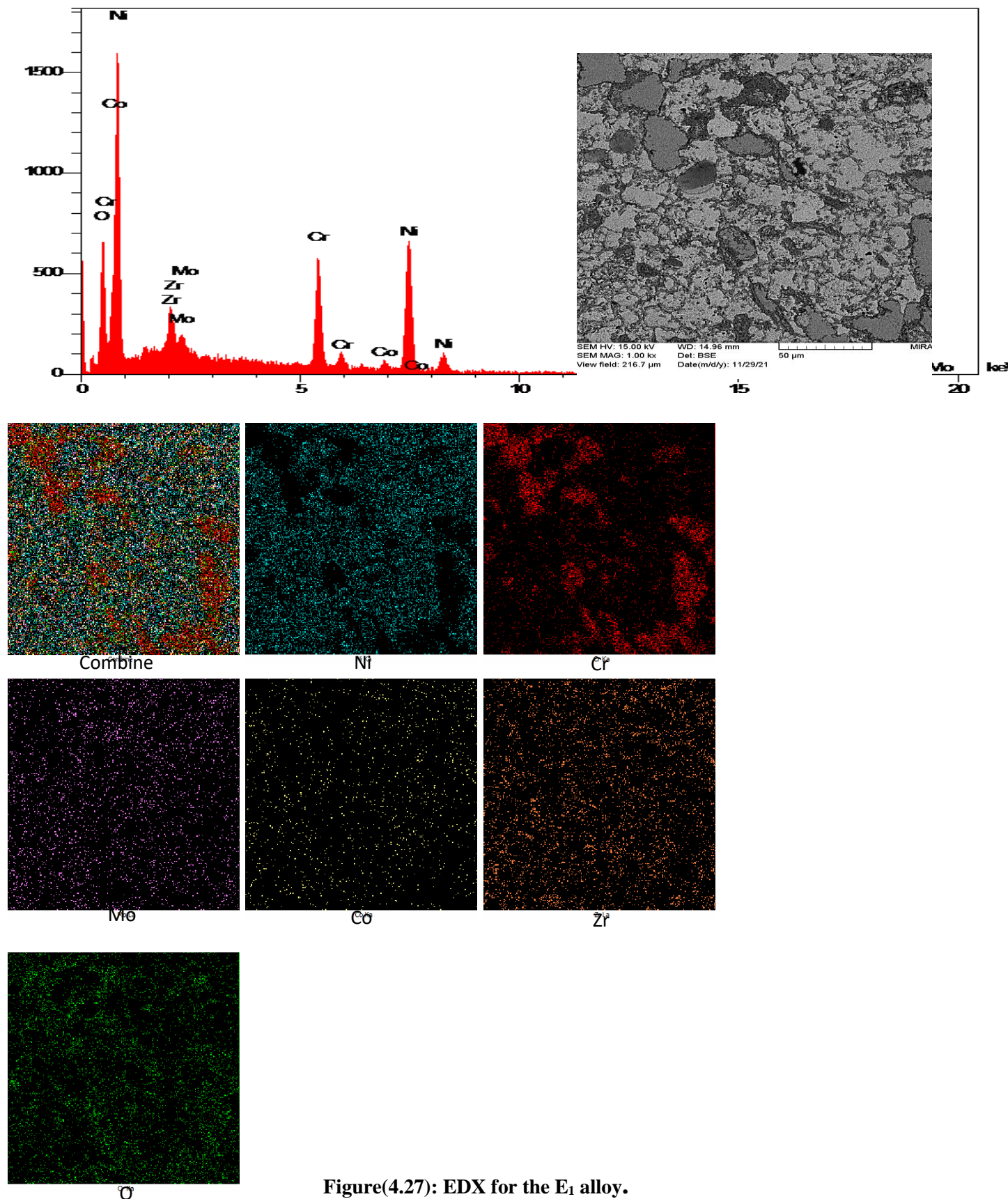
Figure(4.24):EDX for D<sub>1</sub> alloy



Figure(4.25):EDS for D<sub>2</sub> alloy



Figure(4.26):EDX for D<sub>3</sub> alloy



Figure(4.27): EDX for the E<sub>1</sub> alloy.

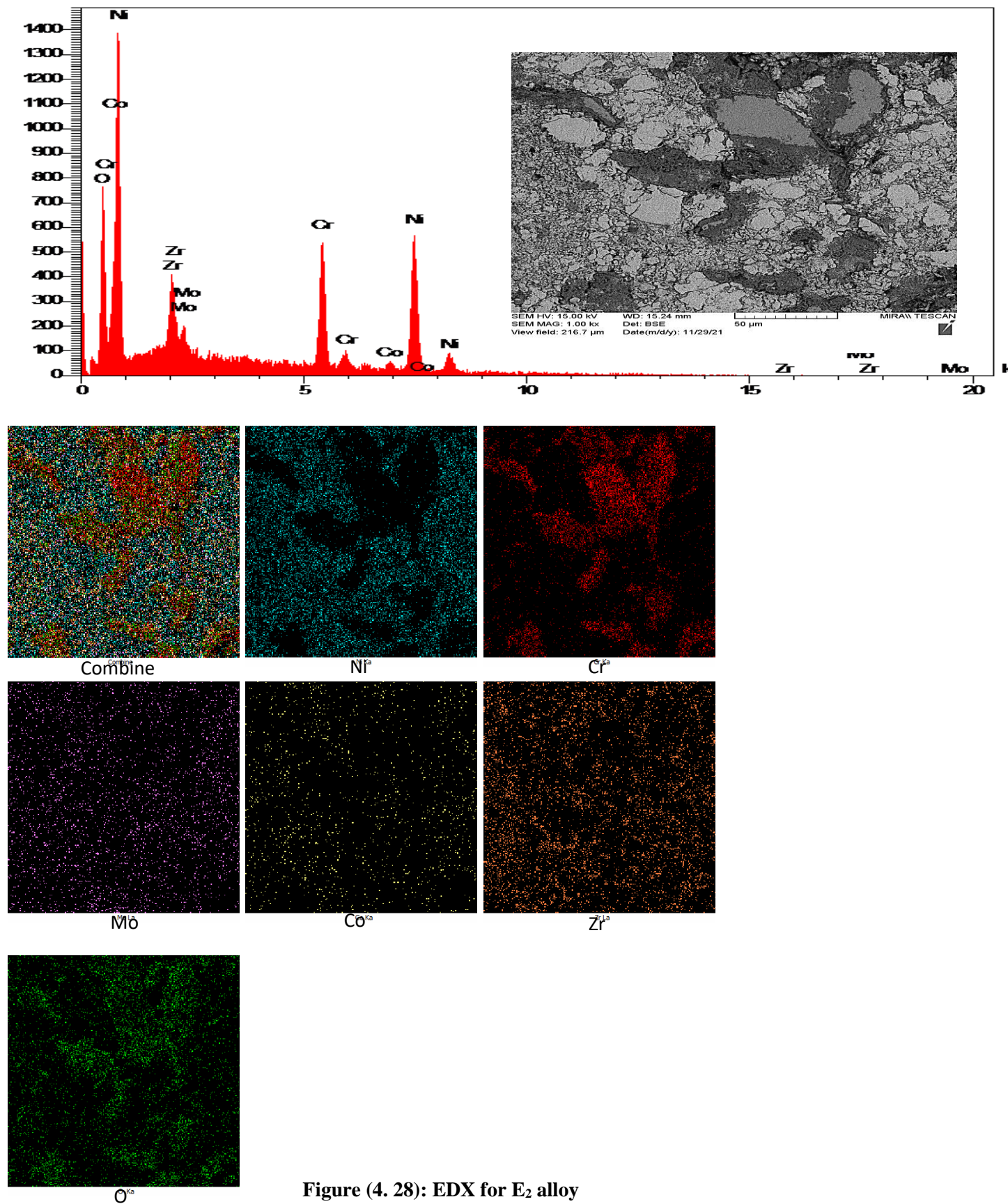


Figure (4. 28): EDX for E<sub>2</sub> alloy

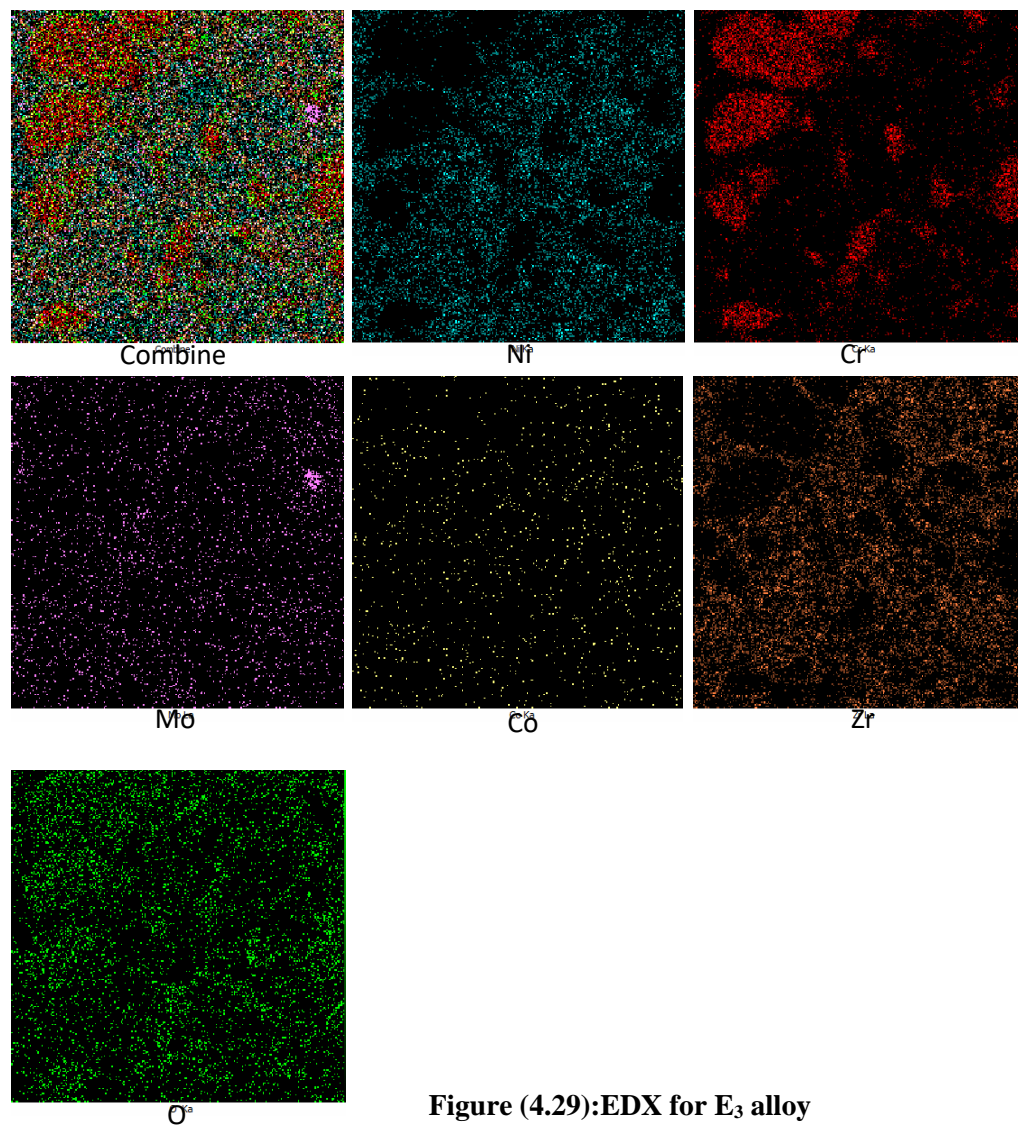
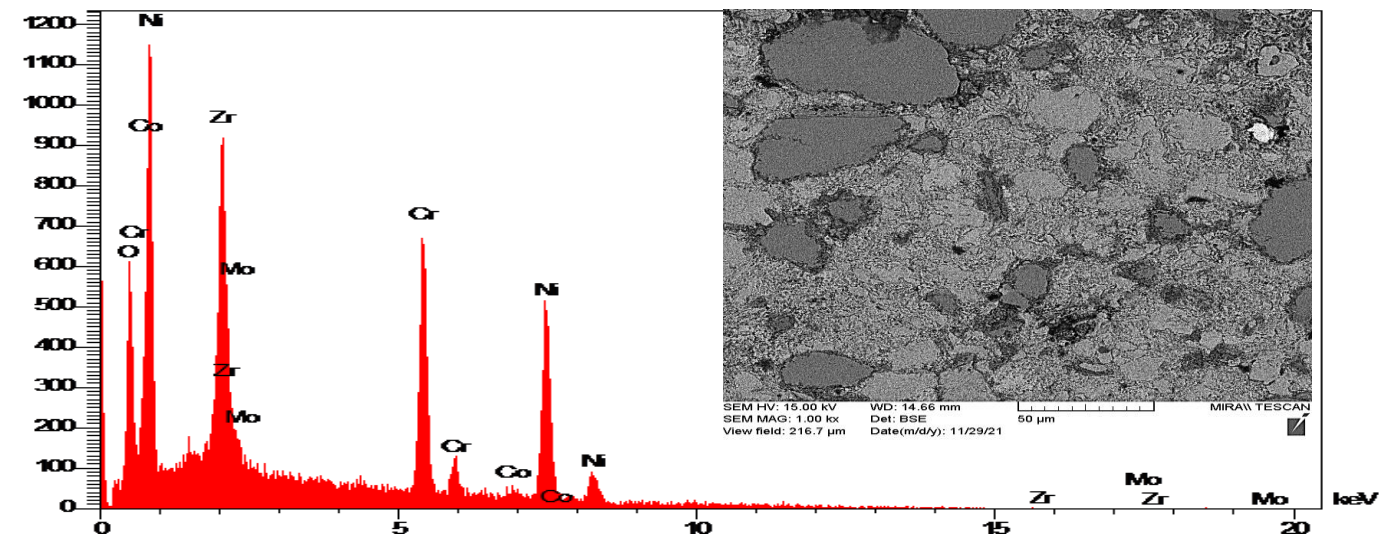


Figure (4.29):EDX for E<sub>3</sub> alloy

## 4.4 Physical Properties Tests

### 4.4.1 Compacting Pressure

Various compacting pressures were used to determine the appropriate compacting pressure. The appropriate compacting pressure is the pressure at which we obtain the least porosity and the highest density of the compacted sample. The pressures that were used are as follows: 300,370,450,520,600,670MPa. The figure (4.30) depicts that green density is increased as the pressure rises, which is due to a decrease in pores as the compacting pressure increases.

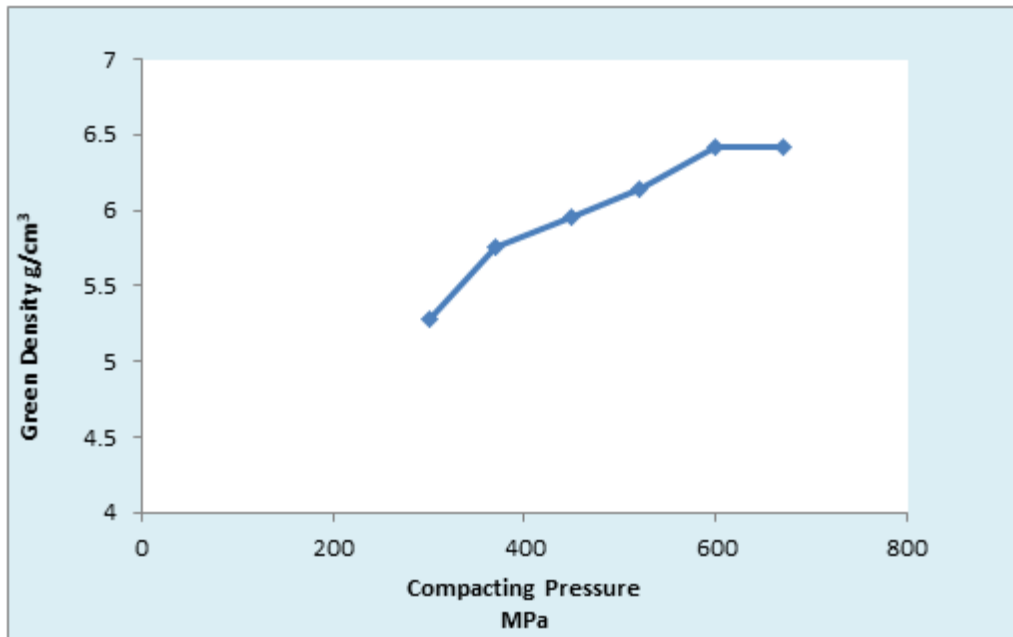


Figure (4.30):The compacting pressure for base (A) alloy versus green density.

When pressure is applied, a rearrangement of the powder will occur resulting in localized deformation. An increase in pressure leads to the elimination of pores and the formation of new contacts, and eventually a homogeneous deformation of the fully compressed sample occurs [113].

#### 4.4.2 Effect of B addition on density and porosity

The Figure (4.31) illustrates effects of adding boron on green density of the alloy. An increase in the proportion of boron leads to a decrease in green density. This is because boron density is  $2.34 \text{ g/cm}^3$  and is less than the density of nickel is  $8.9 \text{ g/cm}^3$ , so the increase in boron in the alloy negatively affects the green density, this result agree with [114, 115].

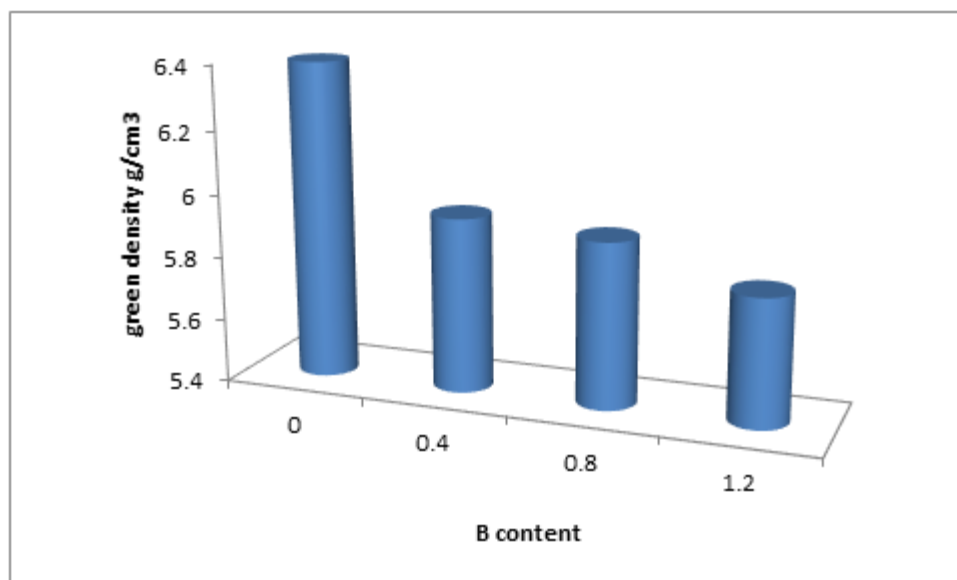


Figure (4.31)Effect B content on green density of A,B1,B2,B3 alloys.

After sintering at  $1000 \text{ c}$  in argon atmosphere the final density calculated by Archimedes method. Figure (4.32) illustrates effects of the addition of the boron on the final density of an alloy, where final density is increased with the increases of the proportion of boron. Adding the boron results in improving densification by enhancing the kinetics of solid-state diffusion. The adding of boron occurs in low melting phases that results in greatly increasing the rate of diffusion during the high-temperature sintering processes [116]. Figure (4.33) shows effects of adding boron on green porosity and the final porosity. The final porosity less than green porosity this attributed to the sintering. The green porosity increases with the increase in the

proportion of boron. The calculation of green porosity depends on the theoretical density, and therefore the porosity increases with the addition of boron. In contrast, the final porosity will be decreased with increasing the proportion of boron, because adding the boron increases the shrinkage and densification.

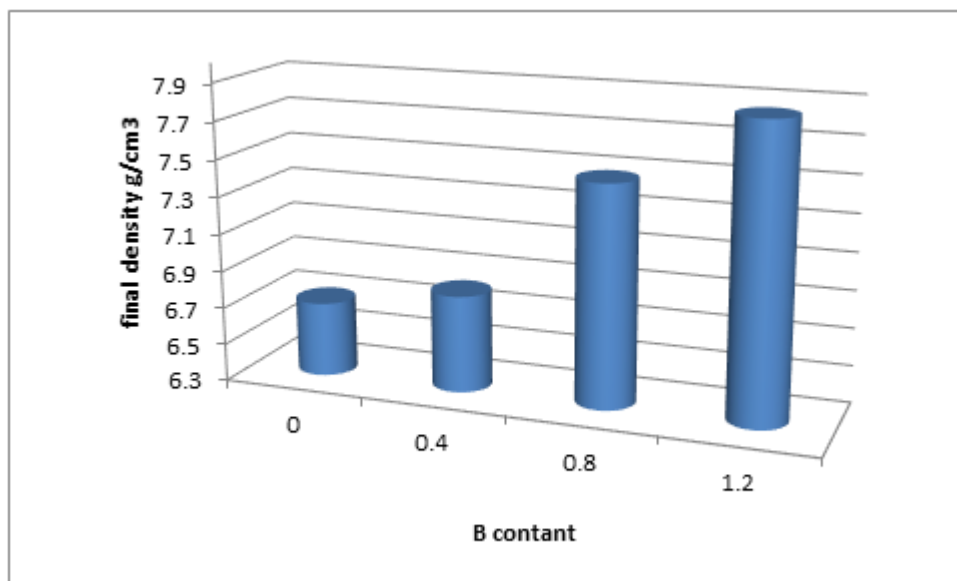


Figure (4.32): The final density of A,B<sub>1</sub>,B<sub>2</sub>,B<sub>3</sub> alloys.

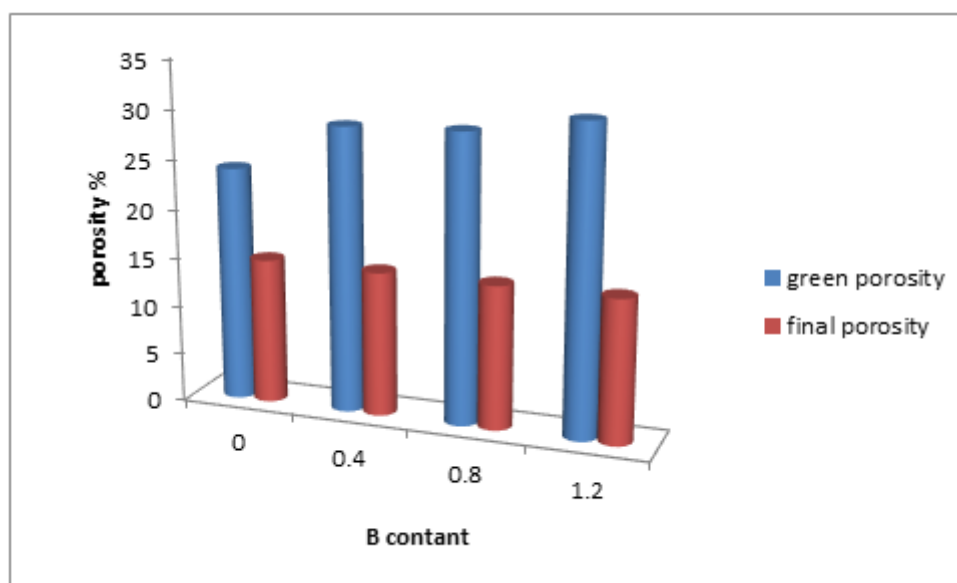


Figure (4.33): The green and final porosity of A,B<sub>1</sub>,B<sub>2</sub>,B<sub>3</sub> alloys.

#### 4.4.3 Effect of Zr addition on density and porosity:

The effects of adding zirconium on green density of alloys have been shown in the figure (4.34). Increasing zirconium will decrease the green density and this is due to the fact that the density of zirconium which is  $6.5\text{g/cm}^3$  is less than the density of nickel  $8.9\text{g/cm}^3$ .

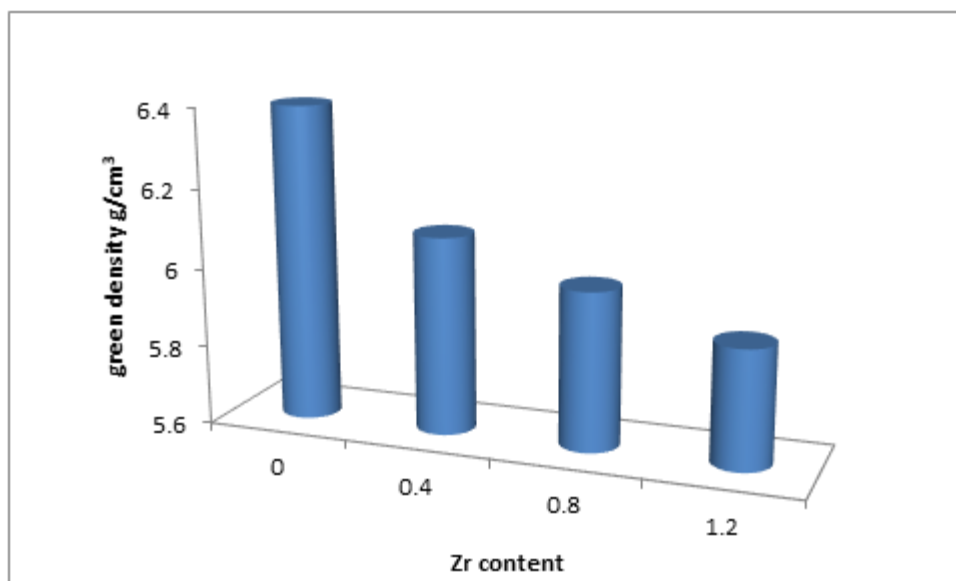
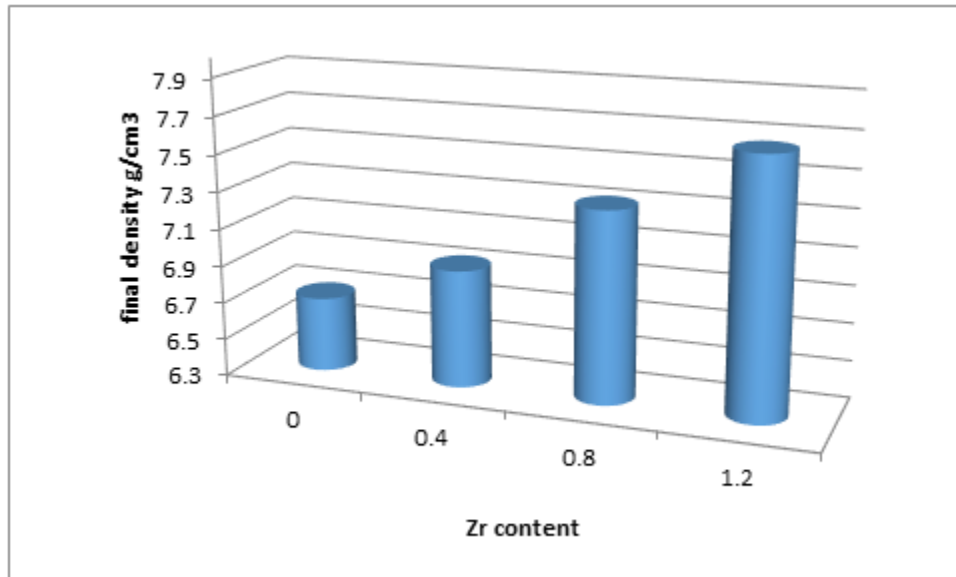


Figure (4. 34): Effect Zr content on green density of A, C<sub>1</sub>, C<sub>2</sub>, C<sub>3</sub> alloys.

Figure (4.35) illustrates effects of adding zirconium on the final density. With the increase of the density after the sintering process, as well as the final density increases when the proportion of zirconium increases, because the presence of zirconium improves the densification process, reduces melting point and decreases sintering temperature, which agrees with [117]. The effects of the addition of zirconium on final porosity is clear as well, as the porosity decreases with the increase in the proportion of zirconium, as shown in Figure (4.36).



Figure(4.35): The final density of A,C<sub>1</sub>,C<sub>2</sub>,C<sub>3</sub> alloys.

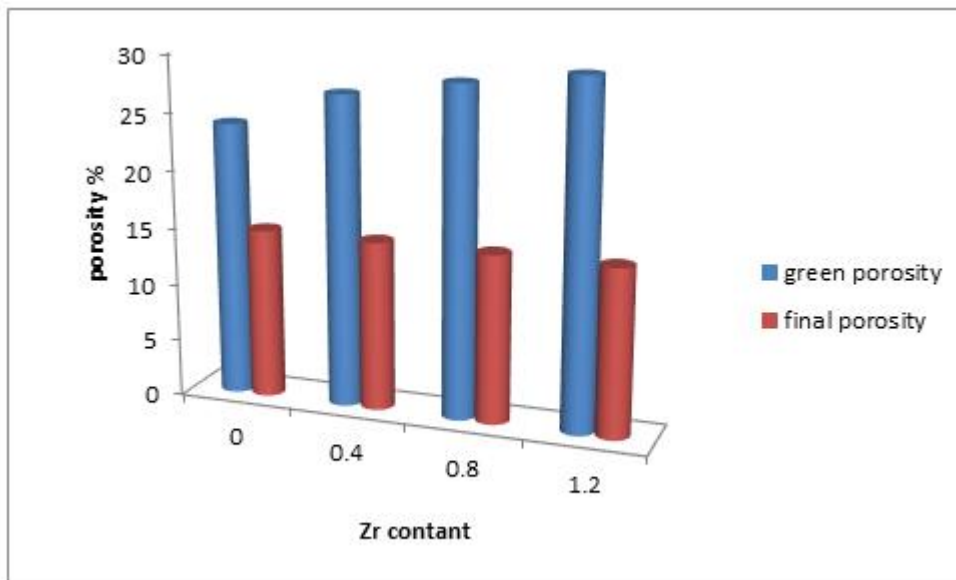


Figure (4.36): The green and final porosity of A,C<sub>1</sub>,C<sub>2</sub>,C<sub>3</sub> alloys.

#### 4.4.4 Effect of In addition on density and porosity:

The figure (4.37) shows effects of changing percentage of indium on green density of the alloy. Increasing the percentage of indium results in decreasing the value of green density and this is due to the fact that the density of indium ( $7.3\text{g/cm}^3$ ) is less than the density of nickel ( $8.9\text{g/cm}^3$ ).

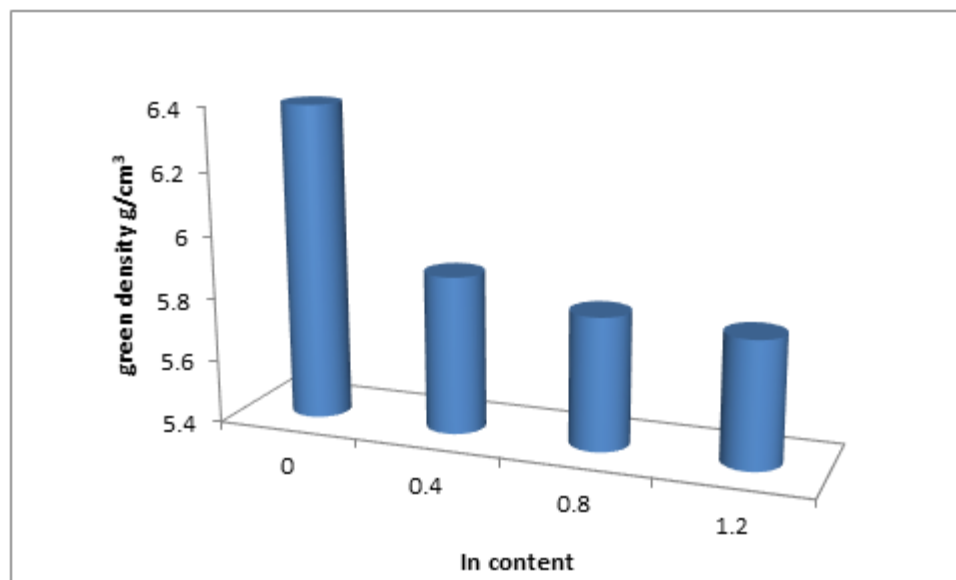


Figure (4.37): Effect In content on green density of A, D<sub>1</sub>, D<sub>2</sub>, D<sub>3</sub> alloys.

Adding indium will affect the density after sintering, as increasing the proportion of indium will increase the final density as shown in Figure (4.38). This is due to the low melting point of indium ( $256.5\text{C}^\circ$ ), so during the sintering process and the high temperature indium fills the pores and the porosity of the solid body decreases and this leads to a rise in the final density as shown in Figure (4.39), this agrees with [118].

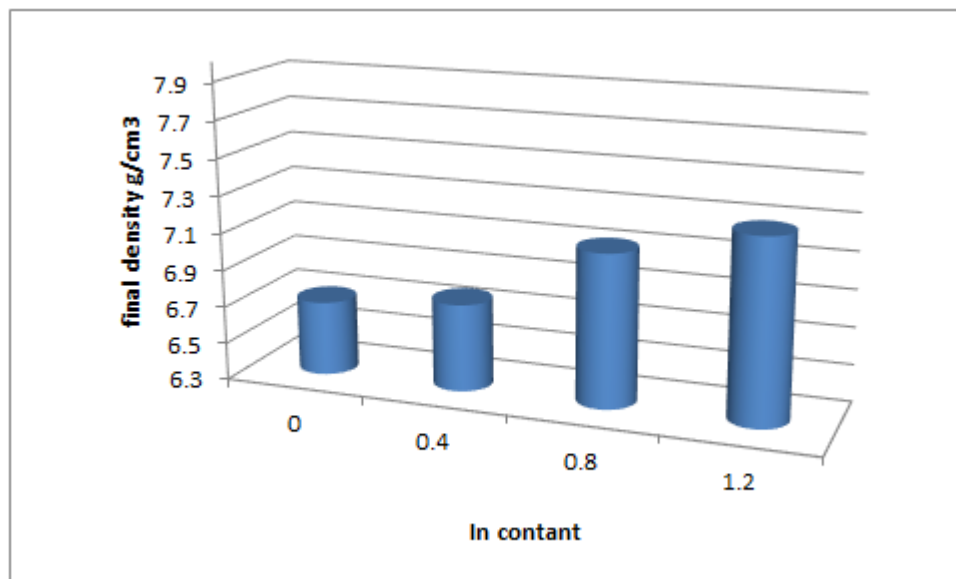


Figure (4.38): Effect In content on final density of A,D<sub>1</sub>,D<sub>2</sub>,D<sub>3</sub> alloys.

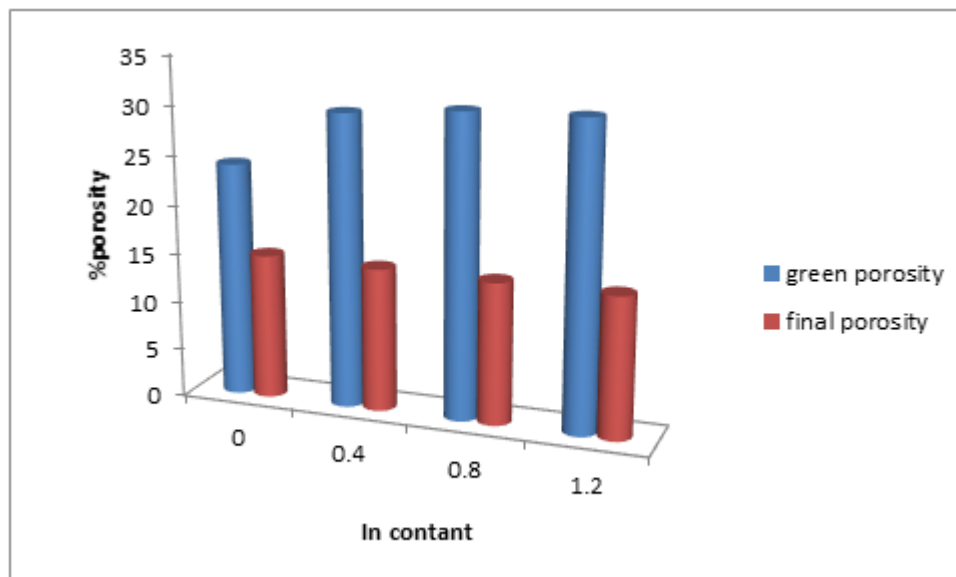
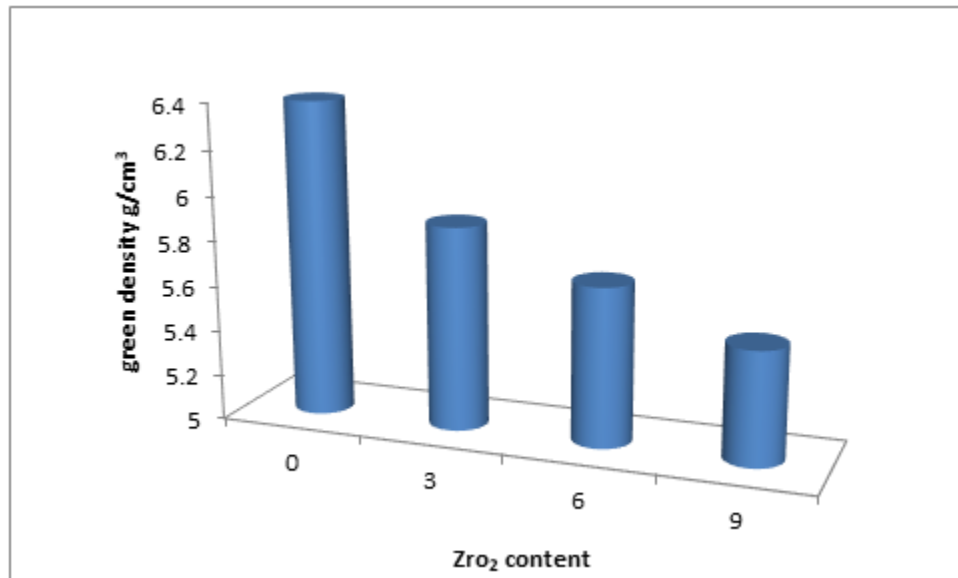


Figure (4.39): The green and final porosity of A,D<sub>1</sub>,D<sub>2</sub>,D<sub>3</sub> alloys.

#### 4.4.5 Effect of ZrO<sub>2</sub> addition on density and porosity:

The figure (4.40) illustrates effects of adding ZrO<sub>2</sub> on green density of the alloy. An increase in the proportion of Zr leads to a reduction in green density. This is because ZrO<sub>2</sub> density is 5.89 g/cm<sup>3</sup> and is less than the density of nickel is 8.9g/cm<sup>3</sup>

also the  $ZrO_2$  amount effect on compressibility behaviour of alloy this agree with [119].



**Figure (4.40):**Effect  $ZrO_2$  content on green density of A, $E_1$ , $E_2$ , $E_3$  alloys.

Figures (4.41), (4.42) show the density and porosity after sintering, where the addition of  $ZrO_2$  leads to a reduction in the density and increasing the porosity. The hardness of  $ZrO_2$  is usually higher when compared to the base alloy, so, addition of  $ZrO_2$  particles will affect the densification ability of the alloy containing  $ZrO_2$ . The sintering ability of the alloys decreases when the proportion of zirconia is increased, due to the poor diffusion, and this corresponds to [120].

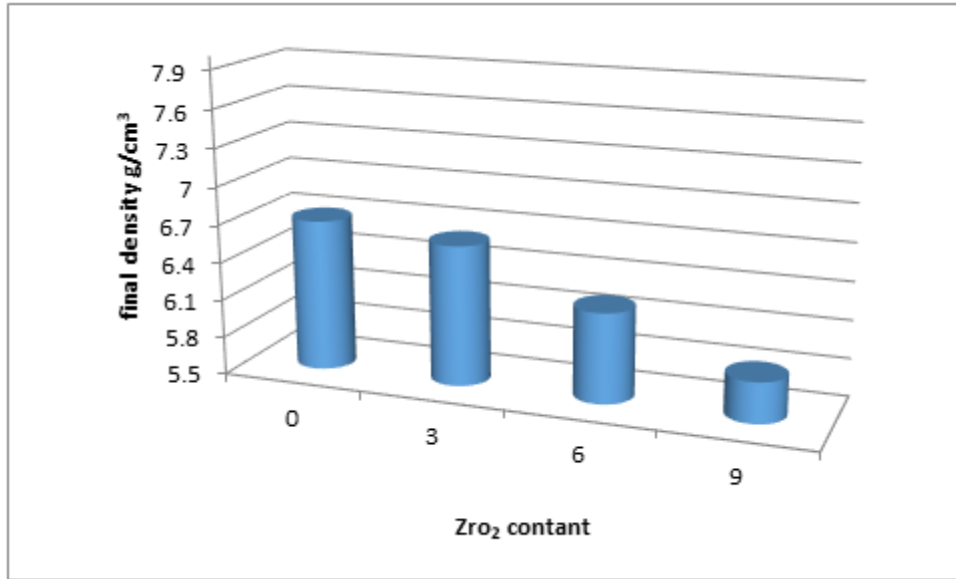


Figure (4.41):Effect ZrO<sub>2</sub> content on final density of A,E<sub>1</sub>,E<sub>2</sub>,E<sub>3</sub> alloys.

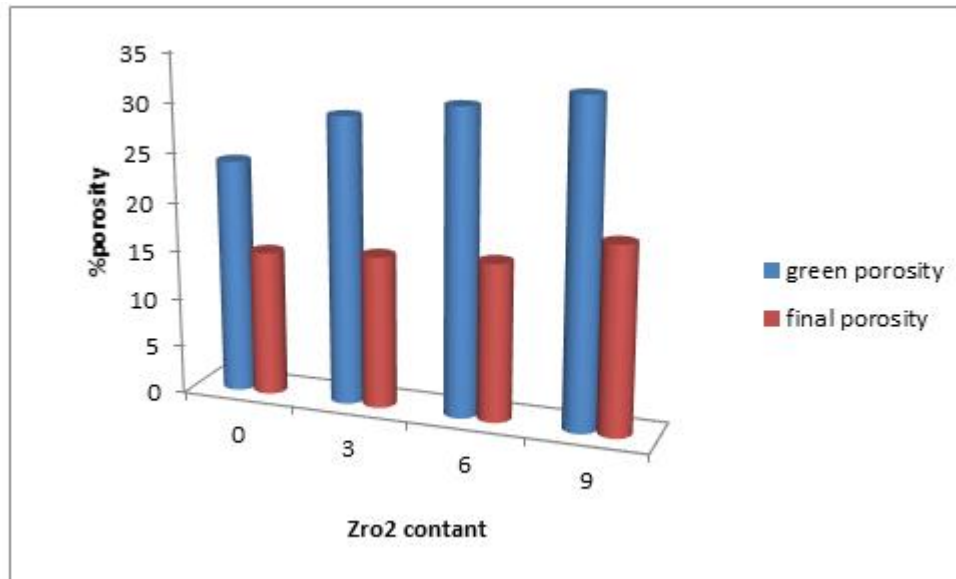
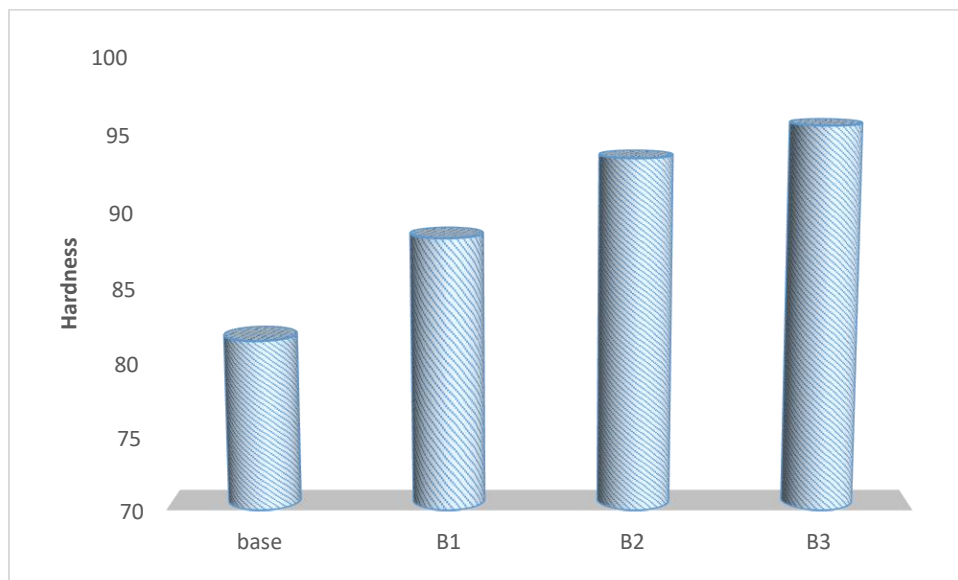


Figure (4.42) :Effect ZrO<sub>2</sub> content on final density of A,E<sub>1</sub>,E<sub>2</sub>,E<sub>3</sub> alloys.

## 4.5 Mechanical Characteristics

### 4.5.1 Brinall Hardness Test

The hardness of the samples has been measured for all alloys as shown in the Figures (4.43-4.46) by using brinall hardness test. The Figure (4.43) illustrates the effect of adding boron on the hardness values, as it was noticed that the hardness value improved when adding boron, and it increased with increasing amount of boron addition. The hardness value of (A)alloy is (81.5) and when added (0.4,0.8,1.2) %wt of B the hardness become to (88.3,93.5,95.6) respectively. This is due to the effect of boron in refining, as well as the diffusion of solid particles in the alloy, which impades the dislocation movement, which increases the hardness value this agree with [121]. The increase in hardness when adding boron can also be attributed to the fact that the porosity of the alloy decreased when boron was added, and since the hardness is inversely proportional to the porosity, it increases with the decrease in the porosity[121].



**Figure (4.43) Brinall hardness of A,B<sub>1</sub>,B<sub>2</sub>,B<sub>3</sub> alloys**

The effect of adding Zr on the hardness shown in Figure (4.44). From this figure it has been noticed that the addition of zirconium had an important impact upon the hardness of the alloy, as increasing the amount of Zr in the alloy leads to the increase in hardness. The values of the hardness of the alloy with (0.4,0.8,1.2)% wt Zr equals (90,92.7,100.3) as the hardness values of the alloy increased due to the presence of zirconium. This is due to the reduction of porosity and refinement of grain after sintering with the addition of Zr this agree with [122].

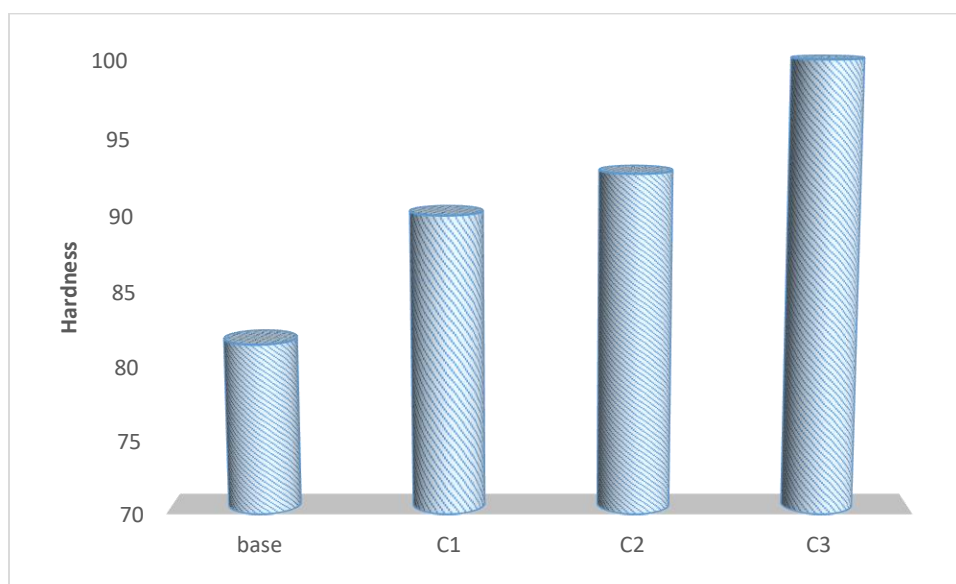


**Figure (4.44) Brinall hardness of A,C<sub>1</sub>,C<sub>2</sub>,C<sub>3</sub> alloys**

The Figure (4.45) shows the effect of adding indium on the hardness of the alloy, where the addition of indium showed an improvement in the hardness values compared to the base alloy. The hardness value of (A)alloy is (81.5) and when added (0.4,0.8,1.2) %wt of In the hardness become to (84.2,86.5,87.1 ) respectively. The hardness increases when Indium is added due to solid solution strengthening and refining[124].

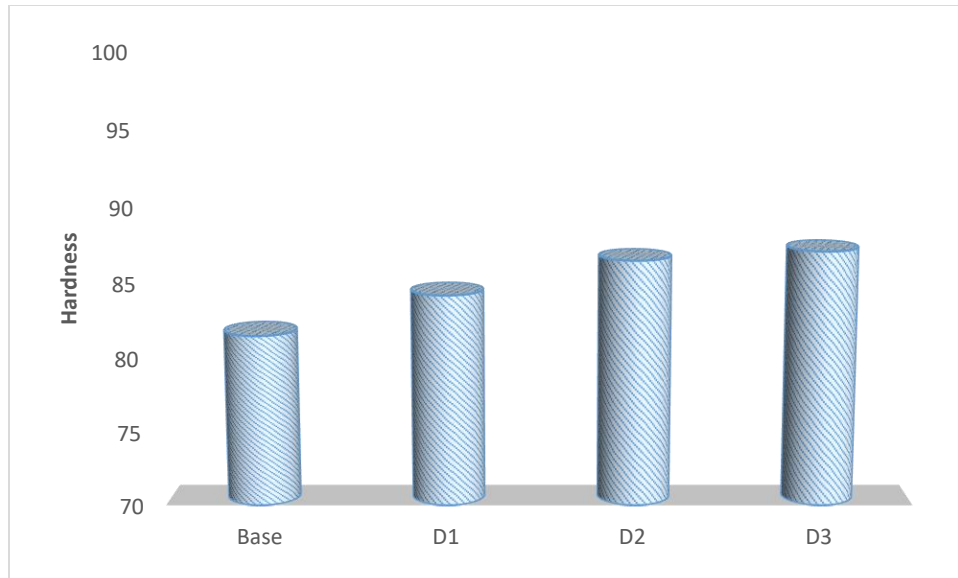


**Figure (4.45) Brinall hardness of A,D<sub>1</sub>,D<sub>2</sub>,D<sub>3</sub> alloys**

Figure (4.46) showed the effect of adding zirconia on the hardness of the alloy. The hardness increase when adding (3,6,9)% wt ZrO<sub>2</sub>, as it becomes (90.1,95.7,93.9) respectively. As the hardness increases gradually when zirconia is added, this is due to the addition of particles that strengthen the solid solution by impeding the dislocation movement. The hardness at E<sub>3</sub> starts to decrease. This is due to the fact that the increase in zirconia leads to increasing the porosity and this results in a decrease of hardness value[125].

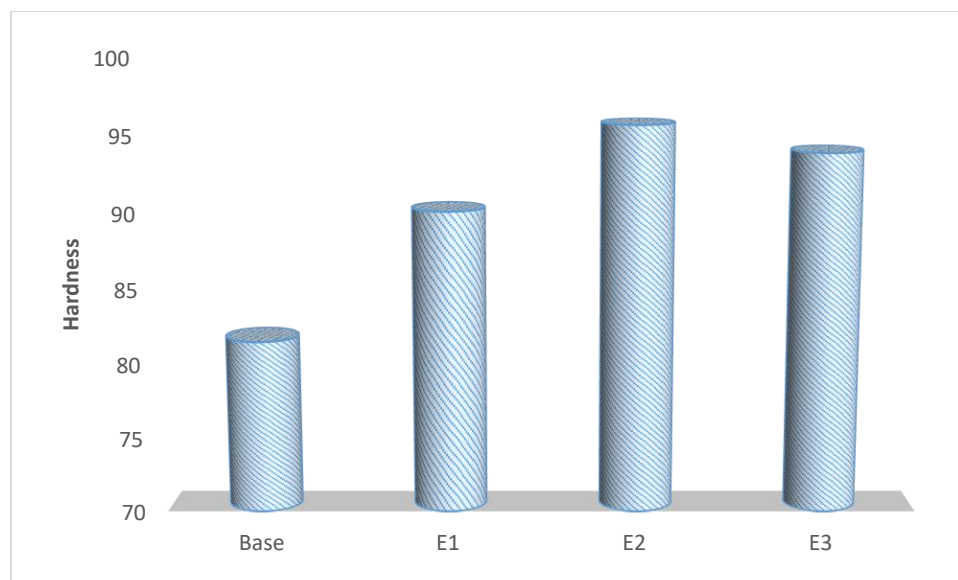


**Figure (4.46) Brinall hardness of A,E<sub>1</sub>,E<sub>2</sub>,E<sub>3</sub> alloys.**

#### 4.5.2 Compression Test

The compression test results illustrated in the Figures (4.47 to 4.48). The compressive strength of the alloy with (0.4,0.8,1.2) %wt of B showed in Figure (4.47), where the addition of boron led to an increase in the compressive strength of the alloy. The compressive strength depends on several factors, including the particle size and the composition of the alloys. The strengthening process can occur by changing the composition of the matrix alloy, which occurs through the addition of reinforcing particles. The rate of grain size will be reduced by the presence of the strengthening particles, which work to impede grain growth and this gives good mechanical properties[126].The Figure (4.48) illustrated the compressive strength of alloy with different addition of Zr. The compressive strength increase with increase of Zr amount in the matrix alloy, and this is due to the presence of Zr refining the grain size, reducing the porosity and increasing the hardness.

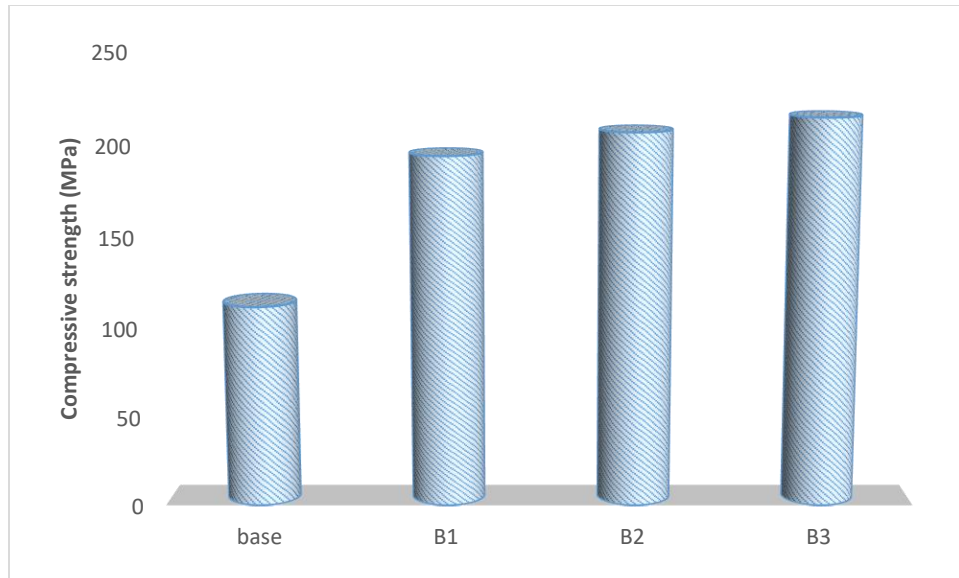


**Figure (4.47) shows the compressive strengths of the A,B<sub>1</sub>,B<sub>2</sub>,B<sub>3</sub> alloys.**

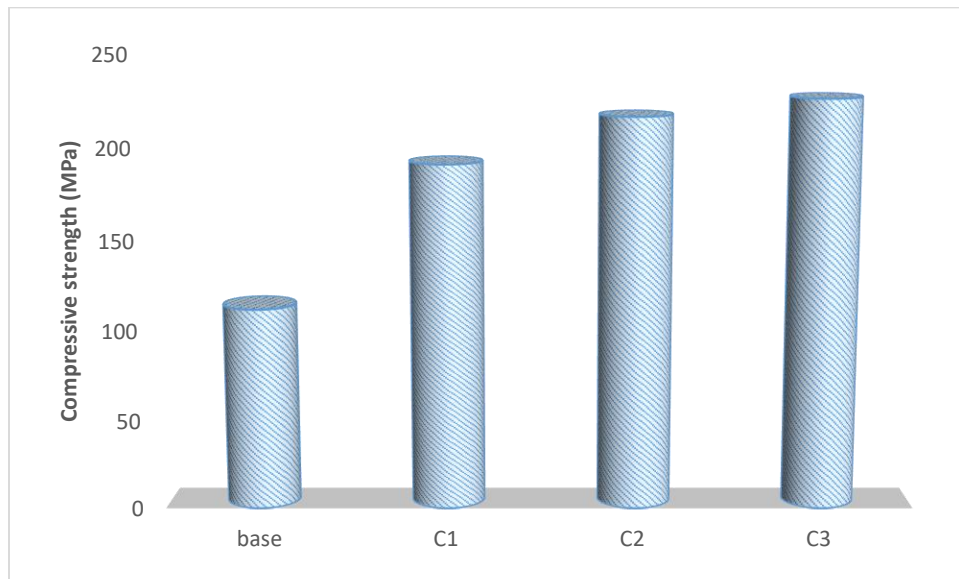


**Figure (4.48) shows the compressive strength of the A,C<sub>1</sub>,C<sub>2</sub>,C<sub>3</sub> alloys.**

The compressive strength of base alloy is affected by the amount of Indium. It is improved by adding Indium, as can be seen in the Figure (4.49).

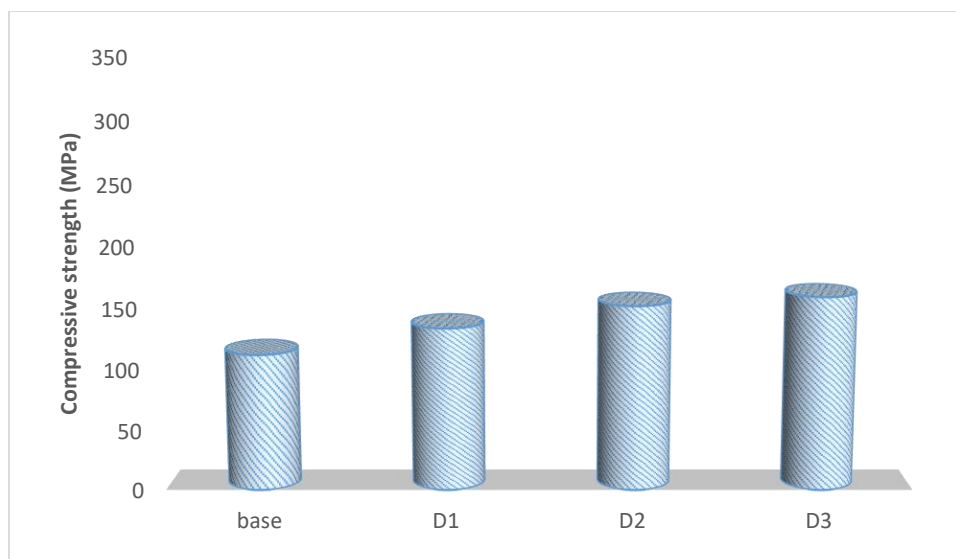


**Figure (4.49): compressive strength of A,D<sub>1</sub>,D<sub>2</sub>,D<sub>3</sub> alloys.**

The Figure (4.50) illustrates effects of adding zirconia on compressive strength. Adding a small percentage (3%) of zirconia to the alloy improved the compressive strength, but the increase in the proportion (6%,9%) of zirconia led to a decrease in the compressive strength. As a result, the gap between reinforcements becomes less when more reinforcement added to the matrix and dislocation pile up occurs which causes reduction in elongation [140]. Table (4.1) shows the compressive strength for all alloys (A,B<sub>1</sub>,B<sub>2</sub>,B<sub>3</sub>,C<sub>1</sub>,C<sub>2</sub>,C<sub>3</sub>,D<sub>1</sub>,D<sub>2</sub>,D<sub>3</sub>,E<sub>1</sub>,E<sub>2</sub>,E<sub>3</sub>).

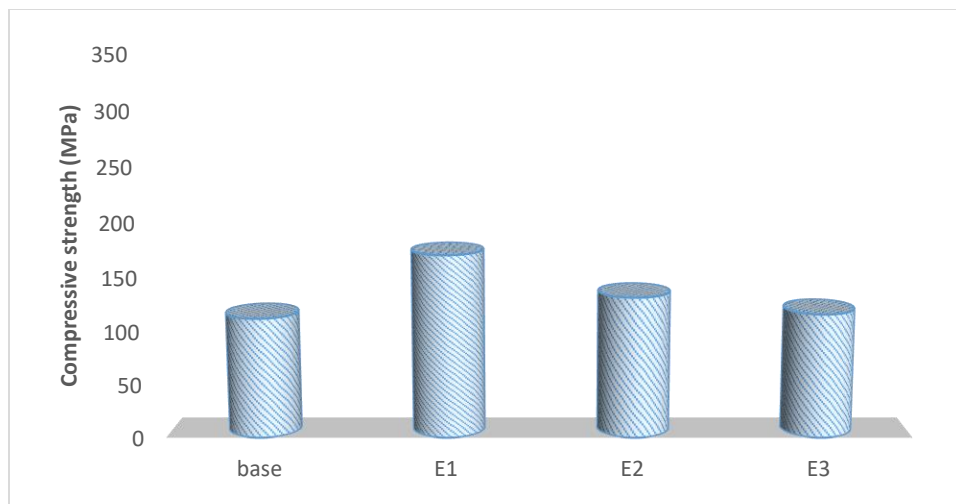


**Figure (4.50) shows the compressive strength of A,E<sub>1</sub>,E<sub>2</sub>,E<sub>3</sub> alloys.**

**Table (4.1) : The Compressive strength for all alloys in MPa.**

<b>Code</b>	<b>Compressive Strength (MPa)</b>
<b>A</b>	<b>111.9</b>
<b>B<sub>1</sub></b>	<b>194.3</b>
<b>B<sub>2</sub></b>	<b>207</b>
<b>B<sub>3</sub></b>	<b>214.9</b>
<b>C<sub>1</sub></b>	<b>191</b>
<b>C<sub>2</sub></b>	<b>216.5</b>
<b>C<sub>3</sub></b>	<b>226.1</b>
<b>D<sub>1</sub></b>	<b>133.7</b>
<b>D<sub>2</sub></b>	<b>151.9</b>
<b>D<sub>3</sub></b>	<b>159.2</b>
<b>E<sub>1</sub></b>	<b>170.2</b>
<b>E<sub>2</sub></b>	<b>131.4</b>
<b>E<sub>3</sub></b>	<b>115.9</b>

### 4.5.3 Ultrasonic wave test

Ultrasonic testing is a non-destructive test used in calculating mechanical characteristics such as Yong's modulus and Poisson's ratio. In this type of test, ultrasound waves are used that pass through the material, and the time of passage of this wave is measured by electronic time instruments. Increasing the density of the material leads to an increase in the speed of the ultrasound wave ( $V_L$ ) and thus leads to an increase in the elastic modulus because it is directly proportional to the speed of ( $V_L$ ) [106]. Figure (4.51) illustrated the elastic modulus of all samples and Table (4.2) showed the mechanical

properties[Transverse velocity  $V_T$ , Longitudinal velocity ( $V_L$ ), young's modulus ( $E$ ), poisons ratio ( $\nu$ )] of each samples.

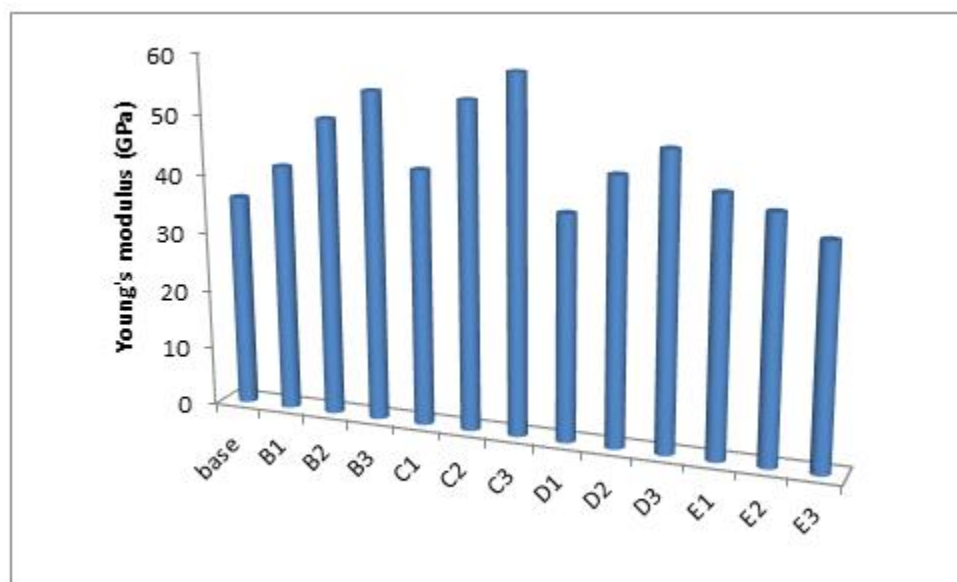


Figure (4.51) Young Modulus of samples.

Table (4.2):The mechanical properties[ $V_L$ ,  $V_T$ ,  $E$ , poisons ratio ( $\nu$ )] of each samples.

Code	$V_L$ (m/sec)	$V_T$ (m/sec)	$E$ (GPa)	$\nu$
A	2647	1200	35.7	0.2442
B <sub>1</sub>	2727	1364	41.5	0.2000
B <sub>2</sub>	3050	1406	49.9	0.2371
B <sub>3</sub>	3158	1440	54.9	0.2418
C <sub>1</sub>	2813	1216	40.1	0.2636
C <sub>2</sub>	3103	1429	54.4	0.2377
C <sub>3</sub>	3214	1452	59.2	0.2443
D <sub>1</sub>	2687	1216	37.6	0.2443
D <sub>2</sub>	2857	1353	44.3	0.2282
D <sub>3</sub>	2950	1440	48.2	0.2113
E <sub>1</sub>	2752	1395	42.8	0.1933
E <sub>2</sub>	2706	1333	40.5	0.2071
E <sub>3</sub>	2650	1216	36.9	0.2391

#### 4.5.4 Wear Testing

This test has been carried out on samples with a diameter of (13) mm using different loads (5, 10, 15) and with the different durations of time (5,10,15,20,25,30) min. Figures (4.52-4.62) showed the wear rate vs time for all samples under different loads. An increase in load that has been applied to the sample increased rate of wear. The wear rate is the highest value at which the applied load is 15 N. This is due to the fact that the weight loss rises when a high load is applied because of the friction on the surface increase and the removal of the material is more when the applied load increases, because contact pressure and temperature between sample and the steel pin increase this agree with [127, 128]. The addition of reinforcing particles to the alloy reduces the wear rate because it prevents the plastic deformation of the material, so when adding boron, a reduction in wear rate was observed under different loads as shown in the Figures (4.52-4.53). Also, the addition of boron has resulted in increasing hardness of the alloy and this would reduce wear rate.

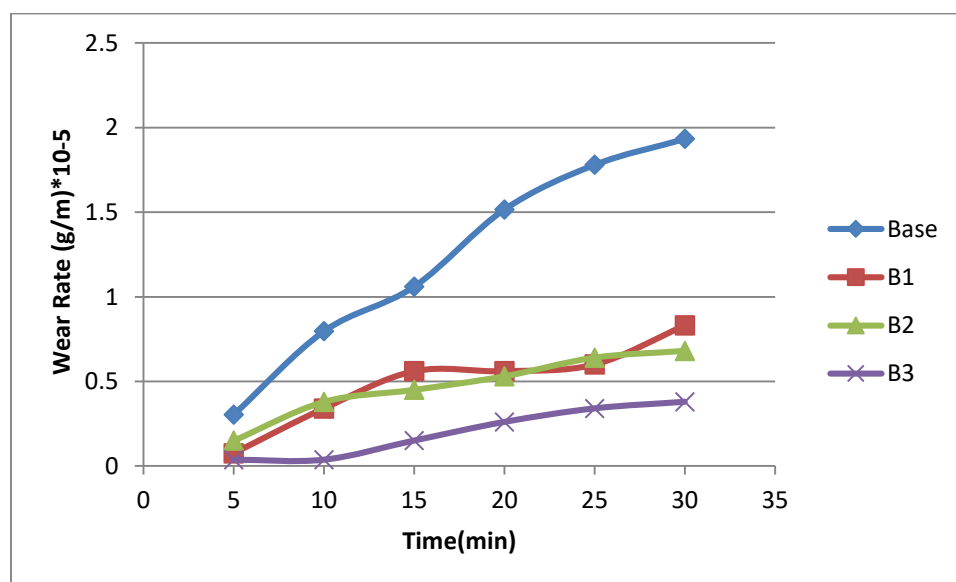
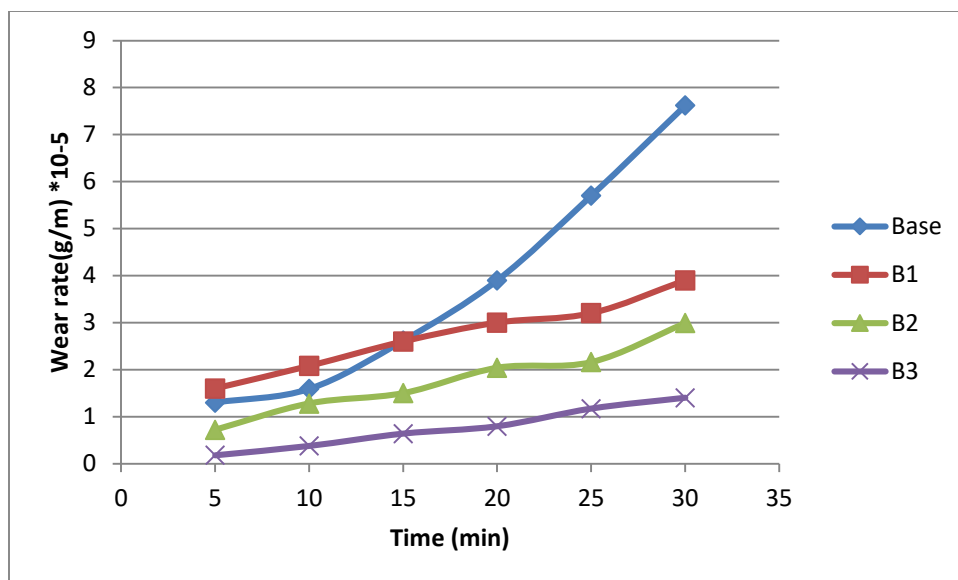
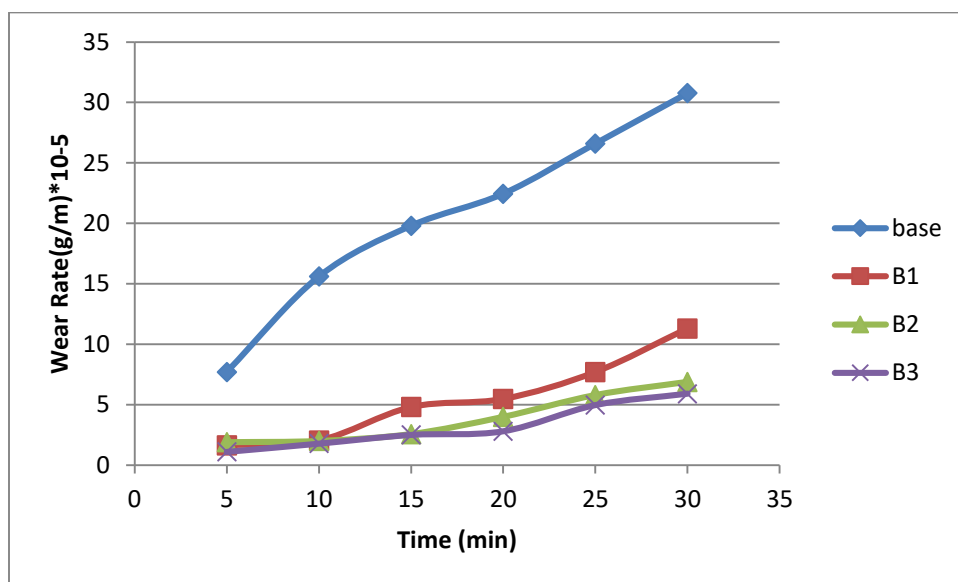


Figure (4.52): Wear rate for A, B<sub>1</sub>, B<sub>2</sub> and B<sub>3</sub> alloy under 5N load



**Figure (4.53):** Wear rate for A, B<sub>1</sub>, B<sub>2</sub> and B<sub>3</sub> alloy under 10N load



**Figure (4.54):** Wear rate for the A, B<sub>1</sub>, B<sub>2</sub> and B<sub>3</sub> alloy under 15N load

The addition of zirconium had a major role in increasing the hardness, and the higher the percentage of addition, the higher the hardness. Therefore, adding zirconium would reduce the wear rate, as shown in the figures (4.55-4.57).

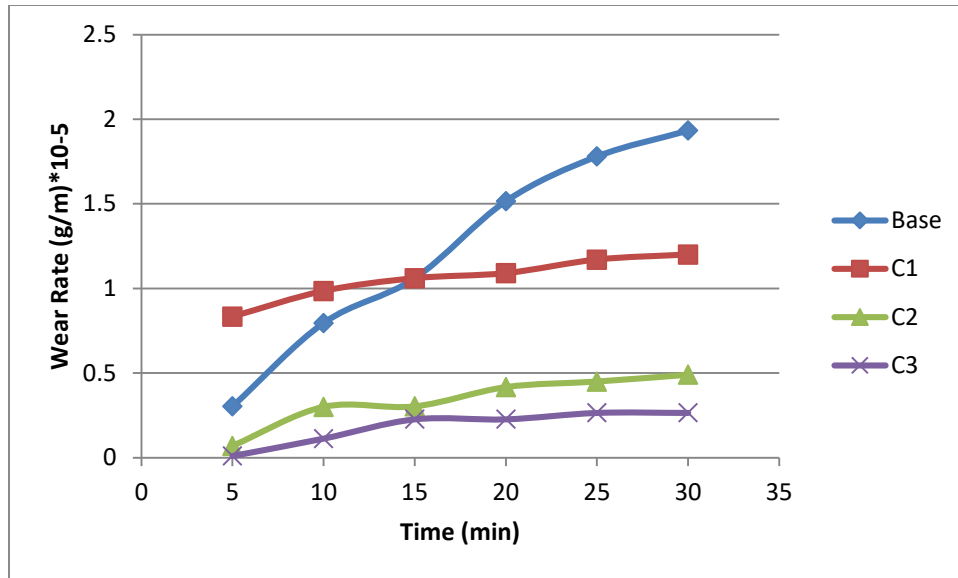


Figure (4.55): Wear rate for the A, C<sub>1</sub>, C<sub>2</sub> and C<sub>3</sub> alloy under 5N load

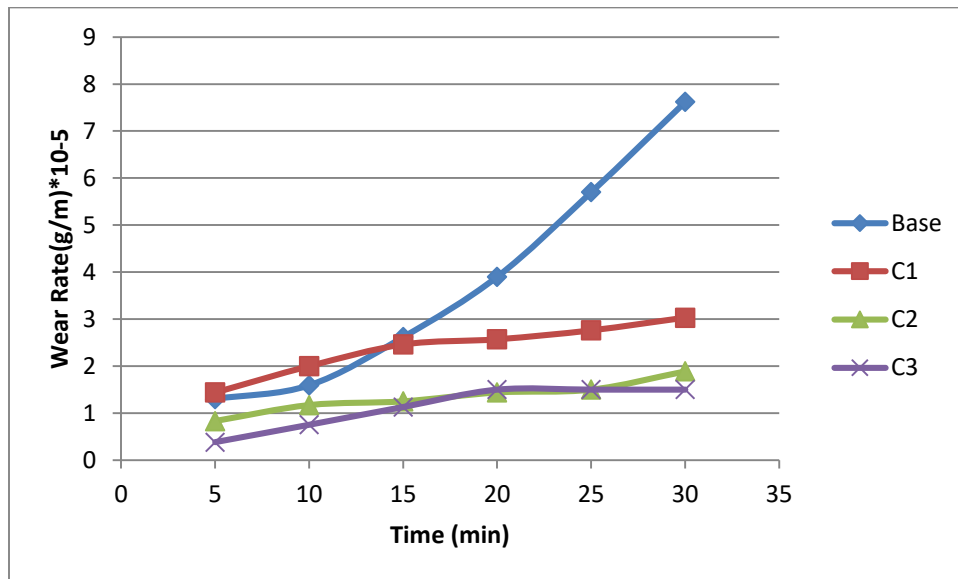
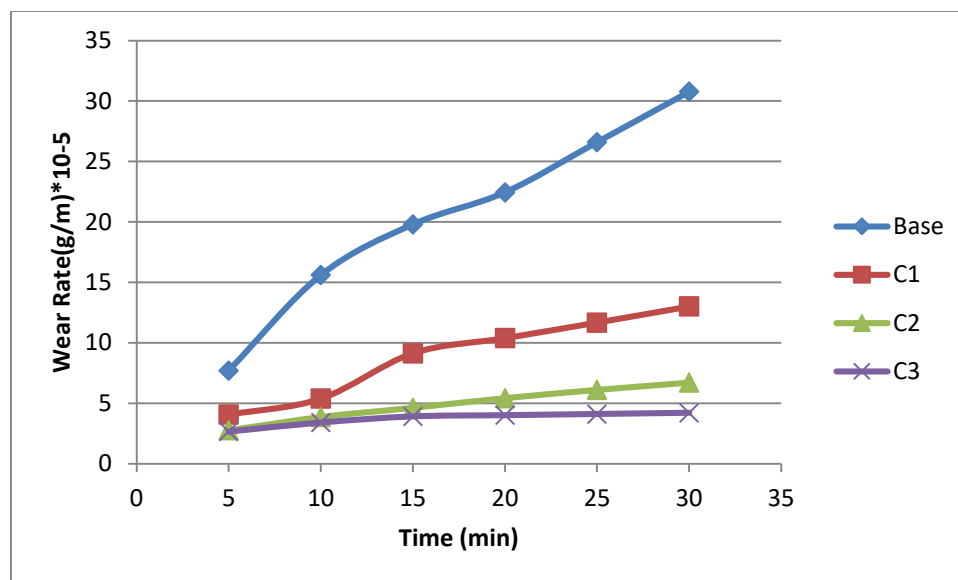


Figure (4.56): Wear rate for A, C<sub>1</sub>, C<sub>2</sub> and C<sub>3</sub> alloy under 10N load



**Figure (4.57):** Wear rate for the A, C<sub>1</sub>, C<sub>2</sub> and C<sub>3</sub> alloy under 15N load

The Figures (4.58-4.60) show effects of adding indium on wear rate, where it was notice a decrease in wear rate in the case of increasing the amount of indium, and this is attributed to the effect of indium in reducing the porosity and increasing the hardness of the alloy. When adding ceramic particles to the alloy, it will improve the wear resistance because of its high hardness that resists friction and this is clear in the figures (4.61-4.63) where the effect of adding zirconia on the wear rate was observed. Increasing the amount of zirconia to 6% had resulted in a decrease in wear rate, but when adding an amount of higher (6%) of zirconia led to an increase in the wear rate and this is because the increase in the proportion of zirconia had led to the increase in the porosity and thus a reduction in the hardness of the alloy.

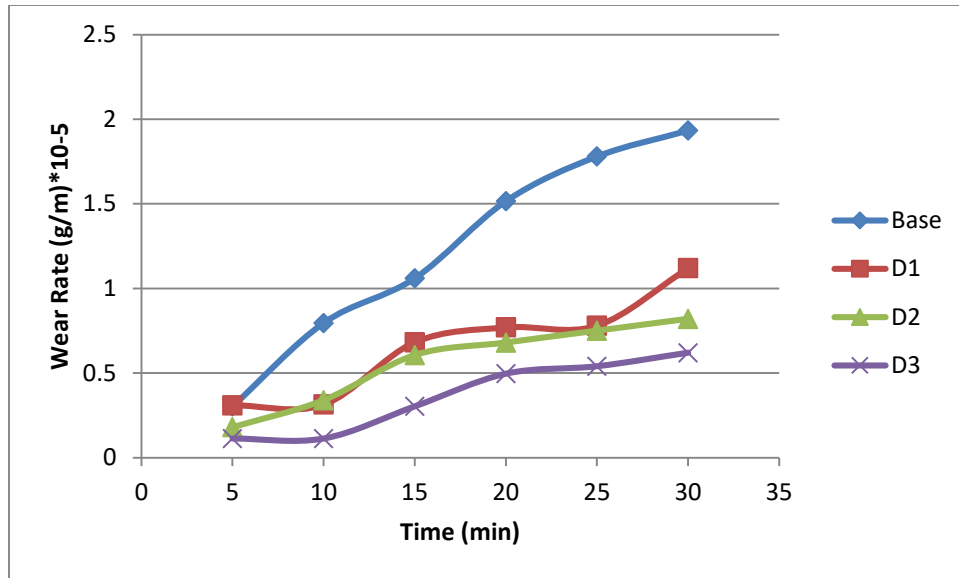


Figure (4.58): Wear rate for the A, D<sub>1</sub>, D<sub>2</sub> & D<sub>3</sub> alloy under 5N load

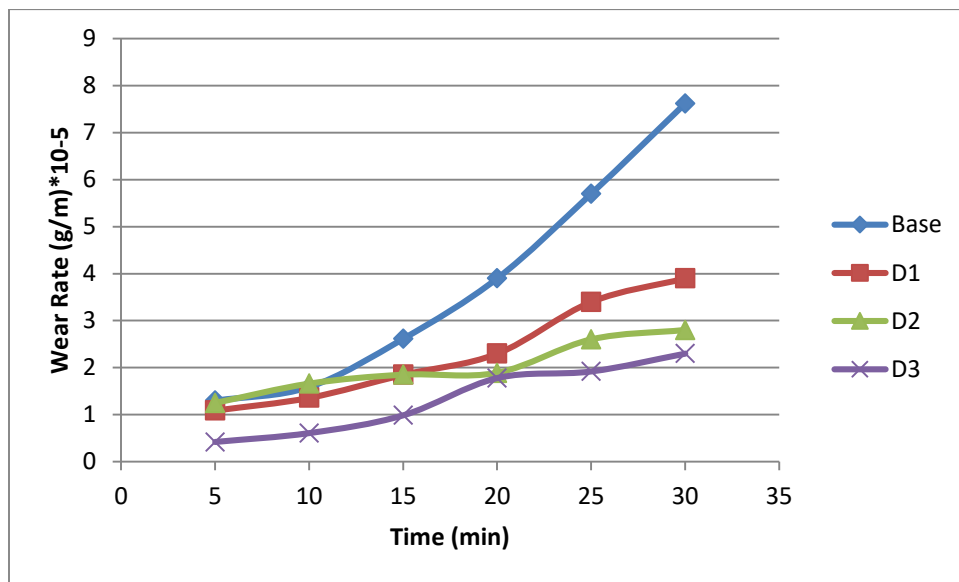


Figure (4.59): Wear rate for the A, D<sub>1</sub>, D<sub>2</sub> & D<sub>3</sub> alloy under 10N load

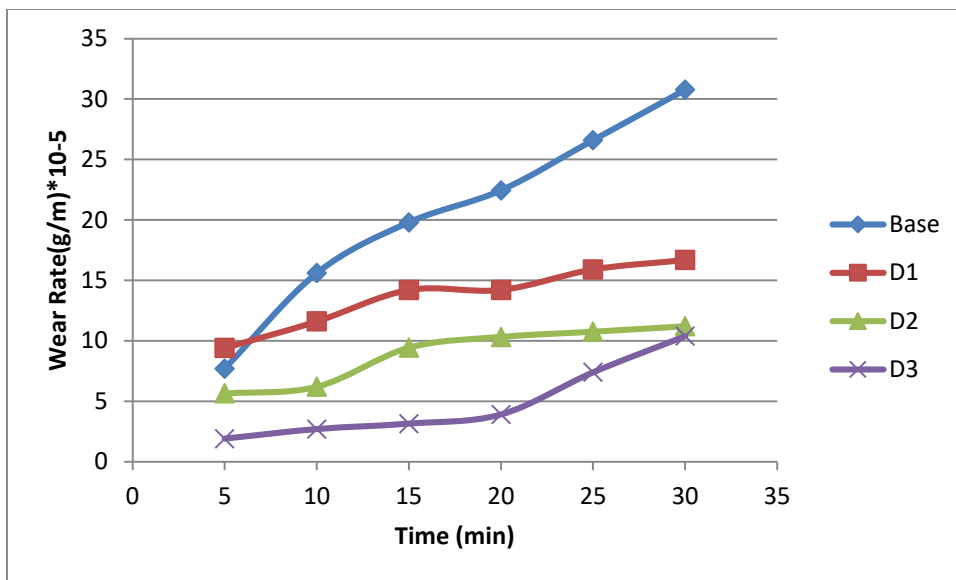


Figure (4.60): Wear rate for the A, D1, D2 & D3 alloy under 15N load

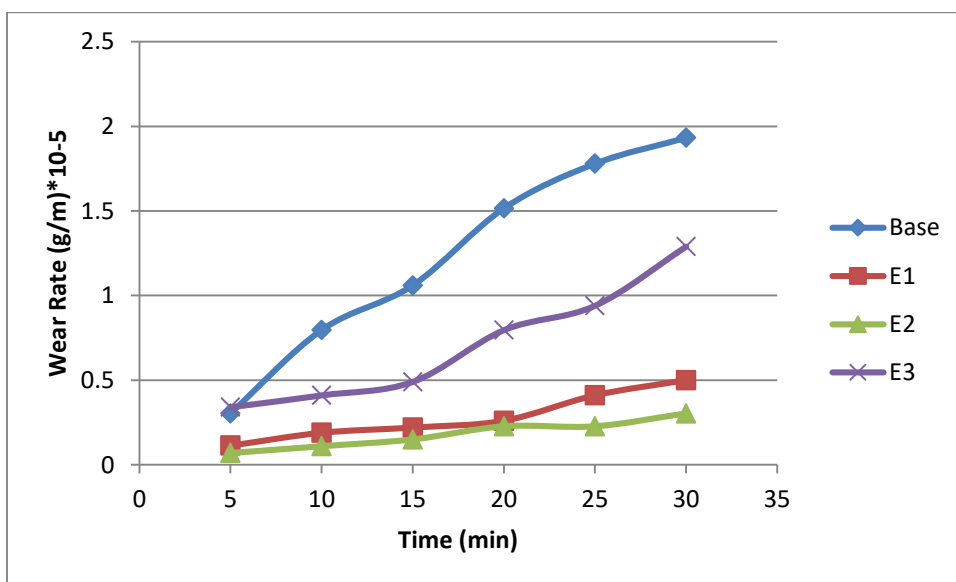


Figure (4.61): Wear rate for A, E1, E2 and E3 alloy under 5N load

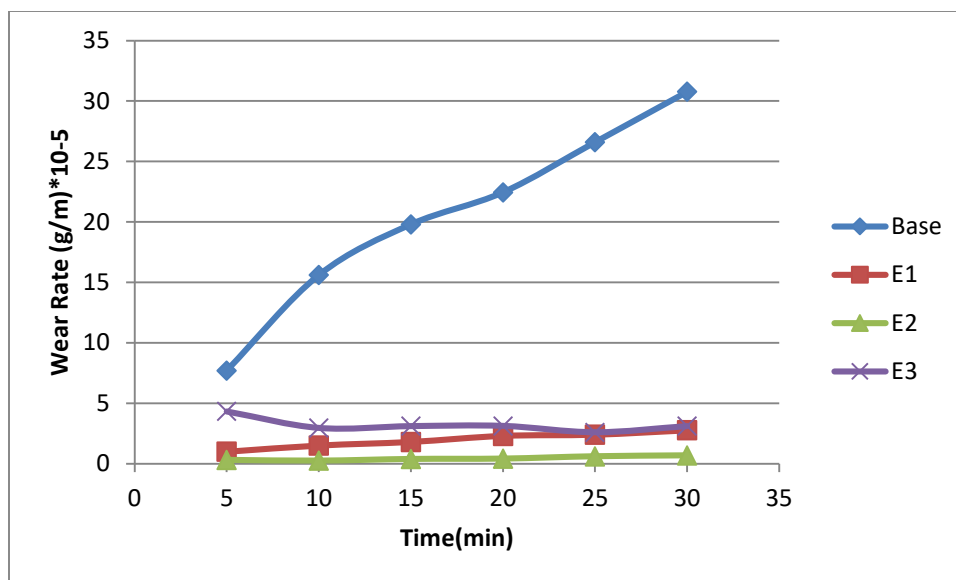


Figure (4.62): Wear rate for A, E<sub>1</sub>, E<sub>2</sub> and E<sub>3</sub> alloy under 10N load

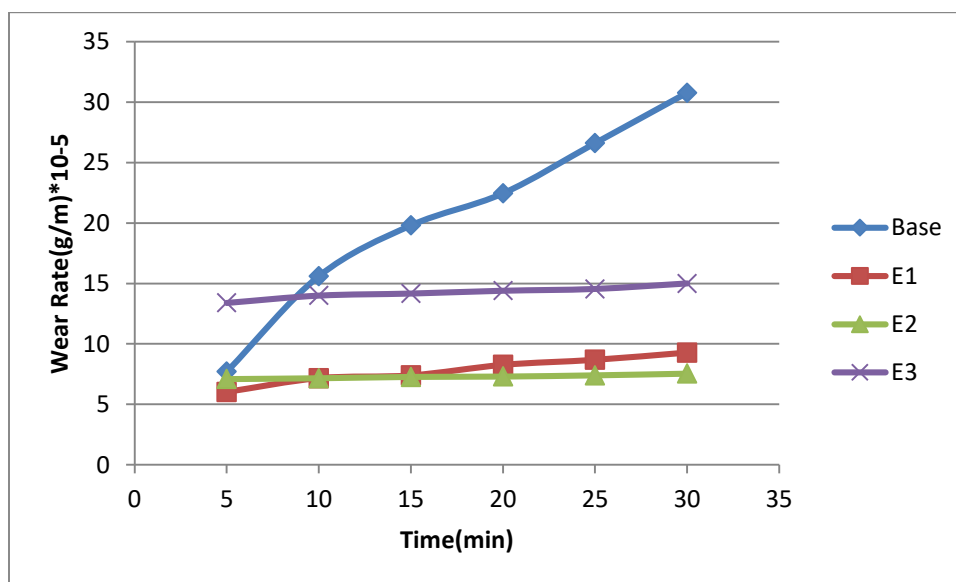
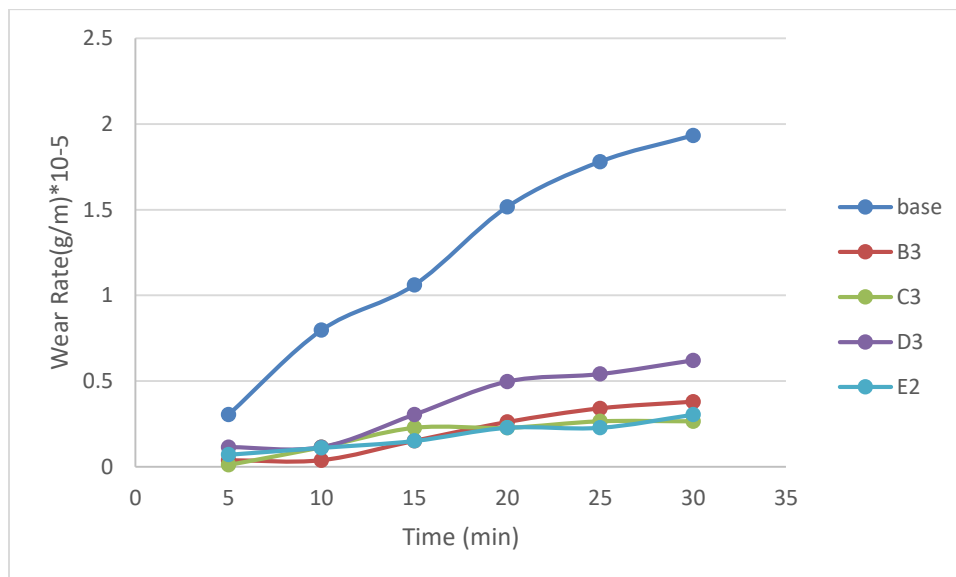


Figure (4.63): Wear rate for A, E<sub>1</sub>, E<sub>2</sub> and E<sub>3</sub> alloy under 15N load

In Figure (4.64) shows the comparison of wear rate of all alloys under 5N load. The best decrease in wear rate appear in C<sub>3</sub> alloy with comparison with all alloys. This is due to the fact that C<sub>3</sub> alloy have higher hardness and lower porosity compared to other alloys.



**Figure(4.64): Comparison of wear rate of all alloys under 5N load.**

Figures (4.65), (4.66), (4.67),(4.68)and (4.69) show the image of the wear tracks taken by an optical microscopy after the wear test. Through Figure (4.65) it was notice that the alloy (A) shows a groove in addition to the wear lines, and this indicates the occurrence of continuous plastic deformation. In the Figures (4.66-4.69) it was observed the appearance of fine wear lines and small areas of wear and the grooves did not appear. This is due to the increase in hardness when adding (B,Zr,In,ZrO<sub>2</sub>) this resulted in reduced weight loss and reduced wear rate and the extrusion deformation it is more difficult when performing a wear test.

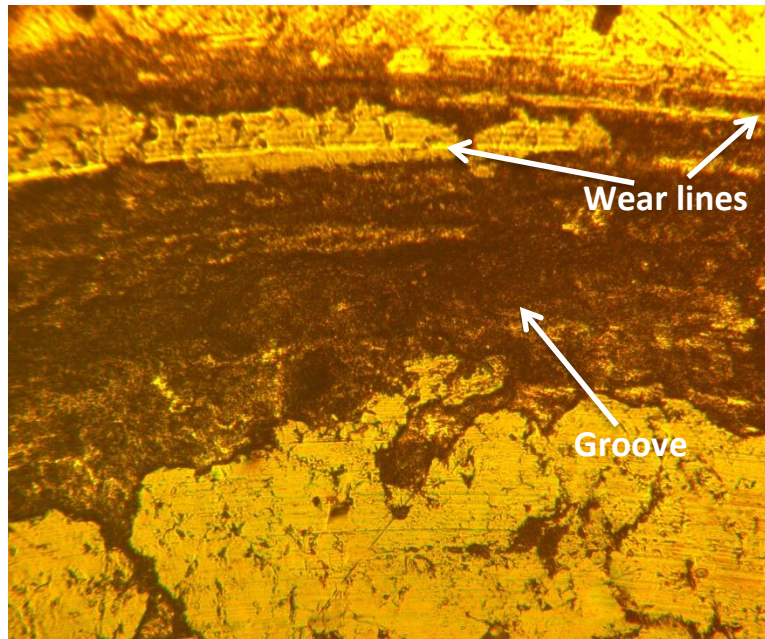


Figure (4.65): Topographic for (A) alloy through using light optical microscope with magnification 200X under (10N) load and (30min) duration.

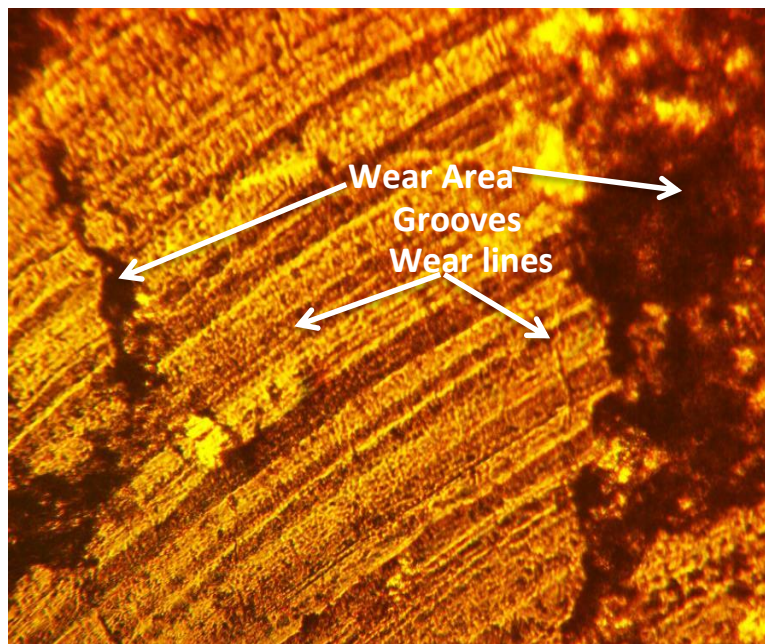
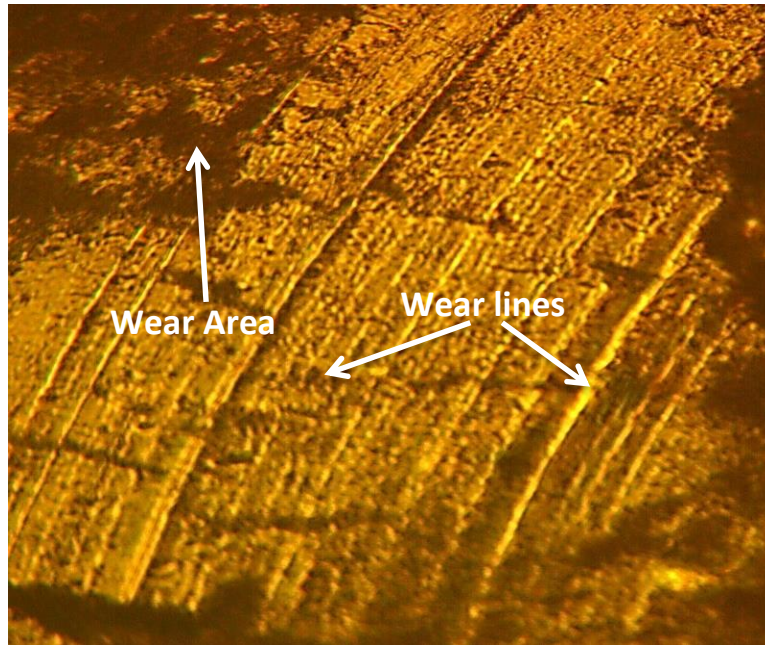
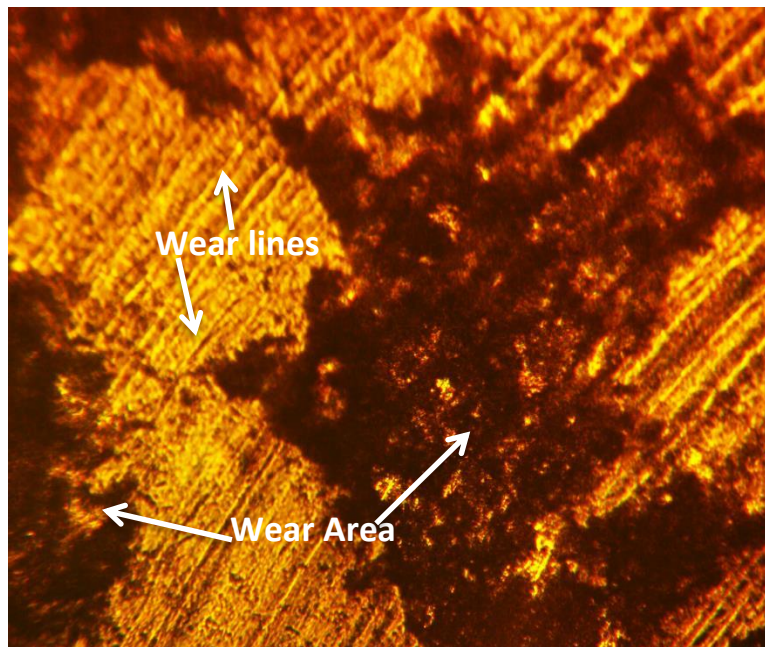


Figure (4.66): Topographic for (B<sub>3</sub>) alloy using the light optical microscope with magnification 200X under (10N) load and (30min) duration.



**Figure (4.67):** Topographic for the (C<sub>3</sub>) alloy using the light optical microscope with magnification 200X under (10N) load and (30min) duration.



**Figure (4.68):** Topographic for the (D<sub>3</sub>) alloy using the light optical microscope with magnification 200X under (10N) load and (30min) duration.

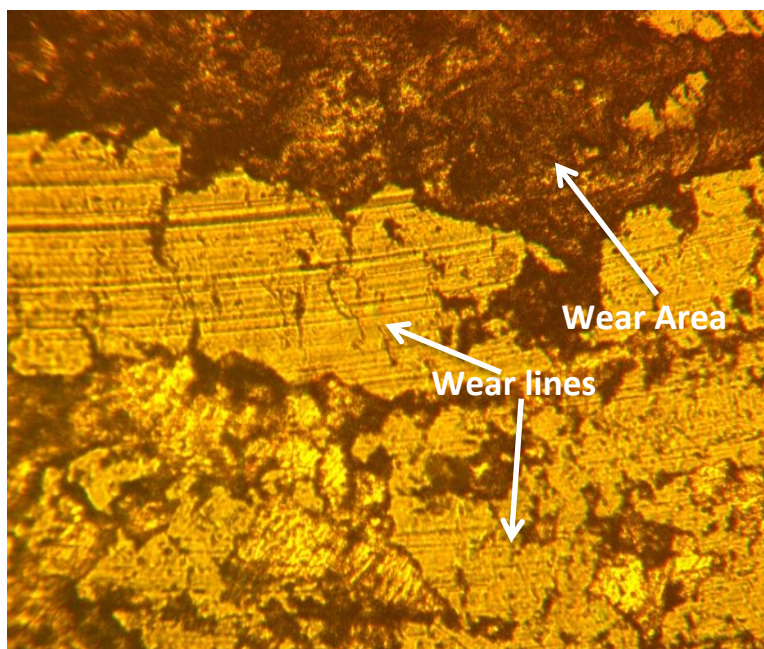


**Figure (4.69): Topographic for the (E<sub>2</sub>)alloy using the light optical microscope with magnification 200X under(10N) load and (30min) duration.**

## 4.6. Electrochemical Tests

### 4.6.1. Open circuit potential (OCP)-time measurement

OCP-time was calculated for all alloys using two solutions artificial saliva and normal saline solution at  $37\pm 1C^{\circ}$ . Figures (4.70-4.73) shows the measurement of corrosion potential over time in an artificial saliva at  $37\pm 1C^{\circ}$  for all of the alloys. The open circuit potential of the alloy starts at a certain value and then gradually decreases. The potential for corrosion that appears is associated with the formation of an oxide film on the metal surface and the ability to protect against corrosion. From the figures below, it was notice that the corrosion potential rises and falls, and this is a result of the formation of oxide layer and then its destruction. Then, the open circuit potential reaches a level that tends to be stable where the potential remains constant even when the test time increases. Consistent corrosion potential means that there is a balance between decomposition and precipitation. Adding

elements(B,Zr,In,ZrO<sub>2</sub>) to the alloy increases the potential for corrosion and this makes the alloy more noble. The OCP-time curves for all alloys in normal saline solution at a temperature of 37±1 °C illustrated in Figures (4.74-4.77).

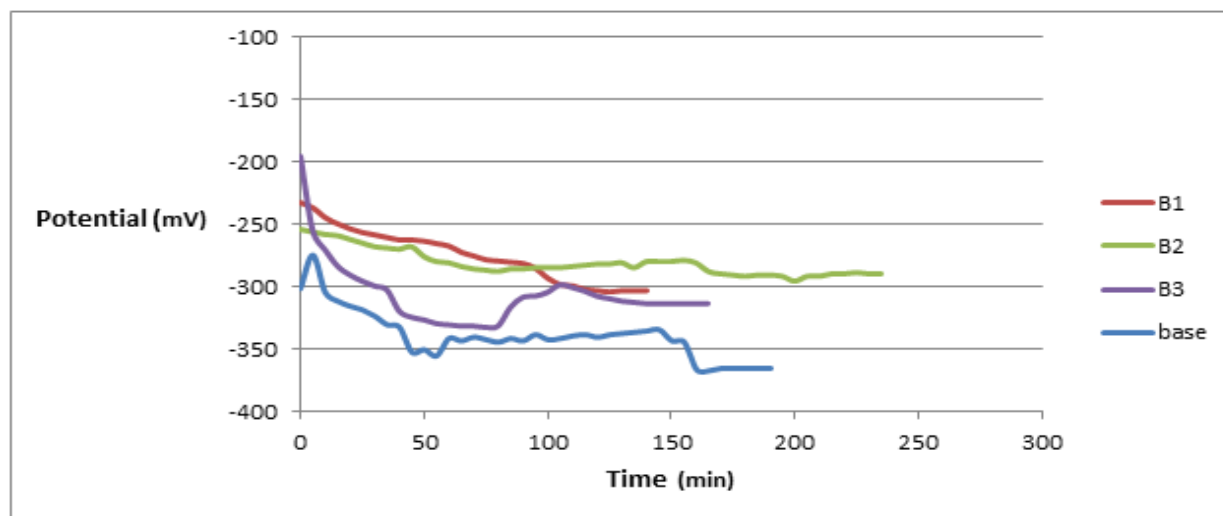


**Figure (4.70):**The OCP-time in solution of saliva at a temperature of 37±1°C for all (A,B<sub>1</sub>,B<sub>2</sub>,B<sub>3</sub>) alloys.

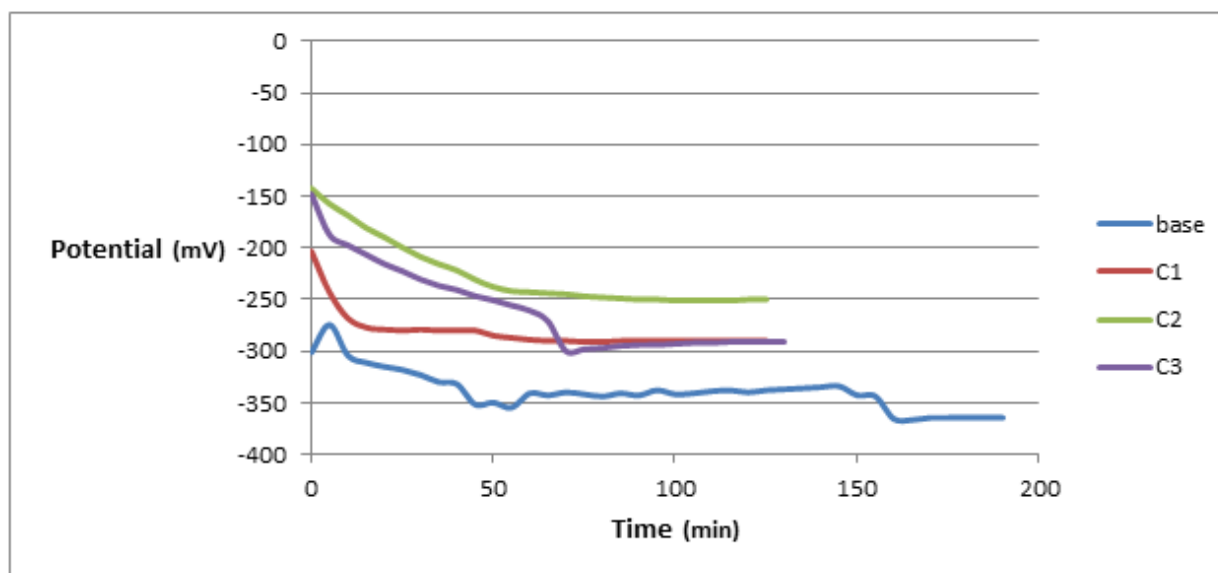


**Figure (4.71):**The OCP-time in saliva solution at 37±1 C° for all (A,C<sub>1</sub>,C<sub>2</sub>,C<sub>3</sub>) alloys.

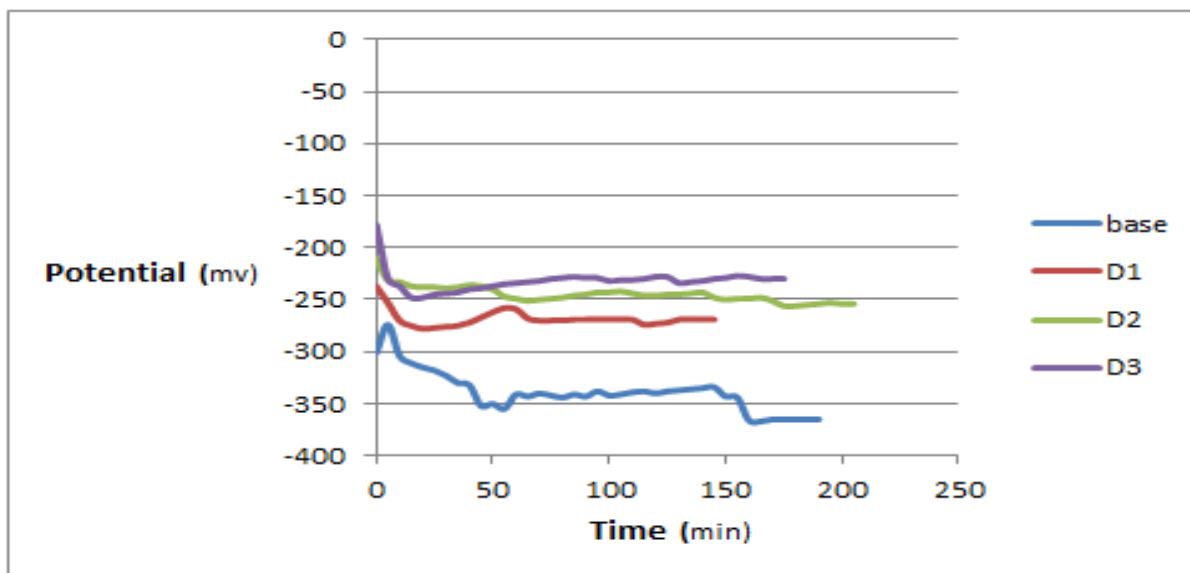


Figure (4.72):The OCP-time in solution of saliva at a temperature of  $37\pm 1^\circ\text{C}$  for all (A,D<sub>1</sub>,D<sub>2</sub>,D<sub>3</sub>) alloys.

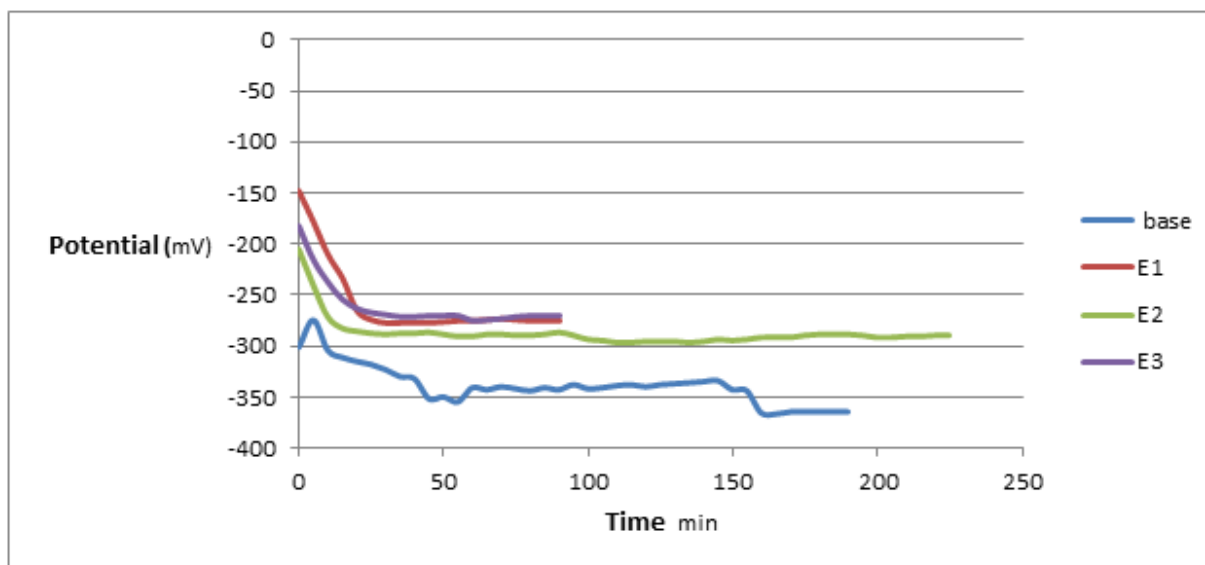


Figure (4.73):The OCP-time in solution of saliva at a temperature of  $37\pm 1^\circ\text{C}$  for all (A,E<sub>1</sub>,E<sub>2</sub>,E<sub>3</sub>) alloys.

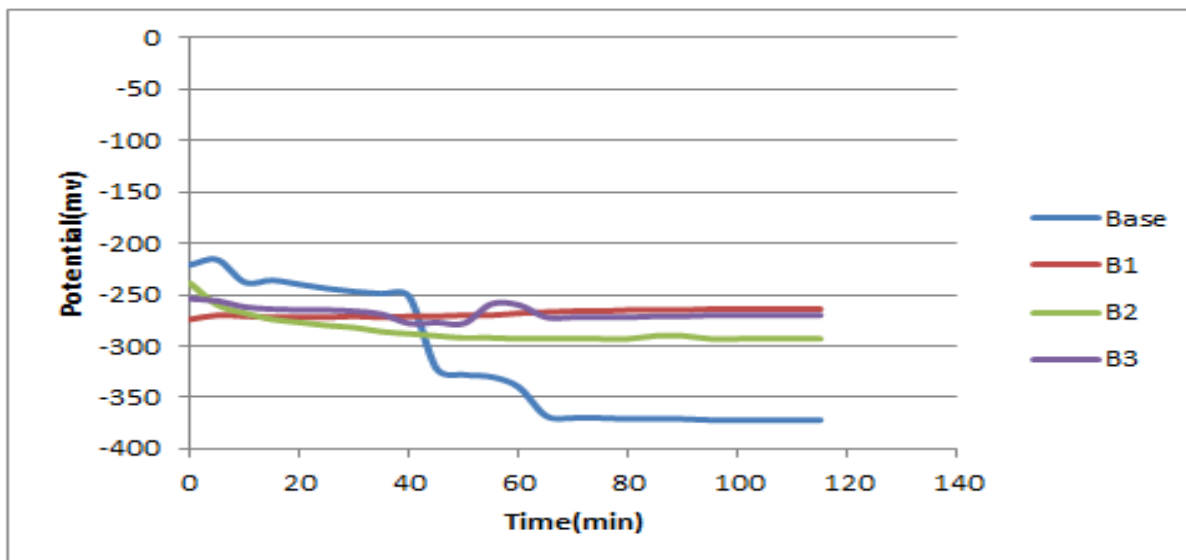


Figure (4.74):The OCP-time in normal saline solution at a temperature of  $37\pm 1$  °C for all (A,B1,B2,B3) alloys.

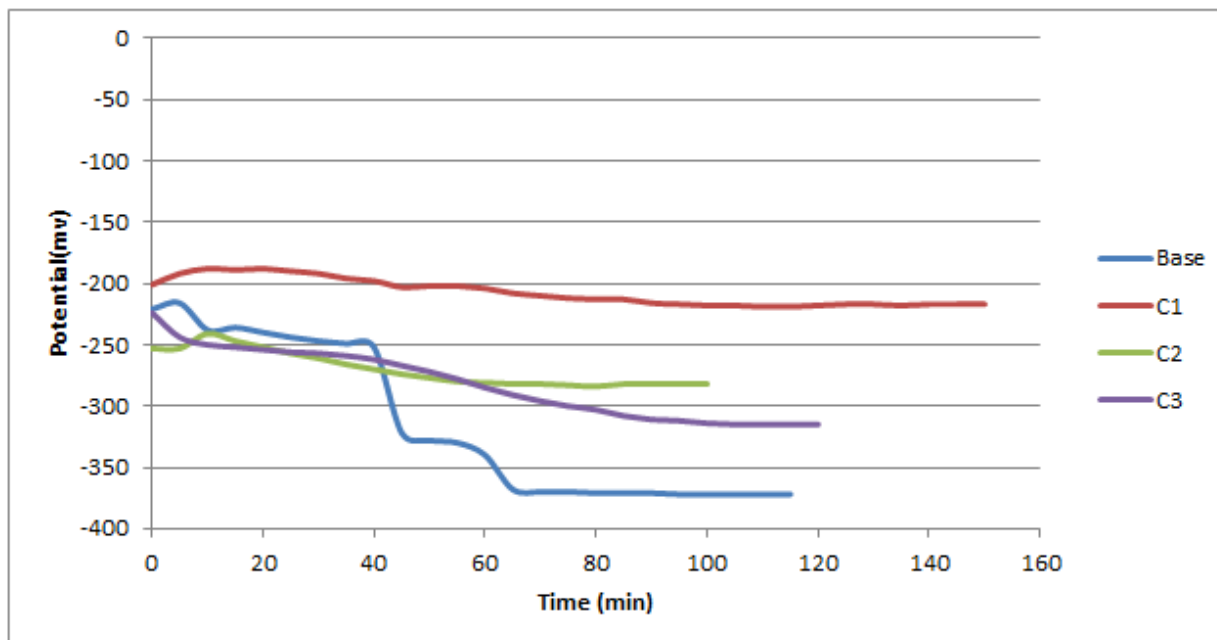


Figure (4.75):The OCP-time in normal saline solution at a temperature of  $37\pm 1$  °C for all (A,C1,C2,C3) alloys.

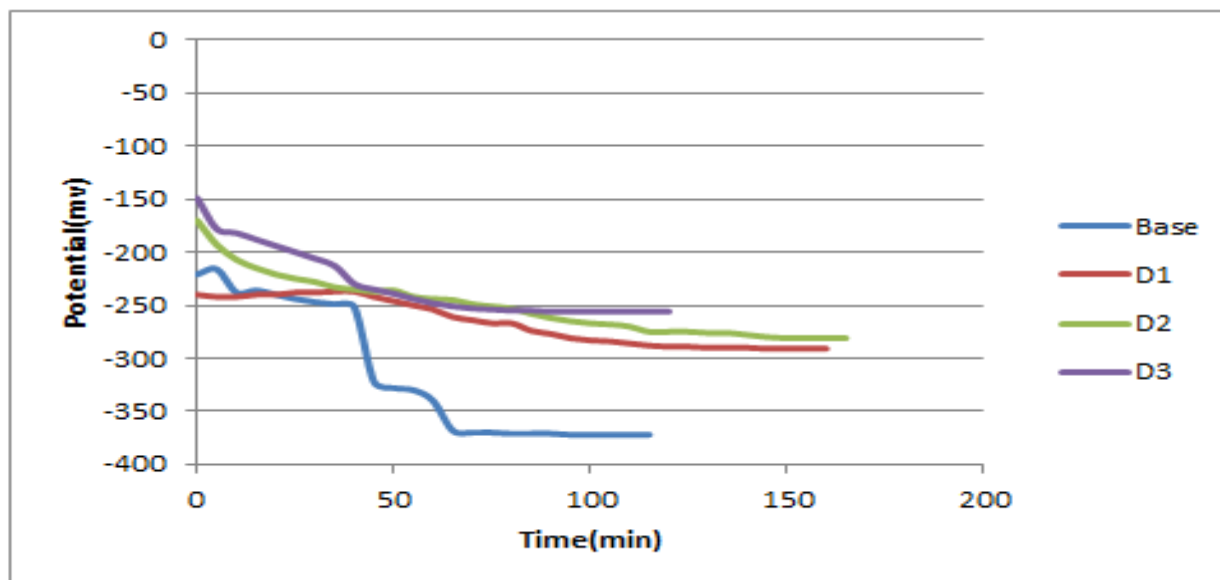


Figure (4.76):The OCP-time in normal saline solution at a temperature of  $37\pm 1$  °C for all (A,D<sub>1</sub>,D<sub>2</sub>,D<sub>3</sub>) alloys.

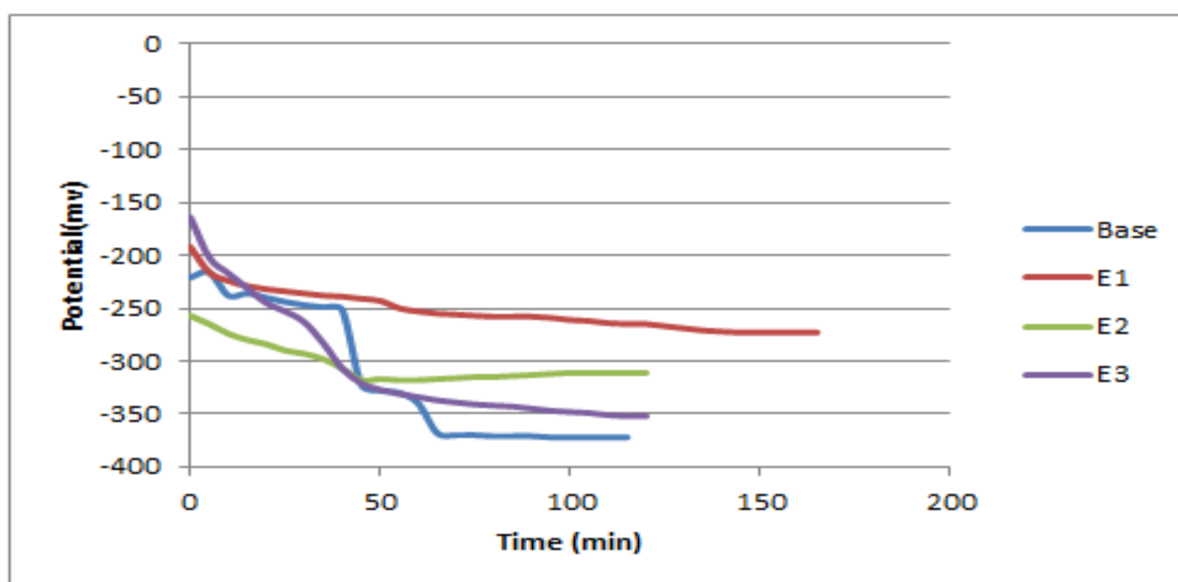
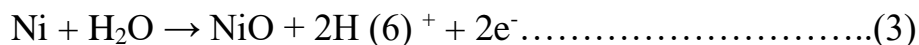
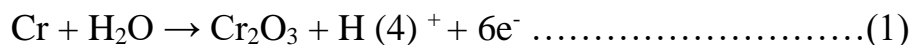


Figure (4.77):The OCP-time in normal saline solution at a temperature of  $37\pm 1$  °C for all (A,E<sub>1</sub>,E<sub>2</sub>,E<sub>3</sub>) alloys.

## 4.6. 2 Potentiodynamic Polarization

The corrosion behaviour of samples in artificial saliva and normal saline solution was studied using a potentiodynamic polarization test. The Log current density-to-

potential diagrams obtained from polarization in an artificial saliva solution are shown in the Figures (4.78-4.81). The consequent reactions of oxidation regarding metals that contain alloy are due to metal dissolution at anodic branch; such dissolution has been translated through an increase in anodic current, succeeded by current's stability and appearance of passive plateau, specifying formation of protective film on the surface of the alloy. On the previously generated Cr oxide, the Nickel and Molybdenum steps of oxidation have been carried out as it has been described by the equilibrium process below [129]:



The amount of molybdenum and chromium in a Ni-Cr alloy's composition influences its corrosion resistance. The development of molybdenum oxide and chromium layers is typically attributed for Ni-Cr alloy passivation. A passive film with greater levels of molybdenum oxide ( $\text{MoO}_3$ ) and chromium oxide ( $\text{Cr}_2\text{O}_3$ ) was shown to inhibit metal ion transfer. In comparison to chromium oxide ( $\text{Cr}_2\text{O}_3$ ), nickel oxide is likely to have a high porosity. The corrosion potential, corrosion current density, corrosion rate, and improvement percentage for all of the alloys in the solution of the saliva at a temperature of  $37^\circ \pm 1^\circ\text{C}$  are shown in Table (4.3). The effect of Boron addition in decreasing the rate of the corrosion for the alloys was noted by Figure (4.78) and Table (4.3). The corrosion rate has been decreased in the case of the addition of the Bo for the alloy in comparison to the base alloy(A) because it leads to enhanced corrosion resistance and passive film stability, this agree with [130, 131]. The presence of boron in the alloy in a small amount reduced the

current density as it becomes  $(16.89, 4.45, 6.89) \mu\text{A}/\text{cm}^2$  for the B<sub>1</sub>, B<sub>2</sub>, B<sub>3</sub> alloys respectively compared to the current density of the A alloy  $(31.80) \mu\text{A}/\text{cm}^2$ .

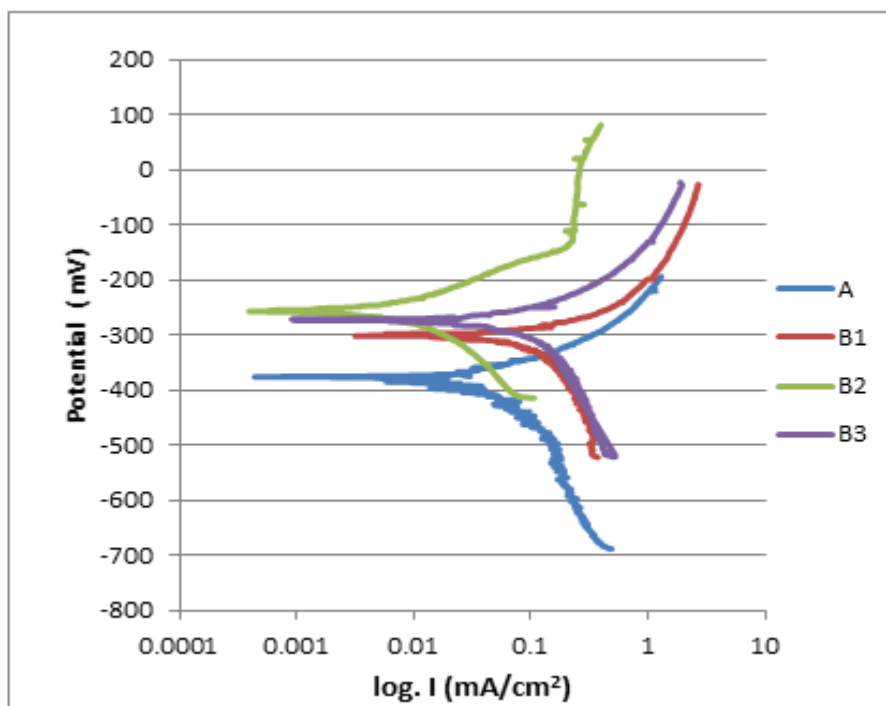


**Figure (4.78): Potentiodynamic Polarization for (A,B<sub>1</sub>,B<sub>2</sub>,B<sub>3</sub>) specimens in artificial saliva solution.**

Figure (4.79) shows the curve of polarization for the samples (A, C<sub>1</sub>, C<sub>2</sub>, C<sub>3</sub>) at 37 °C in artificial saliva solution. Through the polarization curve, it was noticed that the addition of zirconium led to an improvement in corrosion resistance, and this is due to the fact that the presence of zirconium in the alloy led to stabilization of protective oxide layer on surface [132]. When zirconium is added to the alloy, the corrosion rate improves attributable to a rise in the corrosion potential ( $E_{\text{corr}}$ ) and a reduction in the current density ( $I_{\text{corr}}$ ), Table (4.3). The dissolution of the alloy decreases when zirconium is added, so the corrosion current density will decrease when zirconium is added, and this is consistent with [133, 134]. The presence of Zr in the alloy in a

small amount reduced the current density as it becomes  $(13.9, 4.84, 8.76) \mu\text{A}/\text{cm}^2$  for the  $C_1, C_2, C_3$  alloys respectively compared to the current density of the A alloy  $(31.80) \mu\text{A}/\text{cm}^2$ .

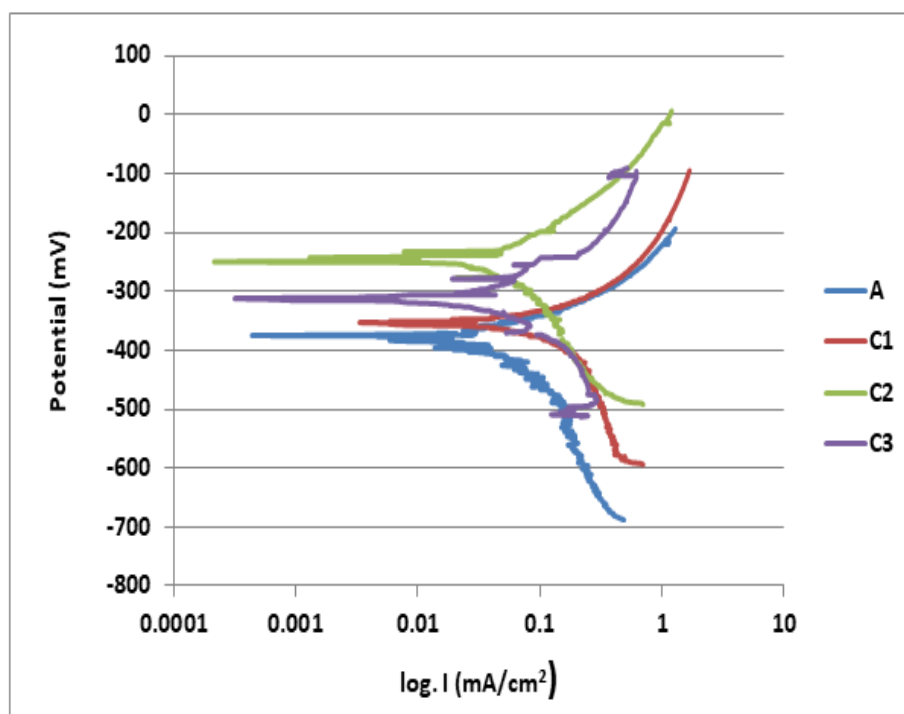


**Figure (4.79): Potentiodynamic Polarization for (A, C<sub>1</sub>, C<sub>2</sub>, C<sub>3</sub>) specimens in artificial saliva solution.**

Figure (4.80) shows the polarization curve for samples (A, D<sub>1</sub>, D<sub>2</sub>, D<sub>3</sub>) at 37 °C in artificial saliva solution. The presence of In in the alloy in a small amount reduced the current density as it becomes  $(14.49, 8.05, 6.53) \mu\text{A}/\text{cm}^2$  for D<sub>1</sub>, D<sub>2</sub>, D<sub>3</sub> alloys respectively compared to current density of A alloy  $(31.80) \mu\text{A}/\text{cm}^2$ . The  $E_{\text{corr}}$  value for alloys with In addition is ranged from  $(-334 \text{ mV})$  to  $(-251.7 \text{ mV})$  which are higher than  $E_{\text{corr}}$  for A alloy which is  $(-336.6 \text{ mV})$ , which means that In addition made the A alloy nobler.

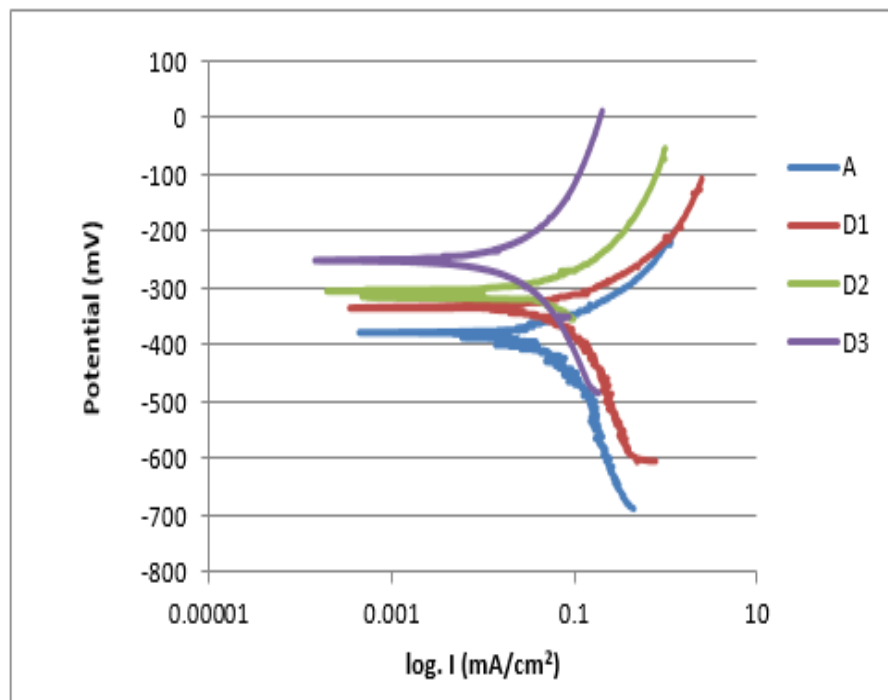


**Figure (4.80): Potentiodynamic Polarization for (A,D<sub>1</sub>,D<sub>2</sub>,D<sub>3</sub>) specimens in artificial saliva solution.**

Figure (4.81) shows the polarization curve for samples (A, E<sub>1</sub>, E<sub>2</sub>, E<sub>3</sub>) at 37 °C in artificial saliva solution. Addition of ZrO<sub>2</sub> to base alloy shifts corrosion potential ( $E_{corr}$ ) to more active direction with decreasing corrosion current density especially in presence 6 and 9 wt% ZrO<sub>2</sub>. The  $E_{corr}$ . value for alloys with ZrO<sub>2</sub> addition is ranged from (-327 mV) to (-249 mV) which are higher than  $E_{corr}$ . for A alloy which is (- 336.6 mV), which means that ZrO<sub>2</sub> addition made the A alloy nobler. The presence of ZrO<sub>2</sub> in the alloy in a small amount reduced the current density as it becomes (18.7,12.06,14.93)  $\mu\text{A}/\text{cm}^2$  for D<sub>1</sub>, D<sub>2</sub>, D<sub>3</sub> alloys respectively compared to current density of A alloy (31.80)  $\mu\text{A}/\text{cm}^2$ .

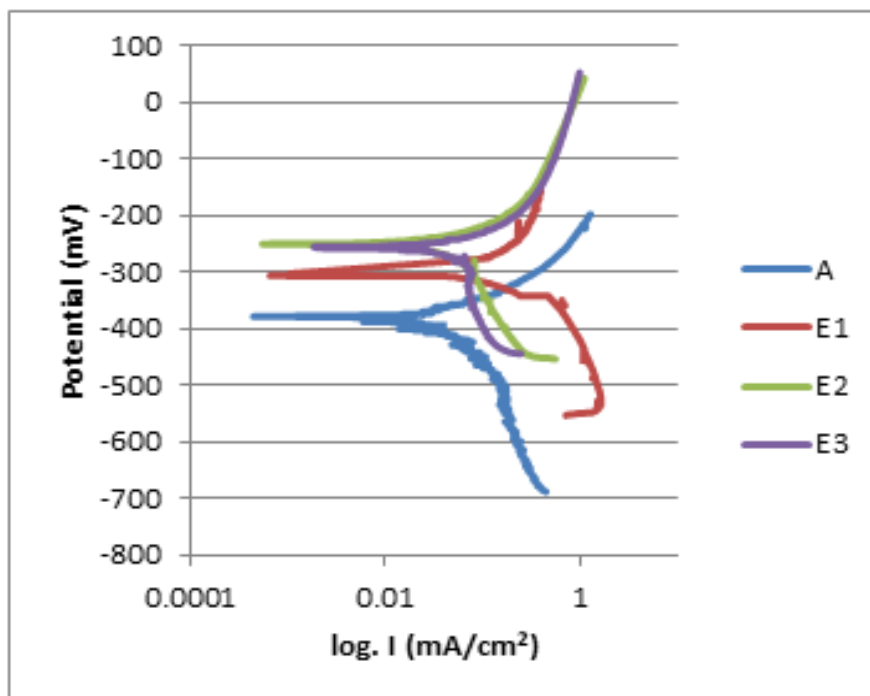


Figure (4.81): Potentiodynamic Polarization for (A,E1,E2,E3) specimens in artificial saliva solution.

Table(4.3): The  $I_{corr}$ ,  $E_{corr}$ . and Corrosion Rate (C.R.) for all alloys in the solution of the saliva at a temperature of  $37^{\circ}\pm 1^{\circ}\text{C}$ .

Synthesized Composition	Code	$I_{corr}$ ( $\mu\text{A}/\text{cm}^2$ )	Potential $E_{corr}$ (mV)	(C.R.) $\text{mpy}\cdot 10^{-3}$	Improvement%
Ni-21%Cr-2%Mo-2%Co	A	31.80	-386.6	10.03	
Ni-21%Cr-2%Mo-2%Co-0.4B	B <sub>1</sub>	16.89	-299.4	5.61	44
Ni-21%Cr-2%Mo-2%Co-0.8B	B <sub>2</sub>	4.45	-254.6	1.54	84.6
Ni-21%Cr-2%Mo-2%Co-1.2B	B <sub>3</sub>	6.98	-273.3	2.450	75.5
Ni-21%Cr-2%Mo-2%Co-0.4Zr	C <sub>1</sub>	13.9	-251.5	5.70	43
Ni-21%Cr-2%Mo-2%Co-0.8Zr	C <sub>2</sub>	4.84	-347.5	1.81	81.9
Ni-21%Cr-2%Mo-2%Co-1.2Zr	C <sub>3</sub>	8.76	-315	2.99	70.1
Ni-21%Cr-2%Mo-2%Co-0.4In	D <sub>1</sub>	14.49	-334	5.24	47.6

Ni-21%Cr-2%Mo-2%Co-0.8In	D <sub>2</sub>	8.05	-318.2	2.95	70.5
Ni-21%Cr-2%Mo-2%Co-1.2In	D <sub>3</sub>	6.53	-251.7	2.54	74.6
Ni-21%Cr-2%Mo-2%Co-3%ZrO <sub>2</sub>	E <sub>1</sub>	18.7	-327	6.59	34.1
Ni-21%Cr-2%Mo-2%Co-6%ZrO <sub>2</sub>	E <sub>2</sub>	12.06	-249	4.69	53.1
Ni-21%Cr-2%Mo-2%Co-9%ZrO <sub>2</sub>	E <sub>3</sub>	14.93	-257.5	6.153	38.4

Figures (4.82 to 4.85) show the potentiodynamic polarization curves for all specimens in normal saline solution and Table (4.3) illustrates the corrosion potential, corrosion rate, corrosion current density, and improvement percentage for all alloys in normal saline solution at  $37\pm 1^\circ\text{C}$ . The corrosion rate was found to be strongly related to pH, where corrosion rate decreases with the increase of pH, ie, an inverse relationship [134]. Where, the pH of artificial saliva and normal saline solutions at  $37\text{ C}^\circ \pm 1$  were 5.8 and 6.5 respectively. Tables (4.3) and (4.4) show that all specimens in normal saline have lower rate and current density of corrosion when compared to those in artificial saliva solution at a temperature of  $37^\circ\text{C}$ . Those findings support the theory that the corrosion resistance regarding a pure metal or an alloy is highly influenced by the environment to which it is exposed as well as the metal's chemical composition [136].

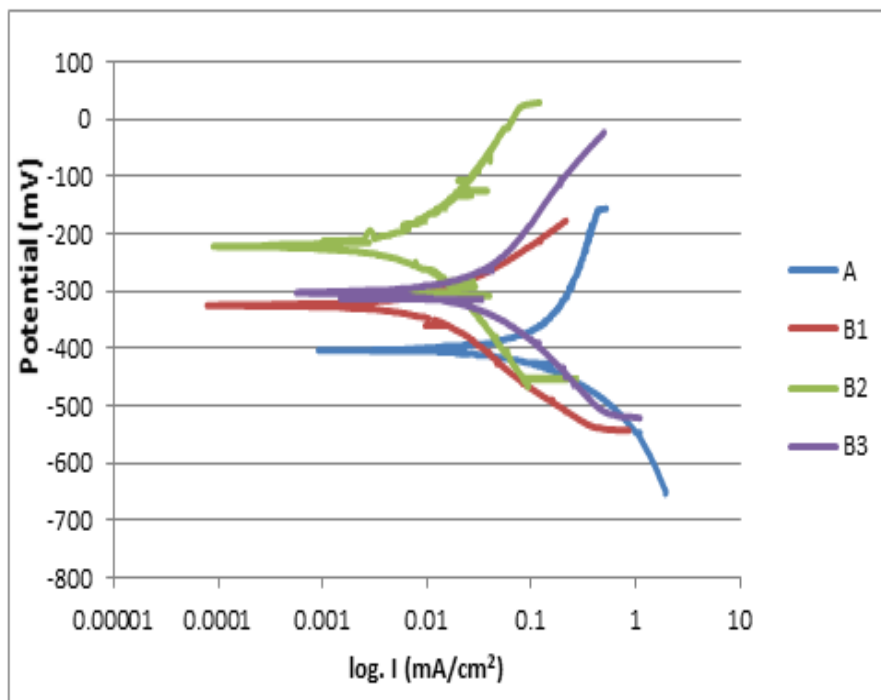


Figure (4.82): Potentiodynamic Polarization curve for (A,B1,B2,B3) samples in normal saline solution.

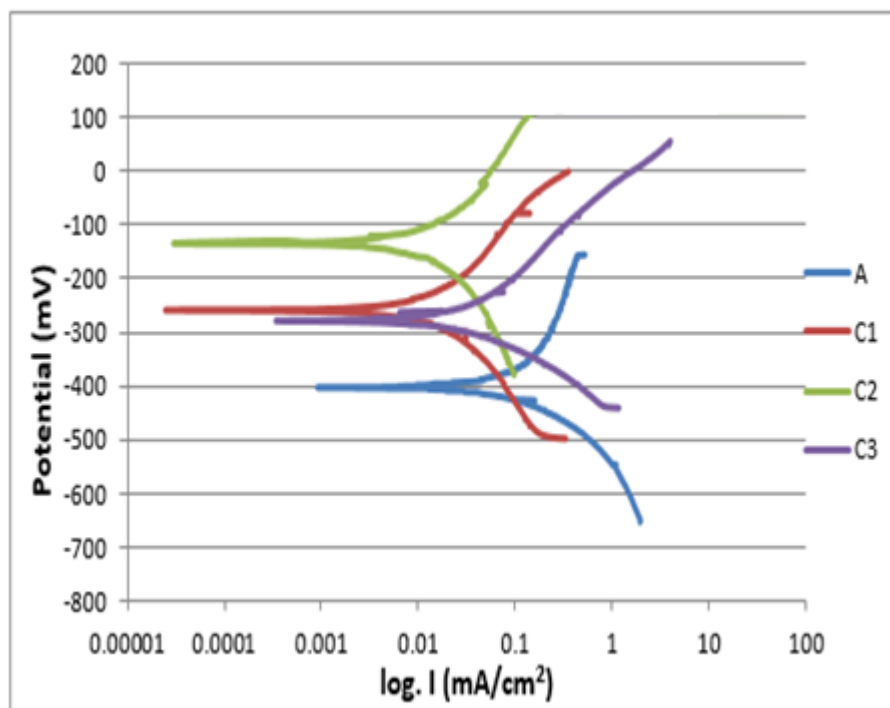


Figure (4.83): Potentiodynamic Polarization curves for the (A,C1,C2,C3) specimens in normal saline solution.

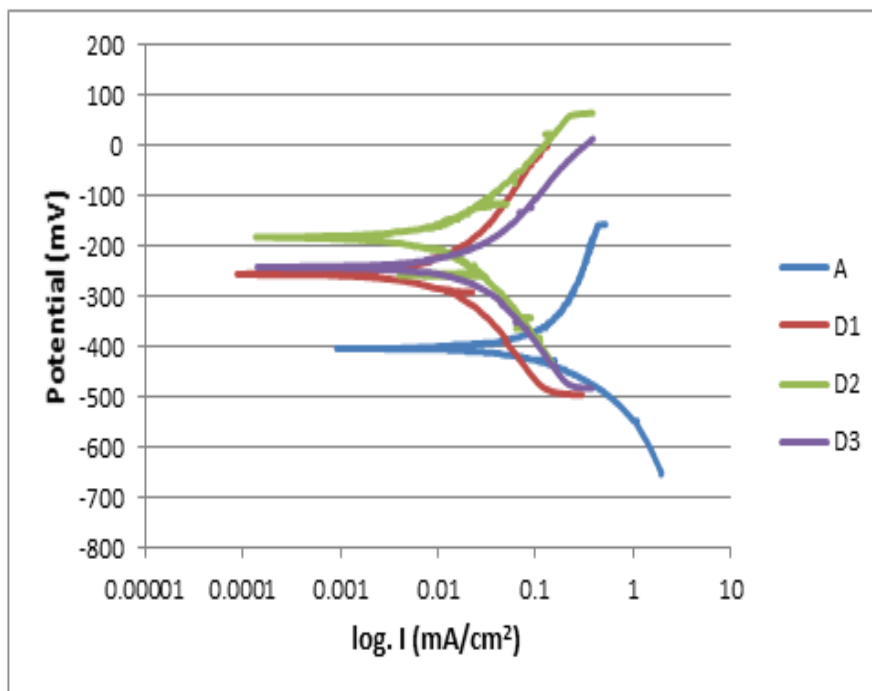


Figure (4.84): Potentiodynamic Polarization curve for specimens of (A,D1,D2,D3) in normal saline solution .

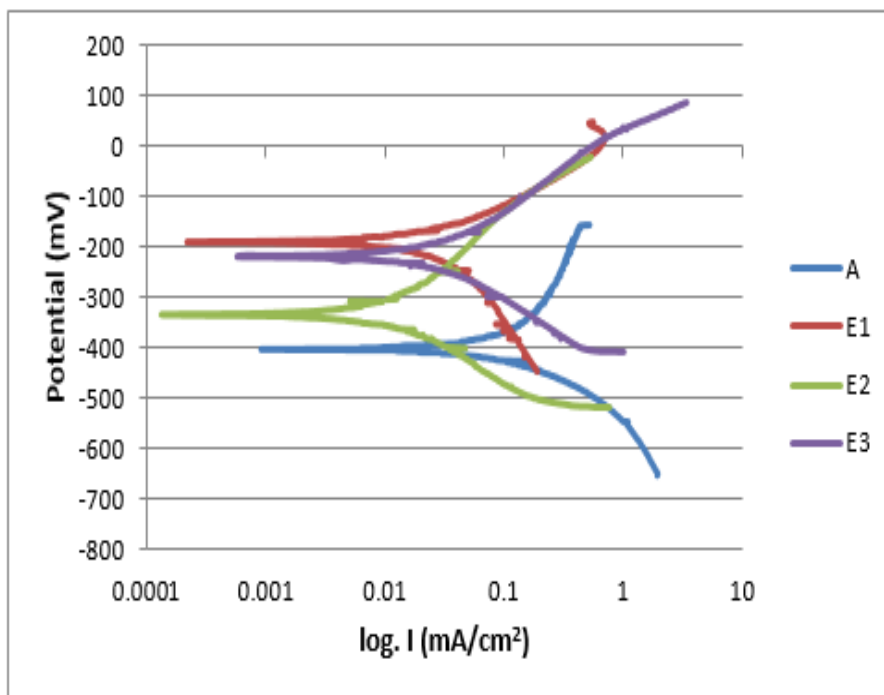
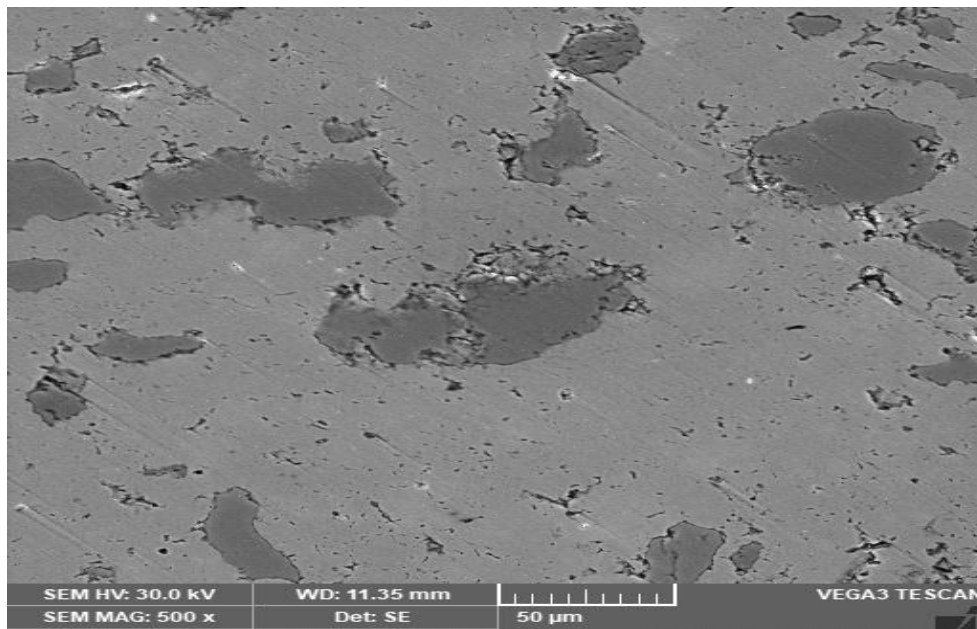


Figure (4.85): Potentiodynamic Polarization curve for specimens of (A,E1,E2,E3) in normal saline solution .

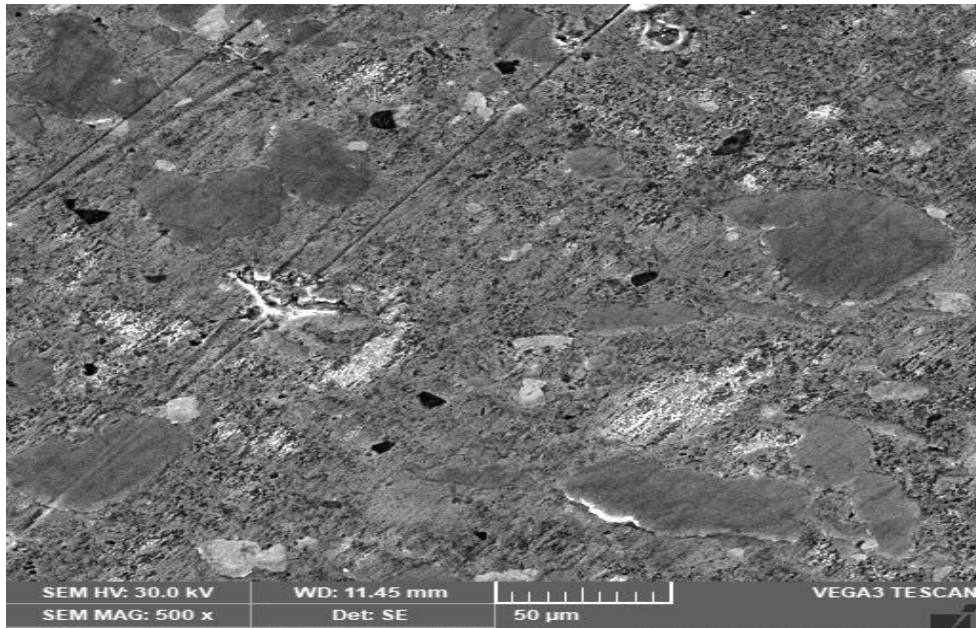
Table(4.4): The  $I_{corr}$ ,  $E_{corr}$ . and C.R. for All of the Alloys in normal saline at  $37\pm 1^\circ\text{C}$ .

Synthesized Composition	Code	$I_{corr}$ ( $\mu\text{A}/\text{cm}^2$ )	$E_{corr}$ (mV)	(C.R.) $\text{mpy} * 10^{-3}$	Improvement%
Ni-21%Cr-2%Mo-2%Co	A	6.98	- 403	2.20	
Ni-21%Cr-2%Mo-2%Co-0.4B	B <sub>1</sub>	1.44	- 325	0.50	77.2
Ni-21%Cr-2%Mo-2%Co-0.8B	B <sub>2</sub>	0.84	-223	0.280	87.2
Ni-21%Cr-2%Mo-2%Co-1.2B	B <sub>3</sub>	2.27	-304	0.79	64
Ni-21%Cr-2%Mo-2%Co-0.4Zr	C <sub>1</sub>	1.43	-258	0.544	75.2
Ni-21%Cr-2%Mo-2%Co-0.8Zr	C <sub>2</sub>	1.32	-133	0.533	75.7
Ni-21%Cr-2%Mo-2%Co-1.2Zr	C <sub>3</sub>	3.24	-277	1.106	49.7
Ni-21%Cr-2%Mo-2%Co-0.4In	D <sub>1</sub>	2.00	-240	0.7366	66.5
Ni-21%Cr-2%Mo-2%Co-0.8In	D <sub>2</sub>	1.82	-253	0.704	68
Ni-21%Cr-2%Mo-2%Co-1.2In	D <sub>3</sub>	1.32	-190	0.480	78.1
Ni-21%Cr-2%Mo-2%Co-3%ZrO <sub>2</sub>	E <sub>1</sub>	4.26	-190	1.48	32.7
Ni-21%Cr-2%Mo-2%Co-6%ZrO <sub>2</sub>	E <sub>2</sub>	2.35	-332	0.969	55.9
Ni-21%Cr-2%Mo-2%Co-9%ZrO <sub>2</sub>	E <sub>3</sub>	4.01	-217	1.56	29

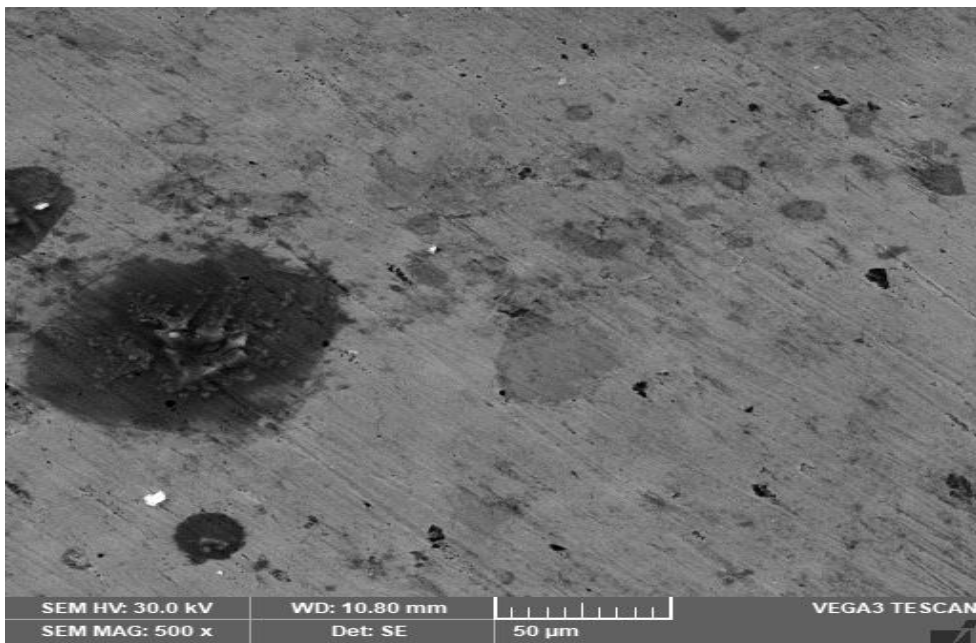
Figure (4.86) shows the SEM image of alloys before and after corrosion test in artificial saliva. When we compared the Figure(4.86-A&B), we noticed the effect of corrosion on the surface of the sample due to the products of corrosion. From Figure (4.86) can be seen that the surface of base alloy as shown in Figure (4.38A) have more cracks in the oxide layer as compared with the surface of B<sub>2</sub> alloy as shown in Figure (4.86- C) . This is mean that the oxide become more adhesive and has less brittleness. Therefore, that the alloys become more resistant to corrosion and more noble. The above results explained a decrease in corrosion current with addition of alloying element .



(A)



(B)



(C)

**Figure( 4.86): SEM for Alloys (A) A alloy before corrosion test (B) A alloy after corrosion in Artificial Saliva solution & (C) B2 alloy after corrosion in Artificial Saliva solution .**

### 4.6.3 Ni and Cr ions release measurement:

Ni sensitization or allergic contact dermatitis can be caused by Ni ions released in significant quantities from Ni-containing alloys[66]. The Ni ions release test is utilized for determining that Ni-Cr-Mo alloys are capable of being employed in human bodies. Immersion experiments with Ni-Cr-Mo alloy were done using two solutions (normal saline and artificial saliva) for getting quantitative data required for selecting adequate materials in line with various medical usage conditions. Figures (4.87) and (4.88) indicate the Ni ions' concentration that are released following immersion in the solution of artificial saliva and normal saline solution for 21 days at  $37^{\circ}\text{C} \pm 2$  as it has been presented in Table 4.3. which shows that measurable Ni ion amounts that have been released from base alloy (A) are larger than those released from other alloys with additives (Zr, B, In,  $\text{ZrO}_2$ ), which are substantially lower compared with the base alloy. These results indicate that (B, Zr, In,  $\text{ZrO}_2$ ) addition reduce Ni ions release from base alloy. This can be attributed to the ability of additives (B, Zr, In,  $\text{ZrO}_2$ ) to formation of stable protective oxide layer, limiting release of Ni ions.

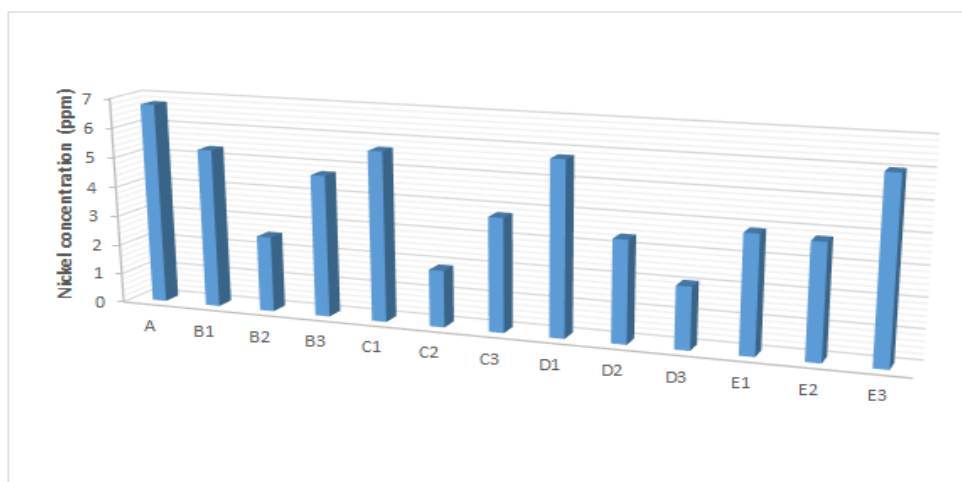


**Figure (4.87):** Nickel ion release values for all of the samples in the solution of the artificial saliva.

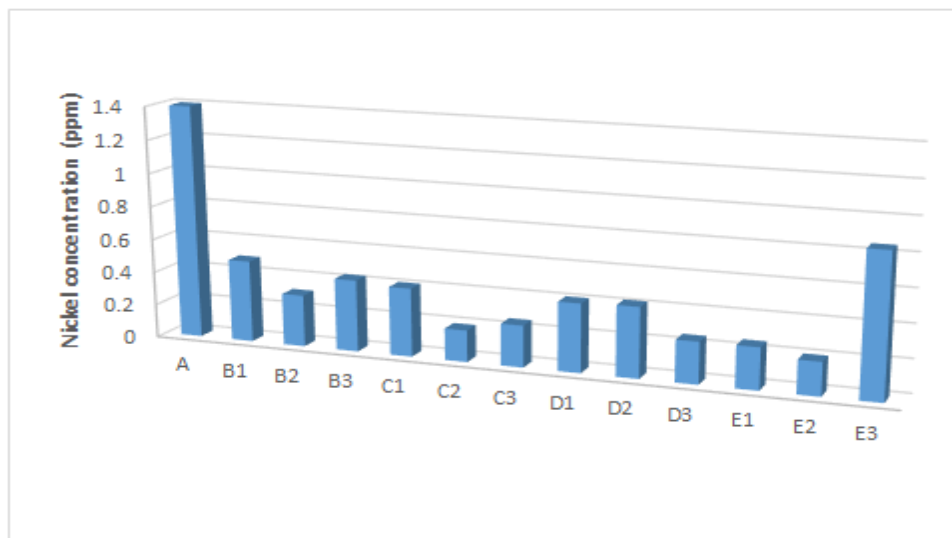


**Figure (4.88): Nickel ion release values for all samples in normal saline solution.**

Figures (4.89) and (4.90) show the concentration of Cr ions released for all of the samples after immersion in the solution of the artificial saliva and normal saline solution for 21 days at  $37\text{ C} \pm 2$  as presented in Table (4.5). The quantities of Cr ions released from the alloys with additives (B, Zr, In,  $\text{ZrO}_2$ ) are much lower than base alloy (A). These results indicate that additives (B, Zr, In,  $\text{ZrO}_2$ ) reduce Cr ions release from NiCrMo alloy. The results indicate that Ni-Cr-Mo alloy releases more Ni than Cr; however, Cr release from Ni-Cr alloy has been considerably lower when compared with Ni release in the artificial saliva and normal saline solution. This can be due to the alloy's lower Cr content; however, there is an increase in the amount of element release with the increase in the percentage of Cr in the alloy [137].

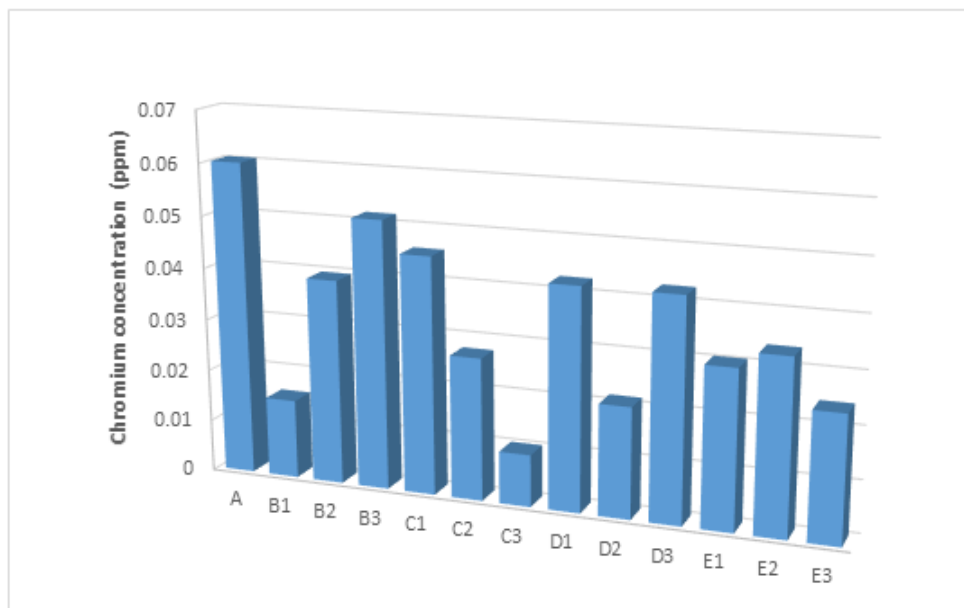


**Figure (4.89): Chromium ion release values for all of the samples in the solution of the artificial saliva.**

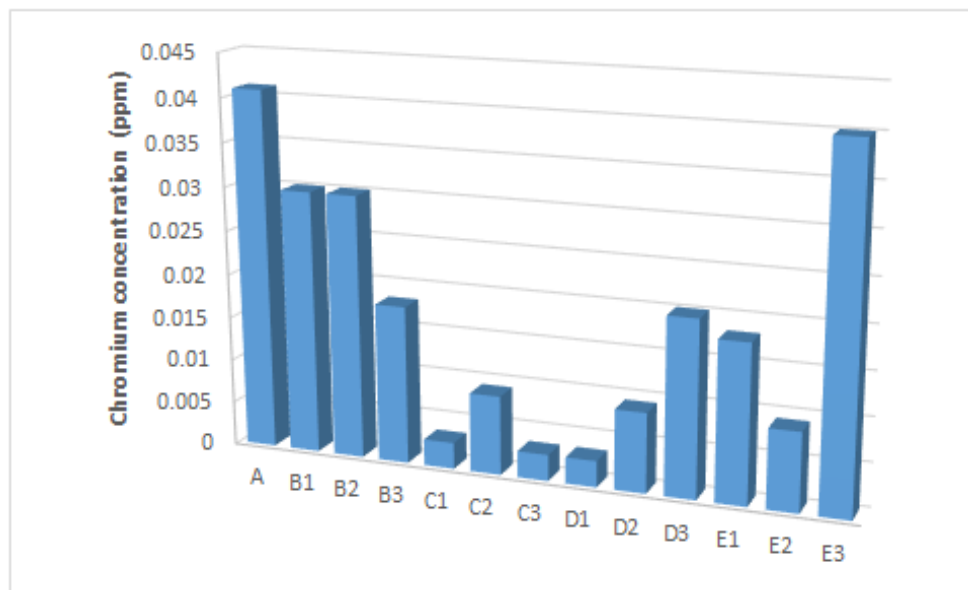


**Figure (4.90): Chromium ion release values for all samples in normal saline solution.**

The corrosion properties related to Ni-Cr alloys are influenced by their microstructure, bulk composition, and development of protective surface oxide, as well as the composition regarding the surrounding electrolyte [135]. Along with improving the existence of  $\text{Cr}_2\text{O}_3$  passive film, the existence of additives (Zr, B, In,  $\text{ZrO}_2$ ) in alloy operate as cathodic regions, reducing dissolution of Ni-Cr from the alloy and so eliminating corrosion rate.

**Table 4.5: Concentration of Nickel and Chromium ions that have been released from the all of the samples in the synthetic saliva and normal saline solutions after 3 weeks of immersion at 37 °C.**

Sample code	Amounts of Ni release (ppm) in saliva	Amounts of Ni release (ppm) in normal saline	Amounts of Cr release (ppm) in saliva	Amounts of Cr release (ppm) in normal saline
A	6.76	1.4	0.0603	0.041
B1	5.35	0.49	0.0152	0.03
B2	2.54	0.31	0.0394	0.03
B3	4.75	0.43	0.0515	0.018
C1	5.68	0.41	0.0455	0.003
C2	1.9	0.19	0.0273	0.009
C3	3.8	0.25	0.01	0.003
D1	5.8	0.41	0.0424	0.003
D2	3.4	0.42	0.0212	0.0091
D3	2.07	0.25	0.0424	0.02
E1	3.9	0.25	0.0303	0.018
E2	3.8	0.2	0.0333	0.009
E3	6.03	0.85	0.0242	0.04

## 4.7 Biological Test

### 4.7.1 Antibacterial Test

The antibacterial test was done for samples ( $B_1, B_4, B_7, B_{10}, B_{12}$ ), where  $B_1$  refer to the alloy without addition,  $B_4$  refer to the alloy with 1.2B addition,  $B_7$  refer to the alloy with 1.2 Zr addition,  $B_{10}$  refer to alloy with 1.2In addition and  $B_{12}$  refer to alloy

with %6 ZrO<sub>2</sub> addition. It was notice that the presence of samples led to a reduction in the effect of bacteria. The Table (4.6) shows the antibacterial test results include (viable count, reduction percentage and Log.reduction) for all samples at Bacteria ( Streptococcus mutans (Gr+, Facultative Anaerobe)) and Fungi( Candida albicans ) after 1h and 12h . Figure (4.91) shows the effect of adding samples on the percentage of reduction after 1h and 12h for all samples in Bacteria(Streptococcus mutans )and Fungi (Candida albicans ) , where it was notice a noticeable decrease in the percentage of bacteria after incubation for 12 hours. Sample B<sub>10</sub> and then sample B<sub>12</sub> had the highest antibacterial effect on both indices compared to other samples. It seems that due to the slow release of the material, the antibacterial effect of the samples on both indicators is more noticeable in a longer time (12 hours). The presence of indium does not help to carry out the vital activities of any living organism, as it is considered a moderately toxic metal, which means that if it is injected directly, it can cause poisoning. Therefore, it was noticed an increase in the resistance of the sample (B<sub>10</sub>) to bacteria when indium is present in the alloy. For zirconia, the particle size of zirconia(0.3μ) is smaller than the size of bacteria (Streptococcus mutans)(0.5 μ), so it is easy for ceramic particles to attack or destroy the bacterial cell or try to penetrate its protein membrane. For fungi ( Candida albicans ), their size is already very large(5-6 μ) , so we noticed that all samples have high effectiveness.

**Table (4.6):** The antibacterial test results include (viable count, reduction percentage and Log.reduction) for all samples at Bacteria ( *Streptococcus mutans* (Gr+, Facultative Anaerobe)) and Fungi( *Candida albicans* ) after 1h and 12h.

<b>I.</b>		<b>Strain: <i>Streptococcus mutans</i></b>		<b>Gram Positive Bacteria</b>			
Time	Item	Blank	B1	B4	B7	B10	B12
1h	VC <sup>1</sup> (CFU/ml)	1 × 10 <sup>6</sup>	5 × 10 <sup>5</sup>	6 × 10 <sup>5</sup>	5 × 10 <sup>5</sup>	1 × 10 <sup>5</sup>	7 × 10 <sup>5</sup>
	RP <sup>2</sup> (%)	-	50%	40%	50%	90%	30%
	LR <sup>3</sup> (Log <sub>10</sub> )	-	0.301	0.222	0.301	1	0.155
12h	VC <sup>1</sup> (CFU/ml)	1 × 10 <sup>6</sup>	6 × 10 <sup>5</sup>	1 × 10 <sup>5</sup>	5 × 10 <sup>5</sup>	<1 × 10 <sup>1</sup>	<1 × 10 <sup>1</sup>
	RP <sup>2</sup> (%)	-	40%	90%	50%	>99.9%	>99.9%
	LR <sup>3</sup> (Log <sub>10</sub> )	-	0.222	1	0.301	>5	>5
1- Viable Count, 2- Reduction Percentage, 3- Logarithmic Reduction							
<b>II.</b>		<b>Strain: <i>Candida albicans</i> ATCC 10231</b>		<b>Fungi (Yeast)</b>			
Time	Item	Blank	B1	B4	B7	B10	B12
1h	VC <sup>1</sup> (CFU/ml)	1 × 10 <sup>6</sup>	8 × 10 <sup>5</sup>	8 × 10 <sup>5</sup>	8 × 10 <sup>5</sup>	6 × 10 <sup>5</sup>	8 × 10 <sup>5</sup>
	RP <sup>2</sup> (%)	-	20%	20%	20%	40%	20%
	LR <sup>3</sup> (Log <sub>10</sub> )	-	0.097	0.097	0.097	0.222	0.097
12h	VC <sup>1</sup> (CFU/ml)	1 × 10 <sup>6</sup>	1 × 10 <sup>4</sup>	5 × 10 <sup>4</sup>	<1 × 10 <sup>4</sup>	<1 × 10 <sup>1</sup>	<1 × 10 <sup>4</sup>
	RP <sup>2</sup> (%)	-	99%	95%	>99%	>99.9%	>99%
	LR <sup>3</sup> (Log <sub>10</sub> )	-	2	1.301	>2	>5	>2
1- Viable Count, 2- Reduction Percentage, 3- Logarithmic Reduction							

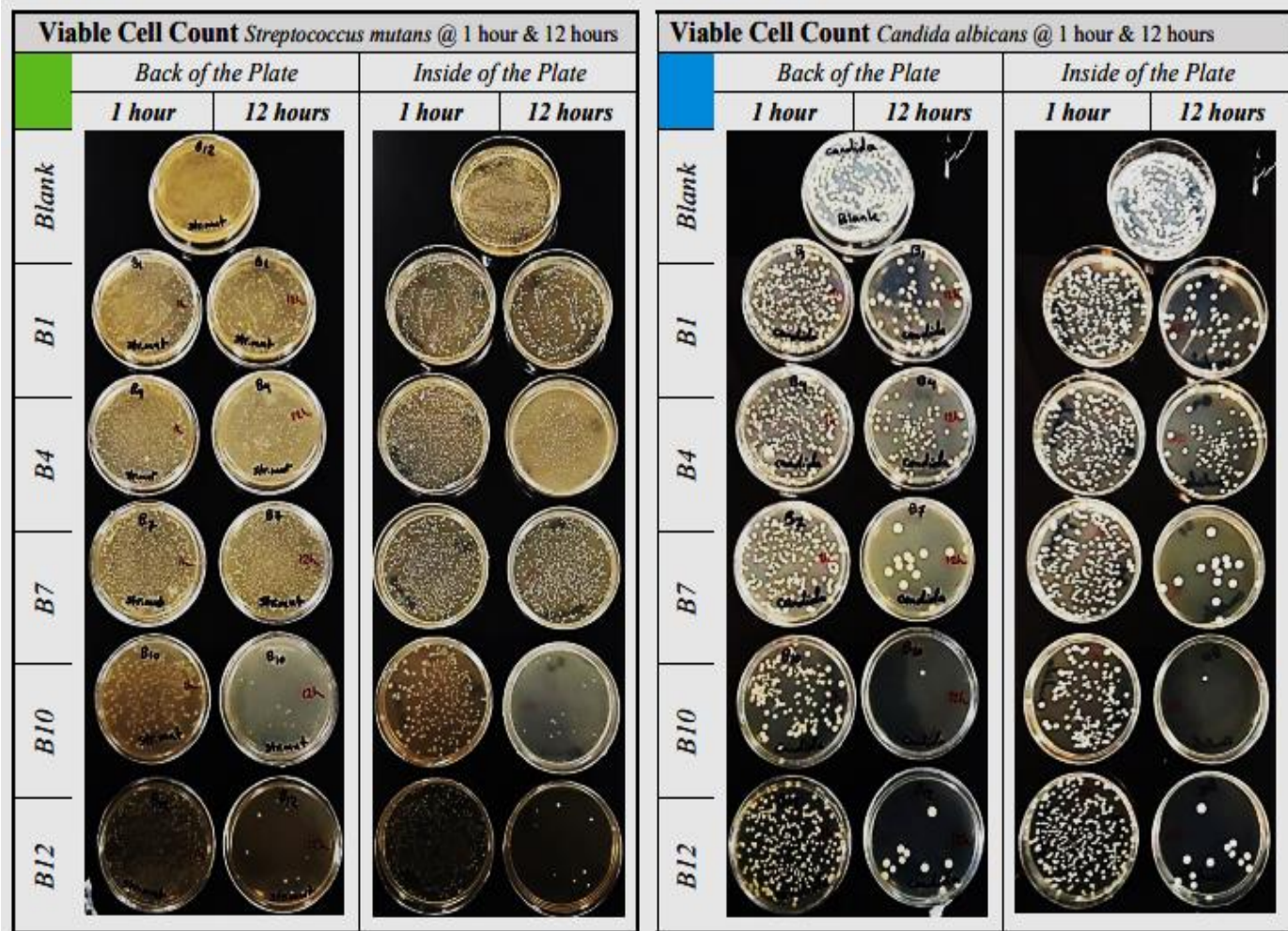


Figure (4.91): The effect of adding samples on the percentage of reduction after 1h and 12h for all samples in Bacteria(*Streptococcus mutans*) and Fungi (*Candida albicans*)

## Chapter Five

### Conclusions & Suggestions for future works

#### 5.1 Conclusions:

From the experimental and numerical modeling results and their discussion, several conclusions may be drawn as follows:

- 1- The best compacting pressure for NiCrMo alloy that used in this work was 600 MPa, in this compacting pressure obtained the least porosity and the highest density of the compacted sample.
- 2- sintering at 1000° C for 8h of samples (with and without additives) is efficient to complete the transformation process of Ni, Cr and Mo to alloy structure.
- 3- At room temperature, just three phases structure appear in all alloys (with and without additives),  $\gamma$  (Ni),  $\text{Cr}_3\text{Ni}_2$ ,  $\text{MoNi}_4$ .
- 4- The addition of B, Zr and In with (0.4 ,0.8 and 1.2) wt. % to NiCrMo alloy resulted in decreasing the porosity compared to base alloy without B,Zr and In. While, the addition of  $\text{ZrO}_2$  with (3,6and 9) wt.% causes increasing in of NiCrMo alloys porosity compared to base alloy without  $\text{ZrO}_2$ .
- 5- The alloys with B, Zr and In additives (0.4 ,0.8 and 1.2) wt. % and  $\text{ZrO}_2$  with(3,6 and 9) wt.% have hardness values higher than that for NiCrMo alloy without B,Zr,In and  $\text{ZrO}_2$  additives .
- 6- The compression strength values with B,Zr ,In and  $\text{ZrO}_2$  additives was higher than that for NiCrMo alloy without B, Zr and  $\text{ZrO}_2$  additives.
- 7- The values of modulus of elasticity an increase in the addition of B, Zr , In and  $\text{ZrO}_2$  compared with the NiCrMo alloy without additive.

- 8- The wear resistance increased with addition of B,Zr,In and ZrO<sub>2</sub> to NiCrMo alloys , The sample of (1.2 %)Zr has lower weigh loss during wear test under different loads.
- 9- The corrosion resistance of CoCrMo alloys with B,Zr,In and ZrO<sub>2</sub> additives was higher than that for NiCrMo alloys without B, Zr,In and ZrO<sub>2</sub> additives in artificial saliva solution and 0.9%NaCL.The higher improvement with the addition of the 0.8wt% B was 84.6% , 87.2% in Saliva and 0.9%NaCl solution , respectively.
- 10- In the Ion release result after immersion in solutions its show that the base alloys with B,Zr,In and ZrO<sub>2</sub> additives exhibited enhances the passive layer to a more area by reduce the ionic release.
- 11- In the antibacterial test it was notice a decrease in the percentage of bacteria after incubation for 12 hours. Sample D<sub>3</sub> and then sample E<sub>2</sub> had the highest antibacterial effect on both indices compared to other samples.

## **5.2. Suggestions for future works**

1- Study the effect of B and Zr additives together on mechanical and electrochemical properties of NiCrMo alloy.

2- Adding other alloying elements like Niobium or Cerium and study the effect of these elements on the mechanical and electrochemical properties of NiCrMo alloy in vitro.

3- Using surface coating treatment to modify the surface properties of NiCrMo and study the effect of the surface treatment on the corrosion resistance of these alloys.

4- Study of the effect of heat treatment after sintering on the mechanical and electrochemical properties of NiCrMo alloy with and without addition.

5- Study the effects of parameters such as shape and practical size of the used powders on the mechanical and electrochemical properties of prepared alloys.

## References

1. Roach, Michael. "Base metal alloys used for dental restorations and implants." *Dental Clinics of North America* 51.3 (2007): 603-627.
2. Gladwin, M. and M. Bagby, *Clinical Aspects of Dental Materials Theory, Practice, and Cases*. 2004.
3. Anusavice, Kenneth J., Chiayi Shen, and H. Ralph Rawls, eds. *Phillips' science of dental materials*. Elsevier Health Sciences, 2012.
4. Manappallil, John J. *Basic dental materials*. JP Medical Ltd, 2015.
5. Mahalaxmi, S. *Materials used in Dentistry*. Wolters kluwer india Pvt Ltd, 2020.
6. O'brien, William J. "Dental materials and their selection." *Quintessence* (2002).
7. Niinomi, Mitsuo, ed. *Metals for biomedical devices*. Woodhead publishing, 2019.
8. Grgur, Branimir N., Vojkan Lazić, Dragana Stojić, and Rebeka Rudolf. "Electrochemical testing of noble metal dental alloys: The influence of their chemical composition on the corrosion resistance." *Corrosion Science* 2021 May 15;184:109412.
9. Hong, Min-Ho, Takao Hanawa, Si Hoon Song, Bong Ki Min, and Tae-Yub Kwon. "Enhanced biocompatibility of a Ni–Cr alloy prepared by selective laser melting: a preliminary in vitro study." *Journal of Materials Research and Technology* 8, no. 1 (2019): 1587-1592.

## References

10. Sakaguchi, Ronald L., and John M. Powers. *Craig's restorative dental materials-e-book*. Elsevier Health Sciences, 2012.
11. Elshahawy, W. and I. Watanabe, Biocompatibility of dental alloys used in dental fixed prosthodontics. *Tanta Dental Journal*, 2014. 2(11): p. 150-159.
12. Liliana, Porojan, Savencu Cristina Elena, Costea Liviu Virgil, Dan Mircea Laurentiu, and Porojan Sorin Daniel. "Corrosion behavior of Ni-Cr dental casting alloys." *Int J Electrochem* 13 (2018): 410-423
13. Bauer, José Roberto de Oliveira, Alessandro Dourado Loguercio, Alessandra Reis, and Leonardo Eloy Rodrigues Filho. "Microhardness of Ni-Cr alloys under different casting conditions." *Brazilian oral research* 20 (2006): 40-46.
14. Mansoor, Nidhal Sahib, Arash Fattah-alhosseini, Arash Shishehian, and Hassan Elmkhah. "Corrosion behavior of single and multilayer coatings deposited on Ni-Cr Dental Alloy by CAE-PVD technique in artificial saliva." *Analytical and Bioanalytical Electrochemistry* 11, no. 3 (2019): 304-320.
15. Manaranche, C. and H. Hornberger, A proposal for the classification of dental alloys according to their resistance to corrosion. *Dental materials*, 2007. 23(11): p. 1428-1437.
16. Schmalz, G. and D. Arenholt-Bindslev, Biocompatibility of dental materials. Vol. 1. 2009: Springer.
17. Renita, D., S. Rajendran, and A. Chattree, Influence of artificial saliva on the corrosion behavior of dental alloys: a review. *Indian J. Adv. Chem. Sci*, 2016. 4(4): p. 478-483.
18. House, Kate, Friedrich Sernetz, David Dymock, Jonathan R. Sandy, and Anthony J. Ireland. "Corrosion of orthodontic appliances—should we

## References

- care?." *American journal of orthodontics and dentofacial orthopedics* 133, no. 4 (2008): 584-592.
19. Graf, K., G. H. Johnson, A. Mehl, and P. Rammelsberg. "The influence of dental alloys on three-body wear of human enamel and dentin in an inlay-like situation." *Operative Dentistry* 27, no. 2 (2002): 167-174.
20. Shi, Donglu , Introduction To Biomaterials. 2005: World Scientific.
21. Quezada-Castillo, Elvar, Wilder Aguilar-Castro, and Bertha Quezada-Alván. "Corrosion of galvanic couplings of Ni-Cr and Co-Cr alloys with Ti-6Al-4V in artificial saliva using electrochemical methods." *Matéria (Rio de Janeiro)* 25 (2020).
22. Muris, Joris, and Cees J. Kleverlaan. "Hypersensitivity to dental alloys." In *Metal allergy*, pp. 285-300. Springer, Cham, 2018.
23. Powers, J.M. and J.C. Wataha, Dental Materials-E-Book: Properties and Manipulation. 2014: Elsevier Health Sciences.
24. Lins, Sâmira Ambar, Áquira Ishikiriama, Fabio Antonio Piola Rizzante, Adilson Yoshio Furuse, José Mondelli, Sérgio Kiyoshi Ishikiriama, and Rafael Francisco Lia Mondelli. "Use of restorative materials for direct and indirect restorations in posterior teeth by Brazilian dentists." *RSBO Revista Sul-Brasileira de Odontologia* 11, no. 3 (2014): 238-244.
25. Setcos, James C., Amir Babaei-Mahani, Lucy Di Silvio, Ivar A. Mjör, and Nairn HF Wilson. "The safety of nickel containing dental alloys." *Dental materials* 22, no. 12 (2006): 1163-1168.

## References

26. He, Longwen, Danni Dai, Liben Xie, Yuming Chen, and Chao Zhang. "Biological effects, applications and strategies of nanomodification of dental metal surfaces." *Materials & Design* 207 (2021): 109890.
27. Hollinger, J.O. and S.A. Guelcher, An introduction to biomaterials. 2012: CRC Press/Taylor & Francis Boca Raton, Florida. USA.
28. Wagner, W.R., et al., Biomaterials science: An introduction to materials in medicine. 2020: Academic Press.
29. Asri, R., et al., A review of hydroxyapatite-based coating techniques: Sol–gel and electrochemical depositions on biocompatible metals. *Journal of the mechanical behavior of biomedical materials*, 2016. 57: p. 95-108.
30. Ratner, B.D., et al., Biomaterials science: an introduction to materials in medicine. 2004: Elsevier.
31. Elshahawy, W. and I. Watanabe, Biocompatibility of dental alloys used in dental fixed prosthodontics. *Tanta Dental Journal*, 2014. 11(2): p. 150-159.
32. Megremis, S. and C.M. Carey, Corrosion and tarnish of dental alloys. 2006.
33. Wataha, J.C., Principles of biocompatibility for dental practitioners. *The Journal of prosthetic dentistry*, 2001. 86(2): p. 203-209.
34. Van Noort, R. and M. Barbour, Introduction to Dental Materials-E-Book. 2014: Elsevier Health Sciences.
35. Scheller-Sheridan, C., Basic guide to dental materials. Vol. 4. 2010: John Wiley & Sons.
36. Brizuela, A., et al., Influence of the elastic modulus on the osseointegration of dental implants. *Materials*, 2019. 12(6): p. 980.

## References

37. Ahmed, H., Craig's restorative dental materials. *British Dental Journal*, 2019. 226(1): p. 9-9.
38. Wataha, J.C., Alloys for prosthodontic restorations. *Journal of Prosthetic Dentistry*, 2002. 87(4): p. 351-363.
39. Teoh, S.H., *Engineering materials for biomedical applications*. Vol. 1. 2004: World scientific.
40. Givan, D., *Precious metal alloys for dental applications*. *Precious metals for biomedical applications*, 2014: p. 109-129.
41. Slokar, L., J. Pranjić, and A. Carek, *Metallic materials for use in dentistry*. *The holistic approach to environment*, 2017. 7(1): p. 39-58.
42. Powers, J. and J. Wataha, *Dental materials: foundations and applications*. 11. painos. St. Louis Missouri: Elsevier, 2017.
43. Rezaie, H.R., et al., *A Review on Dental Materials*. 2020: Springer.
44. Rathi, S. and A. Verma, *Material selection for single-tooth crown restorations*, in *Applications of nanocomposite materials in dentistry*. 2019, Elsevier. p. 225-235.
45. McCabe, J.F. and A.W. Walls, *Applied dental materials*. 2013: John Wiley & Sons.
46. Roach, M., *Base metal alloys used for dental restorations and implants*. *Dental Clinics of North America*, 2007. 51(3): p. 603-627.
47. Wataha, J.C., J.L. Drury, and W.O. Chung, *Nickel alloys in the oral environment*. *Expert review of medical devices*, 2013. 10(4): p. 519-539.

## References

48. Cwalina, K.L., et al., Revisiting the effects of molybdenum and tungsten alloying on corrosion behavior of nickel-chromium alloys in aqueous corrosion. *Current Opinion in Solid State and Materials Science*, 2019. 23(3): p. 129-141.
49. Haider, A., et al. Ni-Cr-Mo alloy for dental prostheses with low melting temperature. in *Key Engineering Materials*. 2018. Trans Tech Publ.
50. Baran, G., The metallurgy of Ni-Cr alloys for fixed prosthodontics. *The Journal of prosthetic dentistry*, 1983. 50(5): p. 639-650.
51. Turchi, P.E., L. Kaufman, and Z.-K. Liu, Modeling of Ni–Cr–Mo based alloys: Part I—phase stability. *Calphad*, 2006. 30(1): p. 70-87.
52. Lippold, J.C., S.D. Kiser, and J.N. DuPont, *Welding metallurgy and weldability of nickel-base alloys*. 2011: John Wiley & Sons.
53. Davis, J.R., *Nickel, cobalt, and their alloys*. 2000: ASM international.
54. Rebak, R.B., *2 Corrosion of Non-Ferrous Alloys. I. Nickel-, Cobalt-, Copper-, Zirconium-and Titanium-Based Alloys*.
55. Ebrahimi, N., *The Influence of Alloying Elements on The Crevice Corrosion Behaviour of Ni-Cr-Mo Alloys*. 2015.
56. Upadhyay, D., et al., Corrosion of alloys used in dentistry: A review. *Materials Science and Engineering: A*, 2006. 432(1-2): p. 1-11.
57. Park, J. and R.S. Lakes, *Biomaterials: an introduction*. 2007: Springer Science & Business Media.
58. Al-Hity, R.R., et al., Corrosion resistance measurements of dental alloys, are they correlated? *Dental Materials*, 2007. 23(6): p. 679-687.

## References

59. Chaturvedi, T., An overview of the corrosion aspect of dental implants (titanium and its alloys). *Indian J Dent Res*, 2009. 20(1): p. 91.
60. Aliofkhazraei, M., *Developments in corrosion protection*. 2014: BoD–Books on Demand.
61. Pedefferri, P. and M. Ormellese, *Corrosion science and engineering*. 2018: Springer.
62. Zohdi, H., M. Emami, and H.R. Shahverdi, *Galvanic Corrosion Behavior of Dental Alloys*. substance, 2012. 4: p. 6.
63. Spencer, P. and A. Misra, *Material-tissue Interfacial Phenomena: Contributions from Dental and Craniofacial Reconstructions*. 2016: Woodhead Publishing.
64. Smallman, R.E. and R.J. Bishop, *Modern physical metallurgy and materials engineering*. 1999: Butterworth-Heinemann.
65. Wessel, J.K., *The handbook of advanced materials: enabling new designs*. 2004: John Wiley & Sons.
66. Huang, H.H., Effect of chemical composition on the corrosion behavior of Ni-Cr-Mo dental casting alloys. *Journal of Biomedical Materials Research*, 2002. 60(3): p. 458-465.
67. Elshahawy, W. and I. Watanabe, *Biocompatibility of dental alloys used in dental fixed prosthodontics*. 2014.
68. Zhou, Z. and J. Zheng, Tribology of dental materials: a review. *Journal of physics D: applied physics*, 2008. 41(11): p. 113001.

## References

69. Heintze, S.D., F.-X. Reichl, and R. Hickel, Wear of dental materials: Clinical significance and laboratory wear simulation methods—A review. *Dental materials journal*, 2019. 38(3): p. 343-353.
70. Gladwin, M. and M. Bagby, *Clinical aspects of dental materials: theory, practice, and case* 3rd ed. West Camden Street: Lippincott Williams & Wilkins, A Walters Kluwer Business, 2009.
71. Zhou, Z.-R., et al., *Dental biotribology*. 2013: Springer.
72. Lanza, A., A. Ruggiero, and L. Sbordone, Tribology and dentistry: A commentary. *Lubricants*, 2019. 7(6): p. 52.
73. Wu, Y.-Q., J.A. Arsecularatne, and M. Hoffman, Effect of acidity upon attrition–corrosion of human dental enamel. *Journal of the mechanical behavior of biomedical materials*, 2015. 44: p. 23-34.
74. Sharma, P., *A Textbook of Production Technology (Manufacturing Processes): Manufacturing Processes*. 2007: S. Chand Publishing.
75. Beddoes, J. and M. Bibby, *Principles of metal manufacturing processes*. 1999: Butterworth-Heinemann.
76. Upadhyaya, G.S., *Powder metallurgy technology*. 1997: Cambridge Int Science Publishing.
77. Kim, S.J., Y.M. Ko, and H.C. Choe. Pitting corrosion of TiN coated dental cast alloy with casting methods. in *Advanced Materials Research*. 2007. Trans Tech Publ.

## References

78. Dewidar, M.M., H.-C. Yoon, and J.K. Lim, Mechanical properties of metals for biomedical applications using powder metallurgy process: A review. *Metals and Materials International*, 2006. 3(12): p. 193-206.
79. Arifin, A., et al., Material processing of hydroxyapatite and titanium alloy (HA/Ti) composite as implant materials using powder metallurgy: a review. *Materials & Design*, 2014. 55: p. 165-175.
80. Tsutsui, T., Recent technology of powder metallurgy and applications. Hitachi Chemical Technical Report. 54: p. 12-20.
81. Neikov, O.D. and N. Yefimov, Handbook of non-ferrous metal powders: technologies and applications. 2009: Elsevier.
82. Angelo, P. and R. Subramanian, Powder metallurgy: science, technology and applications. 2008: PHI Learning Pvt. Ltd.
83. Fang, Z.Z., Sintering of advanced materials. 2010: Elsevier.
84. Bäbler, R., Materials Handbook—A Concise Desktop Reference. 2020.
85. Shah, F.U., S. Glavatskih, and O.N. Antzutkin, Boron in tribology: from borates to ionic liquids. *Tribology letters*, 2013. 51(3): p. 281-301.
86. Alfantazi, A.M. and R. Moskalyk, Processing of indium: a review. *Minerals Engineering*, 2003. 16(8): p. 687-694.
87. Banerjee, S. and P. Mukhopadhyay, Phase transformations: examples from titanium and zirconium alloys. 2010: Elsevier.
88. Ong, J., M.R. Appleford, and G. Mani, Introduction to biomaterials: basic theory with engineering applications. 2014: Cambridge University Press.
89. Darvell, B.W., Materials science for dentistry. 2018: Woodhead publishing.

## References

90. Rao, S.B. and R. Chowdhary, Evaluation on the corrosion of the three Ni-Cr alloys with different composition. *International journal of dentistry*. 2011.
91. Gatin, E., D. Pirvu, and R. Cara, Biocompatibility and sensitization to nickel related corrosion process of Ni–Cr dental metal alloys.
92. Galo, R., et al., Effects of chemical composition on the corrosion of dental alloys. *Brazilian dental journal*, 2012. 23: p. 141-148.
93. Yavuz, T., et al., Effect of Surface Treatment on Elemental Composition of Recast NiCr Alloy. *Materials Sciences and Applications*, 2012. 3: p. 163-167.
94. de Mattias Sartori, I.A., et al., Mechanical behavior of NiCr and NiCrTi alloys for implant prosthetic components. *Brazilian Dental Science*, 2013. 16(2): p. 37-43.
95. Kim, H.S., et al., Corrosion behaviors and biocompatibility of the Ni-Cr-Mo dental casting alloy. *대한금속재료학회지*, 2014. 52(1): p. 67-72.
96. Sousa, L., et al., Corrosion process development of a Ni-Cr-Mo alloy used in dental prosthesis.
97. Loch, J., et al., Electrochemical Behaviour of Co-Cr and Ni-Cr Dental Alloys. *Solid State Phenomena*, 2015. 227: p. 451.
98. Park, S.-Y., et al., Corrosion Properties of Ni–13Cr–(4~ 10) Mo for Dental Casting Alloys. *Science of Advanced Materials*, 2016. 8(12): p. 2248-2252.
99. Augustyn-Nadzieja, J., A. Łukaszczyk, and J. Loch, Effect of remelting of the Ni-22Cr-9Mo alloy on its microstructural and electrochemical properties. *Archives of Metallurgy and Materials*, 2017. 62(1): p. 411--418.

## References

100. Liliana, P., et al., Corrosion behavior of Ni-Cr dental casting alloys. *Int J Electrochem Sci*, 2018. 13: p. 410-23.
101. Moslehifard, E., S. Ghasemzadeh, and F. Nasirpouri, Influence of pH level of artificial saliva on corrosion behavior and nickel ion release of a Ni-Cr-Mo alloy: an in vitro study. *Anti-Corrosion Methods and Materials*, 2019.
102. Turdean, G.L., et al., Study of electrochemical corrosion of biocompatible Co-Cr and Ni-Cr dental alloys in artificial saliva. Influence of pH of the solution. *Materials Chemistry and Physics*, 2019. 233: p. 390-398.
103. dos Reis Barros, C.D., et al., Galvanic corrosion of Ti6Al4V coupled with NiCr as a dental implant alloy in fluoride solutions. *Int. J. Electrochem. Sci*, 2020. 15: p. 394-411.
104. Yun, Chang-Su, Takao Hanawa, Min-Ho Hong, Bong Ki Min, and Tae-Yub Kwon. "Biocompatibility of Ni-Cr alloys, with the same composition, prepared by two new digital manufacturing techniques." *Materials Letters* 305 (2021): 130761.
105. ASTM, B., 328" Standard Test Method for Density. Relative Density (Specific Gravity), and Absorption of Fine Aggregate, 2003.
106. Al-Maamoria, M., J.M. Salmana, and O. Ihsana, Testing the Mechanical Properties of the Alloy (Al-Cu-Mg) by Ultrasonic Technology. 2013.
107. Fontana, M.G. and N.D. Greene, Corrosion engineering. 2018: McGraw-hill.
108. Karaköse, E. and M. Keskin, Effect of microstructural evolution and elevated temperature on the mechanical properties of Ni-Cr-Mo alloys. *Journal of Alloys and Compounds*, 2015. 619: p. 82-90.

## References

109. Martínez, Carola, Claudio Aguilar, Francisco Briones, Danny Guzmán, E. Zelaya, Loreto Troncoso, and P. A. Rojas. "Effects of Zr on the amorphization of Cu-Ni-Zr alloys prepared by mechanical alloying." *Journal of Alloys and Compounds* 765 (2018): 771-781.
110. Ogden, H.R. and F. Holden, *Metallography of titanium alloys*. 1958: Titanium Metallurgical Laboratory, Battelle Memorial Institute.
111. Sampath, V. and U. Mallik. Influence of minor additions of boron and zirconium on shape memory properties and grain refinement of a Cu-Al-Mn shape memory alloy. in *European Symposium on Martensitic Transformations*. 2009. EDP Sciences.
112. Huang, L., *Microstructural Evolution of TiAl-Intermetallic Alloys Containing W and B*. 2005.
113. AYDOĞMUŞ, T. and A.Ş. BOR, Production and characterization of porous TiNi shape memory alloys. *Turkish Journal of Engineering and Environmental Sciences*, 2011. 35(2): p. 69-82.
114. Kolawole, Maruf Yinka, Jacob Olayiwola Aweda, Farasat Iqbal, Asif Ali, and Sulaiman Abdulkareem. "Mechanical properties of powder metallurgy processed biodegradable Zn-based alloy for biomedical application." *Int. J. Mater. Metall. Eng* 13, no. 12 (2019): 558-563.
115. Szewczyk-Nykiel, A., The effect of the addition of boron on the densification, microstructure and properties of sintered 17-4 PH stainless steel. *Czasopismo Techniczne*.
116. Ali, Muhammad, Faiz Ahmad, Puteri Sri Melor, Noorhana Yahya, and Muhammad Aslam. "Investigation of boron effect on the densification of Fe-50%

## References

Ni soft magnetic alloys produced by powder metallurgy route." *Materials Today: Proceedings* 16 (2019): 2210-2218.

117. Soyama, Juliano, Michael Oehring, Wolfgang Limberg, Thomas Ebel, Karl Ulrich Kainer, and Florian Pyczak. "The effect of zirconium addition on sintering behaviour, microstructure and creep resistance of the powder metallurgy processed alloy Ti–45Al–5Nb–0.2 B–0.2 C." *Materials & Design* 84 (2015): 87-94.

118. Romero-Resendiz, L., P. Gómez-Sáez, A. Vicente-Escuder, and V. Amigó-Borrás. "Development of Ti–In alloys by powder metallurgy for application as dental biomaterial." *Journal of Materials Research and Technology* 11 (2021): 1719-1729.

119. Canakci, A. and T. Varol, Microstructure and properties of AA7075/Al–SiC composites fabricated using powder metallurgy and hot pressing. *Powder Technology*, 2014. 268: p. 72-79.

120. Veerappan, G., M. Ravichandran, M. Meignanamoorthy, and V. Mohanavel. "Characterization and properties of silicon carbide reinforced Ni-10Co-5Cr (Superalloy) matrix composite produced via powder metallurgy route." *Silicon* 13 (2021): 973-984.

121. Málek, Jaroslav, František Hnilica, Jaroslav Veselý, Bohumil Smola, Vítězslav Březina, and Kamil Kolařík. "The effect of boron addition on microstructure and mechanical properties of biomedical Ti35Nb6Ta alloy." *Materials characterization* 96 (2014): 166-176.

122. Cabral Miramontes, J. A., Jose Dolores Oscar Barceinas Sánchez, F. Almeraya Calderón, A. Martínez Villafañe, and J. G. Chacón Nava. "Effect of boron

## References

additions on sintering and densification of a ferritic stainless steel." *Journal of materials engineering and performance* 19 (2010): 880-884.

123. Tsai, Yi-Lung, Sea-Fue Wang, Hui-Yun Bor, and Yung-Fu Hsu. "Effects of Zr addition on the microstructure and mechanical behavior of a fine-grained nickel-based superalloy at elevated temperatures." *Materials Science and Engineering: A* 607 (2014): 294-301.

124. Shalaby, R., Effect of indium content and rapid solidification on microhardness and micro-creep of Sn-Zn eutectic lead free solder alloy. *Crystal Research and Technology: Journal of Experimental and Industrial Crystallography*, 2010. 45(4): p. 427-432.

125. Syarifudin, M., E.N. Hale, and B.T. Sofyan. Effect of ZrO<sub>2</sub> addition on mechanical properties and microstructure of Al-9Zn-6Mg-3Si matrix composites manufactured by squeeze casting. in *IOP Conference Series: Materials Science and Engineering*. 2019. IOP Publishing.

126. Li, W., et al., Enhanced compressive strength and tailored microstructure of selective laser melted Ti-46.5 Al-2.5 Cr-2Nb-0.5 Y alloy with different boron addition. *Materials Science and Engineering: A*, 2018. 731: p. 209-219.

127. Sozhamannan, G. G., M. Mohamed Yusuf, G. Aravind, G. Kumaresan, K. Velmurugan, and V. S. K. Venkatachalapathy. "Effect of applied load on the wear performance of 6061 Al/nano TiCp/Gr hybrid composites." *Materials Today: Proceedings* 5, no. 2 (2018): 6489-6496.

128. Arul, S., Effect of nickel reinforcement on micro hardness and wear resistance of aluminium alloy Al7075. *Materials Today: Proceedings*, 2020. 24: p. 1042-1051.

## References

129. Mouflih, K., K. El Mouaden, M. Boudalia, A. Bellaouchou, M. Tabyaoui, A. Guenbour, I. Warad, and A. Zarrouk. "The Effect of the Moroccan *Salvadora Persica* Extract on the Corrosion Behavior of the Ni–Cr Non-precious Dental Alloy in Artificial Saliva." *Journal of Bio-and Tribo-Corrosion* 7 (2021): 1-10.
130. Hernandez-Rodriguez, Marco AL, Dionisio A. Laverde-Cataño, Diego Lozano, Gabriela Martinez-Cazares, and Yaneth Bedolla-Gil. "Influence of boron addition on the microstructure and the corrosion resistance of CoCrMo alloy." *Metals* 9, no. 3 (2019): 307.
131. Qurashi, M.S., et al., Corrosion Resistance and Passivation Behavior of B-containing S31254 Stainless Steel in a low pH medium. *Int. J. Electrochem. Sci*, 2019. 14: p. 10642-10656.
132. Zhang, Yue, Alison J. Davenport, Bernard Burke, Nina Vyas, and Owen Addison. "Effect of Zr addition on the corrosion of Ti in acidic and reactive oxygen species (ROS)-containing environments." *ACS Biomaterials Science & Engineering* 4, no. 3 (2018): 1103-1111.
133. Al-DEEN, H.H.J., EFFECT OF ZIRCONIUM ADDTION ON CORROSION RESISTANCE OF ALUMINUM–BRONZE ALLOYS IN (3.5% NaCl AND 2M HCl) SOLUTIONS.
134. Jayapriya, J., Post Welded Offsw Joints On Acrolein Coating. *Turkish Journal of Computer and Mathematics Education (TURCOMAT)*, 2021. 12(7): p. 2598-2608.
135. Barão, Valentim AR, Mathew T. Mathew, Wirley Gonçalves Assunção, Judy Chia-Chun Yuan, Markus A. Wimmer, and Cortino Sukotjo. "Stability of cp-Ti and

## References

Ti-6 Al-4 V alloy for dental implants as a function of saliva pH—an electrochemical study." *Clinical oral implants research* 23, no. 9 (2012): 1055-1062.

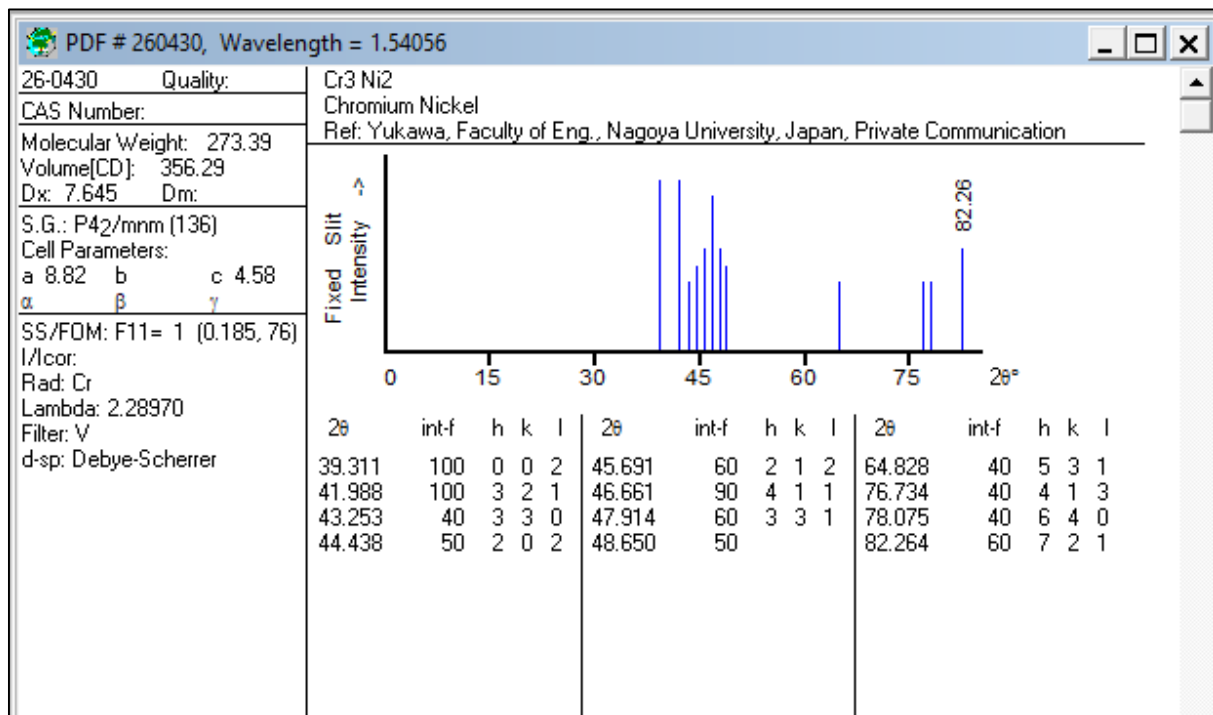
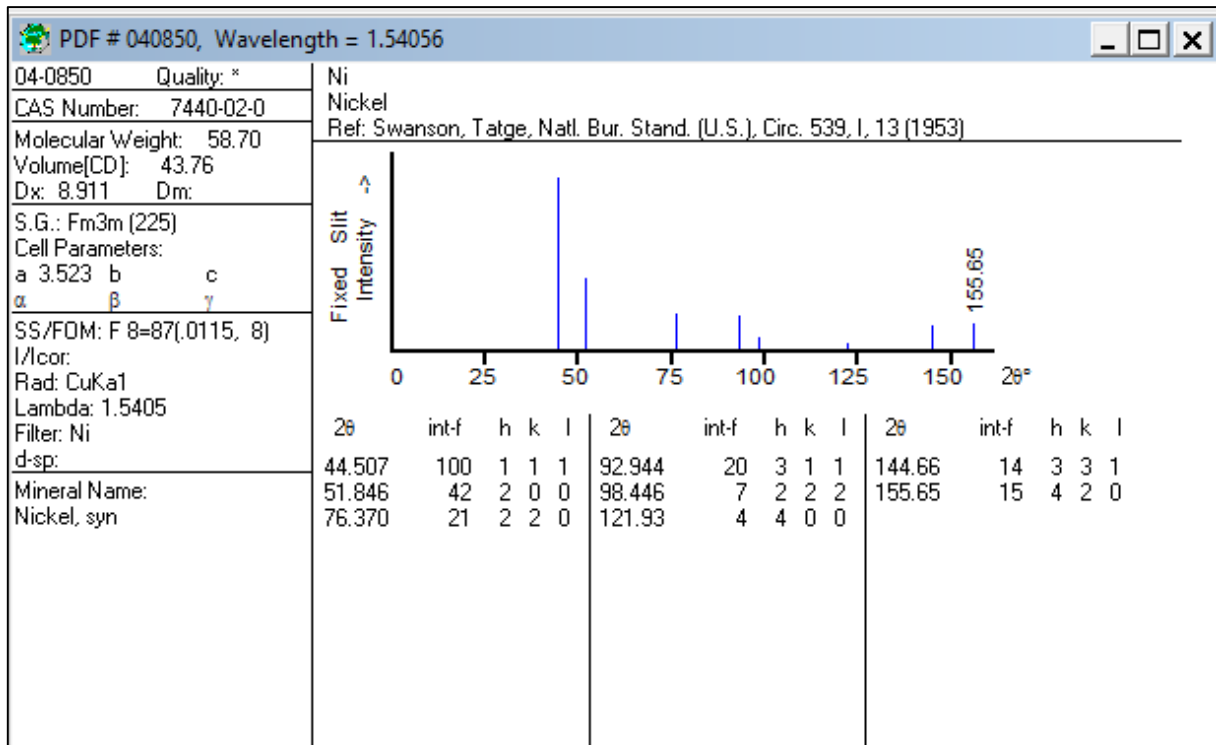
136. Singh, R. and N.B. Dahotre, Corrosion degradation and prevention by surface modification of biometallic materials. *Journal of Materials Science: Materials in Medicine*, 2007. 18(5): p. 725-751.

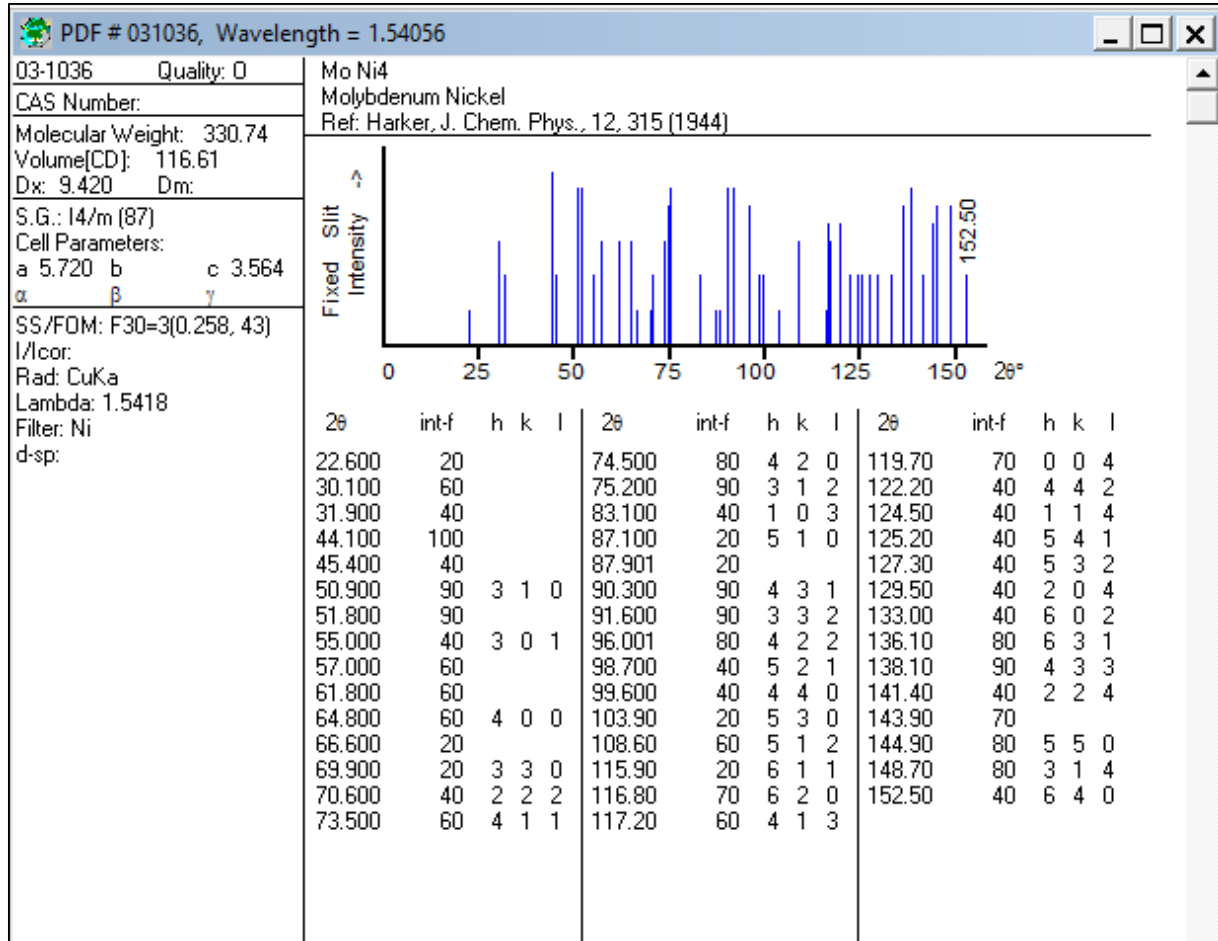
137. Al-Jmmal, A.Y., Metal ion release from Ni-Cr alloy with different artificial saliva acidities. *Al-Rafidain Dental Journal*, 2014. 14(2): p. 266-271.

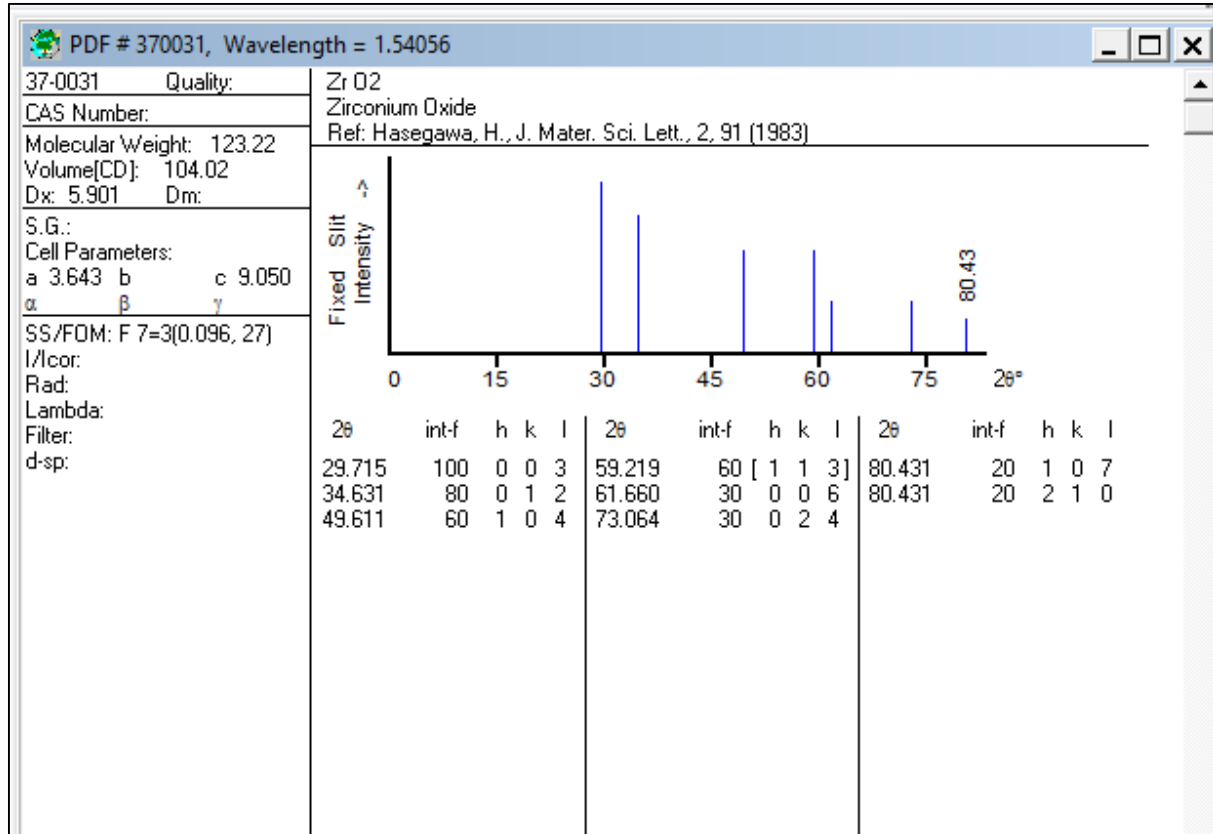
138-Angelo, P. C., and Ramayyar Subramanian. *Powder metallurgy: science, technology and applications*. PHI Learning Pvt. Ltd., 2008.

139-K. Praveenkumar, and V. R. Kabadi "Realistic Approach to Pin –onDisc Wear Testing Measurement" *International Journal of Advanced Production and Industrial Engineering*, vol.610,pp.47-53, 2017.

140- Azaath, L. Mamundi, U. Natarajan, G. Veerappan, M. Ravichandran, and S. Marichamy. "Experimental Investigations on the Mechanical Properties, Microstructure and Corrosion Effect of Cu-20Al-4Ni/SiC Composites Synthesized Using Powder metallurgy Route." *Silicon* 14, no. 11 (2022): 5993-6002.







## EDX FOR ALLOYS

## Quantitative Results for A Alloy

Elt	Line	Int	Error	K	Kr	W%	A%
Cr	Ka	531.6	0.8502	0.3853	0.3822	37.03	40.63
Co	Ka	16.5	0.6943	0.0213	0.0211	2.20	2.13
Ni	Ka	341.2	0.6943	0.5563	0.5519	55.94	54.36
Mo	La	59.1	2.1160	0.0371	0.0368	4.83	2.87
				1.0000	0.9921	100.00	100.00

## Quantitative Result for B1 Alloy

Elt	Line	Int	Error	K	Kr	W%	A%
B	Ka	0.6	71.7450	0.0046	0.0044	2.81	13.07
Cr	Ka	544.9	0.8506	0.4405	0.4253	41.61	40.19
Co	Ka	12.0	0.6313	0.0173	0.0167	1.77	1.51
Ni	Ka	285.2	0.6313	0.5187	0.5008	51.42	43.99
Mo	La	27.0	0.7448	0.0189	0.0182	2.39	1.25
				1.0000	0.9655	100.00	100.00

## Quantitative Results B2 alloy

Elt	Line	Int	Error	K	Kr	W%	A%
B	Ka	0.6	62.1288	0.0050	0.0048	3.13	14.62
Cr	Ka	411.5	0.5894	0.3350	0.3217	31.24	30.32
Co	Ka	16.3	0.7071	0.0237	0.0227	2.38	2.04
Ni	Ka	330.1	0.7071	0.6046	0.5806	59.21	50.90
Mo	La	45.0	1.0116	0.0318	0.0305	4.04	2.12
				1.0000	0.9603	100.00	100.00

## Quantitative Results for B3 alloy

Elt	Line	Int	Error	K	Kr	W%	A%
<b>B</b>	Ka	0.9	34.8448	0.0062	0.0059	4.20	19.12
<b>Cr</b>	Ka	253.9	0.6125	0.1856	0.1763	16.87	15.97
<b>Co</b>	Ka	19.6	0.5962	0.0256	0.0243	2.50	2.09
<b>Ni</b>	Ka	458.0	0.5962	0.7530	0.7154	72.62	60.87
<b>Mo</b>	La	46.7	1.0336	0.0296	0.0281	3.81	1.95
				1.0000	0.9500	100.00	100.00

## Quantitative Results for C1 alloy

Elt	Line	Int	Error	K	Kr	W%	A%
<b>Cr</b>	Ka	447.7	0.7055	0.3469	0.3410	33.02	36.93
<b>Co</b>	Ka	11.9	0.5898	0.0164	0.0161	1.67	1.65
<b>Ni</b>	Ka	327.5	0.5898	0.5708	0.5612	56.52	55.99
<b>Zr</b>	La	53.0	1.9274	0.0237	0.0233	3.29	2.10
<b>Mo</b>	La	62.9	1.9274	0.0422	0.0415	5.49	3.33
				1.0000	0.9832	100.00	100.00

## Quantitative Results for C2 alloy

Elt	Line	Int	Error	K	Kr	W%	A%
<b>Cr</b>	Ka	461.2	0.6441	0.3977	0.3894	37.86	42.27
<b>Co</b>	Ka	13.2	0.8287	0.0203	0.0199	2.07	2.04
<b>Ni</b>	Ka	260.6	0.8287	0.5056	0.4950	49.90	49.35
<b>Zr</b>	La	86.4	0.7187	0.0430	0.0421	5.86	3.73
<b>Mo</b>	La	44.6	0.7187	0.0333	0.0326	4.31	2.61
				1.0000	0.9790	100.00	100.00

## Quantitative Results for C3 alloy

Elt	Line	Int	Error	K	Kr	W%	A%
Cr	Ka	329.9	0.6870	0.2813	0.2740	26.45	30.35
Co	Ka	15.7	1.0143	0.0239	0.0233	2.39	2.42
Ni	Ka	309.8	1.0143	0.5942	0.5789	57.79	58.72
Zr	La	89.7	0.8607	0.0441	0.0430	6.03	3.95
Mo	La	76.5	0.8607	0.0566	0.0551	7.34	4.56
				1.0000	0.9743	100.00	100.00

## Quantitative Results for D1 alloy

Elt	Line	Int	Error	K	Kr	W%	A%
Cr	Ka	359.2	0.9845	0.2814	0.2785	26.83	30.21
Co	Ka	17.0	0.6230	0.0237	0.0234	2.41	2.40
Ni	Ka	359.7	0.6230	0.6341	0.6273	63.00	62.84
Mo	La	66.5	0.8506	0.0452	0.0447	5.91	3.61
In	La	18.1	0.8506	0.0156	0.0155	1.85	0.94
				1.0000	0.9894	100.00	100.00

## Quantitative Results for D2 alloy

Elt	Line	Int	Error	K	Kr	W%	A%
Cr	Ka	366.6	0.6257	0.3039	0.3010	29.06	32.57
Co	Ka	16.4	0.8633	0.0242	0.0240	2.48	2.45
Ni	Ka	330.1	0.8633	0.6156	0.6099	61.36	60.91
Mo	La	50.0	1.3654	0.0359	0.0356	4.70	2.86
In	La	22.3	1.3654	0.0204	0.0202	2.41	1.22

				1.0000	0.9907	100.00	100.00
--	--	--	--	--------	--------	--------	--------

## Quantitative Results for D3 alloy

Elt	Line	Int	Error	K	Kr	W%	A%
Cr	Ka	380.1	0.7383	0.2933	0.2903	28.00	31.51
Co	Ka	19.5	0.9406	0.0268	0.0265	2.73	2.72
Ni	Ka	356.0	0.9406	0.6180	0.6116	61.44	61.24
Mo	La	61.7	0.9699	0.0413	0.0409	5.39	3.29
In	La	24.2	0.9699	0.0206	0.0204	2.43	1.24
				1.0000	0.9896	100.00	100.00

## Quantitative Results for E1 alloy

Elt	Line	Int	Error	K	Kr	W%	A%
O	Ka	120.2	20.2083	0.0762	0.0683	12.95	35.43
Cr	Ka	280.2	0.8401	0.2142	0.1921	19.02	16.01
Co	Ka	17.3	0.5942	0.0235	0.0211	2.23	1.66
Ni	Ka	363.3	0.5942	0.6250	0.5606	58.11	43.31
Zr	La	70.1	1.8497	0.0309	0.0277	4.00	1.92
Mo	La	45.5	1.8497	0.0302	0.0271	3.68	1.68
				1.0000	0.8969	100.00	100.00

## Quantitative Results for E2 alloy

Elt	Line	Int	Error	K	Kr	W%	A%
<b>O</b>	Ka	123.7	18.0723	0.0873	0.0770	14.72	38.97
<b>Cr</b>	Ka	257.6	0.7186	0.2192	0.1935	19.27	15.70
<b>Co</b>	Ka	14.3	0.7885	0.0216	0.0191	2.03	1.46
<b>Ni</b>	Ka	314.8	0.7885	0.6027	0.5319	55.36	39.94
<b>Zr</b>	La	90.4	1.3584	0.0444	0.0392	5.62	2.61
<b>Mo</b>	La	33.6	1.3584	0.0248	0.0219	2.99	1.32
				1.0000	0.8826	100.00	100.00

## Quantitative Results for E3 alloy

Elt	Line	Int	Error	K	Kr	W%	A%
<b>O</b>	Ka	112.8	14.1073	0.0771	0.0659	14.72	39.83
<b>Cr</b>	Ka	314.7	0.8333	0.2596	0.2217	22.33	18.59
<b>Co</b>	Ka	10.7	0.6379	0.0157	0.0134	1.42	1.04
<b>Ni</b>	Ka	265.4	0.6379	0.4926	0.4206	43.42	32.02
<b>Zr</b>	La	265.4	6.8304	0.1264	0.1079	14.76	7.01
<b>Mo</b>	La	39.9	6.8304	0.0286	0.0244	3.35	1.51
				1.0000	0.8538	100.00	100.00

## خلاصة

سبائك الأسنان ذات الأساس المعدني هي واحدة من أكثر المواد المستخدمة على نطاق واسع في طب الأسنان. سبائك الكوبالت والكروم والنيكل والكروم لها تطبيقات عديدة في مجال طب الأسنان إلى جانب سبائك الذهب والمعادن الثمينة المستخدمة في هذا المجال. ركزت هذه الدراسة على تصنيع وتوصيف مركبات سبائك النيكل والكروم المقويات بإضافة بعض العناصر (مادة البورون والزركونيوم والإنديوم والزركونيا) وتأثيرها على الخصائص الفيزيائية والميكانيكية والكهروكيميائية والطبية لهذه السبيكة.

طريقة ميتالورجيا المساحيق المستخدمة في تحضير السبائك تمت بإضافة كل من البورون والزركونيوم والإنديوم بنسب مختلفة (0.4، 0.8، 1.2) wt% بينما أضيف الزركونيا بنسب مختلفة (3، 6 و 9) wt%. تمت عملية الخلط لمدة 6 ساعات ، ثم تم كبسها بضغط ثابت قدره 600 ميجا باسكال. كانت أبعاد العينات بعد عملية الضغط  $d = 13\text{mm}$  و  $t = 4\text{mm}$ . إن عملية التلبيد التي يتم إجراؤها عند درجة حرارة 1000 درجة مئوية لمدة 8 ساعات لجميع العينات كافية تمامًا لتحويل كل العناصر إلى هيكل سبيكة.

تم إجراء اختبارات مختلفة على العينات ، بما في ذلك الاختبارات الميكانيكية (الصلادة ، معامل يونك ، مقاومة الانضغاط ، والبلى ) ، الاختبارات الفيزيائية (الكثافة والمسامية ) ، اختبار البنية المجهرية (تحليل حيود الأشعة السينية ، المجهر الإلكتروني الماسح الضوئي والانبعث الميداني ) ، الاختبارات الكهروكيميائية (جهد الدائرة المفتوحة ، الاستقطاب الديناميكي وإطلاق الأيونات) ، والاختبارات البيولوجية (مضاد للبكتيريا).

أشارت النتائج إلى أن إضافة البورون والزركونيوم والإنديوم أدى إلى انخفاض واضح في المسامية ، بينما أدت إضافة الزركونيا إلى زيادة ملحوظة في قيم مسامية السبيكة. تظهر نتائج الكثافة بعد التلبيد زيادة في كثافة العينات المحتوية على البورون والزركونيوم والإنديوم وانخفاض كبير في كثافة العينات المحتوية على الزركونيا.

أظهرت نتائج XRD أن جميع العينات (مع وبدون إضافات) عند درجة حرارة الغرفة ، تظهر فقط ثلاث اطوار في جميع السبائك ،  $\gamma$  (Ni) ،  $\text{Cr}_3\text{Ni}_2$  ،  $\text{MoNi}_4$  ولكن في حالة إضافة الزركونيا إلى السبيكة ، فقد أظهرت الاطوار السابقة مع وجود بيك واضح من الزركونيا في الرسم التخطيطي.

تمت زيادة صلادة برنل للسبائك المحضرة بشكل كبير مع إضافة القليل من البورون والزركونيوم في جميع النسب ، وكان لإضافة الإنديوم تأثير طفيف على قيمة الصلادة. العينات التي تحتوي على 1.2% بالوزن من الزركونيوم لها صلابة أعلى لجميع عناصر الإضافة.

زادت مقاومة البلى بإضافة B و Zr و In و ZrO<sub>2</sub> إلى سبائك NiCrMoCo ، فإن العينة (1.2) Zr لديها خسارة أقل في الوزن أثناء اختبار التآكل تحت الأحمال المختلفة.

من نتائج الخواص الكهروكيميائية اظهرت مقاومة التآكل لسبيكة NiCrMoCo تحسناً ملحوظاً بعد إضافة كل من B و Zr و In و ZrO<sub>2</sub> في اللعاب الصناعي و المحلول الملحي . وقد تبين أن التحسن أعلى مع إضافة 0.8wt% B حيث كانت نسبة التحسن 84.6% و 87.2% في اللعاب و المحلول الملحي على التوالي.

يوضح اختبار إطلاق الأيونات لجميع السبائك لمدة 21 يوماً في اللعاب الاصطناعي والمحلل الملحي أنه لوحظ وجود تركيزات منخفضة جداً من إطلاق أيونات المعادن. في الاختبار المضاد للبكتيريا لوحظ أن وجود العينات أدى إلى انخفاض تأثير البكتيريا. حيث لوحظ انخفاض ملحوظ في نسبة البكتيريا بعد فترة الحضانة لمدة 12 ساعة. العينة المضاف إليها (1.2 wt %) انديوم و العينة المضاف إليها (6 wt %) ZrO<sub>2</sub> كان لها أعلى تأثير مضاد للجراثيم على كلا المؤشرين مقارنة بالعينات الأخرى.



وزارة التعليم العالي والبحث العلمي  
جامعة بابل  
كلية هندسة المواد  
قسم هندسة المعادن

تقصي تأثير إضافة عناصر السبك / سيراميك على سلوك  
سبيكة  $Ni-Cr-Mo-Co$  كمواد حيائية

اطروحة

مقدمة إلى مجلس كلية هندسة المواد/ جامعة بابل وهي جزء من متطلبات نيل شهادة  
الدكتوراه فلسفة في هندسة المواد/ المعادن

من قبل

بان احمد شنان جاسم

بكالوريوس هندسة معادن (2011)

ماجستير هندسة معادن (2017)

بإشراف

أ. د. علي هوبي حليم

أ. د. حيدر حسن جابر